THE DETECTION STABILITY OF A SINGLE BIT

SAMPLING CROSS-CORRELATOR FOR DETECTING

RANDOM GAUSSIAN SIGNALS

by E. V. Hoversten

THE DETECTION RELIABILITY OF A SINGLE-BIT SAMPLING CROSS-CORRELATOR FOR DETECTING RANDOM GAUSSIAN REFLECTIONS

John Edward Howard

A Thesis Submitted to the Faculty of Engineering,
University of the Witwatersrand, Johannesburg,
for the Degree of Doctor of Philosophy

Johannesburg 1974

I hereby declare that this is my own work and has not been submitted before to any university for a degree.

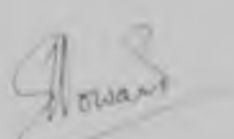

John Edward Howard

Johannesburg, June 1974.

ABSTRACT

In this thesis the detection reliability of a single-bit, digital, sampling cross-correlator used for detecting either single-bit or analog bandlimited Gaussian signals is investigated. This is done by deriving the exact output probability mass function of the cross-correlator, as this directly yields the Detection and False Alarm probabilities.

The cross-correlator output mass function is derived for the following cases:

(a) a single-bit bandlimited Gaussian signal cross-correlated with an attenuated reflection corrupted by wideband Gaussian noise, and

(b) an analog bandlimited Gaussian signal cross-correlated with an attenuated reflection corrupted by wideband Gaussian noise.

The extraneous noise is not necessarily always wideband random noise, and in many applications the interfering signal can be periodic in nature; thus the output mass function is also considered

(c) for a single-bit bandlimited Gaussian signal cross-correlated with an attenuated reflection corrupted by a random phase sinusoid, and

(d) for an analog bandlimited Gaussian signal cross-correlated with an attenuated reflection corrupted by a random phase sinusoid.

In all cases except (d), the cross-correlation function is derived first, and then the probability mass functions are derived for both burst and continuous transmitted signal operation. In (d) the cross-correlation function cannot be derived in a closed form, and a series approximation is given. However, the zero delay (i.e. peak) cross-correlation function is derived exactly, and this yields information on the detection

probabilities to be expected. The cross-correlator output probability mass functions are discussed qualitatively in this case.

It is found that in general the detection reliability obtained using single-bit bandlimited Gaussian signals is higher than that achievable with analog signals, and that a random phase sine wave has a more adverse effect on the cross-correlator's detection performance than wideband Gaussian noise has.

The theoretical derivations of (a), (b) and (c) are verified by extremely close agreement with experimental results taken on a specially built single-bit, sampling cross-correlator.

The cross-correlator's performance under multiple reflection conditions is considered, and the cross-correlation function of a single-bit or an analog bandlimited Gaussian signal with two attenuated reflections corrupted by wideband Gaussian noise is derived. An extension of the theory to more than two reflections is discussed in both cases. The derivation of the cross-correlator output mass functions is considered for both burst and continuous signal operation. It is shown that under conditions where there are two overlapping single-bit reflections in a low extraneous noise environment, there is a high probability of missing the smaller of the two reflections completely, even though it may be only slightly smaller than the larger one. This defect does not occur with analog Gaussian signals, and, although the peaks in their case are not so sharp or well-defined, under these conditions analog signals offer a distinct advantage over single-bit signals.

The practical application of the detection scheme to acoustics is briefly discussed, and it is found that the Gaussian signal centre frequency and the cross-correlator sampling frequency must be matched. A sampling frequency of between one and ten times the signal centre frequency yields satisfactory results. There are several constraints on the signal bandwidth, and octave bandwidths are found to offer a good compromise.

To my Parents, with my thanks

ACKNOWLEDGMENTS

The author very gratefully acknowledges the generous financial support in the form of a scholarship given by C. J. Fuchs Ltd., and the assistance and encouragement given by the members of the Fuchs Electronics Laboratories, in particular Martyn Schriro, during the experimental stage of this project. He is also very grateful indeed for the help and guidance given throughout the project by his supervisor, Professor H. E. Rauhahan.

For many enlightening discussions on statistics, the author is indebted to Mr. Paul Fatti and Professor D. M. Hawkins of the Department of Applied Mathematics and Statistics at this University.

Finally, he would like to thank the Sun Life Assurance Company of Canada for the loan of the typewriter with which to type the final draft.

CONTENTS

CHAPTER I

INTRODUCTION

1.1 General Background

The importance of correlation as a signal detection technique is already well established. Very briefly, the three basic operational configurations are as shown in Fig. 1-1. Figure 1-1a corresponds to a simple auto-correlator for detecting a signal, usually of a periodic nature, immersed in noise. In more demanding applications such as may arise, for example, in astronomy or sonar, the outputs from arrays of receivers are cross-correlated (Fig. 1-1b), and the output is examined

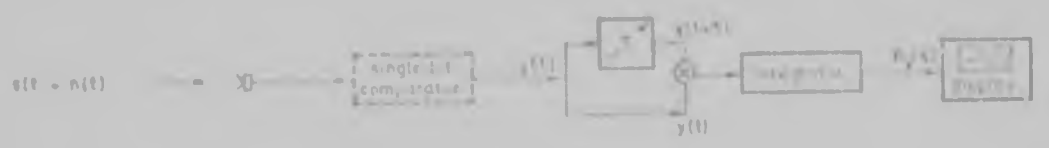

(a) Simple auto-correlation detector

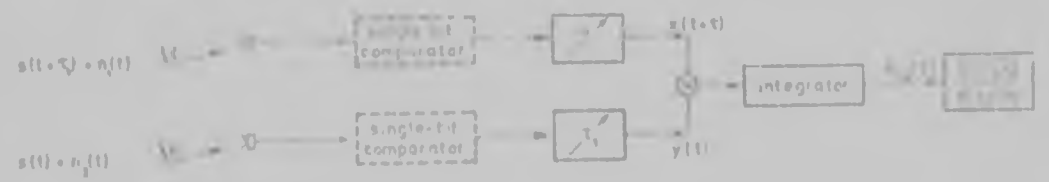

(b) Array cross-correlation detector

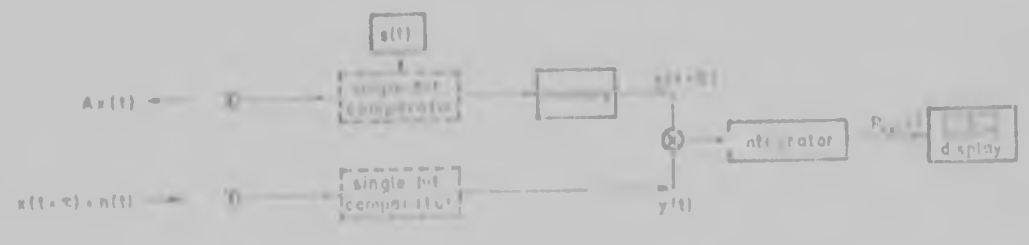

(c) Cross-correlation reflection detector

FIGURE 1-1 Basic configurations of correlation detectors.

for peaks or other characteristics indicating the presence of a common input signal s(t). The third basic application (Fig. 1-1c) is to reflection detection, for example in radar, acoustics or vibration analysis.

For cross-correlation reflection detection, the ideal waveform for precise and unambiguous range and delay measurements is that possessing a 'thumbtack-shaped' auto-correlation function. Gaussian noise is one such waveform, provided, of course, that the duration-bandwidth product is large enough. In addition, the auto-correlation function of an analog Gaussian waveform is simply related to that of its severely-clipped, single-bit version[1]. The computational simplification gained by having to process only a single-bit waveform as compared to the original analog version, especially in the case of a digital processor, is substantial.

With the advent of high speed logical circuitry, many of the problems that had previously made correlators complicated instruments to build were alleviated. However, as the basic circuitry became simpler, so the mathematical processing techniques which the digital circuitry now made it possible to exploit became more complex. As a result, modern correlation detectors tend, as before, to be complicated and sophisticated instruments.

There are many applications of cross-correlation detectors in radar, sonar, communications, acoustics and vibration analysis where detection error probabilities of below 10^{-6} are not really necessary and false alarms could not cause traumatic consequences (as, for example, in missile detection). For these applications it is obviously desirable to be able to use as simple and hence inexpensive a cross-correlator as possible. Moreover, many of these applications often require on-site, real-time measuring, and cross-correlation detectors which are either large or which have to be connected to a large computer would clearly be quite unsuitable. For such applications, therefore, there is a need for a small, self-contained, simple yet reliable cross-correlation

detector. A sampling, single-bit, digital serial cross-correlator used in conjunction with Gaussian random waveforms constitutes an obvious yet most promising solution, combining one of the simplest and hence most inexpensive cross-correlators and a waveform having desirable attributes for reflection detection and single-bit processing.

Although the idea of using a single-bit cross-correlator for detecting Gaussian waveforms is not new, no thorough analysis of the detection reliability of a sampling, single-bit digital cross-correlator has been found in the literature. The work done on analysing their performance in detecting Gaussian waveforms has been limited to the determination of the mean output of a single-bit cross-correlator like that in Fig. 1-1b and an associated signal-to-noise ratio describing the ratio of the mean output to the fluctuation caused by the non-infinite time-constant of the RC integrators usually used. Such an analysis yields only a 'figure of merit' for the detection scheme. It does not yield the detection or false alarm probabilities and it gives no idea of the influence of the number of samples used on the cross-correlation function distribution, since the variance is determined primarily by the integrator time-constant. This would not be so were a digital counter to be used, as is envisaged in this case, rather than an RC integrator. A much more useful analysis would be given by the derivation of the exact output probability distribution of the cross-correlator because this would directly yield the detection and false alarm probabilities and would show the effects of sample size variation.

The development over the past few years of surface acoustic wave devices and techniques, with their enormous potential for high speed single-bit signal processing and matched filtering etc., has certainly revolutionised the possibilities of building very simply such instruments as random signal, single-bit digital cross-correlation radars, and it now seems perfectly feasible that in the future such instruments could be

made cheaply enough to be used for more mundane applications such as traffic monitoring and control, simple collision avoidance radars, or even burglar alarms! Already the possible application of these surface acoustic wave devices to the single-bit cross-correlation of single-bit random waveforms for identification purposes, to increase the reliability of communication between aircraft and ground controllers, has been suggested.

The application of interest to the author is that of acoustic reflection detection, but since the basic correlation detection scheme proposed is potentially suitable for so many other applications besides acoustics, in communications, radar, sonar, ultrasonics, etc., it is considered that a thorough analysis of its detection reliability would be of some value in assessing its suitability for these applications.

1.2 Scope and Organization of the Present Work

This thesis presents an analysis of the detection reliability of a digital, single-bit sampling cross-correlator for detecting both analog and single-bit bandlimited Gaussian reflections (Fig. 1-2).

The discrete probability mass function of the single-bit cross-correlator output is derived in Sections 2.1 and 2.2 for the cases where these two types of reflection are corrupted by wideband Gaussian noise. The analyses deal with the detection of both continuous and burst waveform reflections.

Although the corrupting extraneous noise is often random in nature, acoustic measurements, for example, are often carried out amid more deterministic extraneous noises such as machine hums, i.e. waveforms which are of a periodic nature; similar situations arise in other applications, for instance in radar applications, the chance (or otherwise) occurrence of radio signals within the radar operating frequency band.

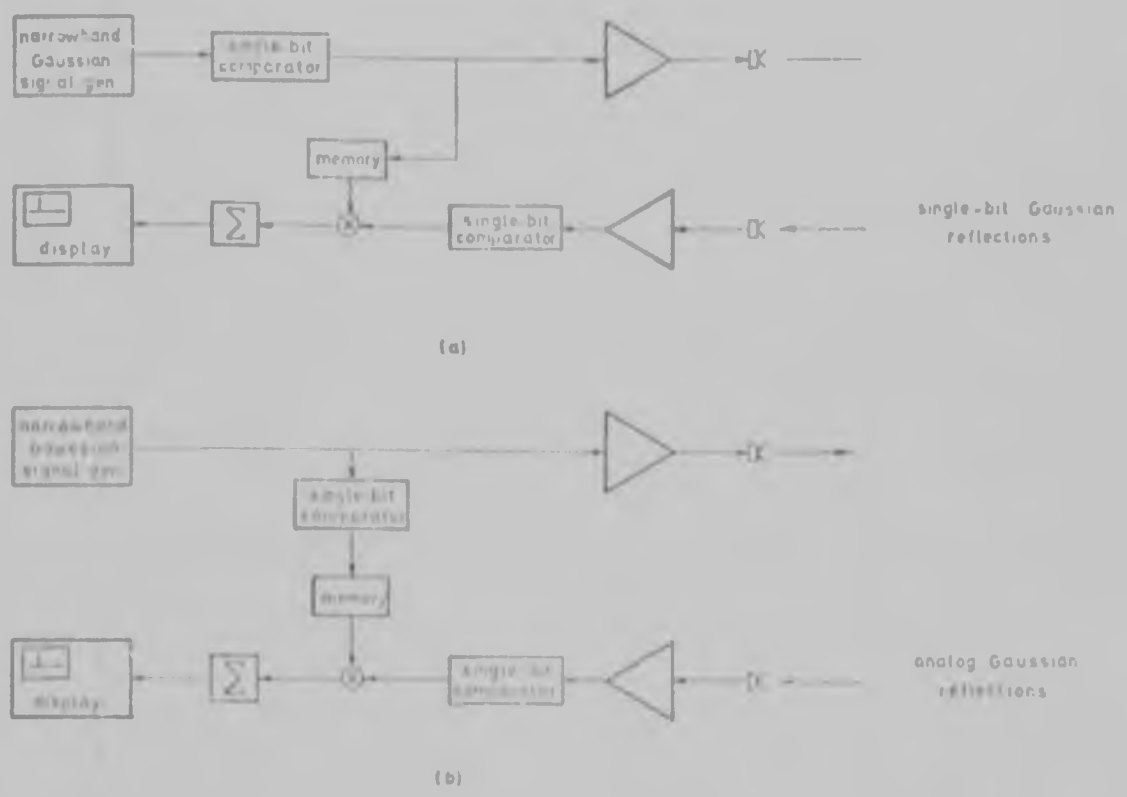

FIGURE 1-2 Single-bit cross-correlation detection (a) of single-bit Gaussian reflections, and (b) of analog Gaussian reflections.

No work has been found in the literature analysing the effects of extraneous periodic waveforms on the detection by single-bit cross-correlation of random waveforms, most analyses having in fact concentrated on the reverse situation. Accordingly, since such situations can arise in practice, the next two sections (2.3 and 2.4) present a derivation of the single-bit cross-correlation function and the output probability mass function of the single-bit cross-correlator when the single-bit or analog Gaussian reflections are corrupted by a random phase sine wave. An extension to other types of periodic waveform is discussed in the case of single-bit reflection detection. Again, both continuous and burst waveform reflections are dealt with.

Chapter three considers the single-bit cross-correlation of a single-bit or analog bandlimited Gaussian signal with a reflection consisting of two delayed, attenuated replicas corrupted by wideband Gaussian noise. The practical significance of such an analysis is illustrated in Fig. 1-3.

An extension of the theory to the detection of more than two simultaneous reflections is discussed.

Experimental results verifying the theory of Chapter two are given and discussed in Chapter four. These results are found to agree extremely accurately with the theoretical predictions, thereby substantiating the major simplifying assumptions and methods used in the theoretical analysis.

FIGURE 1-3 An example of multiple reflection detection.

In Chapter five, the practical application of the cross-correlator to acoustic reflection detection is considered, and Chapter six summarises and discusses the main conclusions to be drawn from the theoretical and experimental results.

The design and construction of the digital single-bit cross-correlator are briefly set out in Appendix T, together with some general remarks on its operation.

1.3 Survey of the Literature

This thesis is concerned with the derivation of the output probability distribution function of a single bit digital cross-correlator for detecting random waveforms. For the sake of completeness, the literature survey will be split into topics as follows: Section 1.3.1 deals with the work done on deriving the output probability density functions of various correlators; Section 1.3.2 covers the work done on analysing hard-limiting cross-correlators used for detecting Gaussian waveforms, and Section 1.3.3 deals with literature on possible applications of the

proposed cross-correlation detection scheme.

1.3.1 Probability Density Function Derivations

Most of the derivations of probability density functions of correlator outputs have been tackled by first deriving the output characteristic function, usually on the simplifying assumption of independent random or jointly normal inputs.

Lampard[2] (1956) derived the characteristic function and hence the probability density function of the output of an analog correlator consisting of a multiplier and low pass filter, whose inputs were correlated, stationary Gaussian waveforms, and solved the specific case of one input being a low pass filtered version of the other. Roe and White[3] (1961) derived the output characteristic function of a sampling cross-correlator whose two inputs consisted of a signal plus noise bandlimited to -W to W hertz. They assumed (1) that the sampling was done at the Nyquist rate so that successive noise and hence input samples were independent, and (2) that corresponding input samples followed a bivariate normal distribution with mean values equal to the respective signal waveforms. The output probability density function was derived for certain extreme values of input signal-to-noise ratio. The problem of determining the output probability density function of an analog cross-correlator like that in Fig. 1-1b, whose two inputs consisted of a correlated, RC filtered Gaussian signal plus uncorrelated white noise, was investigated by Jacobson[4] (1963). Cooper[5] (1965) considered the output probability density function of a correlator whose inputs both consisted of a sine wave plus noise that had been passed through a narrowband filter centred on the sine wave frequency. He obtained solutions for certain special input conditions.

Stremler and Jensen[6] (1970) noted that the problem of the characteristic function approach lay in the transformation to the density

function. They generalised Cooper's results by deriving some simplifying assumptions to ease the transformation. Murarka[7] (1971) further generalised Cooper's and Roe and White's work by deriving an expression for the probability density function of a cross-correlator for detecting an 'in phase' sine wave immersed in narrowband noise. He evaluated this for the cases of perfectly correlated and completely uncorrelated noise waveforms. All restrictions on phase between input signals and degree of correlation between input noise waveforms were eliminated in the analysis of Andrews[11] (1973). He assumed that the correlator output was low pass filtered, leaving only dc terms and the noise component amplitudes. Since these follow a joint normal distribution, their characteristic function and hence the correlator output probability density function can be derived.

Very recently, Andrews[9] (1974) has extended the work of Roe and White[3] to cater for non-zero correlation between the input waveforms.

1.3.2 Analyses of Hard-limiting Correlators

As stated in Section 1.1, most of the work on clipped random waveform correlation has been limited to deriving the mean output of cross-correlators such as that in Fig. 1-1b excited by Gaussian noise, and a representative signal-to-noise ratio describing the ratio of the mean value to the fluctuating component resulting from the non-infinite integration interval.

Thomas and Williams[10] (1959) compared the output signal-to-noise ratios of a full analog and a single-bit cross-correlator consisting of a multiplier and a low pass filter, with input waveforms consisting of a narrowband Gaussian signal plus noise - i.e. $K_1 s(t) + n_1(t)$ and $K_2 s(t) + n_2(t)$. They showed that for stationary or 'nearly stationary' noise the full analog cross-correlator performs best, but for non-stationary noise the single-bit cross-correlator is invariably the better of the two.

The use of a single-bit cross-correlator for the detection of weak

Gaussian signals immersed in Gaussian noise was considered by Ekre[11] (1963). On the assumptions (a) that the input signal and noise were independent stationary random functions with Gaussian amplitude distributions, (b) that the normalised power density spectra of the input signal and noise were identical, and (c) that the input signal-to-noise ratio was much less than one, so that the input waveforms could be assumed uncorrelated, he evaluated the cross-correlation function and the output signal-to-noise ratio for a single-bit cross-correlator (sampling and non-sampling) using an RC integrator. He then compared this to the signal-to-noise ratio that would be achieved using an analog multiplier cross-correlator, showing how the loss in output signal-to-noise ratio due to the clipping operation is only 1.19 dB for low input signal-to-noise ratios.

Cheng[12] (1968) extended the work of Ekre by deriving the exact cross-correlation function and output signal-to-noise ratio for any input signal-to-noise ratio. In addition, his analysis does not entail the simplifying assumption that the input waveforms remain uncorrelated even in the presence of a small input signal. This he obviates by using a quadrivariate normal distribution to describe the joint probability density function of the four input components $[s(t)+n_1(t)]$, $[s(t-\tau)+n_1(t-\tau)]$, $[s(t)+n_2(t)]$, and $[s(t-\tau)+n_2(t-\tau)]$, $s(t)$ and $n(t)$ being uncorrelated Gaussian signal and noise waveforms, respectively. He compares the output signal-to-noise ratios of an analog multiplier cross-correlator and a sampling and non-sampling single-bit cross-correlator, showing how above a certain critical input signal-to-noise ratio, the single-bit cross-correlator's output signal-to-noise ratio is greater than that of the analog multiplier cross-correlator.

Gassner, McGillem and Cooper[13] (1965) consider the use of a single-bit cross-correlator for estimating the cross-correlation function of the two input waveforms, each consisting of the sum of a zero mean Gaussian

signal and zero mean Gaussian noise. They derive a signal-to-noise ratio for the output of the cross-correlator (and hence for the estimate of the input cross-correlation function) defined as $[\rho_y^2(\tau)/\mathrm{var}\{\rho_y(\tau)\}]$, where $\rho_y(\tau)$ is the normalised cross-correlation function after clipping. This is derived on the assumption that the sampling rate is much lower than the signal bandwidth so that consecutive samples of the inputs can be assumed independent. They then consider an envelope single-bit cross-correlator for use on narrow bandpass random signals where the cross-correlation function would be modulated at the central r.f. frequency. By again deriving an output signal-to-noise ratio, they show that this detection scheme has no advantage over a conventional cross-correlator.

McGillem, Cooper and Waltman[14] (1967) apply some of the above results to a radar system having bandpass Gaussian noise as transmitted signal, and a bandpass, single-bit cross-correlation detector. They use the results to derive an approximate signal-to-noise ratio for the output, again on the assumption that the sampling rate is much less than the Nyquist rate.

Aein[15] (1967) considers the detection error rate at the output of a hard-limiting cross-correlator whose inputs consist of a binary deterministic signal plus noise, the output consisting of the sum of n independent random variables (due to the presence of the noise). He shows that although the sum tends to normal, one is not in general justified in using the complementary error function to calculate the error probabilities on the tails of the distribution. By using the Chernov bound, he derives an expression for the error probability P_e which, for the assumptions of low input signal-to-noise ratios and $P_e < 10^{-2}$ (i.e. inferring a sufficiently long correlation interval), simplifies to a good approximation of the complementary error function, suggesting a normal distribution.

1.3.3 Applications

As mentioned in Section 1.1, virtually all of the applications of random waveform single-bit cross-correlation at radar frequencies have arisen due to the development of surface acoustic wave devices. The topic is extensively covered by Collins and Hagon[16] (1970), Kino and Shaw[17] (1972), Maines and Paige[18] (1973) and Morgan[19] (1974).

An application to air traffic control communications is discussed by Grant, Collins, Darby and Morgan[20] (1973). To increase the reliability of communication between aircraft and ground, a single-bit, random coded waveform can be sent prior to the message and single-bit cross-correlated by a surface acoustic wave matched filter in the receiver; the cross-correlation peak serves to announce the arrival of a message and also to synchronise the receiver to the ensuing single-bit coded message.

Broch[21] (1970) discusses some of the practical uses and possibilities of cross-correlation and cross-spectral density techniques in acoustic delay measurements and vibration analysis. He points out that cross-correlation techniques (with fairly narrowband noise) only give meaningful results when (a) the transmission characteristics of the various propagation paths are frequency independent, and (b) the noise signal used has a wide enough bandwidth. In cases where this is not so, the output tends to be oscillatory, making peak detection and discrimination difficult. He derives an approximate empirical expression for the minimum bandwidth in terms of the required resolution. As this criterion leads to required bandwidths often in excess of three hundred hertz, he concludes that the use of cross-correlation is of very limited value in acoustics. He then considers the use of cross-spectral density techniques and derives a criterion in this case for the bandwidth of the sampling filter. This is inversely proportional to the delay being measured and hence renders this technique unattractive for acoustic purposes, where delays of several seconds can be encountered.

Many papers on the application of random waveform cross-correlation to sonar are to be found in the Journals of the Acoustic Society of America, and a very comprehensive text on correlation techniques and their applications has been written by Lange[22] (1967). He gives an extremely comprehensive bibliography on the subject.

CHAPTER II

CROSS-CORRELATION DETECTION OF SINGLE REFLECTIONS

It is impossible to foresee the exact operating conditions that a detection system will encounter. One must resort, therefore, to analysing a situation which is as accurate a representation as possible of the type of conditions likely to be met with in practice, and then interpret the results from an engineering point of view rather than a purely mathematical one, bearing in mind that they apply only to representative conditions.

This chapter presents the derivation of the output probability mass function of a single-bit, sampling cross-correlator for detecting

(a) a single-bit bandlimited Gaussian reflection (Fig. 1-2a, page 5) corrupted by wideband Gaussian noise (Section 2.1),

(b) an analog bandlimited Gaussian reflection (Fig. 1-2b) corrupted by wideband Gaussian noise (Section 2.2),

(c) a single-bit bandlimited Gaussian reflection corrupted by a random phase sine wave (Section 2.3), and

(d) an analog bandlimited Gaussian reflection corrupted by a random phase sine wave (Section 2.4).

In all cases except (d), the cross-correlation function is derived first, and then the probability mass functions are derived for both burst and continuous transmitted signal operation. In (d) the cross-correlation function cannot be derived in a closed form, and a series approximation is given. However, the zero delay (i.e. peak) cross-correlation function is derived exactly, and the probability mass functions are discussed

qualitatively.

In all probability the extraneous noise will rarely be pure Gaussian or a perfect sinusoid, and it is unlikely that the reflection will be linearly attenuated. Nevertheless, these simulated conditions are representative of those that might prevail on average. They do have some advantages. Firstly, they can be readily simulated in a laboratory and hence the theoretical predictions can be reliably checked. Secondly, they provide a realistic basis for comparison between different systems subjected to them. Finally, the fact that the mathematics involved under these idealised, simplified but mathematically representable conditions can prove somewhat intractable suggests what lies in store were a strictly realistic analysis to be undertaken!

2.1 Detection of a Single-bit Gaussian Reflection Corrupted by Wideband Gaussian Noise

2.1.1 Derivation of the Cross-correlation Function

Consider the two waveforms

$$x_1(t) = \mathrm{sgn}[f_n(t)] \quad \ldots\ldots\ldots\ldots\ldots\ldots 2.1.1$$

$$x_2(t+\tau) = \mathrm{sgn}[\beta x_1(t+\tau) + n(t)] \quad \ldots\ldots\ldots\ldots 2.1.2$$

where

$$\mathrm{sgn}[a] = \begin{cases} +1 & a \geq 0 \\ -1 & a < 0 \end{cases}$$

and $f_n(t)$ is a random Gaussian waveform of zero mean, bandlimited to $(\omega_b/2\pi)$ Hz. $n(t)$ is wideband Gaussian noise of zero mean and variance σ^2, and β is an attenuation factor which is assumed to be a real constant.

Defining P_{++} as the probability that $x_1(t)$ and $x_2(t+\tau)$ are both equal to +1, and P_{-+} similarly as the probability that $x_1(t)=-1$ and $x_2(t+\tau)=+1$, etc.,

$$P_{++} + P_{+-} + P_{-+} + P_{--} = 1$$
$$P_{++} + P_{+-} - P_{-+} - P_{--} = E\{x_1(t)\} = 0 \qquad \ldots\ldots 2.1.3$$
$$P_{++} - P_{+-} + P_{-+} - P_{--} = E\{x_2(t+\tau)\} = 0$$
$$P_{++} - P_{+-} - P_{-+} + P_{--} = E\{x_1(t).x_2(t+\tau)\} = \psi_{x_1x_2}(\tau)$$

$E\{x_1(t).x_2(t+\tau)\}$ is the same as the cross-covariance of $x_1(t)$ and $x_2(t+\tau)$ as they have zero mean, and in this case is identical to their cross-correlation function $\psi_{x_1x_2}(\tau)$. By symmetry $P_{++} = P_{--}$ and $P_{+-} = P_{-+}$. Hence, solving for $\psi_{x_1x_2}(\tau)$

$$\psi_{x_1x_2}(\tau) = 4P_{++} - 1 \qquad \ldots\ldots 2.1.4$$

For $x_2(t+\tau)$ to be +1, either $x_1(t+\tau) = +\beta$ and $n(t) > -\beta$, or $x_1(t+\tau) = -\beta$ and $n(t) > +\beta$. Therefore

$$P_{++} = P\{x_1(t)=+1\}.\ P\{x_1(t+\tau)=+1/\ x_1(t)=+1\}.P\{n(t) > -\beta\} +$$
$$P\{x_1(t+\tau)=-1/\ x_1(t)=+1\}.P\{n(t) > +\beta\} \qquad \ldots 2.1.5$$
$$= \tfrac{1}{2}\ P\{x_1(t+\tau)=+1/\ x_1(t)=+1\}.[\tfrac{1}{2} + \tfrac{1}{2}\mathrm{erf}(\beta/\sigma\sqrt{2})] +$$
$$P\{x_1(t+\tau)=-1/\ x_1(t)=+1\}.[\tfrac{1}{2} - \tfrac{1}{2}\mathrm{erf}(\beta/\sigma\sqrt{2})] \qquad \ldots\ldots 2.1.6$$

where

$$\mathrm{erf}(\theta) = \frac{2}{\sqrt{\pi}} \int_0^{\theta} e \quad du$$

$P\{x_1(t+\tau)=+1/\ x_1(t)=+1\}$ is the probability of an even number of zero crossings of $x_1(t)$ in period τ. An analogous set of equations to eqns. (2.1.3) can be written for $x_1(t)$ and $x_1(t+\tau)$, the only difference being that $E\{x_1(t).x_1(t+\tau)\}$ is the auto-covariance of $x_1(t)$ and $x_1(t+\tau)$, and is identical to the auto-correlation function $\psi_{x_1}(\tau)$ of $x_1(t)$, which is

$$\psi_{x_1}(\tau) = \frac{2}{\pi} \mathrm{Arcsin}\left[\rho_n(\tau)\right]. \qquad \ldots\ldots 2,1,7$$

$\rho_n(\tau)$ being the normalised auto-correlation function of $n(t)$.[+] The

---

[+] see Appendix A, (p. 103)

probability of an even number of zero crossings of $x_1(t)$ in time τ can then be written as $(P_{++} + P_{--})$. Similarly, $P\{x_1(t+\tau)=-1/\ x_1(t)=+1\}$ is the probability of an odd number of zero crossings of $x_1(t)$ in time τ, and can be written as $(P_{+-} + P_{-+})$.

Solving the set of equations for these yields

$$P\{x_1(t+\tau)=+1/\ x_1(t)=+1\} = P_{++} + P_{--} = \tfrac{1}{2}[1+\psi_{x_1}(\tau)]$$
$$P\{x_1(t+\tau)=-1/\ x_1(t)=+1\} = P_{+-} + P_{-+} = \tfrac{1}{2}[1-\psi_{x_1}(\tau)] \quad \ldots\ldots\ldots 2.1.8$$

Substituting these two into eqn. (2.1.6), and then substituting eqn. (2.1.6) into eqn. (2.1.4) gives

$$\psi_{x_1 x_2}(\tau) = \operatorname{erf}(\beta/\sigma\sqrt{2}) \cdot \psi_{x_1}(\tau) \quad \ldots\ldots\ldots\ldots 2.1.9$$

The auto-correlation function of $x_2(t)$ can be derived similarly, and is

$$\psi_{x_2}(\tau) = \left[\operatorname{erf}(\beta/\sigma\sqrt{2})\right]^2 \cdot \psi_{x_1}(\tau) \quad \ldots\ldots\ldots 2.1.10^{+}$$

2.1.2 Extension to Digital Sampling Cross-correlation

Consider a digital sampling cross-correlator. N samples, δt apart, of $x_1(t)$ and $x_2(t+\tau)$ are stored, and the products of corresponding sample pairs added to form the cross-correlation operation; i.e.

$$\psi_p(\tau) = \sum_{i=1}^{N} x_1(t_i) \cdot x_2(t_i+\tau) \quad \ldots\ldots\ldots\ldots 2.1.11$$

The probability distribution of $\psi_p(\tau)$ will be considered in two sections, (a) for $\tau=0$ and (b) for $|\tau|>0$.

For $\tau = 0$ and no extraneous noise $n(t)$ in $x_2(t)$, $\psi_p(0) = N$ since all the product terms are +1. With noise present, $\psi_p(0)$ will be reduced by two for every instant t_i at which either (1) $n(t_i) > \beta$ when $\beta x_1(t_i) = -\beta$ or (2) $n(t_i) < -\beta$ when $\beta x_1(t_i) = +\beta$. The probability of (1) or (2)

[+] see Appendix B, (p. 105)

occurring is

$$p = \tfrac{1}{2}.\ \mathrm{erfc}(\beta/\sigma\sqrt{2}) \quad \ldots\ldots\ldots\ldots\ldots\ldots\ 2.1.12$$

which, as n(t) is wideband Gaussian noise, is independent of t_i. Hence, the number of times (N_i) that (1) or (2) occurs in N instants will follow a binomial distribution[23][24] with mean Np and variance Np(1-p). The mean of $\psi_b(0)$ will be

$$\overline{\psi_b(0)} = N - 2Np$$
$$= N.\mathrm{erf}(\beta/\sigma\sqrt{2}) \quad \ldots\ldots\ldots\ldots\ldots\ 2.1.13$$

which agrees with eqn. (2.1.9), and since

$$P\{\psi_b(0) = N-2N_i\} = P\{(1) \text{ or } (2) \text{ occurring } N_i \text{ times}\} \quad 2.1.14$$

the distribution of $\psi_b(0)$ can be derived directly from that of N_i.

Some sample distributions of $\psi_b(0)$ for N=100 are plotted in Fig. 2-1.

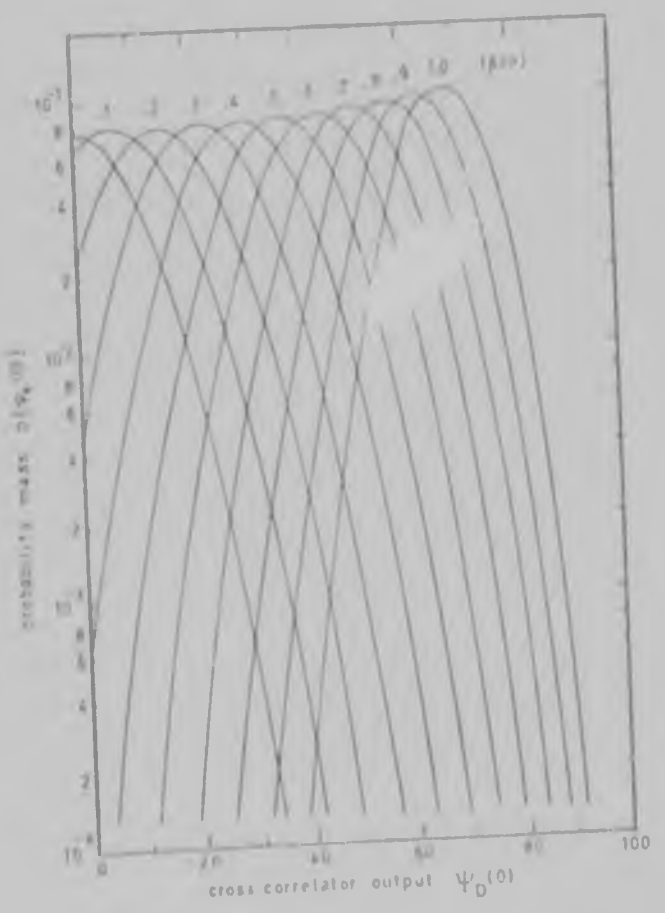

FIGURE 2-1 Probability mass functions of $\psi_b(0)$ for 100 samples

For $|\tau| > 0$, two cases will be considered. The first is where burst waveforms of duration T only are transmitted, so that (see Fig. 2-2) over interval 0 to $(T-\tau)$ $x_1(t)$ is cross-correlated with $\operatorname{sgn}[\beta x_1(t+\tau) + n(t)]$, and over interval $(T-\tau)$ to T with $\operatorname{sgn}[n(t)]$ only. Thus two distributions

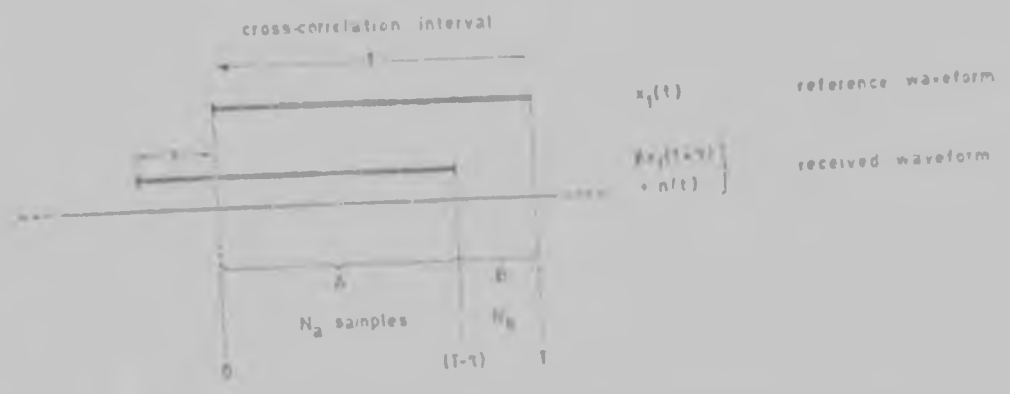

FIGURE 2-2 Cross-correlation of burst waveforms for $|\tau| > 0$

must be derived, and their combination yields the distribution of $\Psi_2(\tau)$.

For the period t_1 to $(t_N-\tau)$ (i.e. region A in Fig. 2-2), as a large[+] number N_a of identically distributed random variables is being summed, the Central Limit Theorem suggests that the distribution of the sum will tend to a normal distribution.[‡] The mean of this sum will be

$$\mu_{N_a} = N_a \cdot \Psi_{x_1 x_2}(\tau) \quad \ldots\ldots\ldots\ldots \quad 2.1.15$$

where $\Psi_{x_1 x_2}(\tau)$ is the cross-correlation function of $x_1(t)$ and $x_2(t+\tau)$ as defined in eqn. (2.1.9). The variance of the sum can be written as

$$\begin{aligned}
\operatorname{var}\Big[\sum_{i=1}^{N_a} x_1(t_i)x_2(t_i+\tau)\Big] &= E\Big\{\Big[\sum_{i=1}^{N_a} x_1(t_i)x_2(t_i+\tau) - E\Big\{\sum_{i=1}^{N_a} x_1(t_i)x_2(t_i+\tau)\Big\}\Big]^2\Big\} \\
&= E\Big\{\Big[\sum_{i=1}^{N_a} x_1(t_i)x_2(t_i+\tau)\Big]^2\Big\} - \Big[E\Big\{\sum_{i=1}^{N_a} x_1(t_i)x_2(t_i+\tau)\Big\}\Big]^2 \\
&= E\Big\{\sum_{i=1}^{N_a} x_1^2(t_i)x_2^2(t_i+\tau)\Big\} + 2E\Big\{\sum_{i=1}^{N_a-1}\sum_{j=i+1}^{N_a} x_1(t_i)x_2(t_i+\tau)x_1(t_j)x_2(t_j+\tau)\Big\} - \mu_{N_a}^2 \\
&= N_a - \mu_{N_a}^2 + 2\sum_{i=1}^{N_a-1}\sum_{j=i+1}^{N_a} E\{x_1(t_i)x_2(t_i+\tau)x_1(t_j)x_2(t_j+\tau)\} \quad \ldots\ldots \quad 2.1.16
\end{aligned}$$

[+] see p. 23

[‡] see Section 2.1.3 (p. 21)

now

$$\mathcal{E}\{x_1(t_i)x_2(t_i+\tau)x_1(t_j)x_2(t_j+\tau)\} = P_{++++} - P_{+++-} - \ldots + P_{++--} - \ldots + P_{----} \quad \ldots\ldots 2.1.17$$

where P_{++++} is the probability that $x_1(t_i)$, $x_2(t_i+\tau)$, $x_1(t_j)$ and $x_2(t_j+\tau)$ are all equal to +1, and P_{+++-} etc., are all similarly defined.

Assuming that the number of zero crossings of $x_1(t)$ and $x_2(t)$ in any given interval is independent of the number in any other non-overlapping interval[+], these joint probabilities may be evaluated as follows:

(a) $t_j < (t_i+\tau)$, so that the non-overlapping intervals are t_i to t_j, t_j to $(t_i+\tau)$, and $(t_i+\tau)$ to $(t_j+\tau)$. In this case

$$\begin{aligned} P_{++++} &= P\{x_1(t_i)=+1,\ x_2(t_i+\tau)=+1,\ x_1(t_j)=+1,\ x_2(t_j+\tau)=+1\} \\ &= P\{x_1(t_i)=+1\}.P\{x_1(t_j)=+1/\ x_1(t_i)=+1\}.P\{x_2(t_i+\tau)=+1/\ x_1(t_j)=+1\} \\ &\qquad .P\{x_2(t_j+\tau)=+1/\ x_2(t_i+\tau)=+1\} \end{aligned} \quad \ldots\ldots\ldots 2.1.18$$

$P\{x_2(t_i+\tau)=+1/\ x_1(t_i)=+1\}$ is the probability of an even number of zero crossings in time $(t_i+\tau-t_j)$, and from eqns. (2.1.3) is given by $\frac{1}{2}[1+\psi_{x_1x_1}(t_i+\tau-t_j)]$. Therefore

$$P_{++++} = \tfrac{1}{2}.\tfrac{1}{2}[1+\psi_{x_1x_1}(t_j-t_i)].\tfrac{1}{2}[1+\psi_{x_2x_2}(t_i+\tau-t_j)].\tfrac{1}{2}[1+\psi_{x_1x_1}(t_j-t_i)] \quad \ldots\ldots 2.1.19$$

Similarly

$$P_{+++-} = \tfrac{1}{16}[1+\psi_{x_1x_1}(t_j-t_i)].[1+\psi_{x_2x_2}(t_i+\tau-t_j)].[1-\psi_{x_1x_1}(t_j-t_i)]$$

Calculating the rest of the terms in eqn. (2.1.17) in the same way and summing,

$$E\{x_1(t_i)x_2(t_i+\tau)x_1(t_j)x_2(t_j+\tau)\} = \psi_{x_1x_1}(t_j-t_i).\psi_{x_2x_2}(t_j-t_i) \quad \ldots 2.1.20$$

from eqns. (2.1.8) and (2.1.9).

[+]see Section 2.1.4 (p. 24)

(b) For $t_j \geq (t_i+\tau)$, so that the non-overlapping intervals are now t_i to $(t_i+\tau)$, $(t_i+\tau)$ to t_j, and t_j to $(t_j+\tau)$, as in (a)

$$\xi\{x_1(t_i)x_2(t_i+\tau)x_1(t_j)x_2(t_j+\tau)\} = [\psi_{x_1x_2}(\tau)]^2 \quad \ldots\ldots\ldots 2.1.21$$

Substituting in eqn. (2.1.17) and collecting like terms*, the variance of the sum of the N_a products is

$$\text{var}_{N_a} = N_a - \mu^2_{N_a} + 2\sum_{i=1}^{N_a-1}(N_a-i)\psi_{x_1}(i\delta\tau).\psi_{x_2}(i\delta\tau) + (2N_a-N+1)(2N_a-N)\left[\psi_{x_1x_2}(\tau)\right]^2 \quad \ldots\ldots 2.1.22$$

Over the remaining interval $(T-\tau)$ to T (region B in Fig. 2-2), the reference signal $x_1(t)$ is cross-correlated with $x_2(t+\tau) = \text{sgn}[n(t)]$. Each of these product terms can have value 1 or -1 (with equal probability in this case) and, as n(t) is wideband random noise, its value will be independent of that of any of the other product terms. Thus the number of product terms (N_i) having value -1, say, will follow a binomial distribution with mean $(N_b \cdot \frac{1}{2})$ and variance $(N_b \cdot \frac{1}{4})$. The sum of the product terms, which is equal to $(N_b - 2N_i)$, will therefore have zero mean and variance N_b, and its distribution can be derived directly from that of N_i.

The output of the cross-correlator, $\psi'_b(\tau)$, is the sum of the N_a and the N_b product terms, and therefore the distribution of $\psi'_b(\tau)$ is obtained by combining the two distributions derived above. These may be combined directly as they are independent of one another.** The mean of the combined distribution will be $\rho'_{x_1x_2}$.

If the received signal consisted of noise only, the distribution of $\psi'_b(\tau)$ would be derived exactly as for the product sum in the interval $(T-\tau)$ to T above, except that the number of terms having value -1 would in this case have mean $(N.\frac{1}{2})$ and variance $(N.\frac{1}{4})$. The mean and variance

---

*See Appendix C(1), (p. 106) **See Appendix C(3), (p. 107)

of $\psi_3(\tau)$ would be zero and N, respectively. Due to its symmetry about zero, this distribution would tend to normal rapidly with increasing N.

The second case to be analysed is for continuous transmitted waveforms. This situation is simpler than the burst waveform analysis in that $x_2(t+\tau) = \text{sgn}[\beta x_1(t+\tau) + n(t)]$ over the whole of the correlation interval T so that only one distribution need be derived. This one is directly analogous to the distribution calculated for the sum of the N_a terms in the previous analysis, and thus the sum of the N product terms will tend to normal with mean and variance[+]

$$\psi_3(\tau) = \mu_3 = N.\psi_{x_1x_2}(\tau) \quad \ldots\ldots\ldots\ldots\ldots \quad 2.1.23$$

$$\text{var}[\psi_3(\tau)] = N - \mu_3^2 + 2\sum_{i=1}^{N-N_a-1}(N-i)\psi_{x_1}(i\delta t).\psi_{x_2}(i\delta t) + N_a(N_a+1)\left[\psi_{x_1x_2}(\tau)\right]^2 \quad 2.1.24$$

respectively, where N_a is again the number of samples in the interval 0 to $(T-\tau)$.

Two points in the above theory warrant a more detailed consideration; the first is the assumption that the sum of the N_a product terms will tend to normal, and the second is the assumption in the evaluation of the fourth order moment in eqn. (2.1.16).

2.1.3 Application of the Central Limit Theorem

The basic theorem states[25] that the area under the curve of the density function of the normalised sum of a large number of independent, identically distributed random variables over a fixed interval (i.e. independent of the number of variables) approaches the value of the normal integral evaluated over the same interval, the agreement becoming closer as the number of variables increases without limit; i.e. if $\{y_i\}$ is a set of independent, random variables having zero mean, variance σ_y^2, and

---

[+] see Appendix C(2), (p. 107)

with identical density functions $p_y = p_{y_i}$, then, if

$$z = \frac{1}{\sqrt{n}} \sum_{i=1}^{n} y_i$$

the variance of z equals that of y_i (i.e. σ_y^2), the mean of z is zero, and

$$\lim_{n \to \infty} P\{t_1 \leq z \leq t_2\} = \frac{1}{\sigma_y \sqrt{2\pi}} \int_{x_1}^{x_2} e^{-y^2/2\sigma_y^2} dy$$

the general conditions for its application being that (a) the variances of the components exist, are finite, and that their sum tends to infinity with n, and (b) the contribution of each component to the sum is small and no one term predominates.

It has also been shown[26] that if $\{x_i\}$ is a set of independent, random variables having mean μ and variance σ^2, then, if

$$\xi = \frac{1}{n} \sum_{i=1}^{n} x_i$$

so that $\bar{\xi} = \mu$ and $\text{var}(\xi) = \sigma^2/n$,

$$\lim_{n \to \infty} P(t_1 \leq z \leq t_2) = \frac{\sqrt{n}}{\sigma\sqrt{2\pi}} \int_{t_1}^{t_2} e^{-(x-\mu)^2/2(\sigma/n)^2} dx$$

$$= \frac{1}{\sqrt{2\pi}} \int_{(t_1-\mu)\sqrt{n}/\sigma}^{(t_2-\mu)\sqrt{n}/\sigma} e^{-y^2/2} dy$$

but here the limits are functions of n, so the rate of convergence may not be so rapid.[25]

Central Limit Theorems have been proved for sequences of non-independent random variables, and these are reviewed in Feller[27]. In particular, he showed that if in a fixed number of trials n, a recurrent event ε occurs N_n times, then, if N_n can be regarded as a random variable (definitely not independent in this case), as n tends to infinity, N_n tends to a normal distribution, provided that the mean recurrence rate of ε and its variance are non-infinite.

Considering N_n an equivalent to n, and ε the event $\{x_1(t_i)x_2(t_i+\tau)\} = 1$, N_n, the number of times that ε occurs, will then tend to normal as n

increases. Thus the product sum, which equals $2N_n - N_a$, also tends to normal. The mean value and variance of N_n in this case are clearly not infinite. Noting that the general conditions (a) and (b) are both satisfied by the product terms, ((b) being in fact ideally satisfied since each product term contributes equally), there is sufficient evidence to support the use of the Central Limit Theorem in this case.

As far as the expected accuracy of the Central Limit Theorem is concerned, if one obtains 2:1 agreement with measured values at probability density levels of 10^{-5} using one hundred random variables, then practically speaking this constitutes a 'good fit'. Obtaining a density of 10^{-15} compared to an actual density of 10^{-20}, say, would not be unreasonable when one considers that although the normal distribution is the limiting form of many distributions, for example Poisson, Chi-square, etc., its rate of roll-off on the tails is proportional to $e^{-x^2/2}$, which is of a completely different order to that of the original distributions. As a result, large discrepencies can exist at low density levels, and little significance can be attached to Central Limit Theorem results at these levels.

Another relevant question is how large a 'large' number of variables is. This is entirely dependent upon the statistic being measured, some converging more rapidly than others. The sampling variance of any moment is dependent upon the population moment of twice its order, thus where fifty or one hundred could be 'large' for a mean or variance estimate, five hundred might not be large enough for a fourth moment estimate. Kendall[28] states that as far as can be generalised with safety, over five hundred can usually be assumed large, over one hundred often so, less than one hundred is sometimes suspect and less than thirty is rarely large. In the present case, the correlation function is second order, and for $|\tau|>0$ has almost zero mean. As a result, the distribution will be almost perfectly symmetrical about the mean and should therefore

converge rapidly to normal. Hence in this case one hundred samples should adequately constitute a large number for convergence to normality.

To sum up, where one has sums of random variables having finite means and variances, the Central Limit Theorem may often apply. However, it does not necessarily apply, and even if it does, it is only an approximation (except where the component variables are themselves normal), and may or may not yield accurate results, especially on the tails of the distribution, depending upon the order of the variable, the symmetry of the distribution and the number of components. Often it is only the experimental results which finally confirm or disprove the validity of its application in a particular case.

2.1.4 Evaluation of the Fourth Order Moment

The second point to be considered is the evaluation of $E\{x_1(t_i)x_2(t_i+\tau)x_1(t_j)x_2(t_j+\tau)\}$. It is not possible, in general, to express higher order moments in terms of first and second order moments only, and hence reasonable simplifying assumptions have to be made.

To assume that $x_1(t_i)$, $x_2(t_i+\tau)$, $x_1(t_j)$ and $x_2(t_j+\tau)$ are all independent would clearly be wrong. To assume that the number of zero crossings in any interval is independent of the number in any other non-overlapping interval does to some extent permit a 'semi-dependence' between samples which are in close proximity, and independence between those spaced further apart; i.e. it implies a Markov process of limited but non-zero order. This ties up with the 'quasi-independence' of random function zero crossings suggested by McFadden[29]. Hence, since the exact distribution of the zero crossings of bandlimited Gaussian noise is not known, the above assumption seems reasonable. Once again, the final decision as to whether the assumption is reasonable or not lies in the degree of agreement between the experimental results and the theoretical predictions.

2.2 Detection of an Analog Gaussian Reflection Corrupted by Wideband Gaussian Noise

A theoretical analysis analogous to that in the last section is given here for the detection of an analog bandlimited Gaussian reflection corrupted by wideband Gaussian noise.

2.2.1 Derivation of the Cross-correlation Function

In this case the two waveforms to be considered are

$$x_1(t) = \mathrm{sgn}[f_n(t)] = \mathrm{sgn}[I_1(t)] \quad \ldots\ldots\ldots\ldots\ldots 2.2.1$$

$$x_2(t+\tau) = \mathrm{sgn}[\beta f_n(t+\tau) + n(t)] = \mathrm{sgn}[I_2(t+\tau)] \quad \ldots\ldots\ldots 2.2.2$$

where $f_n(t)$ is a bandlimited Gaussian waveform with zero mean and variance s^2. $n(t)$ is wideband Gaussian noise of zero mean and variance σ^2, and β is the attenuation factor.

As in Section 2.1.1, the cross-correlation function of $x_1(t)$ and $x_2(t+\tau)$ can be written as

$$\psi_{x_1x_2}(\tau) = 4P_{++} - 1 \quad \ldots\ldots\ldots\ldots\ldots\ldots 2.2.3$$

where

$$P_{++} = P\{x_1(t)=+1,\ x_2(t+\tau)=+1\}$$
$$= P\{I_1(t) \geq 0,\ I_2(t+\tau) \geq 0\} \quad \ldots\ldots\ldots 2.2.4$$

$f_n(t)$ and $f_n(t+\tau)$, being values of the same Gaussian waveform, will follow a bivariate normal density function[30][31] with mean $\{0,0\}$ and variances $\{s^2,s^2\}$. For the purposes of computation, $I_2(t+\tau)$ may be regarded as a Gaussian waveform having the amplitude distribution of $\beta f_n(t+\tau)$ but with an instantaneous mean value of $n(t)$. Hence, since $I_2(t+\tau)$ is a linear function of $f_n(t+\tau)$, $I_1(t)$ $(= f_n(t))$ and $I_2(t+\tau)$ will also follow a bivariate normal distribution[32] with mean $\{0,n(t)\}$ and variances $\{s^2,(\beta s)^2\}$. An instantaneous value of $P\{I_1(t)\geq 0,\ I_2(t+\tau)\geq 0\}$ can now be

evaluated, but before substitution into eqn. (2.2.3), this must be averaged over all n(t). Letting $n(t)=\eta$,

$$P_{++}(\text{inst.}) = \frac{1}{2\pi\beta s^2(1-\rho^2)^{1/2}} \int_0^{\infty} du \int_0^{\infty} \exp\left\{\frac{-1}{2(1-\rho^2)}\left[\frac{u^2}{s^2} - \frac{2\rho u(v-\eta)}{\beta s^2} + \frac{(v-\eta)^2}{(\beta s)^2}\right]\right\} dv \quad . \quad 2.2.5$$

where ρ is the normalised cross-covariance of $f_n(t)$ and $\beta f_n(t+\tau)$ which is the same as that of $f_n(t)$ and $f_n(t+\tau)$, and is thus the normalised auto-correlation function of $f_n(t)$ and $f_n(t+\tau)$, i.e. $\rho_f(\tau)$. This integral may be expanded into a Maclaurin series in terms of ρ, and averaged term by term, giving[+]

$$P_{++} = \frac{1}{4} + \frac{1}{2\pi} \text{Arcsin}\left\{\sqrt{\frac{(\beta s/\sigma)^2}{1+(\beta s/\sigma)^2}} \cdot \rho_f(\tau)\right\} \quad . \quad . \quad . \quad . \quad . \quad . \quad 2.2.6$$

Substituting into eqn. (2.2.3)

$$\Psi_{x_1 x_2}(\tau) = \frac{2}{\pi} \text{Arcsin}\left\{\sqrt{\frac{(\beta s/\sigma)^2}{1+(\beta s/\sigma)^2}} \cdot \rho_f(\tau)\right\} \quad . \quad . \quad . \quad . \quad . \quad . \quad . \quad 2.2.7$$

The auto-correlation function of $x_2(t)$ may be derived similarly,[‡] and is

$$\Psi_{x_2}(\tau) = \frac{2}{\pi} \text{Arcsin}\left\{\frac{(\beta s/\sigma)^2}{1+(\beta s/\sigma)^2} \cdot \rho_f(\tau)\right\} \quad . \quad . \quad . \quad . \quad . \quad . \quad . \quad 2.2.8$$

which is the same result as eqn. (12) of Ekre[11].

2.2.2 Extension to Digital Sampling Cross-correlation

For a digital, single-bit sampling cross-correlator as in Section 2.1.2, the cross-correlation is performed as

$$\Psi_2(\tau) = \sum_{i=1}^{N} x_1(t_i).x_2(t_i+\tau) \quad . \quad . \quad . \quad . \quad . \quad . \quad . \quad . \quad 2.2.9$$

For the special case of $\tau = 0$, $\Psi_2(0)$ will again be equal to N when there is no corrupting noise n(t) in $x_2(t)$. At any instant t_i, if $f_n(t_i) = -\alpha$, the probability of n(t) causing an error by changing the

---

[+] see Appendix D, (p. 110) [‡] see Appendix D(2), (p. 111)

sign of $x_2(t_i)$, is

$$p_e(\alpha) = \frac{1}{\sigma\sqrt{2\pi}} \int_{-\infty}^{0} e^{-y^2/2\sigma^2} dy \quad \ldots\ldots\ldots\ldots 2.2.10$$

Expanding in a Maclaurin series

$$p_e(\alpha) = \frac{1}{\sigma\sqrt{2\pi}} \left[-\sqrt{\frac{\pi}{2}} - \alpha + \frac{\alpha^3}{3!\sigma^2} - \frac{\alpha^5}{5!\sigma^4} + \frac{15\alpha^7}{11\sigma^6} - \cdots\cdots \right]$$

Averaging over all negative α and noting that the identical situation exists, by symmetry, for α positive, the error probability p is given by[4]

$$p = \tfrac{1}{2} - \tfrac{1}{\pi} \text{Arctan } (\beta s/\sigma) \quad \ldots\ldots\ldots\ldots 2.2.11$$

$\psi_b(0)$ will again be reduced by two for every instant at which n(t) causes an error. As n(t) is wideband Gaussian noise, the probability of an error at any instant is independent of any other instant. Hence the number of errors will follow a binomial distribution with mean Np and variance Np(1- p). The mean value of $\psi_b(0)$ will be

$$\overline{\psi_b(0)} = N - 2Np$$

$$= N.\tfrac{2}{\pi} \text{Arctan } (\beta s/\sigma) \quad \ldots\ldots\ldots\ldots 2.2.12$$

which agrees with eqn. (2.2.7), and its distribution can be derived directly from that of the number of errors as described in Section 2.1.2. Some sample distributions of $\psi_b(0)$ for N= 100 are plotted in Fig. 2-3.

As in Section 2.1.2, both burst and continuous waveform cross-correlation will be considered for $|\tau|>0$. For burst waveforms (see Fig. 2-4) the two distributions resulting from cross-correlation over intervals 0 to $(T-\tau)$ and $(T-\tau)$ to T must be derived. The variance of the sum of the N_a product terms in interval 0 to $(T-\tau)$ (region A in Fig. 2-4) can be written as in eqn. (2.1.16)

$$\text{VAR}_{N_a} = N_a - \mu_{N_a} + 2 \sum_{i=1}^{N_a-1} \sum_{j=i+1}^{N_a} E\{x_1(t_i)x_2(t_i+\tau)x_1(t_j)x_2(t_j+\tau)\} \quad (2.1.16)$$

---

[4] see Appendix E, (p. 113)

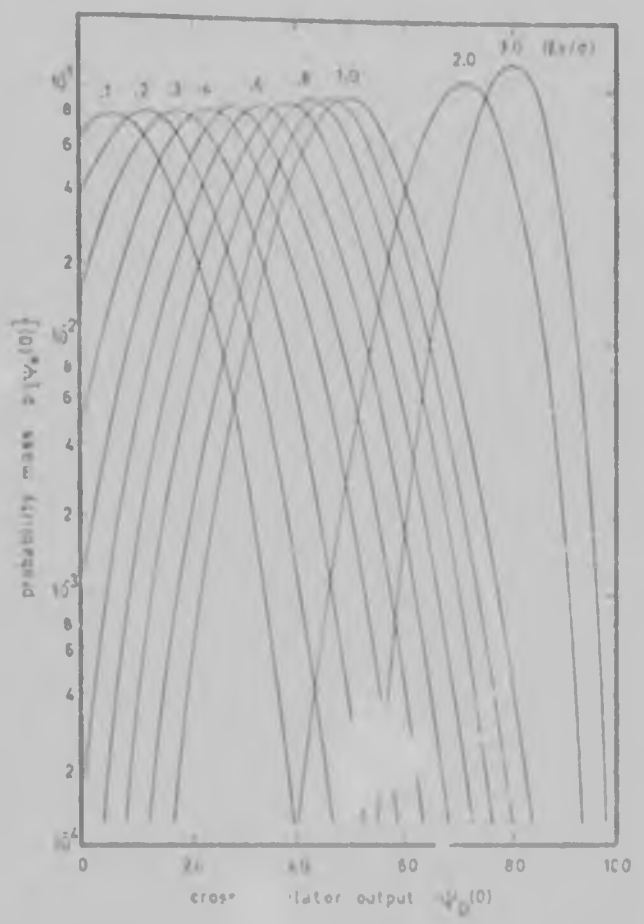

FIGURE 2-3 Probability mass functions of $\psi_0(0)$ for N=100 samples.

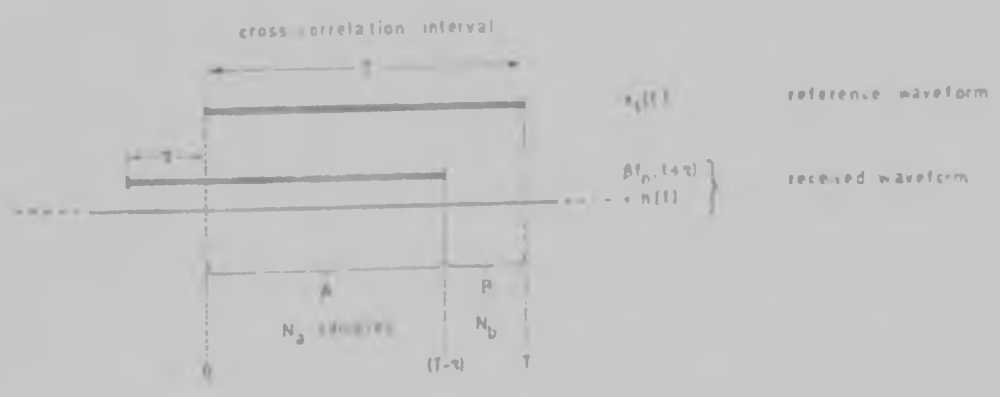

FIGURE 2-4 Cross-correlation of burst waveforms for $|\tau|>0$.

where μ_{N_a} is the mean of the sum, i.e. $N_a.\psi_{x_1x_2}(\tau)$, $\psi_{x_1x_2}(\tau)$ being as defined in eqn. (2.2.7). As in eqn. (2.1.17),

$$E\{x_1(t_i)x_2(t_i+\tau)x_1(t_j)x_2(t_j+\tau)\} = P_{++++} - P_{+++-} - \ldots + P_{++--} - \ldots + P_{----}.$$

where

$$P_{++++} = P\{x_1(t_i)=+1,\ x_2(t_i+\tau)=+1,\ x_1(t_j)=+1,\ x_2(t_j+\tau)=+1\}$$
$$= P\{I_1(t_i) \geqslant 0,\ I_2(t_i+\tau) \geqslant 0,\ I_1(t_j) \geqslant 0,\ I_2(t_j+\tau) > 0\} \quad . \quad 2.2.13$$

Unfortunately, the covariance matrix of the quadrivariate normal distribution of $I_1(t_i)$, $I_2(t_i+\tau)$, $I_1(t_j)$ and $I_2(t_j+\tau)$ is not of a reducible form[+] and thus the integral over zero to infinity cannot be evaluated directly. Hence a simplifying assumption must again be made, and therefore, as in the last section, the number of zero crossings of $x_1(t)$ or $x_2(t+\tau)$ in any interval will be assumed to be independent of the number in any other non-overlapping interval. Thus $E\{x_1(t_i)x_2(t_i+\tau)x_1(t_j)x_2(t_j+\tau)\}$ can now be evaluated as before[++] and eqn (2.1.16) becomes

$$\mathrm{var}_{N_b} = N_a - \mu_{N_b}^2 + 2\sum_{i=1}^{N-N_b-1}(N_a-i)\psi_{x_1}(i\delta t).\psi_{x_2}(i\delta t) + (2N_a-N+1)(2N_a-N)\,\psi_{x_1x_2}(\tau)$$

. . . . . 2.2.14

where ψ_{x_1}, $\psi_{x_1x_2}$ and ψ_{x_2} are as defined in eqns. (2.1.7), (2.2.7) and (2.2.8), respectively.

Over interval (T-τ) to T (region B in Fig. 2-4), the distribution of the sum of the N_b products can be derived exactly as in the previous section (p. 20), and will again have zero mean and variance N_b.

[+]Reduction formulae exist for this type of multivariate normal integral for special cases where the covariance matrix $\{\rho_{ij}\}$ has elements of certain special forms. S. Gupta[33] gives a description of all these forms and the reduction formulae. Kendall[34] gives a general expression for the integral of the multivariate normal distribution over zero to infinity involving an infinite series of second order moment product terms. Cheng[12] has evaluated it exactly, in a closed form, for the special case of the covariance matrix being symmetrical and involving two variables only.

[++]see p. 19 and Appendix C(2), (p. 107)

where μ_{N_a} is the mean of the sum, i.e. $N_a.\psi_{x_1}(\tau)$, $\psi_{x_1x_2}(\tau)$ being as defined in eqn. (2.2.7). As in eqn. (2.1.17),

$$E\{x_1(t_i)x_2(t_i+\tau)x_1(t_j)x_2(t_j+\tau)\} = P_{++++} - P_{+++-} - \ldots + P_{++--} - \ldots + P_{----}$$

where

$$P_{++++} = P\{x_1(t_i)=+1,\ x_2(t_i+\tau)=+1,\ x_1(t_j)=+1,\ x_2(t_j+\tau)=+1\}$$
$$= P\{I_1(t_i) \geq 0,\ I_2(t_i+\tau) \geq 0,\ I_1(t_j) \geq 0,\ I_2(t_j+\tau) \geq 0\} \quad . \ ? \ 2.13$$

Unfortunately, the covariance matrix of the quadrivariate normal distribution of $I_1(t_i)$, $I_2(t_i+\tau)$, $I_1(t_j)$ and $I_2(t_j+\tau)$ is not of a reducible form[+] and thus the integral over zero to infinity cannot be evaluated directly. Hence a simplifying assumption must again be made, and therefore, as in the last section, the number of zero crossings of $x_1(t)$ or $x_2(t+\tau)$ in any interval will be assumed to be independent of the number in any other non-overlapping interval. Thus $E\{x_1(t_i)x_2(t_i+\tau)x_1(t_j)x_2(t_j+\tau)\}$ can now be evaluated as before[+] and eqn (2.1.16) becomes

$$\text{var}_{N_a} = N_a - \mu_{N_a} + 2\sum_{i=1}^{N-N_a-1}(N_a-i)\psi_{x_1}(i\delta t).\psi_{x_2}(i\delta t) + (2N_a-N+1)(2N_a-N)\,\psi_{x_1x_2}(\tau)$$

. . . . . 2.2.14

where ψ_{x_1}, $\psi_{x_1x_2}$ and ψ_{x_2} are as defined in eqns. (2.1.7), (2.2.7) and (2.2.8), respectively.

Over interval (T-τ) to T (region B in Fig. 2-4), the distribution of the sum of the N_b products can be derived exactly as in the previous section (p. 20), and will again have zero mean and variance N_b.

[+]Reduction formulae exist for this type of multivariate normal integral for special cases where the covariance matrix $\{\rho_{ij}\}$ has elements of certain special forms. S. Gupta[33] gives a description of all these forms and the reduction formulae. Kendall[34] gives a general expression for the integral of the multivariate normal distribution over zero to infinity involving an infinite series of second order moment product terms. Cheng[12] has evaluated it exactly, in a closed form, for the special case of the covariance matrix being symmetrical and involving two variables only.

[+]see p. 19 and Appendix C(2), (p. 107)

Combining these two independent distributions yields that of $\psi_b(\tau)$.

For continuous transmitted waveforms, the situation is directly analogous to that analysed in Section 2.1.2 for single-bit reflections. Hence the sum of the N products will tend to a normal distribution with mean and variance as in eqns. (2.1.23) and (2.1.24), i.e.

$$\overline{\psi_b(\tau)} = \mu_b = N.\psi_{s_1 s_2}(\tau) \quad \ldots\ldots\ldots\ldots\ldots 2.2.15$$

$$\text{var}[\psi_b(\tau)] = N\ \mu_n^2 + 2\sum_{i=1}^{N-N_a-1}(N-i)\psi_n(i\delta t).\psi_{s_2}(i\delta t) + N_a(N_a+1)[\psi_{s_1 s_2}(\tau)]^2 . \quad 2.2.16$$

ψ_{s_2}, $\psi_{s_1 s_2}$ and ψ_n being as defined in eqns. (2.1.7), (2.2.7) and (2.2.8), respectively.

2.2.3 Comparison of Analog and Single-bit Reflection Detection

It is of interest to compare the detection characteristics of the two waveforms just analysed. The zero delay cross-correlation functions have been shown to be

$$\psi_b(0) \text{ (analog)} = N.\frac{2}{\pi}\text{Arctan}(\beta s/\sigma) \qquad (2.2.12)$$

$$\psi_b(0) \text{ (single-bit)} = N.\text{erf}(\beta/\sigma\sqrt{2}) \qquad (2.1.13)$$

and the normalised values, $[\psi_b(0)/N]$, are plotted against signal-to-noise ratio in Fig. 2-5. $(\beta s/\sigma)$ and (β/σ) are taken as equivalent signal-to-noise ratios for comparison purposes.

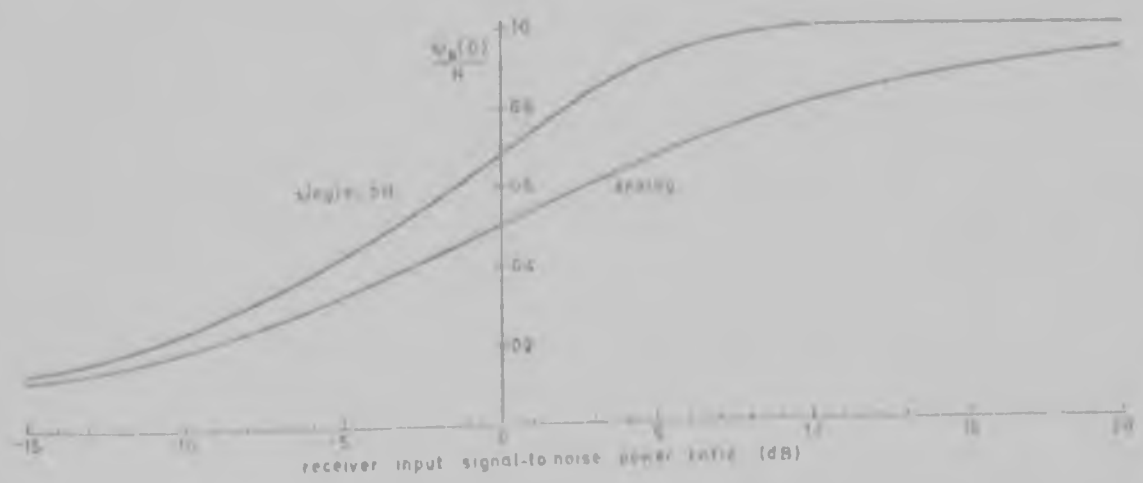

FIGURE 2-5 Comparison of zero delay cross-correlation function values.

The zero delay cross-correlation peak in the case of the single-bit Gaussian reflection can be seen to be considerably higher than that of an equivalent rms valued analog Gaussian reflection; for example, at 0 dB signal-to-noise ratio, the peak would be 68 as compared to 50, with 100 samples. The detection probabilities for the two waveforms are plotted in Figs. 4-5 (p. 74) and 4-13 (p. 80), and a comparison shows that the detection probabilities achievable with single-bit Gaussian waveforms are higher than those achievable with analog Gaussian waveforms. This might intuitively be expected since with a severely clipped Gaussian signal of rms value V, say, the waveform is always at ±V, whereas with an analog Gaussian waveform of rms value V, 68 per cent of the waveform has magnitude less than V. Therefore this waveform is likely to be more susceptible to corruption by extraneous noise than the severely clipped one.

The expressions for the mean values of the distributions of $\Psi_s(\tau)$ for $|\tau| > 0$, when continuous waveforms are transmitted, are

$$\overline{\Psi_s(\tau)}\ \text{(analog)} = N.\frac{2}{\pi}\,\text{Arcsin}\left\{\sqrt{\frac{(\beta s/\sigma)^2}{1+(\beta s/\sigma)^2}}\ \rho_s(\tau)\right\} \qquad (2.2.15)$$

$$\overline{\Psi_s(\tau)}\ \text{(single-bit)} = N.\text{erf}(\beta/\sigma\sqrt{2}).\frac{2}{\pi}\,\text{Arcsin}[\rho_s(\tau)] \qquad (2.1.23)$$

$[\Psi_s(\tau)/N]$ is plotted versus signal-to-noise ratio in Fig. 2-6 for a value of $\rho_s(\tau)$ of 0.1. As can be seen, the mean values in this case are

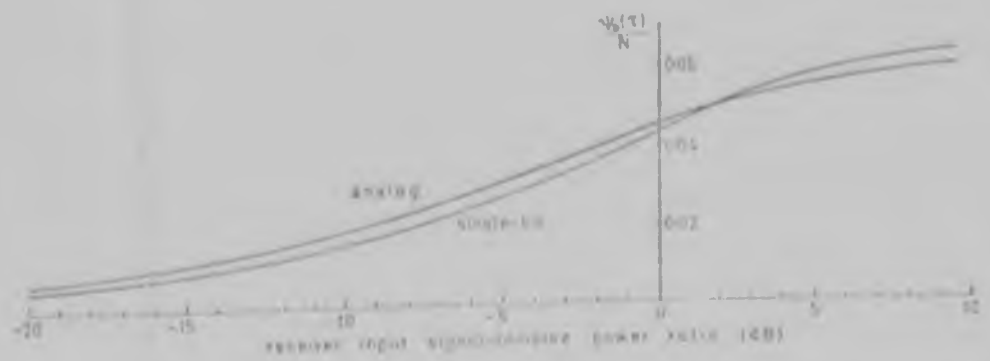

FIGURE 2-6 Comparison of the cross-correlation function values of single-bit and analog Gaussian waveforms for $|\tau|>0$ and $\rho_s(\tau)=0.1$.

much closer together than those of $\psi_s(0)$.

The variances of the respective distributions can be compared by noting that for both waveforms the variance is of the form

$$\text{var}[\psi_s(\tau)] = N - \mu^2 + 2\sum_{i=1}^{N-1}\sum_{j=i+1}^{N}[\text{positive terms much less than one}]. \quad . \quad 2.2.17$$

The dominating term in this expression is N, and hence the variances of $\psi_s(\tau)$ can be expected to be almost equal for both waveforms. Thus, seeing that the means are also close, the distributions of $\psi_s(\tau)$, and therefore the false alarm rates, will be very similar.

For burst waveforms, the variances of the sum of the N_b product terms are in both cases equal to N_b, and it can be reasoned as above that the variances of the sum of the N_a product terms will also be similar. Therefore, in this case too, the distributions of $\psi_s(\tau)$, and hence the false alarm rates will be much the same for both waveforms. The theoretical and experimental results bear this out, and are plotted in Figs. 4-6 and 4-14 on pages 74 and 80, respectively.

To sum up then, the detection probabilities obtained with single-bit bandlimited Gaussian signals are higher than those obtained with equivalent rms valued analog bandlimited Gaussian signals, for the same receiver input signal-to-noise ratio, but the false alarm rates of the two waveforms are almost the same. Thus the single-bit waveform has the better detection characteristics of the two; however, the price of this advantage is the considerably larger transmission bandwidth required by the single-bit waveform as compared to the analog version.

2.3 Detection of a Single-bit Gaussian Reflection Corrupted by a Random Phase Sine Wave

Situations can arise in signal detection where the extraneous noise corrupting the received waveform is of a deterministic nature rather than

purely random. It is of interest to investigate how the cross-correlator would perform under such conditions, and so in this section the situation is considered where a single-bit bandlimited Gaussian signal is transmitted, as in Section 2.1, but in this case the reflection is corrupted by a random phase sine wave. The analysis will follow a form parallel to that of the last two sections.

2.3.1 Derivation of the Cross-correlation Function

The waveforms to be cross-correlated are

$$x_1(t) = \operatorname{sgn}[f_n(t)] \quad \ldots\ldots\ldots\ldots\ldots\ldots \quad 2.3.1$$

$$x_2(t+\tau) = \operatorname{sgn}[\beta x_1(t+\tau) + A \sin(\omega t+\phi)] \quad \ldots\ldots\ldots \quad 2.3.2$$

where as before $f_n(t)$ is a zero mean Gaussian waveform bandlimited to $(\omega_b/2\pi)$ Hz, β is an attenuation factor, and ϕ is a random phase angle which is evenly distributed between zero and 2π radians.

$$\begin{aligned} P_{++} &= P\{x_1(t)=+1,\ x_2(t+\tau)=+1\} \\ &= P\{x_1(t)=+1\}.P\{x_2(t+\tau)=+1/\ x_1(t)=+1\} \\ &= \tfrac{1}{2}\big[P\{\beta x_1(t+\tau)=\beta/\ x_1(t)=+1,\ A\sin(\omega t+\phi) \geq -\beta\} + \\ &\quad P\{\beta x_1(t+\tau)=-\beta/\ x_1(t)=+1,\ A\sin(\omega t+\phi) \geq +\beta\}\big] \\ &= \tfrac{1}{2}\big[P\{x_1(t+\tau)=+1/\ x_1(t)=+1\}.P\{A\sin(\omega t+\phi) \geq -\beta\} + \\ &\quad P\{x_1(t+\tau)=-1/\ x_1(t)=+1\}.P\{A\sin(\omega t+\phi) \geq +\beta\}\big] \quad \ldots\ldots \quad 2.3.3 \end{aligned}$$

The density function of a random phase sine wave $A.\sin(\theta)$ is[35]

$$P_{A\sin\theta}(a) = \begin{cases} \frac{1}{\pi\sqrt{A^2-a^2}} & -A < a < +A \\ 0 & \text{elsewhere} \end{cases}$$

Integrating this over the intervals $-\beta$ to infinity and $+\beta$ to infinity, and using eqns. (2.1.8),

$$\begin{aligned} P_{++} &= \tfrac{1}{2}\big[\tfrac{1}{2}[1+\psi_{x_1}(\tau)]\,[\tfrac{1}{2}+\tfrac{1}{\pi}\operatorname{Arcsin}(\beta/A)] + \tfrac{1}{2}[1-\psi_{x_1}(\tau)]\,[\tfrac{1}{2}-\tfrac{1}{\pi}\operatorname{Arcsin}(\beta/A)]\big] \\ &= \tfrac{1}{4}\big[1+\tfrac{2}{\pi}\operatorname{Arcsin}(\beta/A).\psi_{x_1}(\tau)\big] \quad \ldots\ldots\ldots\ldots\ldots\ldots \quad 2.3.4 \end{aligned}$$

and thus

$$\Psi_{s_1 s_2}(\tau) = 4P_{++} - 1$$
$$= \frac{4}{\pi} \text{Arcsin}(\beta/A).\Psi_{s_1}(\tau). \quad \ldots\ldots\ldots\ldots 2.3.5$$

2.3.2 Extension to Digital Sampling Cross-correlation

The Nyquist sampling rate for a signal bandlimited to 20 kHz is 40 kHz. At this sampling rate, one hundred samples would occupy 2.475 ms. In acoustics measurements, the periodic waveforms encountered can range in frequency from below 100 Hz to above 10 kHz so that the ninety nine sampling intervals could encompass from less than one cycle to above twenty cycles of this interfering waveform. The most convenient way of considering this effect is to divide the cross-correlation interval T into sub-intervals T' and (T-T'), where T' contains an exact number of half-cycles of the interfering waveform, and (T-T') contains the remaining fraction of a half-cycle (Fig. 2-7). The time T_{ez} spent by the sine wave in the 'error zones', i.e. greater than $+\beta$ or less than $-\beta$, can then be

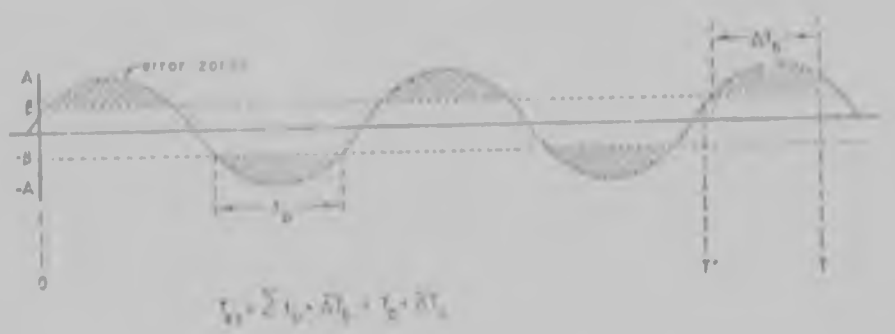

FIGURE 2-7 Splitting of $A.\sin(\omega t+\phi)$ into error and non-error zones.

considered in two corresponding parts, T_b for the interval 0 to T', and $\overline{\Delta T_b}$ for T' to T. Therefore

$$T_{ez} = T_b + \overline{\Delta T_b} \quad \ldots\ldots\ldots\ldots\ldots\ldots 2.3.6$$

It is clear that T_{ez} is dependent upon the sine wave frequency, and

hence the mean and variance of $\psi_s(\tau)$ are also functions of frequency. To find the distribution of $\psi_s(\tau)$, therefore, both the sine wave amplitude and frequency must be known. It is reasonable to assume that the phase angle ϕ will vary from correlation interval to correlation interval, as exact synchronisation with the cross-correlator clock is highly improbable. As a result, the effect of the phase angle ϕ will be averaged out. A detailed discussion of T_b and ΔT_b is given in Appendix F (p. 114).

If the cross-correlation interval T is sufficiently large that T_b is very much greater than $\overline{\Delta T_b}$, $\overline{\Delta T_b}$ can be neglected. Under these circumstances T_{ez} is equal to T_b, is independent of frequency, and is given by+

$$T_{ez} = T[1 - \tfrac{2}{\pi} \text{Arcsin}(\beta/A)] \quad \ldots\ldots\ldots\ldots \quad 2.3.7$$

Considering the special case of $\tau=0$, all product terms not in the error zones will be +1, and the average sum of those in the error zones will be zero because the waveforms are symmetrically distributed about zero. Hence, the mean value of $\psi_s(0)$ will be

$$\begin{aligned}\overline{\psi_s(0)} &= [T - T_{ez}]/\delta t \\ &= [T - T[1 - \tfrac{2}{\pi} \text{Arcsin}(\beta/A)]]/\delta t \\ &= N. \tfrac{2}{\pi} \text{Arcsin}(\beta/A) \quad \ldots\ldots\ldots\ldots \quad 2.3.8\end{aligned}$$

which agrees with eqn. (2.3.5).

To calculate the variance of $\psi_s(0)$, only those terms in the error zones need be considered because the others do not contribute. In each of these zones $x_2(t)$ is either +1 or -1. Hence the distribution of $\psi_s(0)$ may be found by considering the cross-correlation of $x_1(t)$ with a waveform $\xi(t)$ as shown in Fig. 2-8. As the sine wave, and hence $\xi(t)$, has random phase and $x_1(t)$ is random, it is reasonable to assume that the product

---

+see Appendix F, (p. 114)

FIGURE 2-8 The waveform $\xi(t)$. In regions a, b, c ..etc., $x_1(t_i).\xi(t_i) = 0$ so that non-error zone terms do not contribute to the sum.

terms $x_1(t_i).\xi(t_i)$ will be random. They each have zero mean so that their sum will be symmetrically distributed about zero, and, since each term contributes equally to the sum, it is reasonable to assume that their sum will tend to normal, having zero mean, and variance

$$\text{var}[\psi_b(0)] = E\left[\left[\sum_{i=1}^{N} x_1(t_i)\xi(t_i)\right]^2\right] - \left[E\left[\sum_{i=1}^{N} x_1(t_i)\xi(t_i)\right]\right]^2$$

This can be evaluated to give[*]

$$\text{var}[\psi_b(0)] = N\left[1 - \frac{2}{\pi}\text{Arcsin}(\beta/A)\right] + 2\sum_{i=1}^{N-1}(N-i)\psi_1(i\delta t).\psi_\xi(i\delta t) \quad \ldots \quad 2.3.9$$

where $\psi_\xi(\tau)$ is the auto-correlation function of $\xi(t)$ [†]. For the case of a very large interfering sine wave or a very small reflected signal, i.e. (β/A) tending to zero, $\xi(t)$ tends to a square wave and the mean of $\psi_b(0)$ would tend to zero. The dependence of the distribution variance upon the sine wave frequency is illustrated in Fig. 2-9.

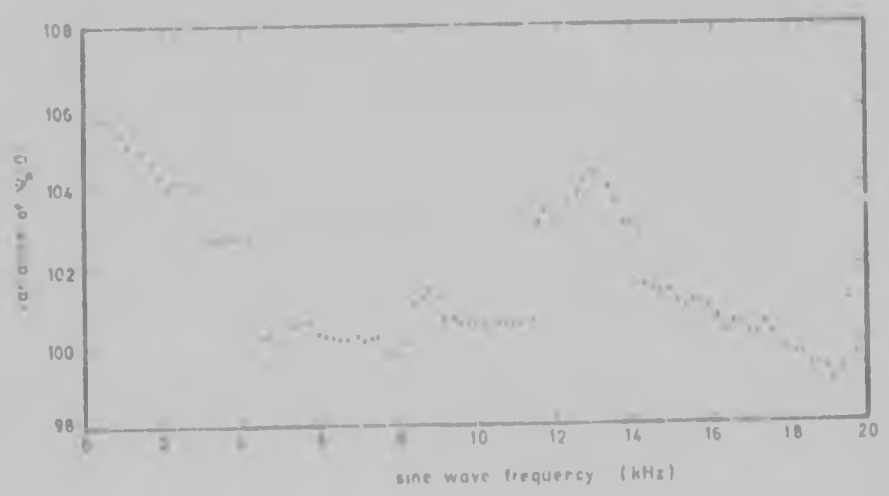

FIGURE 2-9 Variance of $\psi_b(0)$ as a function of the frequency of the interfering random phase sine wave. $(\beta/A)=0.8$ and $N=100$ samples.

---

[*] see Appendix G, (p. 117)

[†] see Appendix H, (p. 119)

The distribution of $\Psi_s(\tau)$ for $|\tau|>0$ is somewhat more complex. Consider the cross-correlation over interval 0 to $(T-\tau)$ for the case of a burst type reflection. As for the analysis with $\tau=0$, $x_2(t+\tau)$ can be split up into error zones and non-error zones (Fig. 2-7), the product terms in the error zones being accounted for by considering the cross-correlation of $x_1(t)$ with a waveform $\xi(t)$ (Fig.2-8). This yields a zero mean distribution that tends to normal for a large number of product terms, with variance as in eqn. (2.3.9), but with N replaced by N_a in this case.[+] The product terms in the non-error zones are of the form $\{\text{sgn}[f_n(t_i)]\cdot \text{sgn}[\beta f_n(t_i+\tau)]\}$ and are not always equal to +1, as was the case for $\tau=0$. The distribution of the sum of these product terms may be considered by noting that they are generated when $x_1(t)$ is cross-correlated with a waveform $y_2(t+\tau)$, where (Fig. 2-10)

$$y_2(t+\tau)= x_1(t+\tau).\gamma(t) \quad \ldots\ldots\ldots\ldots\ldots\ldots 2.3.10$$

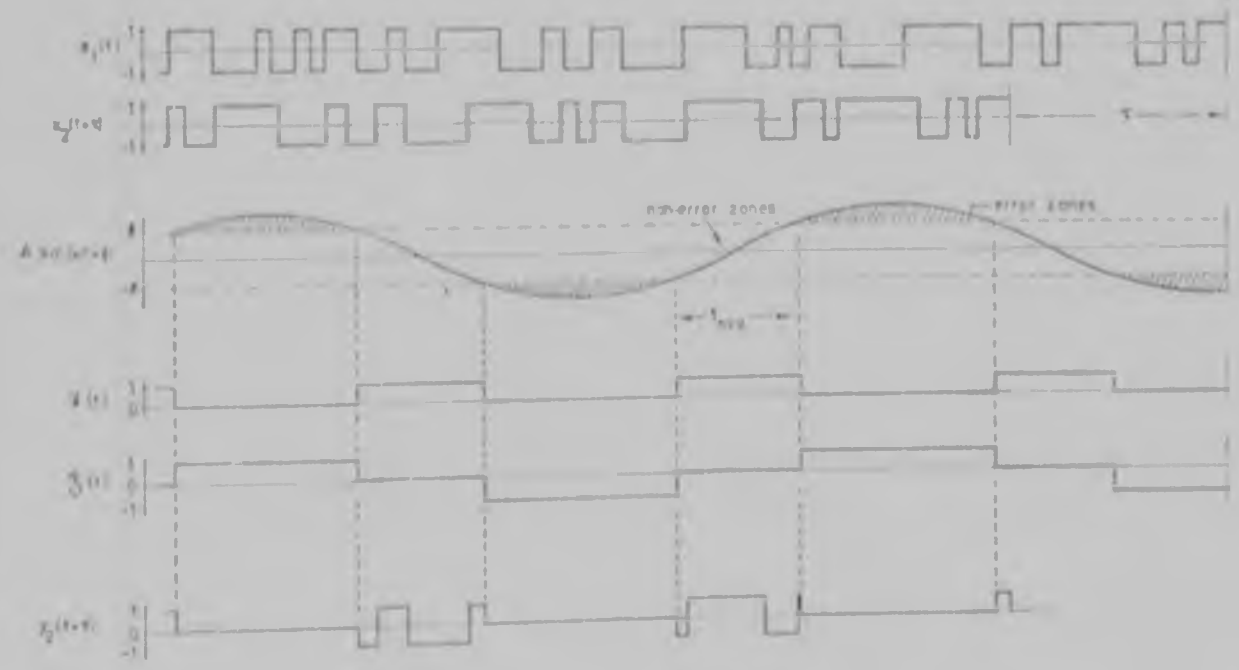

FIGURE 2-10 Cross-correlation waveforms for evaluating the variance of $\Psi_s(\tau)$.

[+]see Note 1 of Appendix G, (p. 118)

$\gamma(t)$ is derived from the corrupting sine wave $A.\sin(\omega t+\phi)$, having value +1 in the non-error zones where $|A.\sin(\omega t+\phi)| < \beta$, and zero elsewhere. The mean value of the non-error zone product terms is therefore

$$E\{x_1(t)y_2(t+\tau)\} = E\{x_1(t).x_1(t+\tau)\gamma(t)\}$$
$$= \psi_x(\tau).E\{\gamma(t)\} \quad \ldots\ldots\ldots\ldots 2.3.11$$

and from Fig. 2-10

$$E\{\gamma(t)\} = t_{nez}/(\pi/\omega)$$
$$= [(2/\omega)\text{Arcsin}(\beta/A)/(\pi/\omega)]$$
$$= \tfrac{2}{\pi}\text{Arcsin}(\beta/A). \quad \ldots\ldots\ldots\ldots 2.3.12$$

hence

$$E\{x_1(t)y_2(t+\tau)\} = \tfrac{2}{\pi}\text{Arcsin}(\beta/A).\psi_x(\tau) \quad \ldots\ldots 2.3.13$$

and the sum of the non-error zone product terms will have mean

$$\mu_{nez} = N_a.[\tfrac{2}{\pi}\text{Arcsin}(\beta/A).\psi_x(\tau)] \quad \ldots\ldots 2.3.14$$

where N_a is the number of samples in period $(T-\tau)$. Since the other two distributions contributing to that of $\psi_x(\tau)$ i.e. those of the sum of the - ve product terms and of the cross-correlation over $(T-\tau)$ to T, have zero mean, eqn. (2.3.14) gives the mean value of $\psi_x(\tau)$. This is the intuitively expected result from eqn. (2.3.5). The variance of the sum of the non-error zone product terms is shown in Appendix I (p. 120) to be

$$\text{var}_{nez} = N_a[\tfrac{2}{\pi}\text{Arcsin}(\beta/A)] + 2\sum_{i=1}^{N_a-1}\sum_{j=i+1}^{N_a}\psi_1(t_j-t_i).E[x_1(t_i)x_2(t_i+\tau)x_1(t_j)x_2(t_j+\tau)]$$
$$-\mu^2_{nez} \quad \ldots\ldots 2.3.15$$

where $\psi_1(\tau)$ is the auto-correlation function of $\gamma(t)$[+]. To evaluate eqn. (2.3.15) the fourth product moment of $x_1(t)$ must be calculated. As explained previously, this cannot be done directly and some simplifying

---

[+] see Appendix J, (p. 122)

assumption must again be made. An assumption similar to that in Section 2.1.2 is thus made; the number of zero crossings of $x_1(t)$ in any interval will be assumed independent of the number in any other non-overlapping interval. In this case it is applied to a bandlimited Gaussian function $f_n(t)$ whereas in Section 2.1.2 it was applied to functions consisting of a bandlimited plus a wideband Gaussian function; hence it can be expected that it will not apply as realistically to the present case[+]. With this assumption, eqn. (2.3.15) may be evaluated as[‡]

$$\text{var}_{nez} = N_a\left[\frac{2}{\pi}\text{Arcsin}(\beta/A)\right] - \omega_{nez}^2 + 2\sum_{i=1}^{N-N_a-1}(N_a-i)\,\psi_1(i\delta t)\left[\psi_1(i\delta t)\right]^2 +$$

$$2\{\psi_1(\tau)\}^2\sum_{i=0}^{N-N_a-1}(2N_a-N-j)\,\psi_1[(N-N_a+j)\delta t] \quad \ldots\ldots\ldots \quad 2.3.16$$

The distribution resulting from the cross-correlation of $x_1(t)$ with $x_2(t+\tau) = \text{sgn}[A.\sin(\omega t+\phi)]$ over interval $(T-\tau)$ to T is identical to the situation analysed above for $\psi_b(0)$ with $(\beta/A)=0$, when $\xi(t)$ became a square wave. The sum of these N_b product terms will tend to normal with zero mean, and variance[++]

$$\text{var}_{N_b} = N_b + 2\sum_{i=1}^{N_b-1}(N_b-i)\,\psi_\xi(i\delta t).\psi_\xi(i\delta t) \quad \ldots\ldots\ldots \quad 2.3.17$$

where $\psi_\xi(\tau)$ is the auto-correlation function of $\xi(t)$[*], which in this case is in its limiting form of a square wave.

For τ small, in which case N_b is small also, errors will obviously occur in assuming that the sum of the N_b products terms is normally distributed. Similarly, when (β/A) is very near zero or one, the number

---

[+]The theoretically predicted distribution of $\psi_b(\tau)$ in Section 2.1.2 for $(\beta/\sigma)=\infty$ (i.e. $n(t)=0$) will be seen in Chapter four to agree extremely accurately with the experimental one, and since the predicted variance in that case relies on the above assumption applied to $f_n(t)$ alone, the assumption would seem to be valid for $f_n(t)$ as well as for $f_n(t)+n(t)$.

[‡]see Appendix I. (p. 120)

[++]see Appendix K, (p. 123)

[*]see Appendix H, (p. 119)

of samples in the non-error or error zones, respectively, will be small, and errors will result from assuming that these product term sums tend to normal. However, when the number of product terms is small, its contribution to the overall distribution of $\Psi_s(\tau)$ is small, and thus the error induced in the overall distribution will be correspondingly small. The approach to normality of the three distributions is aided considerably by the fact that they have zero or near zero means and are hence almost perfectly symmetrical.

To sum up: in the case of burst waveform reflections there are three distributions contributing to that of $\Psi_s(\tau)$. All tend to normal as the respective sample numbers increase. These distributions are:-

(a) Interval 0 to $(T-\tau)$ - error zone product term sum. Mean equal to zero, variance given by

$$\text{var}_{e.z.} = N_{e.z.}\left[1-\tfrac{2}{\pi}\text{Arcsin}(\beta/A)\right] + 2\sum_{i=1}^{N_{e.z.}-1}(N_{e.z.}-i)\Psi_x(i\delta t).\Psi_\xi(i\delta t)$$

$\Psi_\xi(\tau)$ being given in Appendix H. ($\xi(t)$ is a square wave only if $(\beta/A)=0$).

(b) Interval 0 to $(T-\tau)$ - non-error zone product term sum. Mean and variance as given in eqns. (2.3.14) and (2.3.16), respectively.

(c) Interval $(T-\tau)$ to T - mean zero and variance as in eqn. (2.3.17).

The distribution of $\Psi_s(\tau)$ consists of the sum of these three normal distributions. It will therefore also be normal, with mean as given in eqn. (2.3.14). As both waveforms $\xi(t)$ and $\gamma(t)$ have random phase and are independent of $x_1(t)$, and as $x_1(t)$ is random, the error incurred by assuming that the three product sums are independent will be small. In this case, the variance of $\Psi_s(\tau)$ is simply the sum of the three individual variances.

The distribution of $\Psi_s(\tau)$ for the case of continuous transmitted waveforms is analysed exactly as for that of the product term sum over interval 0 to $(T-\tau)$ for burst waveforms. The mean of the non-error zone product term sum is (see eqn. (2.3.14)

$$\mu_N = N.\frac{2}{\pi}\text{Arcsin}(\beta/A).\Psi_2(\tau) \quad \ldots\ldots\ldots\ldots 2.3.18$$

and the variance (see Appendix 1 (p. 120))

$$\text{var}_{nez} = N.\frac{2}{\pi}\text{Arcsin}(\beta/A) - \mu_N^2 + 2\sum_{i=1}^{N-N_a-1}(N-i)\Psi_1(i\delta t)[\Psi_{s_1}(i\delta t)]^2 + 2[\Psi_{s_1}(\tau)]^2\sum_{i=0}^{N_a-1}(N_a-i)\Psi_1[(N-N_a+i)\delta t] \quad \ldots 2.3.19$$

The mean of the sum of the error zone product terms is zero and the variance (from eqn. (2.3.9)) is

$$\text{var}_{ez} = N[1-\tfrac{2}{\pi}\text{Arcsin}(\beta/A)] + 2\sum_{i=1}^{N-1}(N-i)\,\Psi_x(i\delta t).\Psi_\xi(i\delta t). \quad \ldots\ldots 2.3.20$$

where $\Psi_x(i\delta t)$ is as given in Appendix H (p. 119). Adding these two variances gives that of $\Psi_2(\tau)$, again assuming that the two sets of product terms may be regarded as independent. The mean of $\Psi_2(\tau)$ is given by μ_N.

The above analysis is applicable to any type of corrupting periodic waveform having random phase. All that is required is that the appropriate forms of $\xi(t)$ and $\gamma(t)$ and their auto-correlation functions be derived.

2.4 Detection of an Analog Gaussian Reflection Corrupted by a Random Phase Sine Wave

The analysis of the cross-correlator performance in this case has proved less tractable than in the foregoing ones. The general cross-correlation function $\Psi_{x_1y_1}(\tau)$ is obtained in series form for large receiver input signal-to-noise ratios. For the special case of $\tau=0$, $\Psi_{x_1y_1}(0)$ can be expressed in terms of an integral that can be evaluated numerically.

2.4.1 Consideration of the Cross-correlation Function

The reference and received waveforms in this case are, respectively,

$$x_1(t) = \text{sgn}[f_n(t)] = \text{sgn}[y_1] \quad \ldots\ldots\ldots 2.4.1$$

$$x_2(t+\tau) = \mathrm{sgn}[\beta f_n(t+\tau) + A.\sin(\omega t+\phi)] = \mathrm{sgn}[y_2] \quad . \quad . \quad . \quad . \quad 2.4.2$$

As in Section 2.2.1, for the purposes of computation, y_1 and y_2 can be regarded as following a bivariate normal distribution with instantaneous mean $\{0, A.\sin(\omega t+\phi)\}$ and variances $\{s^2, (\beta s)^2\}$. The instantaneous probability that both y_1 and y_2 are positive is

$$P_{++}(\mathrm{inst}) = \frac{1}{2\pi\beta s^2(1-\rho_x^2)^{1/2}} \int_0^\infty d\alpha \int_0^\infty \exp\left\{\frac{-1}{2(1-\rho_x^2)}\left[\frac{\alpha^2}{s^2} - 2\rho_x\frac{\alpha[\epsilon - A\sin(\omega t+\phi)]}{\beta s^2} + \frac{[\epsilon - A\sin(\omega t+\phi)]^2}{(\beta s)^2}\right]\right\} d\epsilon \quad . \quad . \quad . \quad 2.4.3$$

It is shown in Appendix L (p. 124) that this can be written in the form

$$P_{++}(\mathrm{inst}) = K \int_{-u_1}^\infty d\alpha \int_{-u_2}^\infty \exp\left[-\frac{\alpha^2 - 2\rho_x K\lambda + \lambda^2}{2s^2(1-\rho_x^2)}\right] d\lambda$$

and then expanded in a Taylor series in terms of u_1 and u_2. Each term can then be averaged over one cycle of $A.\sin(\omega t+\phi)$. This is the same method as was used by McFadden[36], and, after substitution into eqn. (2.1.4), yields[+]

$$\Psi_{x_1y_1}(\tau) \triangleq \Psi_{x_1}(\tau) - \frac{2}{\pi}\left[\frac{\rho_x}{(1-\rho_x^2)^{1/2}}\cdot\frac{(A/\beta s)^2}{2!}\cdot\frac{1}{2} + \frac{\rho_x(2\rho_x^2-3)}{(1-\rho_x^2)^{3/2}}\cdot\frac{(A/\beta s)^4}{4!}\cdot\frac{1}{2}\cdot\frac{3}{4} + \frac{\rho_x(8\rho_x^4-20\rho_x^2+15)}{(1-\rho_x^2)^{5/2}}\cdot\frac{(A/\beta s)^6}{6!}\cdot\frac{1}{2}\cdot\frac{3}{4}\cdot\frac{5}{6} + \cdots\right] \quad . \quad . \quad . \quad . \quad 2.4.4$$

This result gives an approximation to $\Psi_{x_1y_1}(\tau)$ only for $(A/\beta s)$ very small and hence is of little use.

The special case of $\tau=0$ is simpler, and a result can be derived that holds for all receiver input signal-to-noise ratios. In this case

$$y_1(t) = \mathrm{sgn}[f_n(t)] \quad . \quad . \quad . \quad . \quad . \quad . \quad . \quad . \quad . \quad . \quad . \quad . \quad . \quad . \quad . \quad . \quad 2.4.5$$

$$x_1(t) = \mathrm{sgn}[\beta f_n(t) + A.\sin(\omega t+\theta)] \quad . \quad . \quad . \quad . \quad . \quad . \quad . \quad . \quad . \quad 2.4.6$$

and

$$P_{++}(\mathrm{inst}) = P\{f_n(t) \geq 0,\ \beta f_n(t) > -A.\sin(\omega t+\theta)\}$$

[+] see Appendix L, (p. ---.)

$$= P\{f_n(t) > 0,\ A.\sin(\omega t+\theta) > -\beta f_n(t)\} \quad \ldots\ldots\ldots 2.4.7$$

The probability that the random sine wave is greater than some value $-z$ ($|z|<A$) is[35]

$$\int_{-z}^{A} (\pi\sqrt{A^2 - z^2})^{-1} dz = \tfrac{1}{2} + \tfrac{1}{\pi}\,\mathrm{Arcsin}(z/A) \quad \ldots\ldots\ldots 2.4.8$$

Considering $-\beta f_n(t) = -z$, this expression can be averaged over all $\beta f_n(t) > 0$ to give P_{++}. Therefore

$$P_{++} = \frac{1}{\beta s\sqrt{2\pi}} \left[\int_{0}^{A} \{\tfrac{1}{2} + \tfrac{1}{\pi}\,\mathrm{Arcsin}(z/A)\} e^{-z^2/2(\beta s)^2} dz + \int_{A}^{\infty} e^{-z^2/2(\beta s)^2} dz \right] \quad \ldots\ldots 2.4.9$$

since the probability of $A.\sin(\omega t+\theta)$ being greater than $-z$ for $-z < -A$ is one. Rearranging eqn. (2.4.9)

$$\Psi_{x_1x_2}(0) = 4P_{++} - 1$$
$$= \mathrm{erfc}\left[\frac{A}{\beta s\sqrt{2}}\right] + \frac{4}{\pi}\frac{1}{\beta s\sqrt{2\pi}} \int_{0}^{A} \mathrm{Arcsin}(z/A) e^{-z^2/2(\beta s)^2} dz. \quad \ldots 2.4.10$$

and this integral can be evaluated numerically.

2.4.2 Extension to Digital Sampling Cross-correlation

Little can be said in this case about the output probability distribution of a sampling cross-correlator for which

$$\Psi_s(\tau) = \sum_{i=1}^{N} x_1(t_i).x_2(t_i+\tau)$$

For $\tau = 0$, the mean of the distribution will be $N.\Psi_{x_1x_2}(0)$, with $\Psi_{x_1x_2}(0)$ as defined in eqn. (2.4.10). The variance can be written as

$$\mathrm{var}\ \Psi_s(0) = N - [\overline{\Psi_s(0)}]^2 + 2\sum_{i=1}^{N-1}\sum_{j=i+1}^{N} E\{x_1(t_i)x_2(t_i+\tau)x_1(t_j)x_2(t_j+\tau)\} \quad (2.1.19)$$

but in this case there is no simple way round the evaluation of the fourth order moment. As the interfering waveform is periodic, there is no justification for assuming that the number of zero crossings of $x_2(t)$ in non-overlapping intervals are independent, and in any case the necessary

values of the cross-correlation function of $x_1(t)$ and $x_2(t+\tau)$ and the auto-correlation function of $x_2(t)$ have not been found exactly.

For $|\tau|>0$, the mean of $\psi_s(\tau)$ will be $N.\psi_{x_2}(\tau)$ for continuous waveforms and $N_a.\psi_{x_2}(\tau)$ for burst waveforms. However, these can only be evaluated for $(A/\beta s)$ small. The extreme cases, where the reflection consists of signal only or interfering sine wave only, are the same as those analysed in Section 2.3.2.

2.4.3 Comparison the Detection of Analog and Single-bit Gaussian Reflections Corrupted by a Random Sine Wave or Wideband Gaussian Noise

The detection reliabilities of the two waveforms may be compared by plotting the values of $\psi_{x_1x_2}(0)$ against signal-to-noise ratio at the receiver input (Fig. 2-11). $(\sqrt{2}\beta/A)$ and $(\sqrt{2}\beta s/A)$ are taken as equivalent signal-to-noise voltage ratios.

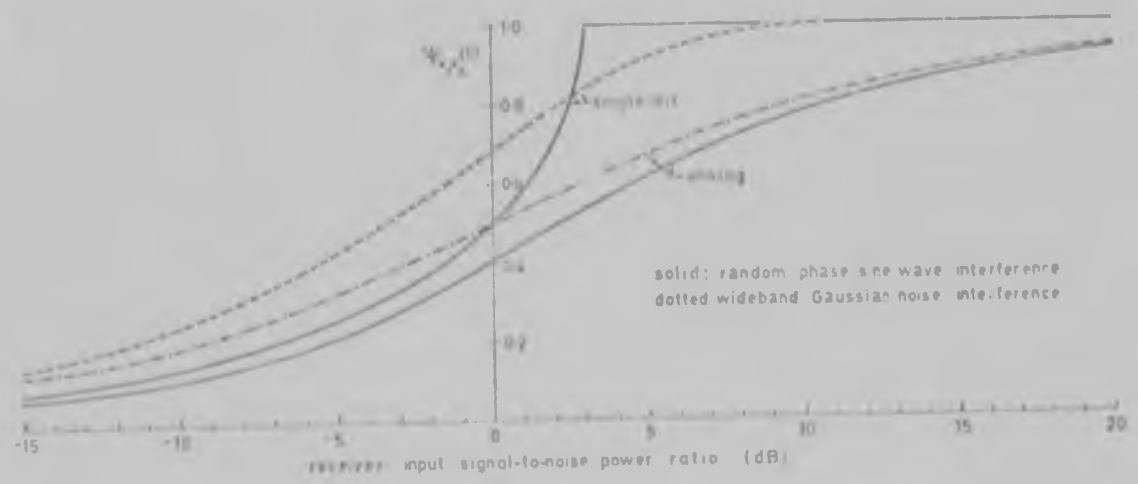

FIGURE 2-11 Zero delay cross-correlation peak values for analog and single-bit reflections corrupted by a random phase sine wave or wideband Gaussian noise.

The single-bit Gaussian waveform is seen to yield higher central cross-correlation peaks in the presence of an interfering sinusoid than the equivalent rms valued analog version. The same result applies when the corrupting waveform is wideband Gaussian noise. It can be seen that

with analog Gaussian signals, the cross-correlation peak values are lower when the corrupting waveform is a random sine wave than when it is equivalent rms valued wideband Gaussian noise. The same is true of single-bit bandlimited Gaussian signals for receiver input signal-to-noise ratios below approximately 2.5 dB. Above that value an interfering random sine wave has a less detrimental effect than wideband Gaussian noise, and above 3 dB it has no effect at all. The detection probabilities of a single-bit Gaussian signal corrupted by wideband Gaussian noise and by a random phase sine wave are plotted in Figs. 4-5 (p. 74) and 4-21 (p. 86), respectively.

Returning to the case of a single-bit or analog reflection being corrupted by a random phase sine wave, the variances of the respective distributions of $\psi_b(\tau)$ for $|\tau|>0$ will, for the same reasons as discussed in Section 2.2.3, be similar, and as the mean value of $\psi_b(\tau)$ varies only over a small range close to zero for $|\tau|>0$, the distributions and hence false alarm rates can be expected to be very similar. In the case of an analog Gaussian reflection, the distributions of $\psi_b(\tau)$ for the extreme values of receiver input signal-to-noise ratio, i.e. zero and infinity, will be identical to those derived for single-bit reflections, and those for intermediate signal-to-noise ratios will lie in between. These two extremes are shown plotted in Fig. 4-20 (p. 85). It can be seen that the range in between is fairly small, so the false alarm rates for analog bandlimited Gaussian reflections corrupted by a random sine wave can be guessed at fairly accurately.

Comparing Figs. 4-6 (p. 74) and 4-22 (p. 86) reveals that the false alarm rates for a single-bit reflection corrupted by a random sinusoid are higher than those when the corrupting waveform is wideband Gaussian noise.

In general, therefore, an interfering random phase sine wave has a more detrimental effect on the detection reliability of the single-bit cross-correlator than wideband Gaussian noise.

CHAPTER III

CROSS-CORRELATION DETECTION OF MULTIPLE REFLECTIONS

In this chapter the single-bit cross-correlation function of a single-bit or an analog bandlimited Gaussian waveform and a reflection consisting of two attenuated, delayed replicas corrupted by wideband Gaussian noise is derived. The practical significance of such an analysis was mentioned in Section 1.2 (Fig. 1-3, p. 6). An extension of the theory to more than two reflections is discussed in each case.

3.1 Detection of Two Single-bit Gaussian Reflections Corrupted by Wideband Gaussian Noise

3.1.1 Derivation of the Cross-correlation Function

The waveforms being cross-correlated are defined by

$$x_1(t) = \operatorname{sgn}[f_n(t)] \quad \ldots\ldots\ldots\ldots\ldots\ldots\ldots\ldots \quad 3.1.1$$

$$x_2(t+\tau) = \operatorname{sgn}[\beta x_1(t+\tau) + \gamma x_1(t+\tau+\Delta) + n(t)] \quad \ldots\ldots\ldots \quad 3.1.2$$

where $f_n(t)$ is zero mean bandlimited Gaussian noise with variance s^2, $n(t)$ is zero mean wideband Gaussian noise with variance σ^2, and β and γ are attenuation factors which are assumed to be real constants.

Once again, The probability P_{++} of $x_1(t)$ and $x_2(t+\tau)$ both being +1 must be derived. For $x_2(t+\tau)$ to be +1, either

$$\left.\begin{array}{ll} \text{(a)} & \beta x_1(t+\tau)=\beta,\ \gamma x_1(t+\tau+\Delta)=\gamma \text{ and } n(t) \geq -(\beta+\gamma) \\ \text{(b)} & \beta x_1(t+\tau)=\beta,\ \gamma x_1(t+\tau+\Delta)=-\gamma \text{ and } n(t) \geq -(\beta-\gamma) \end{array}\right\} \quad \ldots\ldots 3.1.3$$

$$\left.\begin{array}{l} \text{(c)}\quad \beta x_1(t+\tau)=-\beta,\ \gamma x_1(t+\tau+\Delta)=\gamma \text{ and } n(t)\geq -(\gamma-\beta) \\ \text{or (d)}\quad \beta x_1(t+\tau)=-\beta,\ \gamma x_1(t+\tau+\Delta)=-\gamma \text{ and } n(t)\geq (\gamma+\beta) \end{array}\right\} \quad \ldots\ldots 3.1.3$$

Letting $y_1 = f_n(t)/s$, $y_2 = f_n(t+\tau)/s$ and $y_3 = f_n(t+\tau+\Delta)/s$, P_{++} is therefore

$$\begin{aligned} P_{++} = {} & P\{y_1\geq 0,\ y_2\geq 0,\ y_3\geq 0\}.P\{n(t)\geq -(\beta+\gamma)\} + \\ & P\{y_1\geq 0,\ y_2\geq 0,\ y_3< 0\}.P\{n(t)\geq -(\beta-\gamma)\} + \\ & P\{y_1\geq 0,\ y_2< 0,\ y_3\geq 0\}.P\{n(t)\geq +(\beta-\gamma)\} + \\ & P\{y_1\geq 0,\ y_2< 0,\ y_3< 0\}.P\{n(t)\geq +(\beta+\gamma)\} \end{aligned} \quad \ldots\ldots 3.1.4$$

In the same way that $f_n(t)$ and $f_n(t+\tau)$ follow a bivariate normal distribution[30][31], $f_n(t)$, $f_n(t+\tau)$ and $f_n(t+\tau+\Delta)$ will be trivariate normally distributed. The joint probability $P\{y_1\geq 0,\ y_2\geq 0,\ y_3\geq 0\}$ is[34]

$$P\{y_1\geq 0,\ y_2\geq 0,\ y_3\geq 0\} = \tfrac{1}{8}+\tfrac{1}{4\pi}\{\text{Arcsin}\,\rho_{12}+\text{Arcsin}\,\rho_{13}+\text{Arcsin}\,\rho_{23}\}. \quad \ldots 3.1.5$$

The other joint probabilities in eqn. (3.1.4) may be evaluated by noting that $P\{y_1\geq 0,\ y_2\geq 0,\ y_3<0\} = P\{y_1\geq 0,\ y_2\geq 0,-y_3\geq 0\}$. The covariance matrix of y_1, y_2 and y_3 is

$$\lambda_{y_1y_2y_3} = \begin{pmatrix} 1 & \rho_{12} & \rho_{13} \\ & 1 & \rho_{23} \\ & & 1 \end{pmatrix} \quad \ldots\ldots 3.1.6$$

and thus that of y_1, y_2 and $-y_3$ is

$$\lambda_{y_1y_2-y_3} = \begin{pmatrix} 1 & \rho_{12} & -\rho_{13} \\ & 1 & -\rho_{23} \\ & & 1 \end{pmatrix} \quad \ldots\ldots 3.1.7$$

so that

$$P\{y_1\geq 0,\ y_2\geq 0,\ y_3<0\} = \tfrac{1}{8}+\tfrac{1}{4\pi}\{\text{Arcsin}\,\rho_{12}-\text{Arcsin}\,\rho_{13}-\text{Arcsin}\,\rho_{23}\}. \quad \ldots 3.1.8$$

The other terms in eqn. (3.1.5) may be derived likewise. Also

$$\left.\begin{array}{l} P\{n(t)\geq -(\beta+\gamma)\} = \tfrac{1}{2}\left[1+\text{erf}\left(\frac{\beta+\gamma}{\sigma\sqrt{2}}\right)\right] \\ P\{n(t)\geq -(\beta-\gamma)\} = \tfrac{1}{2}\left[1+\text{erf}\left(\frac{\beta-\gamma}{\sigma\sqrt{2}}\right)\right] \end{array}\right\} \quad \ldots\ldots 3.1.9$$

$$P\{n(t) \geq -(\gamma-\beta)\} = \tfrac{1}{2}\left[1 - \operatorname{erf}\left(\tfrac{\beta-\gamma}{\sigma\sqrt{2}}\right)\right] \quad \ldots\ldots\ldots\ldots 3.1.9$$

$$P\{n(t) \geq +(\beta+\gamma)\} = \tfrac{1}{2}\left[1 - \operatorname{erf}\left(\tfrac{\beta+\gamma}{\sigma\sqrt{2}}\right)\right]$$

Substituting into eqn. (3.1.4)

$$P_{++} = \tfrac{1}{4} + \tfrac{1}{4\pi}\left[\operatorname{erf}\left(\tfrac{\beta-\gamma}{\sigma\sqrt{2}}\right)\left\{\operatorname{Arcsin}\rho_{12} - \operatorname{Arcsin}\rho_{13}\right\} + \operatorname{erf}\left(\tfrac{\beta+\gamma}{\sigma\sqrt{2}}\right)\left\{\operatorname{Arcsin}\rho_{12} + \operatorname{Arcsin}\rho_{13}\right\}\right] \ldots\ldots 3.1.10$$

ρ_{12} is the same as $\rho_f(\tau)$, the auto-correlation function of $f_n(t)$. Similarly, ρ_{13} is the same as $\rho_f(\tau+\Delta)$. Thus, noting that $x_1(t)$ and $x_2(t+\tau)$ both have zero mean

$$\psi_{x_1x_2}(\tau) = 4P_{++} - 1$$

$$= \tfrac{1}{\pi}\left[\operatorname{erf}\left(\tfrac{\beta-\gamma}{\sigma\sqrt{2}}\right)\left\{\operatorname{Arcsin}\rho_f(\tau) - \operatorname{Arcsin}\rho_f(\tau+\Delta)\right\} + \operatorname{erf}\left(\tfrac{\beta+\gamma}{\sigma\sqrt{2}}\right)\left\{\operatorname{Arcsin}\rho_f(\tau) + \operatorname{Arcsin}\rho_f(\tau+\Delta)\right\}\right] \quad \ldots\ldots 3.1.11$$

For the trivial case of $\Delta=0$, this resolves into the form expected from eqn. (2.1.8). For $\tau=0$, the expression becomes

$$\psi_{x_1x_2}(0) = \tfrac{1}{2}\left[\operatorname{erf}\left(\tfrac{\beta+\gamma}{\sigma\sqrt{2}}\right) + \operatorname{erf}\left(\tfrac{\beta-\gamma}{\sigma\sqrt{2}}\right) + \psi_{n_1n_2}(\Delta)\left\{\operatorname{erf}\left(\tfrac{\beta+\gamma}{\sigma\sqrt{2}}\right) - \operatorname{erf}\left(\tfrac{\beta-\gamma}{\sigma\sqrt{2}}\right)\right\}\right] \ldots 3.1.12^*$$

as compared to

$$\psi_{x_1x_2}(0) \text{ (single reflection)} = \operatorname{erf}(\beta/\sigma\sqrt{2}) \qquad (2.1.8)$$

As the extraneous noise $n(t)$ tends to zero, an interesting effect appears: the value of $\psi_{x_1x_2}(\tau)$ becomes critically dependent upon which of β or γ is the greater. For $\sigma=0$, if $\beta>\gamma$, eqn. (3.1.11) becomes

$$\psi_{x_1x_2}(\tau) = \tfrac{2}{\pi}\operatorname{Arcsin}\ \rho_f(\tau)$$

and if $\gamma>\beta$

$$\psi_{x_1x_2}(\tau) = \tfrac{2}{\pi}\operatorname{Arcsin}\ \rho_f(\tau+\Delta)$$

---

*Eqn. (3.1.12) can be derived directly, as in Section 2.1.1, i.e. without assuming any multivariate distributions.

In other words, only the larger of the two reflections will be detected. The smaller one will be completely missed and will have no effect whatsoever on the cross-correlator output. The conclusion to be drawn is that single-bit waveforms should not be used for single-bit cross-correlation reflection detection in applications where low extraneous noise and double reflections can be expected, as there is a definite probability that the smaller of the two reflections will be missed. This, incidentally, applies to the single-bit cross-correlation of any severely clipped waveform - pseudo random, square, or whatever.

Eqn. (3.1.11) is plotted in Fig. 3-1 for some representative values of β, γ, σ and Δ. It is notable that whenever there are two reflections, both zero delay peaks are reduced as compared to the single reflection peak in Fig. 3-1a. The worst case arises when $\beta=\gamma$ in which case both peaks are approximately halved.

3.1.2 Extension to Digital Sampling Cross-correlation

Starting with the special case of $\tau=0$ and assuming that the transmitted waveform is continuous, so that $x_2(t+\tau) = \mathrm{sgn}[\beta x_1(t+\tau) + \gamma x_1(t+\tau+\Delta) + n(t)]$ over the whole cross-correlation interval 0 to T, the noise n(t) will cause an error i.e. cause $x_2(t_i+\tau)$ to have opposite sign to $x_1(t_i+\tau)$ when either

$$\left.\begin{array}{l} \text{(a) } \beta x_1(t_i+\tau)=\beta,\ \gamma x_1(t_i+\tau+\Delta)=\gamma \text{ and } n(t_i) < -(\beta+\gamma) \\ \text{(b) } \beta x_1(t_i+\tau)=\beta,\ \gamma x_1(t_i+\tau+\Delta)=-\gamma \text{ and } n(t_i) < -(\beta-\gamma) \\ \text{(c) } \beta x_1(t_i+\tau)=-\beta,\ \gamma x_1(t_i+\tau+\Delta)=\gamma \text{ and } n(t_i) > (\beta-\gamma) \\ \text{or (d) } \beta x_1(t_i+\tau)=-\beta,\ \gamma x_1(t_i+\tau+\Delta)=-\gamma \text{ and } n(t_i) > (\beta+\gamma) \end{array}\right\} \quad \ldots\ldots 3.1.13$$

A set of equations analogous to eqns. (2.1.3) (p. 15) can be written for $x_1(t_i+\tau)$ and $x_1(t_i+\tau+\Delta)$, and from these the probability of an even or odd number of zero crossings of x_1 in period Δ can be expressed as $\frac{1}{2}[1+\psi_{x_1}(\Delta)]$ and $\frac{1}{2}[1-\psi_{x_1}(\Delta)]$, respectively. Using eqns. (3.1.9), the error probability P_e, which is the sum of the probabilities (a), (b), (c) and (d) above, is

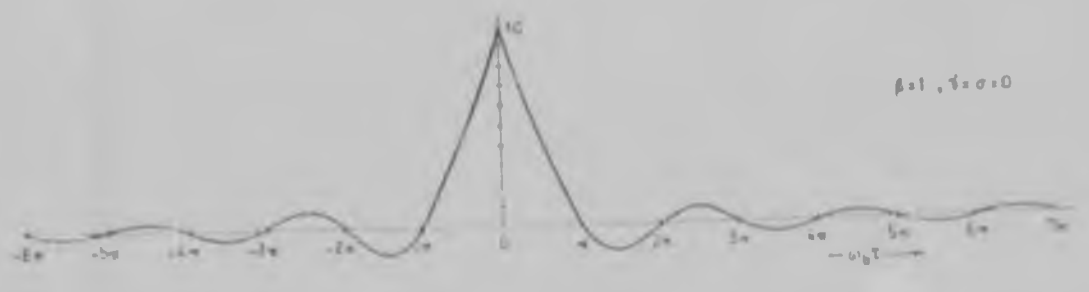

(a)

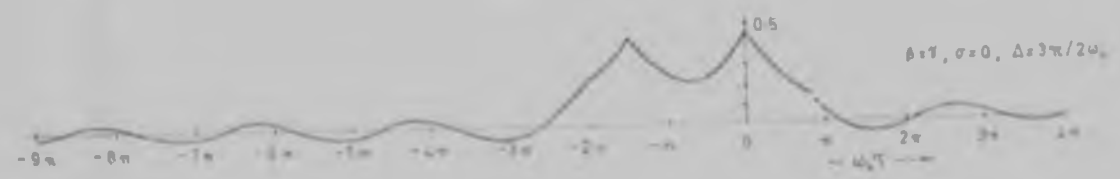

(b)

(c)

(d)

(e)

(f)

FIGURE 3-1 Double single-bit reflection error-correlation functions. Note how in (f) the second peak is almost non-existent even though the one reflection has amplitude 90 per cent of the other. $f_s(t)$ is assumed to have a 'brick wall' frequency spectrum over 0 to $\omega_b/2\pi$ Hz.

$$P_e = \tfrac{1}{4}\left[1+\Psi_n(\Delta)\right]\left[1-\operatorname{erf}\left(\tfrac{\beta+\gamma}{\sigma\sqrt{2}}\right)\right] + \tfrac{1}{4}\left[1-\Psi_n(\Delta)\right]\left[1-\operatorname{erf}\left(\tfrac{\beta-\gamma}{\sigma\sqrt{2}}\right)\right] \quad \ldots 3.1.14$$

The mean of $\Psi_s(0)$, which, as discussed in Section 2.1.2, is given by $N\left[1-2P_e\right]$, is therefore

$$\overline{\Psi_s(0)} = \tfrac{1}{2}.N\left[\operatorname{erf}\left(\tfrac{\beta+\gamma}{\sigma\sqrt{2}}\right) + \operatorname{erf}\left(\tfrac{\beta-\gamma}{\sigma\sqrt{2}}\right) - \Psi_n(\Delta)\left\{\operatorname{erf}\left(\tfrac{\beta+\gamma}{\sigma\sqrt{2}}\right) - \operatorname{erf}\left(\tfrac{\beta-\gamma}{\sigma\sqrt{2}}\right)\right\}\right] \quad . \; 3.1.15$$

which is the same as eqn. (3.1.12). It resolves into the forms expected from eqn. (2.1.11) for the trivial cases of $\gamma=0$ and $\Delta=0$, and into that expected from eqn. (2.1.20) for $\beta=0$.

As $n(t)$ is wideband, the probability of its causing an error at instant t_i is independent of t_i, and therefore, as discussed before, the number of errors occurring in the N instants will follow a binomial distribution with mean and variance NP_e and $NP_e(1-P_e)$, respectively. As before, the distribution of $\Psi_s(0)$ can be derived directly from that of the number of errors.

In the case of $x_1(t)$ being transmitted in bursts so that the received waveform contains both reflections only over period 0 to $(T-\Delta)$ (see Fig. 3-2), and over period $(T-\Delta)$ to T contains only one of the reflections,

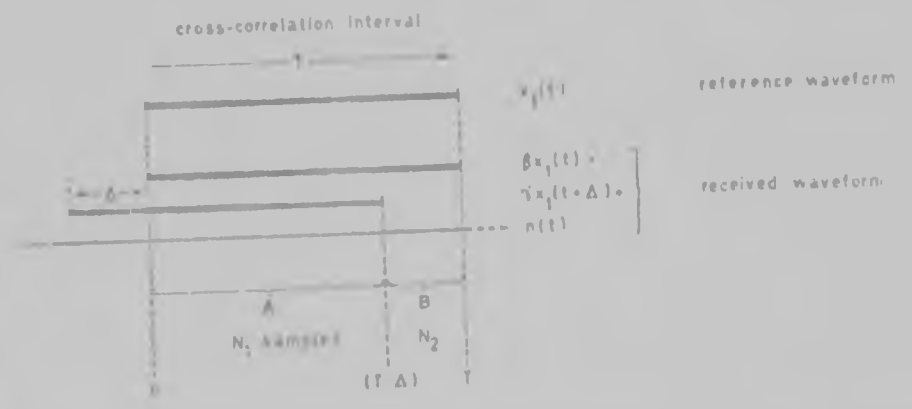

FIGURE 3-2 Zero delay cross-correlation of burst waveforms.

$\beta x_1(t)$, the distribution of $\Psi_s(0)$ must be derived in two parts. The N_1 products in interval 0 to $(T-\Delta)$ are identical to those analysed above for continuous waveforms, except that the number of errors will have mean N_1P_e and variance $N_1P_e(1-P_e)$. The mean of the sum of the N_1 product terms

will be

$$\mu_1 = N_1 \cdot \Psi_{x_1 x_2}(0) \quad \ldots\ldots\ldots\ldots\ldots\ldots \quad 3.1.16$$

The product terms in the interval (T-Δ) to T constitute a situation identical to that of the zero delay cross-correlation of a single reflection in Section 2.1.2 (p. 16). The distribution of their sum can be derived from the binomial distribution of the number of error instants in period (T-Δ) to T which will have mean $N_2[\frac{1}{2}\text{erfc}(\beta/\sigma\sqrt{2})] = N_2 p$ and variance $N_2 p(1-p)$. The mean of the product term sum will be

$$\mu_2 = N_2 \text{erf}(\beta/\sigma\sqrt{2}) \quad \ldots\ldots\ldots\ldots\ldots\ldots \quad 3.1.17$$

Combining these two distributions yields that of $\Psi_b(0)$. Direct combination assumes that the two distributions are independent, but since n(t) is totally uncorrelated with $x_1(t)$, this is a legitimate assumption. The mean of $\Psi_b(0)$ will of course be $(\mu_1 + \mu_2)$.

For $|\tau| > 0$, the mean of $\Psi_b(\tau)$ for $x_1(t)$ being transmitted continuously will just be $N_1 \Psi_{x_1 x_2}(\tau)$, with $\Psi_{x_1 x_2}(\tau)$ as in eqn. (3.1.11). Where $x_1(t)$ is transmitted in bursts, the situation is as depicted below;

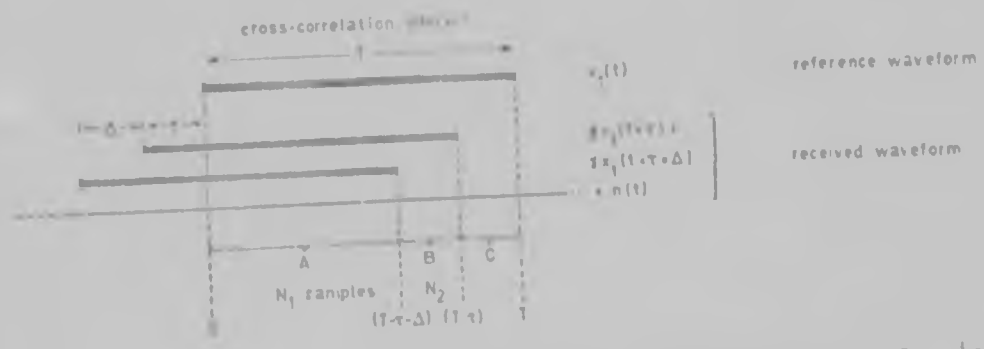

FIGURE 3-3 Cross-correlation of burst waveforms for $|\tau| > 0$.

over the N_1 samples in region A, $x_1(t)$ is being cross-correlated with both reflections plus noise so the mean of the sum of the N_1 product terms will be $N_1 \Psi_{x_1 x_2}(\tau)_a$, $\Psi_{x_1 x_2}(\tau)_a$ being as defined in eqn. (3.1.11). Over region B, $x_2(t+\tau) = \text{sgn}[\hat{a} x_1(t+\tau) + n(t)]$ and thus the mean of the sum of these N_2 product terms will be $N_2 \Psi_{x_1 y}(\tau)_b$ where $\Psi_{x_1 y}(\tau)_b$ is as in eqn. (2.1.9) (p. 16);

the mean of $\Psi_b(\tau)$ is the sum of these two means since the product terms in region C have zero mean.

Little can be said about the variance of $\Psi_b(\tau)$ for either burst or continuous waveform cross-correlation. The fourth order moments that occur in its expression cannot be evaluated easily. However, the term N dominates the expression (constituting typically 90 per cent or more in the variances calculated for the single reflection distributions of $\Psi_s(\tau)$ in Chapter two). One may therefore expect a variance slightly greater than N. For τ not equal to zero or $-\Delta$, $\Psi_b(\tau)$ has mean value close to zero. Each term contributes equally to $\Psi_b(\tau)$ and hence, following the discussion in Section 2.1.3, the distribution of $\Psi_b(\tau)$ will most likely tend to normal for N large. But it must be remembered that since all the N product terms are not identically distributed, the convergence to normality will not be as rapid as for the single reflection case where the product terms were identically distributed.

3.1.3 Extension to More than Two Reflections

In general, it will not be possible to derive closed form expressions like eqn. (3.1.11) for the cross-correlation function when more than two simultaneous reflections are received. The reason is that for more reflections, multivariate normal distributions of higher order than three would be required, and it is only in very exceptional circumstances[+] that joint probabilities of the form of eqn. (3.1.8) can be evaluated exactly.

3.2 Detection of Two Analog Gaussian Reflections Corrupted by Wideband Gaussian Noise

3.2.1 Derivation of the Cross-correlation Function

To start with, consider the case where there is no extraneous noise.

[+]see footnote on p. 29.

The cross-correlator input waveforms are then

$$x_1(t) = \operatorname{sgn}\left[f_n(t)\right] = \operatorname{sgn}\left[I_1\right] \quad \ldots\ldots\ldots\ldots\ldots\ldots \quad 3.2.1$$

$$x_2(t+\tau) = \operatorname{sgn}\left[\beta f_n(t+\tau) + \gamma f_n(t+\tau+\Delta)\right] = \operatorname{sgn}\left[I_2\right] \quad \ldots\ldots\ldots \quad 3.2.2$$

where $f_n(t)$ is as defined in all the previous sections. $f_n(t)$, $f_n(t+\tau)$ and $f_n(t+\tau+\Delta)$ are all correlated Gaussian random variables, and their joint probability can be described by a trivariate normal distribution function; hence any linear combination of them will follow a multivariate normal distribution. In particular, I_1 and I_2 will be bivariate normally distributed with mean $\{0,0\}$ and variances[+] $\{s^2, (\beta^2 + 2\gamma\beta\rho_f(\Delta) + \gamma^2)s^2\}$. The cross-covariance of I_1 and I_2 is

$$\begin{aligned} E\{I_1 I_2\} &= E\{\beta f_n(t) f_n(t+\tau) + \gamma f_n(t) f_n(t+\tau+\Delta)\} \\ &= \beta s^2 \rho_f(\tau) + \gamma s^2 \rho_f(\tau+\Delta) \\ &= R_{I_1 I_2}(\tau) \quad \ldots\ldots\ldots\ldots\ldots\ldots \quad 3.2.3 \end{aligned}$$

Normalising:

$$\begin{aligned} \rho_{I_1 I_2}(\tau) &= \frac{R_{I_1 I_2}(\tau)}{\sqrt{E[I_1^2]\, E[I_2^2]}} \\ &= \frac{\beta \rho_f(\tau) + \gamma \rho_f(\tau+\Delta)}{\sqrt{\beta^2 + 2\beta\gamma\rho_f(\Delta) + \gamma^2}} \quad \ldots\ldots\ldots \quad 3.2.4 \end{aligned}$$

Because I_1 and I_2 are zero mean and bivariate normal, the probability of both being positive is[34]

$$P_{++} = \tfrac{1}{4} + \tfrac{1}{2\pi} \operatorname{Arcsin}\left[\rho_{I_1 I_2}(\tau)\right] \quad \ldots\ldots\ldots\ldots \quad 3.2.5$$

and hence, as before, the cross-correlation function of $x_1(t)$ and $x_2(t+\tau)$ is

$$\psi_{x_1 x_2}(\tau) = \tfrac{2}{\pi} \operatorname{Arcsin}\left[\rho_{I_1 I_2}(\tau)\right] \quad \ldots\ldots\ldots\ldots \quad 3.2.6$$

Considering now the case where wideband Gaussian noise $n(t)$ is present in $x_2(t+\tau)$,

---

[+]Follows directly from $\operatorname{var}\{\xi\} = E\{[\xi - \bar{\xi}]^2\}$

$$x_2(t+\tau) = \operatorname{sgn}[\beta f_n(t+\tau) + \beta f_n(t+\tau+\Delta) + n(t)]$$
$$= \operatorname{sgn}[w(t+\tau) + n(t)] \quad \ldots\ldots\ldots\ldots \quad 3.2.7$$

$w(t+\tau)$ is a linear function of $f_n(t+\tau)$ and $f_n(t+\tau+\Delta)$ and hence $f_n(t)$ and $w(t+\tau)$ will be bivariate normally distributed with mean $(0,0)$ and variance $(\beta^2, (\lambda\beta)^2)$, where $\lambda = \sqrt{2+2\rho_n(\Delta)}$, and will have normalised cross-correlation function $\rho_{II_\lambda}(\tau)$ (see eqn. (3.2.4)). This set up is exactly analogous to that analysed in Section 2.2.1 with $\beta f_n(t+\tau)$ replaced by $w(t+\tau)$. Therefore the cross-correlation function of $x_1(t)$ and $x_2(t+\tau)$ in eqns. (3.2.1) and (3.2.7), respectively, can be written down directly as

$$\psi_{x_1x_2}(\tau) = \frac{2}{\pi} \operatorname{Arcsin}\left[\sqrt{\frac{(\lambda s/\sigma)^2}{1+(\lambda s/\sigma)^2}} \cdot \rho_{II_\lambda}(\tau)\right] \quad \ldots\ldots \quad 3.2.8^+$$

$\psi_{x_1x_2}(\tau)$ is plotted in Fig. 3-4 for some representative values of β, τ, σ, s and Δ. These have been chosen to correspond to those used in Fig. 3-1 for comparison purposes.

The peaks in the case of analog reflections are lower and less well-defined than those for single-bit reflections and the side lobes are higher. However, Fig. 3-4f shows how the possibility of missing a reflection in a low noise environment is not as great as with single-bit reflections, and under these conditions analog waveforms offer a distinct advantage.

3.2.2 Extension to Digital Sampling Cross-correlation

Consider the special case of continuous waveform cross-correlation with $\tau=0$. The error probability P_e cannot be derived directly as in Section 3.1.2; however, under the assumption that the probability of an error at any instant t_i is independent of t_i due to the nature of $n(t)$, the number of errors occurring in the N instants will follow a binomial

---

+The auto-correlation function of $x_2(t)$ can also be derived directly from eqn. (2.2.8) p. 26. This is done in Appendix M, (p. 126).

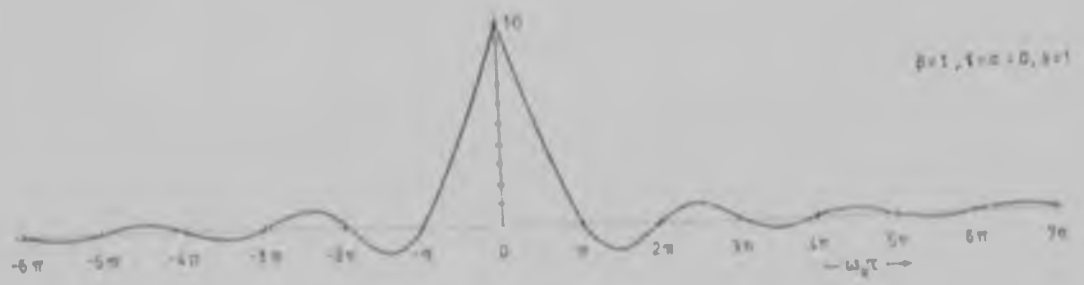

(a)

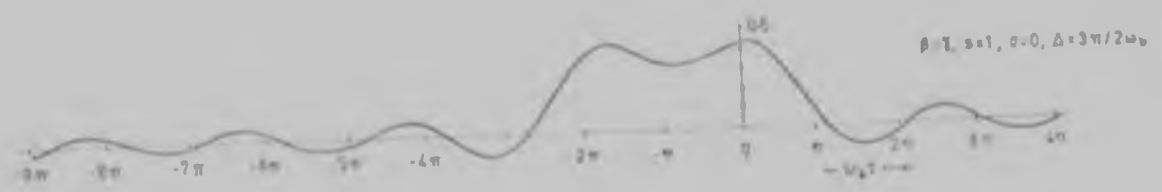

(b)

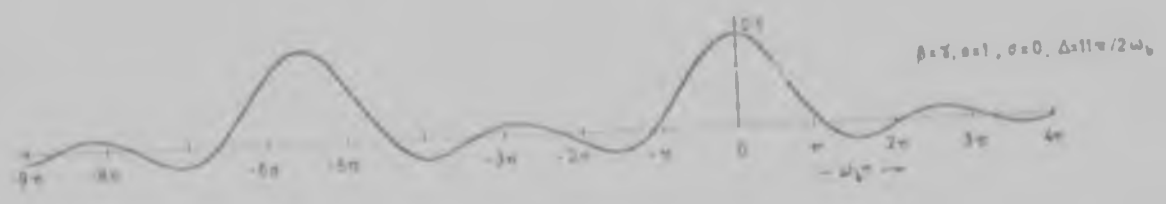

(c)

(d)

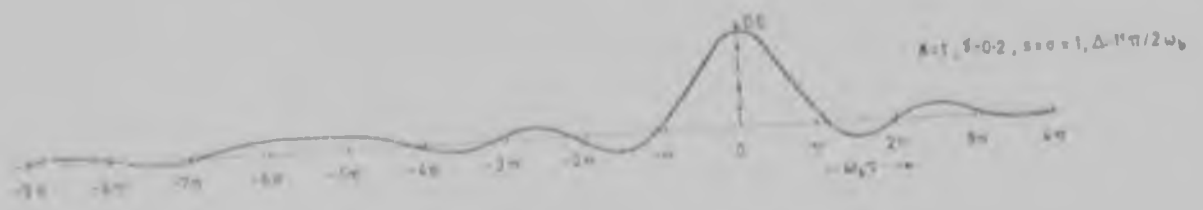

(e)

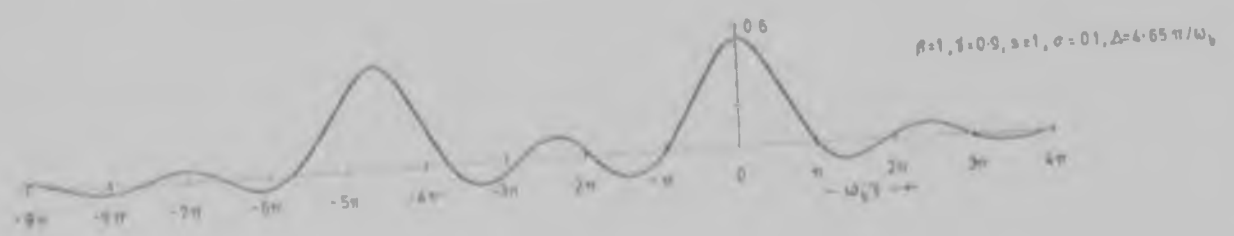

(f)

FIGURE 3-4 Double analog reflection cross-correlation functions. Parameters in (a) to (f) correspond to those in Fig. 3-1(a) to (f).

distribution. Once P_e is found, this distribution is completely defined and the distribution of $\Psi_b(0)$ can then be derived. In all the previous analyses, the mean of $\Psi_b(0)$, as calculated by first deriving P_e, has turned out to be of the form $N.\Psi_{b,x_1}(0)$, as expected, thereby providing a check on the derivation of Ψ_{b,x_1}. Reversing this process,

$$\overline{\Psi_b(0)} = E\left[\sum_{i=1}^{N} x_1(t_i)x_2(t_i)\right]$$
$$= N.\Psi_{b,x_1}(0) \quad \ldots\ldots\ldots\ldots\ldots\ldots 3.2.9$$

where $\Psi_{b,x_1}(0)$ is as defined in eqn. (3.2.8). This is related to P_e by

$$\overline{\Psi_b(0)} = N - 2NP_e$$

and hence

$$P_e = \tfrac{1}{2}[1 - \Psi_{b,x_1}(0)] \quad \ldots\ldots\ldots\ldots\ldots\ldots 3.2.10$$

Thus the distribution of $\Psi_b(0)$ can now be derived as before.

For burst waveform cross-correlation, the distribution of $\Psi_b(0)$ can again be considered in two independent sections (Fig. 3-5). The

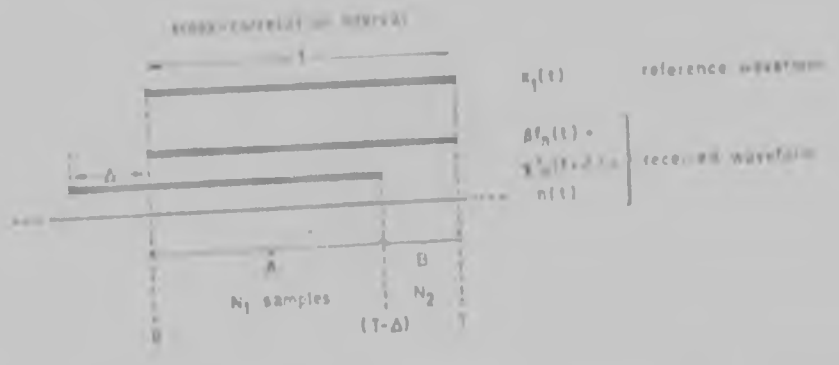

FIGURE 3-5 Burst waveform cross-correlation with $\tau=0$.

distribution of the sum of the N_1 product terms in period 0 to $(T-\Delta)$ can be derived in exactly the same way as that of the continuous waveform product term sum above. The binomial distribution of the number of error instants will have mean N_1P_e and variance $N_1P_e(1-P_e)$, and the mean of the sum of the N_1 product terms will be

$$\mu_1 = N_1 - 2N_1P_e \quad \ldots\ldots\ldots\ldots\ldots\ldots \quad 3.2.11$$

Over period (T-ℓ to T, the situation is identical to that analysed in Section 2.2.2 for the distribution of $\Psi_b(\sigma)$. The mean of the sum of the N_2 product terms will be

$$\mu_2 = N_2 \cdot \tfrac{2}{\pi} \text{Arctan}(\rho s/\sigma) \qquad (2.2.12)$$

These two distributions may, due to the nature of n(t), reasonably be assumed to be independent, and may therefore be combined directly to give the distribution of $\Psi_b(0)$.

For $|\tau| > 0$, the mean of $\Psi_b(\tau)$ for continuous waveform cross-correlation will be $E\cdot\Psi_{a,b}(\tau)$, with $\Psi_{a,b}(\tau)$ as given by eqn. (3.2.8). As mentioned earlier, $f_n(t)$ and $w(t+\tau)$ have a zero mean bivariate normal joint distribution function, and hence, as for all such variables, the probabilities that both are positive or negative are equal (Fig. 3-6) since the distribution is symmetrical. There is no reason why this symmetry should be

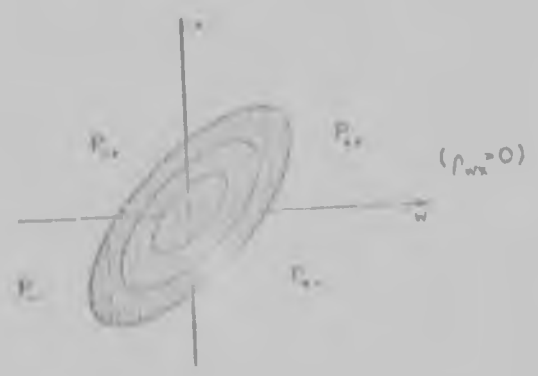

FIGURE 3-6 Zero mean bivariate normal distribution (plan view).

upset by the addition of an independent, symmetrical, zero mean, normally distributed random variable n(t)[+]. Therefore, sets of equations like eqns. (2.1.3) (p. 15) can be written for $x_1(t) = \text{sgn}[f_n(t)]$ and $x_1(t+\tau)$, for $x_1(t)$ and $x_2(t+\tau) = \text{sgn}[w(t+\tau) + n(t)]$, and for $x_2(t)$ and $x_2(t+\tau)$;

[+]see Note 1 at the end of Appendix D, (p. 112)

these can be solved for the probabilities of even or odd numbers of zero crossings of the waveforms in terms of Ψ_{s_1} (eqn. (2.1.7)), $\Psi_{s_1 s_2}$ (eqn. (3.2.6)) and Ψ_{n_1} (Appendix M), and thus the variance of $\Psi_b(\tau)$ can be calculated from eqn. (2.1.19), again assuming that the number of zero crossings of $x_1(t)$ or $x_2(t+\tau)$ in any interval is independent of the number in any other non-overlapping interval.

For burst waveform cross-correlation, the mean of $\Psi_b(\tau)$ can be calculated as the sum of the means of the N_1 and N_2 product term sums in Fig. 3-7, and is thus

$$\overline{\Psi_b(\tau)} = N_1 \cdot \Psi'_{s_1 s_2}(\tau) + N_2 \cdot \Psi''_{s_1 s_2}(\tau) \quad \ldots\ldots\ldots\ldots \quad 3.2.12$$

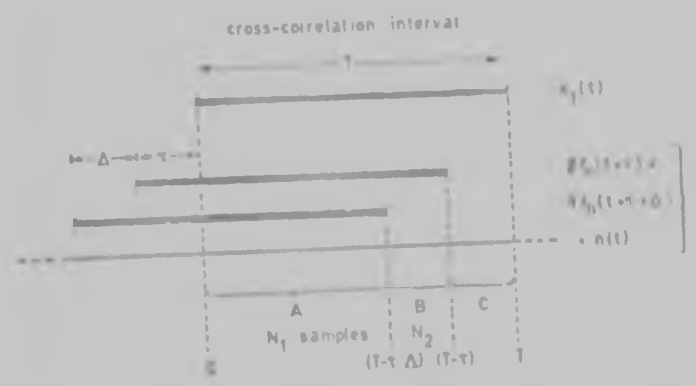

FIGURE 3-7 Burst waveform cross-correlation for $|\tau| > 0$.

where $\Psi'_{s_1 s_2}(\tau)$ and $\Psi''_{s_1 s_2}(\tau)$ are as defined in eqns. (3.2.8) and (2.2.7), respectively. The N_1 and N_2 product term sums cannot be assumed to be totally independent, and so it is not reasonable to consider them separately and then combine their distributions. Therefore, as in the case of double single-bit reflection detection, all that can be said is that the variance of $\Psi_b(\tau)$ for values of τ away from the two peaks will probably range between N and N plus five or ten per cent for receiver input signal-to-noise ratios between zero and infinity. The distribution can be expected to tend to normal as N increases.

3.2.3 Extension to More than Two Reflections

In this case an extension of the theory to the detection of more than two simultaneous reflections is possible. The reason is that the sum of n linearly attenuated Gaussian waveforms will be a normally distributed variable (i.e. I_2 in eqn. (3.2.2)) whose cross-covariance with I_1 in eqn. (3.2.1) can be derived as in eqns. (3.2.3) and (3.2.4). The heuristic derivations of the cross-correlation function in the presence of noise n(t) can also be applied. As the number of reflections increases, so the heights of the individual cross-correlation peaks will drop, since each added reflection effectively decreases the input signal-to-noise ratio at the zero delay instants of the other reflections.

With continuous waveform cross-correlation, an analysis similar to that above may be made of the distributions of $\psi_b(0)$ and $\psi_b(\tau)$; however, this will be proportionately more messy and less accurate with increasing complexity of the received waveform. With burst waveforms, the problem met above with the distribution of $\psi_b(\tau)$, that of the combination of the non-independent distributions of sums of product terms, arises again, in this case for the distribution of $\psi_b(0)$ as well, and so little other than the mean of the distributions can be reliably estimated.

CHAPTER IV

EXPERIMENTAL RESULTS

For the verification of the theory of Chapter two, the detection schemes analysed were simulated as precisely as possible using a specially built digital single-bit cross-correlator. The design and construction of the instrument are discussed in Appendix T (p. 144). As stated in Chapter one, the original application intended for the detection method was to acoustic reflection measurements, and therefore it was decided to use a noise signal having a bandwidth of approximately zero to 20 kHz. Serial processing was chosen for economy of circuitry. Once the maximum number of samples had been chosen as 20%, the speed of the TTL circuitry available at the time (20 Mlz for 9328 sixteen-bit shift registers) set the maximum correlation and hence signal sampling rate ($1/\delta t$) at 80 klhz.

4.1 Measurement of the Discrete Probability Mass Function of $\Psi_s(\tau)$ and the Detection and False Alarm Probabilities

By counting the number of times N_h in a total number of cross-correlations N_R that $\Psi_s(\tau)$ equalled or exceeded a chosen threshold h at a chosen time delay τ, and dividing by N_R, the complement of the cumulative distribution function of $\Psi_s(\tau)$ was obtained (i.e. $1 - P\{\Psi_s(\tau) < h\}$). This yielded directly the detection or false alarm probability, depending upon whether τ was equal to or greater than zero, respectively. The difference between N_h values for successive thresholds h and (h+2), divided by N_R,

gave the probability of $\Psi_b(\tau)$ being equal to h, or in other words, the discrete probability mass function of $\Psi_b(\tau)$, $p_\Psi\{h\}$. Successive thresholds were spaced at intervals of two, corresponding to the smallest possible change in $\Psi_b(\tau)$.

It may be noted here that $P\{\Psi_b(\tau) \geq h\} - P\{\Psi_b(\tau) \geq h+2\}$ is the probability that $\Psi_b(\tau)$ is equal to h and not (h+1), as this is impossible; thus the theoretical value for cases where the discrete mass function is approximated by a continuous density function would be evaluated as the integral of the continuous cumulative distribution function from (h-1) to (h+1), and not from h to (h+2).

4.2 Choice of Delays τ at which to Take Readings

The choice of $\tau=0$ as one of the delays at which to take N_h readings was obvious, as this yields the distribution of the cross-correlation peak and hence the detection probability P_D. The other value of τ chosen was $3\pi/2\omega_b$ (Fig. 4-1), as this gives virtually the highest value of $\Psi_b(\tau)$ away from the central peak and hence intuitively offers the most 'dangerous'

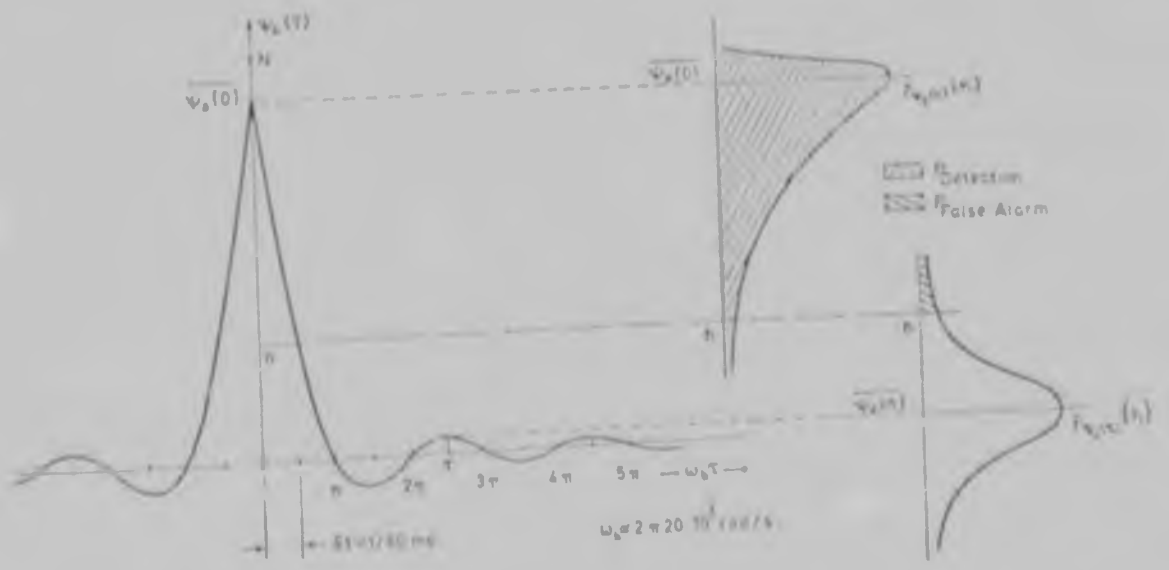

FIGURE 4-1 Measurement of detection and false alarm probabilities. The Gaussian signal $f_n(t)$ has a 'brick wall' frequency spectrum from zero to $\omega_b/2\pi$ Hz, and therefore $\rho_f(\tau) = \sin(\omega_b\tau)/\omega_b\tau$.

false alarm point. Secondly, for τ much larger, $\overline{\psi_b(\tau)}$ falls rapidly to zero and errors in the predicted mean value would be less apparent. Thirdly, for $\tau \gg 0$, the distribution of $\psi_b(\tau)$ tends more and more to a zero mean normal distribution which is independent of τ.

4.3 Practical Limitations

As stated, the probability mass function of $\psi_b(\tau)$ is derived by subtracting successive values of N_h; i.e.

$$p_\psi(h) = (N_h - N_{h+2})/N_R = \Delta N_h/N_R \quad \ldots\ldots\ldots\ldots 4.3.1$$

The value of $p_\psi(h)$ sets the lower limit on N_R because, for example, if $p_\psi(h) = 10^{-3}$, then N_R must be greater than 10^3 in order to be able to detect the difference between N_h and N_{h+2}. In theory there is no upper limit on the value of N_R; however, certain practical limitations were encountered. Difficulties arose in obtaining precise readings of N_h on the upper tails of the distribution where N_h, N_{h+2} and ΔN_h were very small compared to N_R, and where ΔN_h was of the same order of magnitude as N_h and N_{h+2}. To get precise readings on these upper tails required extremely tight control of parameters such as the dc drift in the output of the operational amplifier feeding the sum of signal plus noise to the comparator whose output was $x_2(t+\tau)$. The output of this comparator (μA 710C) changed state over an input range of 2 mV. The operational amplifier feeding it (RCA 3015), chosen for its wide bandwidth, did not have very low drift characteristics, and could drift by up to 10 mV if left for over five minutes. This drift was found to be enough to upset the readings; for example, in the case of the 100 sample cross-correlation detection of an analog Gaussian reflection in wideband noise, $(\beta s/\sigma) = 1.0$, and threshold $h = 40$, the readings of N_{40} were 53, 57, 48, 48, 40, 53 for $N_R = 10^5$. On checking after the reading 40 was obtained, it was discovered that the

dc level of the operational amplifier had drifted up. After resetting it, the value 53 was obtained. (The 40 was of course neglected). When it is considered that the mean of N_{42} was 26, it can be seen that the dc drift caused a change of approximately 50 per cent in ΔN_h. As the output of the operational amplifier was a random waveform whose dc level varied about zero with time, it was impossible to monitor the dc drift during the correlation runs and adjust it when necessary. The output amplitude of the operational amplifier was limited by the bandwidth requirements and could not merely be increased in an attempt to minimise the relative effect of the dc drift.

The other parameters that had to be tightly controlled were the signal and the additive wideband noise amplitudes. With rms amplitudes of, for example, one volt, changes of 50 mV in either amplitude caused noticeable changes in the N_h readings. However, as before, it was only when the N_h readings were small that errors in ΔN_h became large. For instance, a change of 50 mV in either amplitude half way through a run could change N_h readings from around 5300 to 5600, or from 600 to 700 suddenly, the effect obviously being more detrimental in the latter case. Thus before and after every run, the rms values of the signal and noise at the output of the operational amplifier were checked as well as the dc drift, and the input signal and noise rms amplitudes were monitored continuously.

Fortunately, in taking readings of N_h at a particular threshold, it was found that noticeably high or low readings could be consistently traced to one of the above parameters having changed. Screening of the odd high or low reading not attributable to any drift or mis-setting is discussed in the next section. Little trouble was encountered with readings at the low end or the middle of the mass function of $\Psi_b(\tau)$, where N_h and ΔN_h were not both very small compared to N_R.

Hence N_R had to be chosen large enough to give the required resolution N_h on the distribution tails, but not so large that unpredictable drifts

occurring during the run could render a large percentage of the readings useless. It was found that $N_R = 10^5$ gave the best compromise, and it was felt that if the theory and experiment agreed down to 10^{-5} probability mass function levels, this was sufficient to verify the theory.

Each of the 10^5 cross-correlations involved feeding 100 or 200 samples into the shift registers, cross-correlating these six times in the intervals between the next six sampling instants of the received waveform $x_2(t+\tau)$, and noting whether the values of $\psi_b(\tau)$ exceeded the threshold h for the two chosen delays $\tau=0$ and $5\pi/2\omega_b$. Hence each cross-correlation operation took (100/80+6/80) ms i.e. 1.3 ms for 100 samples and 2.6 ms for 200. The run of 10^5 operations thus took four or six minutes, respectively, taking into account the time necessary to note the values of N_h, check the operational amplifier output dc level, signal and noise amplitudes, reset if necessary and start again. On average at least four to eight readings were necessary for each threshold setting, and ten to twelve for those on the upper tails of the distribution, before a definite average could be discerned, so that one probability mass function point for a particular threshold and signal-to-noise ratio took some 40 to 90 minutes to work out for 100 samples, and between 80 minutes and three hours for 200 samples.

It was desirable to take all the readings of N_h and N_{h+2} necessary to work out one probability mass function point in one go and on the same day, as setting up the identical voltage levels the following morning sometimes proved extremely difficult. It was not that the readings changed radically, but, for example, the readings in the evening could be

$$N_{30} = 52930 \qquad \Delta N_{30} = 295$$
$$N_{32} = 52635$$

and the next morning

$$N_{30} = 53300 \qquad \Delta N_{30} = 288$$
$$N_{32} = 53062$$

Therefore, if only two or three readings of N_{32} had been taken the previous

evening and more were required, a lot of time was wasted in having to take additional readings of N_{30} as a check, as well as taking the necessary readings of N_{32}. With $N_R = 10^6$, it proved virtually impossible to take all the necessary readings for one mass function point in a day. Furthermore, it was more reliable to have six readings with $N_R = 10^5$ for which confidence limits could be established and from which dubious readings could be deleted and retaken, than to have one reading for $N_R = 10^6$ for which it was not known if some random drift had occurred sometime during the run, rendering N_h high or low. Finally, the author is somewhat sceptical about the practical significance of false alarm probabilities, etc., at levels of 10^{-6} and below, when so much of the system analysed has had to be idealised.

In practice, small drifts in the amplifier would not be bothered about, firstly because they only affect the tails of the distribution of $V_n(\tau)$ badly and these tail values have a low probability of occurrence, and secondly, being random, the drift would eventually reverse. It was only because the correlator was being used to simulate and verify mathematical theory that these small variations could not be tolerated; and they were only troublesome because of the small differences being measured.

4.4 Screening of the Experimental Readings

The readings of N_h used to obtain the average $\bar{N}_h$ were screened firstly by checking the values of the parameters mentioned above after each run. If any were found to have drifted off the set values, the reading was neglected and retaken. If the input signal or noise amplitudes, which were continuously monitored, were seen to drift during a run, they were reset and the run recommenced. Readings for each threshold h were taken until a definite average could be discerned. In cases where a seemingly high or low reading was obtained and checking revealed no drift in any

parameters, more readings were taken and if, after seven or eight readings, a correspondingly low or high reading was obtained, both readings were accepted. If no complementary reading occurred and the rest of the readings were grouped closely, the extreme value was neglected as a low probability 'tail of distribution' value. In doubtful cases a χ^2-test was performed. If the N_h values varied over a wide range, the number of readings taken was increased.

For example, the N_{60} and N_{62} readings for the 200 sample cross-correlation detection of an analog reflection corrupted by wideband noise, $(\beta s/\sigma) = 0.8$, were:

N_{60}: 97284, 97248, 97258 $\qquad \overline{N_{60}} = 97263.3$

N_{62}: 96211, 96433, 96665, 96420, 96444, 96703, 96583, 96612, 96425

$\overline{N_{62}} = 96499.5$

Mean difference: 763.8 90 per cent confidence interval: 594.7 - 933.0[+]

Here the readings of N_{60} were extremely close and so fewer were taken than for N_{62}.

The N_{10} and N_{12} readings for the 200 sample cross-correlation detection of a single-bit reflection corrupted by a random phase, 3903 Hz sine wave, $(\beta/A) = 0.309$, were:

N_{10}: 97324, 97353, 97368, 97355 $\qquad \overline{N_{10}} = 97350.0$

N_{12}: 96344, 96463, 96474, 96380, 96327 $\qquad \overline{N_{12}} = 96397.6$

Mean difference: 952.4 90 per cent confidence interval: 884.4 - 1020.4

The wider range in the values of N_{62} in the previous example compared to that of the N_{12} values in this one is reflected in the wider confidence interval in that case, even though more readings were taken of N_{62} than of N_{12}.

Another example, this time from the N_h readings for the detection of a single-bit reflection corrupted by a random phase sine wave (100

[+]see next section for method of evaluation

samples, $(\beta/A) = 0.809$) is:

N_{12}: 26187*, 26741, 26679, 26733, 26736

The starred value clearly does not fit in with the rest and could have resulted from a momentary drift in some parameter or else be a 'tail of distribution' value. As no complementary value occurred and the rest of the values were closely grouped, the reading was neglected and retaken.

A typical example of a complete set of experimental readings, including the ones that were screened out for one of the reasons described above, is given in Appendix N (p. 127).

4.5 Evaluation of the Confidence Intervals

The Central Limit Theorem in the form discussed by Feller[27] provides the justification for using the t-test to evaluate the confidence limits of the difference between the mean values of the N_h readings. He showed that if in a fixed number of trials n, a recurrent event ε occurs N_n times, then if N_n may be considered random (not necessarily independent), N_n will tend to normal as n tends to infinity. Regarding ε as the event $\Psi_s(\tau) \geq h$ and $n = N_R = 10^5$, N_h corresponds to N_n and hence tends to normal for large N_R. Also, because the mean values of N_h and N_{h+2} are in general close, it is reasonable to assume that the distributions of N_h and N_{h+2} should have approximately equal variances; hence the two conditions for applying the t-test are satisfied and it may be applied to finding the confidence interval of the difference between the readings of N_h and N_{h+2}, giving[37]

$$\text{Limits of } (\overline{N_h} - \overline{N_{h+2}}) = \overline{x_1} - \overline{x_2} \pm t_{1-(\alpha/2),m+n-2} \cdot \frac{\sqrt{\sum_{i=1}^{m}(x_{1i}-\overline{x_1})^2 + \sum_{k=1}^{n}(x_{2k}-\overline{x_2})^2}}{\sqrt{\frac{m+n}{mn}\left(\frac{m+n-2}{2}\right)}} \quad \ldots\ldots 4.5.1$$

at a confidence level of $(1-\alpha)$ (i.e. $t_{.95}$ is used to find the 90 per cent confidence limits), where $\{x_{1i}\}$ and $\{x_{2k}\}$ are the readings of N_h and N_{h+2}, respectively, and $\overline{x_1}$ and $\overline{x_2}$ are the mean values of N_h and N_{h+2} calculated

from the respective sets of readings. m and n are the numbers of readings of N_h and N_{h+2}, respectively, so that the number of degrees of freedom is (m+n-2).

The validity of the assumption of equal variances for the sets of N_h and N_{h+2} readings is discussed in Appendix O (p. 129), and alternative methods of evaluating the confidence interval of the difference between the means are discussed and shown to give results compatible with the t-test results. The application of the t-test to the odd few sets of readings that quite obviously did not have equal variances is also considered.

4.6 The Noise Signal $f_n(t)$

Gaussian noise having a flat frequency spectrum from zero to approximately 20 kHz was chosen as the signal with which to verify the theoretical analysis of the cross-correlator's performance, although had some other low-pass filtered Gaussian signal been chosen, the theory would still hold with the appropriate expression for $\rho_x(\tau)$ being used in the equations[+]. A fifth order elliptic filter was used to simulate the 'brick wall' response. The frequency spectrum of the bandlimited Gaussian signal used is shown in Fig. 4-2. From this the cut-off frequency f_b was taken as 21 kHz, and this value was used in all the theoretical predictions.

4.7 Presentation of the Results

Experimental readings of $p_v(h)$, the detection probability P_D, and the false alarm probability P_{FA} were taken for 100 and 200 sample cross-correlation

(1) with burst-type single-bit bandlimited Gaussian signals, the

---

[+]see Appendix A, (p. 103)

reflection being corrupted by wideband Gaussian noise (Sections 2.1.1 and 2.1.2),

(2) with continuous analog bandlimited Gaussian signals, the reflection being corrupted by wideband Gaussian noise (Sections 2.2.1 and 2.2.2) and

(3) with continuous single-bit bandlimited Gaussian signals, the reflection being corrupted by a random phase sine wave (Sections 2.3.1 and 2.3.2). The frequency of the sine wave was chosen as 3903 Hz because this gave approximately twenty sampling instants per sine wave period, and the signal-to-noise ratios chosen resulted from the theoretical calculations being carried out for zero to ten samples per error zone period (period t_b in Fig. 2-7, p. 34), for the sake of simplicity.

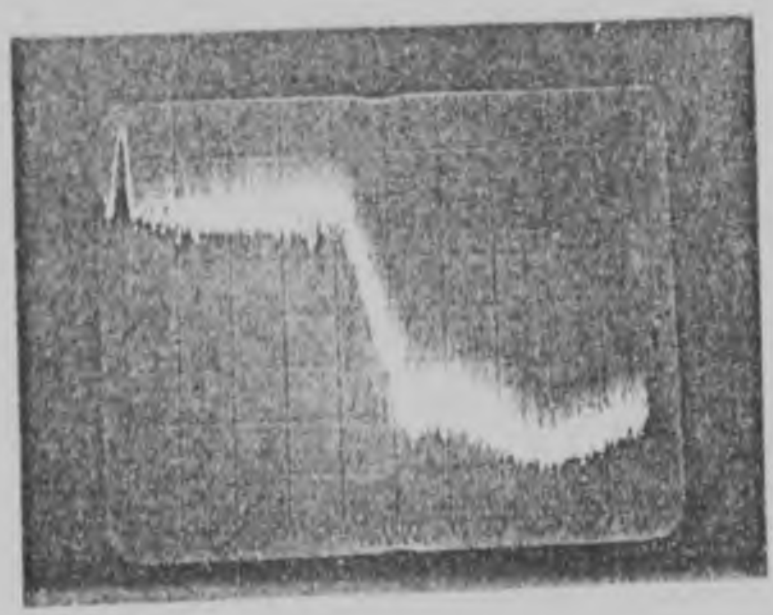

FIGURE 4-2 Frequency spectrum of the bandlimited Gaussian signal.

The results are given here in graphical form together with the theoretically predicted results for comparison purposes. Although the probability density functions and curves of the detection and false alarm rates are all discrete, for clarity the theoretical values have been joined with smooth curves and the experimental ones left as discrete

points. In some cases it was not possible to plot all the experimental values without causing congestion; however, they are all tabulated in Appendix P, p. 132. The 90 per cent confidence limits are denoted by vertical bars drawn through the points, ($\frac{1}{2}$). Where experimental points are very closely spaced, the limits have not been inserted on every point, but only on more widely spaced points spread across the distribution.

Readings could not be taken for all signal-to-noise ratios and so specific values were chosen, for example 0, 0.1, 0.5, 1.0, and infinity. It is highly unlikely that the theory would hold for the spot values only, and not for the rest. Nevertheless, as a check, in the case of the 100 sample cross-correlation detection of a single-bit reflection corrupted by wideband Gaussian noise, closely spaced readings of $P\{\psi_0(0) \geq h\}$ were taken for (β/σ) equal to 0, 0.1, 0.2, 0.3, ... 1.0, and infinity, and for the rest, more widely spaced points spread across the distributions were picked at random.

The voltmeter conversion factors necessary to read the true values of s, σ and β, and the actual values used in taking the experimental readings are given in Appendices Q (p. 135) and R (p. 136), respectively.

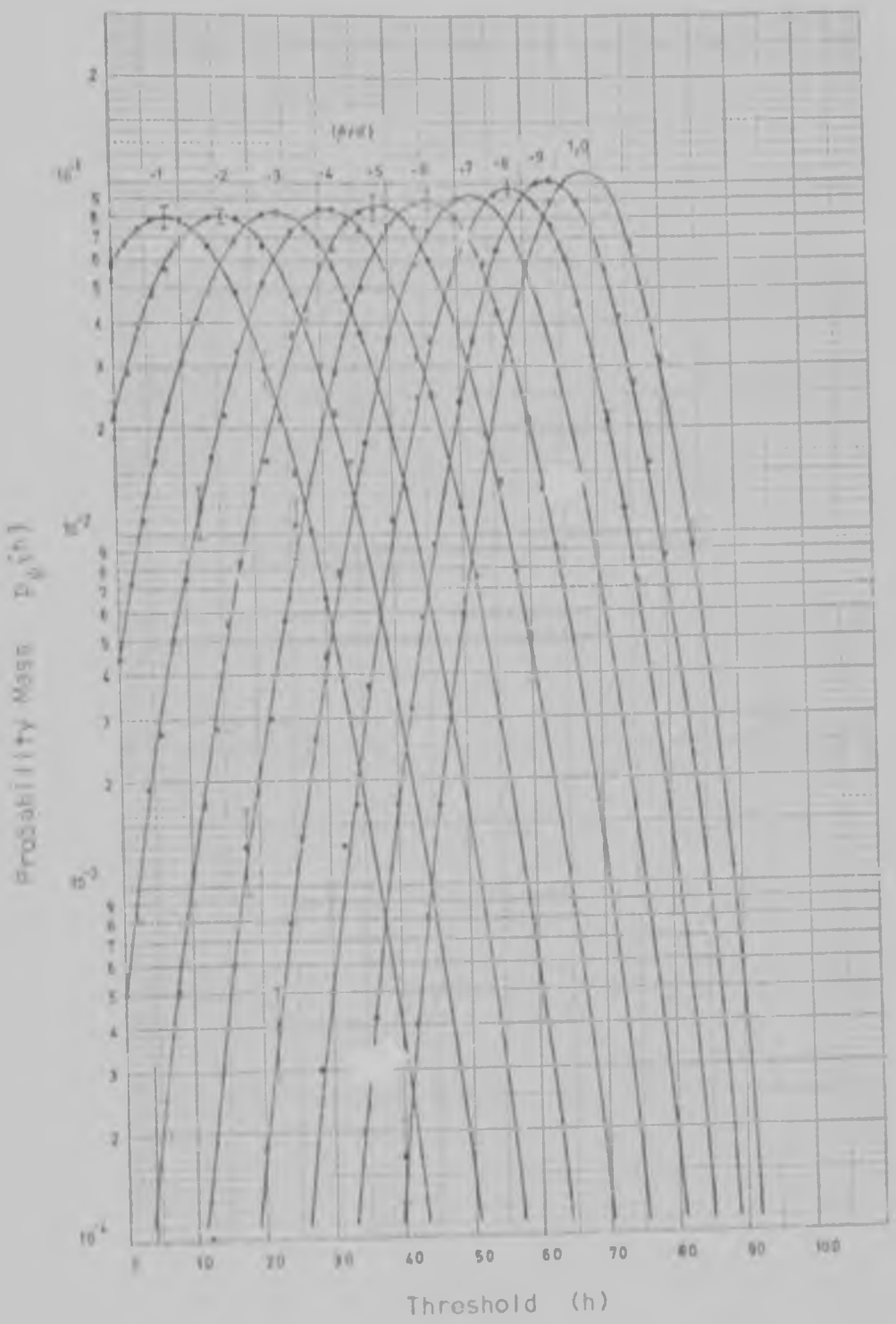

FIGURE 4-3 Probability mass functions of $\psi_0(0)$ for the 100 sample cross-correlation detection of a single-bit Gaussian reflection corrupted by wideband Gaussian noise.
(β and σ are the receiver input rms values of the single-bit Gaussian reflection and the wideband Gaussian noise, respectively).

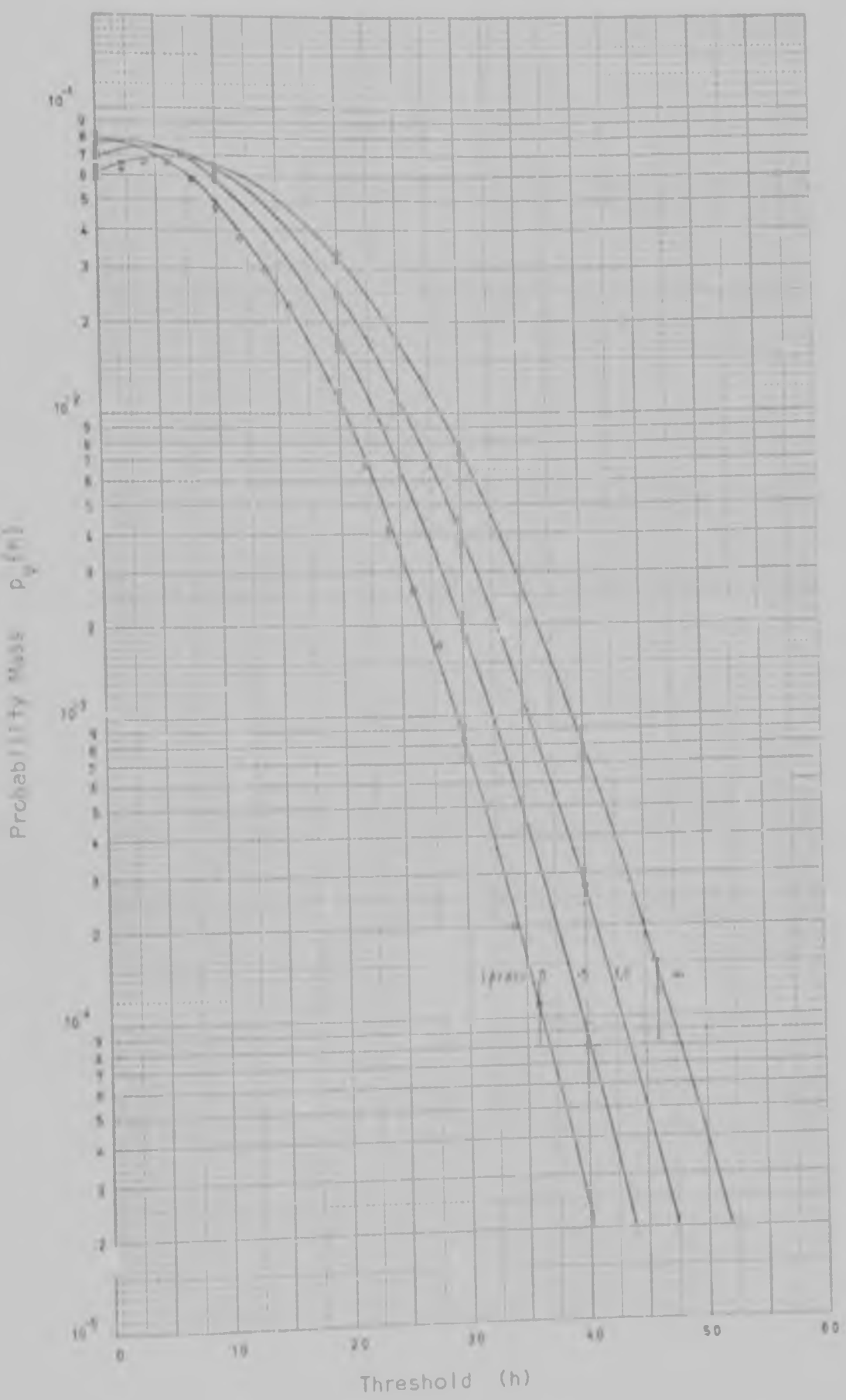

FIGURE 4-4 Probability mass functions of $v_0(\tau)$ for the 100 sample cross-correlation detection of a single-bit Gaussian reflection corrupted by wideband Gaussian noise. ($\tau = 5\pi/2\omega_b$).

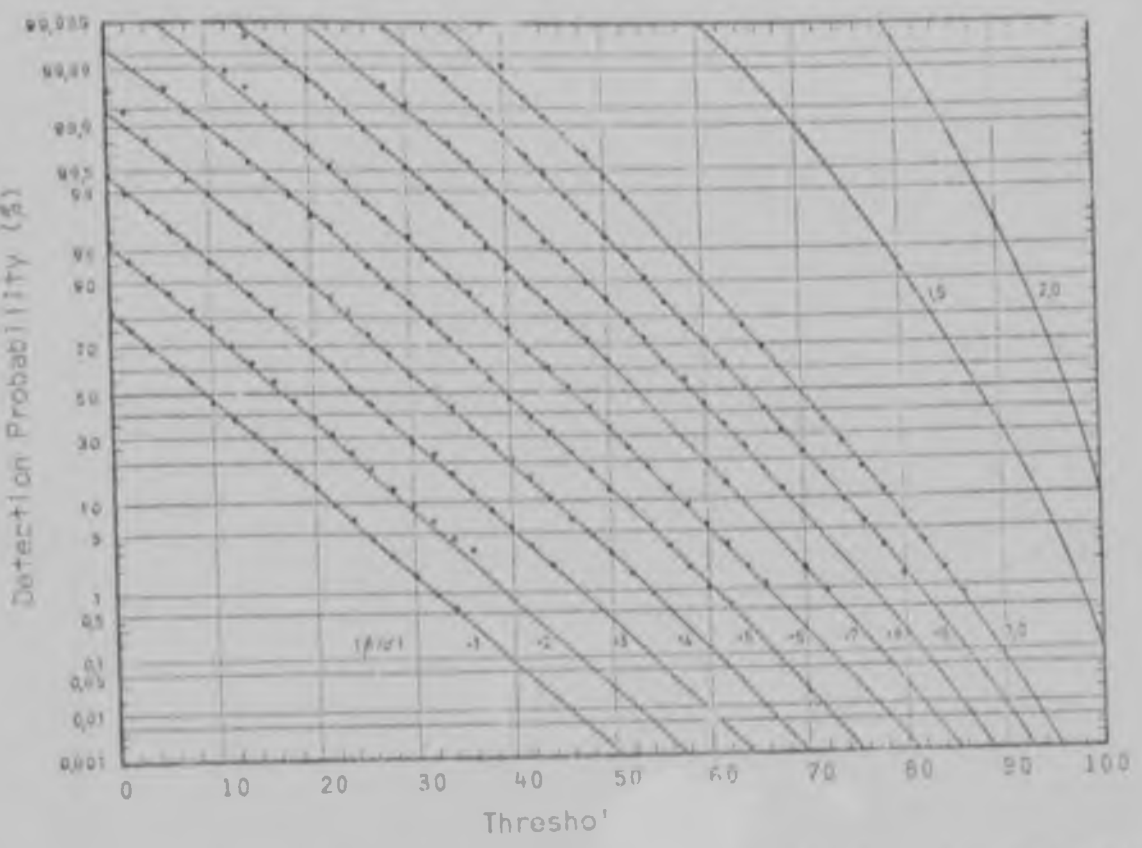

FIGURE 4-5 Detection probabilities of single-bit Gaussian reflection corrupted by wideband Gaussian noise. (100 sample cross-correlation).

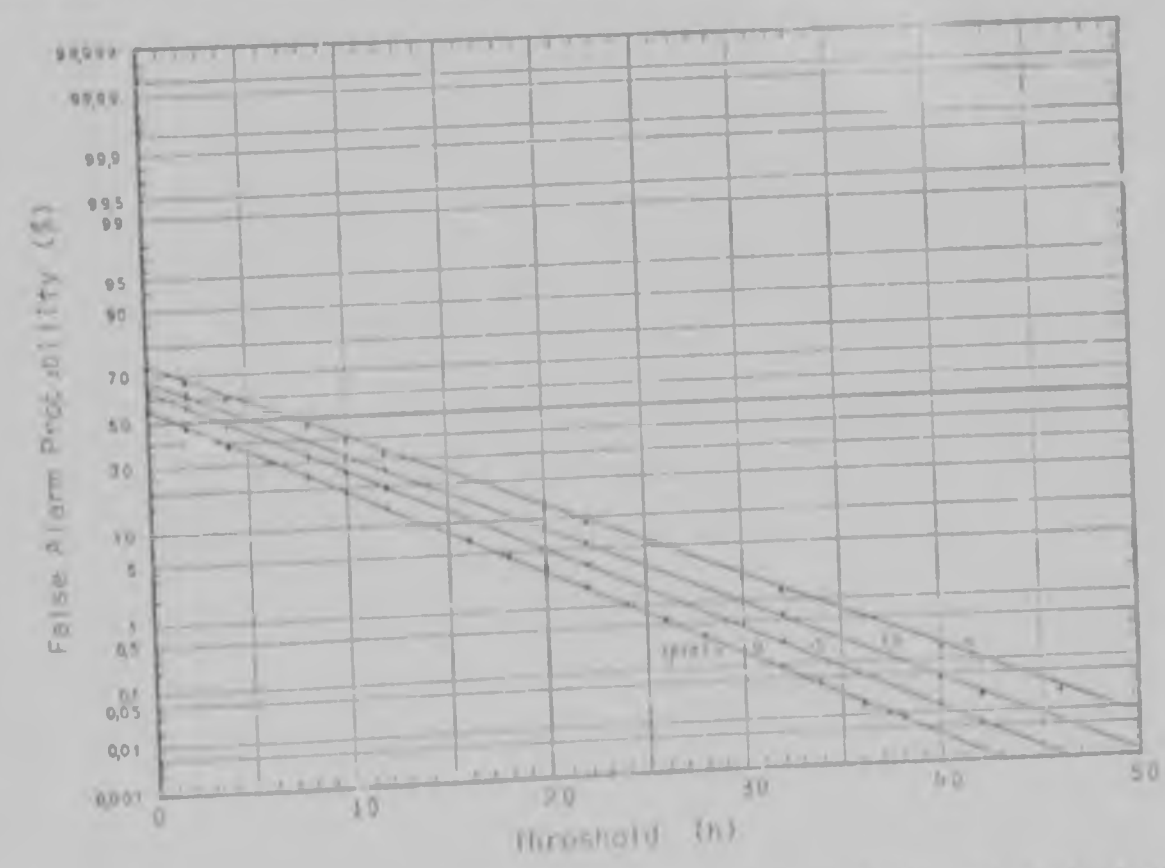

FIGURE 4-6 False alarm probabilities at delay $= 5\pi/2\omega_0$ of a single-bit Gaussian reflection corrupted by wideband Gaussian noise. (100 sample cross-correlation).

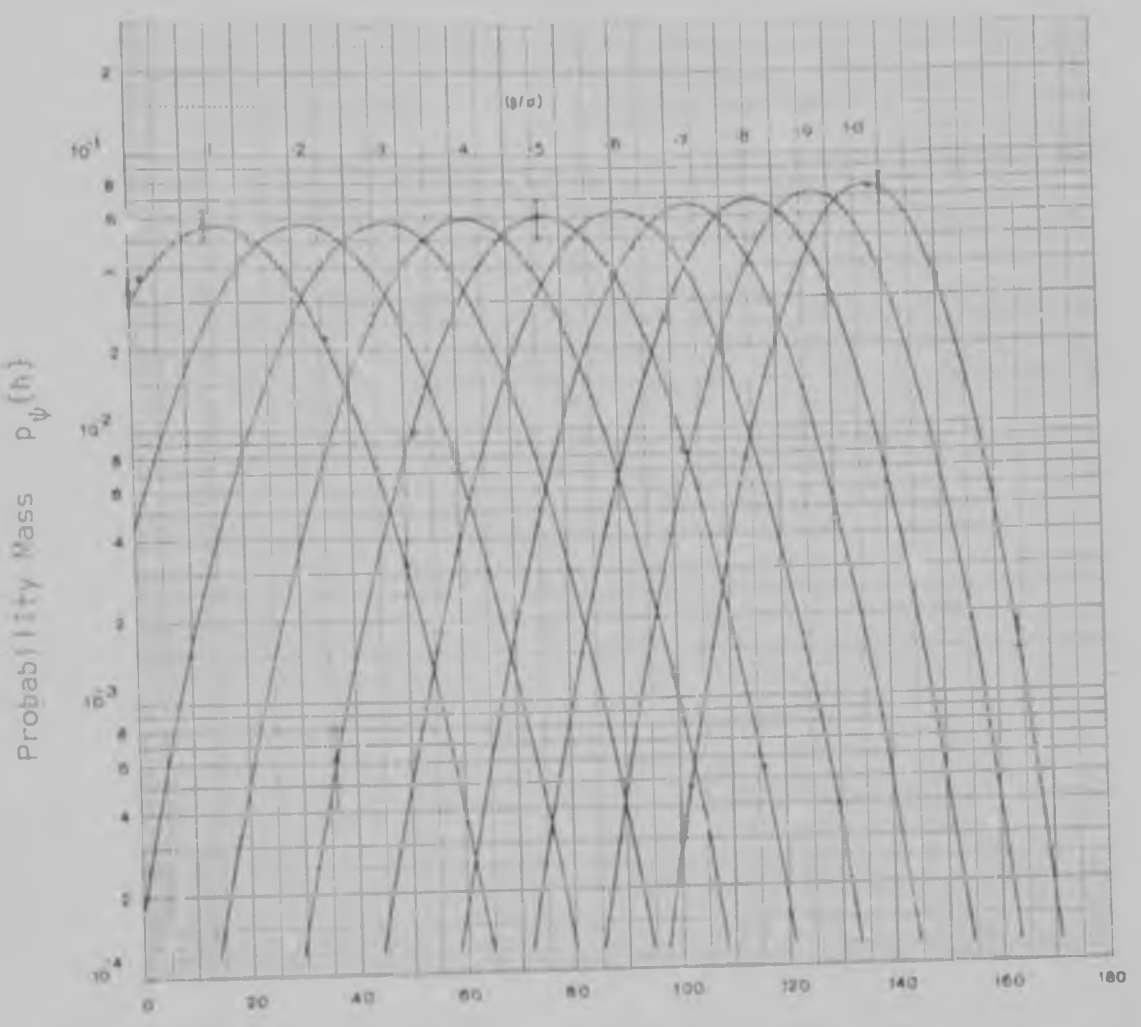

FIGURE 4-7 Probability mass functions of $V_p(0)$ for the 200 sample cross-correlation detection of a single-bit Gaussian reflection corrupted by wideband Gaussian noise.

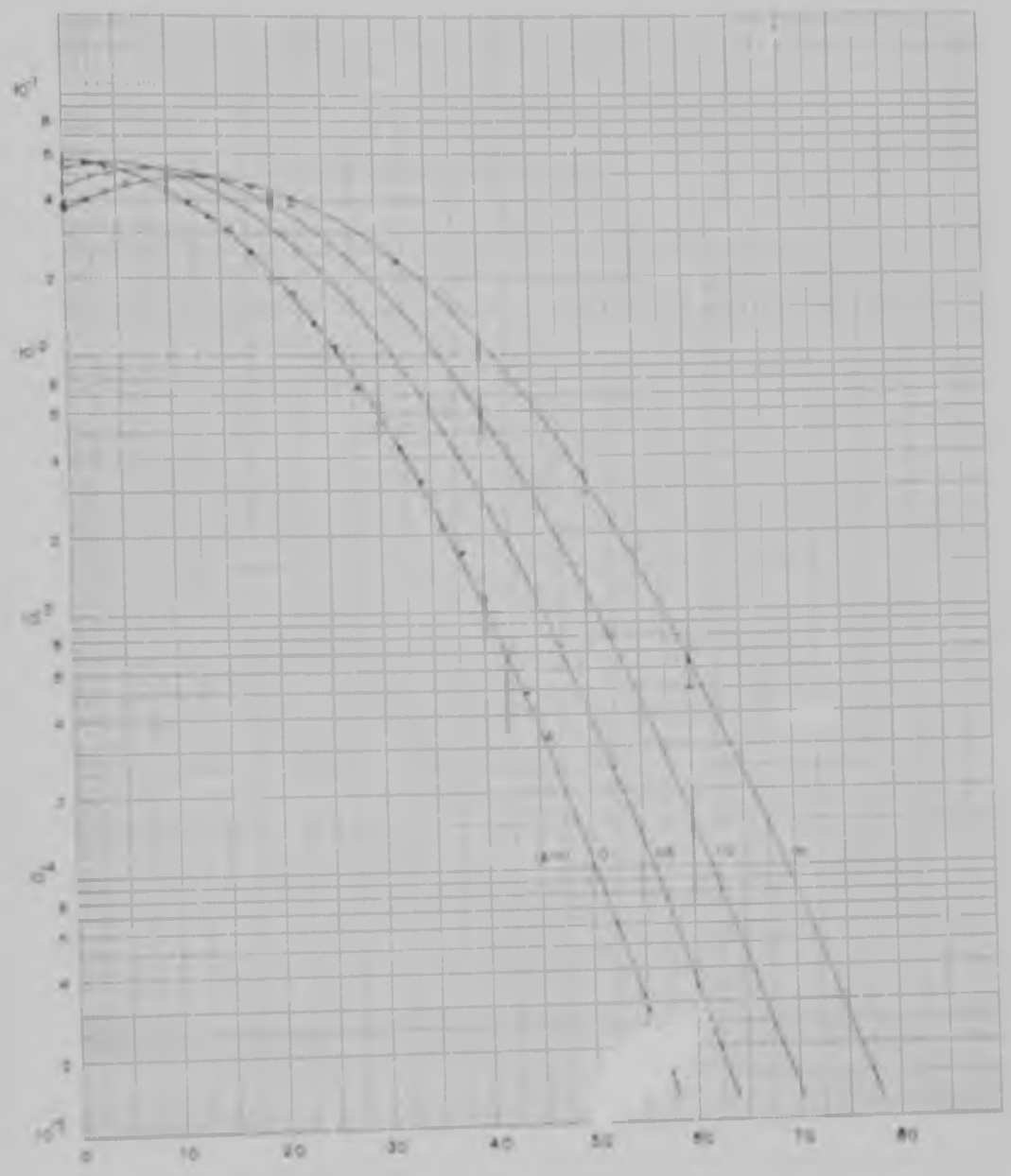

FIGURE 4-8 Probability mass functions of $z_1(r)$ for the 2nd sample cross-correlation detection of a single-bit Gaussian reflection corrupted by wideband Gaussian noise. ($\sigma_w = 5.12$ b).

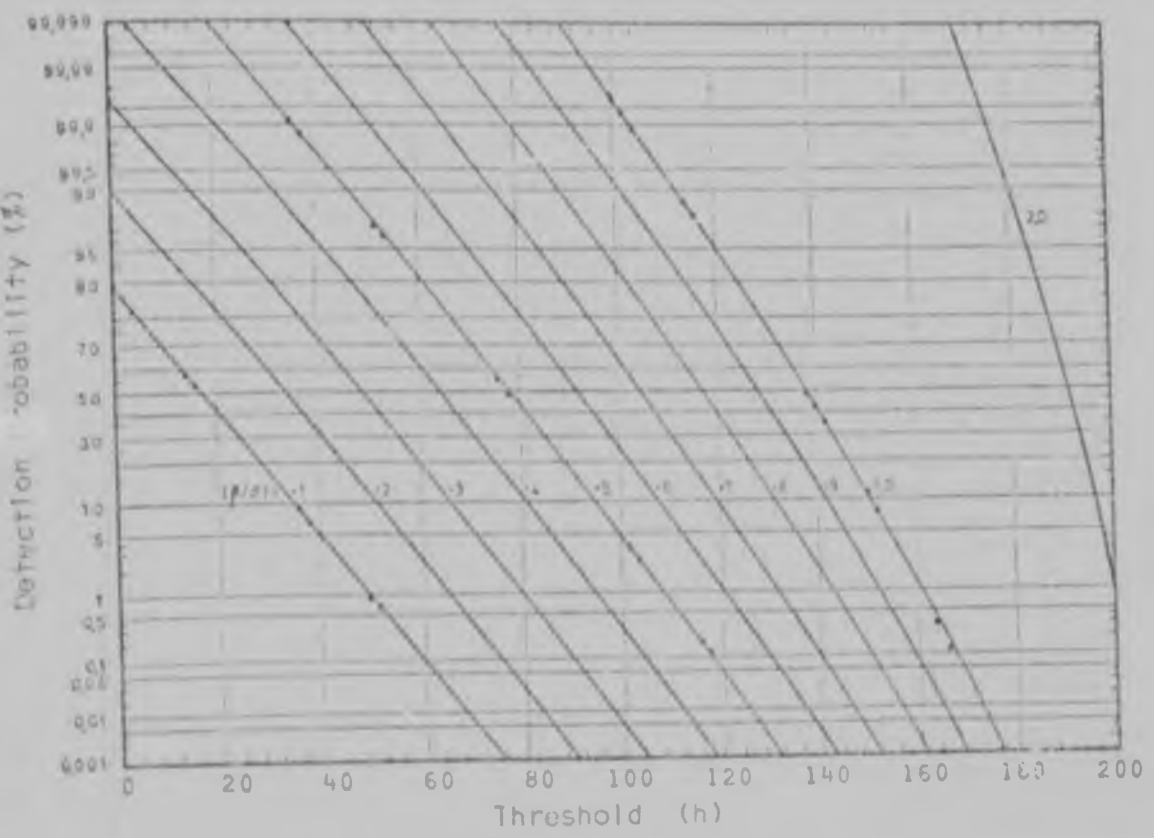

FIGURE 4-9 Detection probabilities of a single-bit Gaussian reflection corrupted by wideband Gaussian noise. (200 sample cross-correlation).

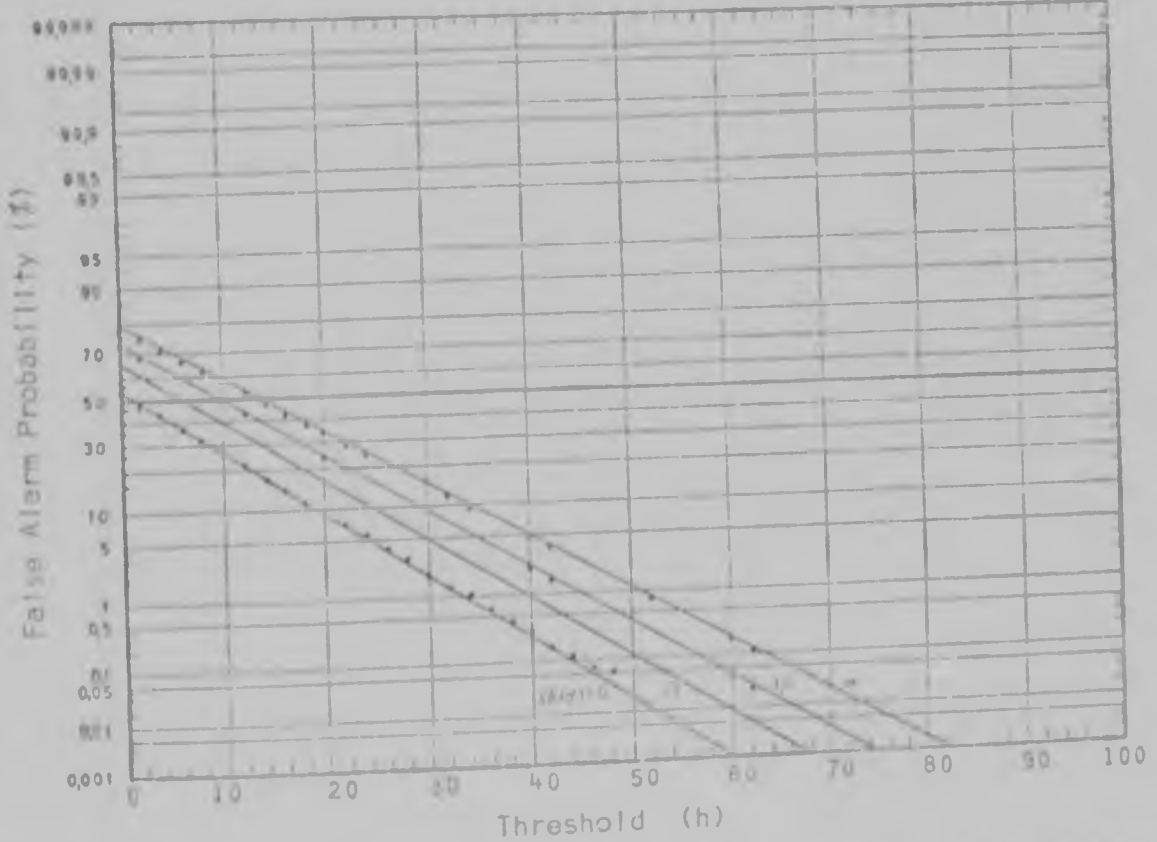

FIGURE 4-10 False alarm probabilities at delay $\tau = 5\pi/2\omega_b$ of a single-bit Gaussian reflection corrupted by wideband Gaussian noise. (200 sample cross-correlation).

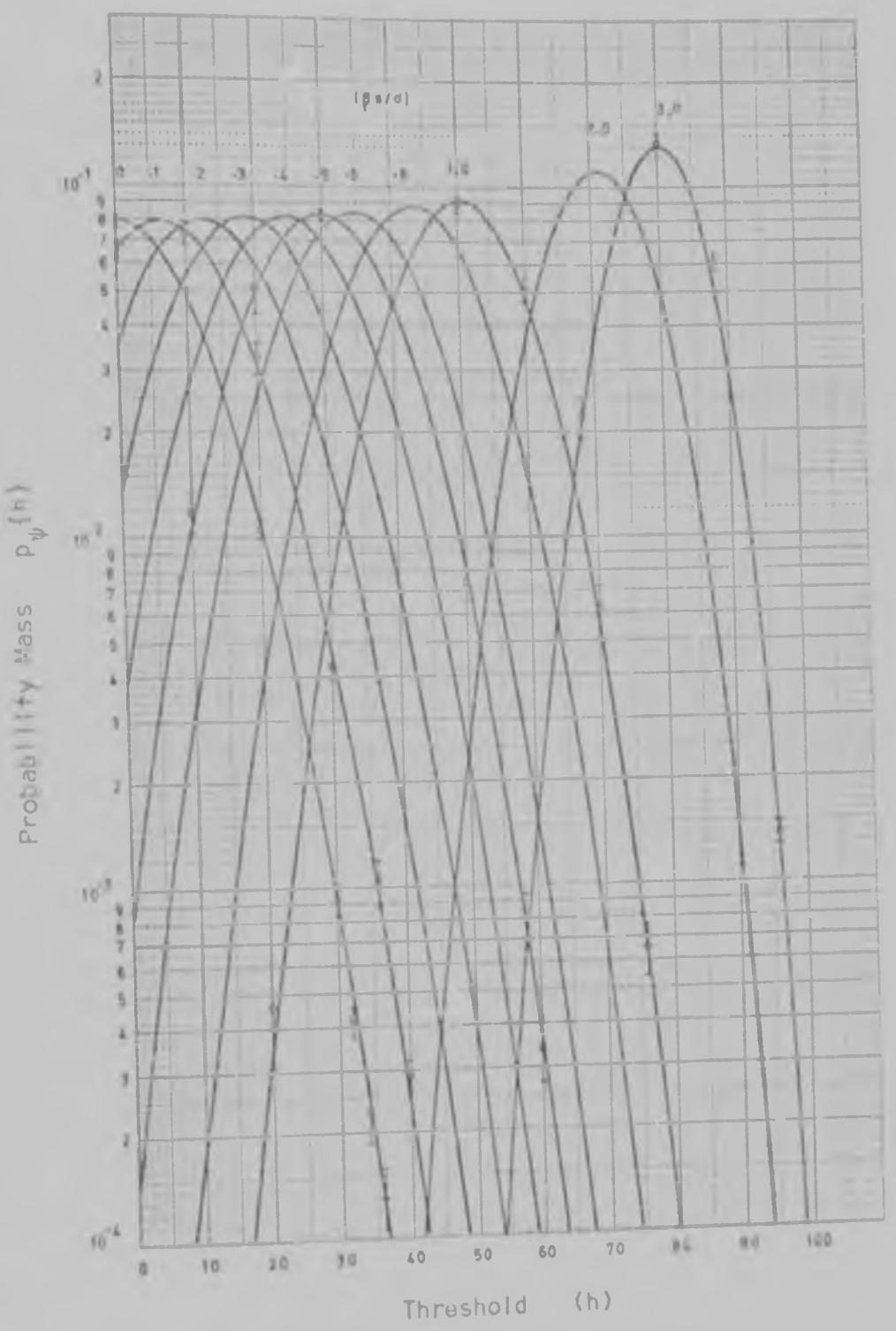

FIGURE 4-11 Probability mass functions of $\psi_R(0)$ for the 100 sample cross-correlation detection of an analog Gaussian reflection corrupted by wideband Gaussian noise.
(βs and σ are the receiver input rms values of the analog Gaussian reflection and the wideband Gaussian noise, respectively).

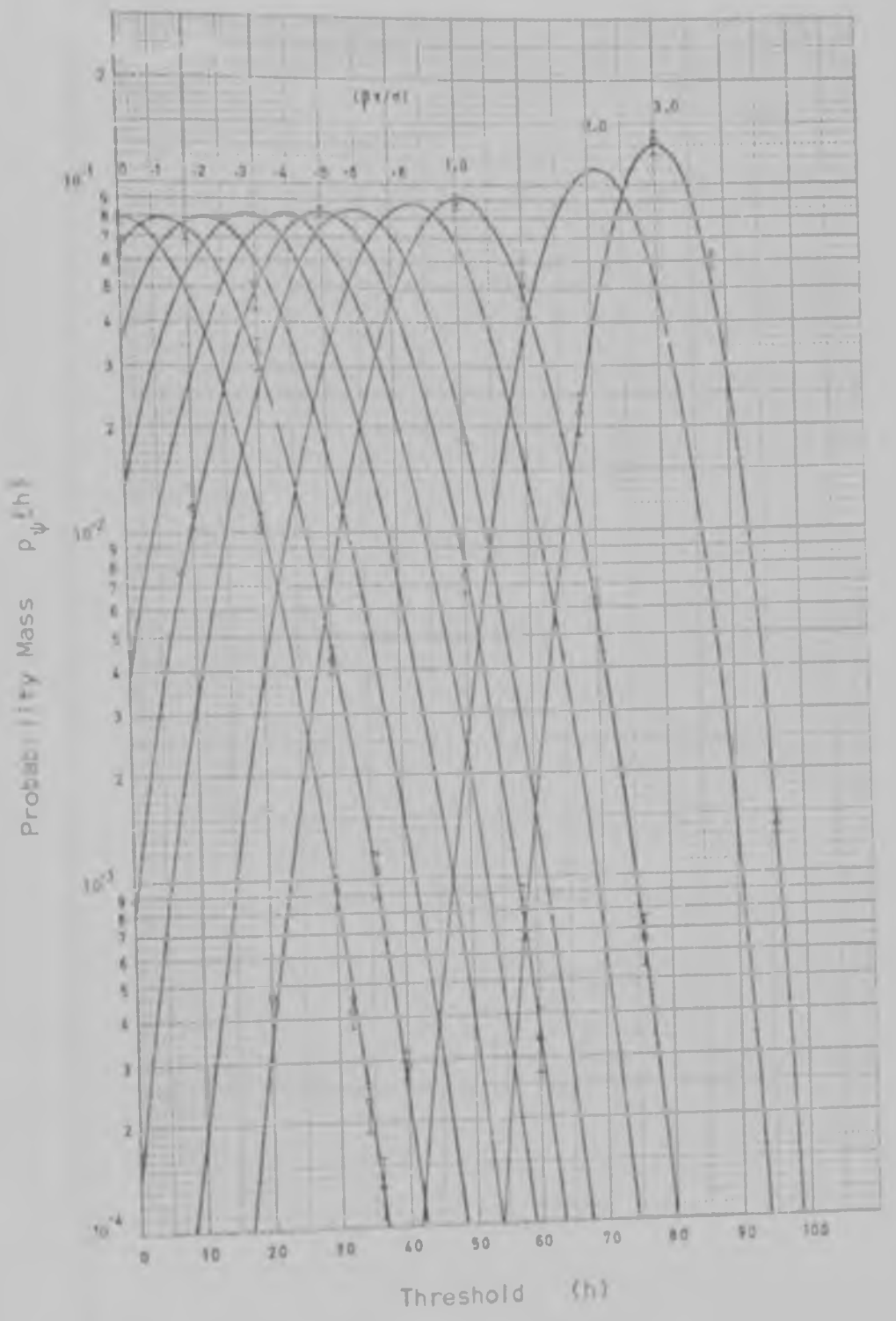

FIGURE 4-11 Probability mass functions of $\psi_0(0)$ for the 100 sample cross-correlation detection of an analog Gaussian reflection corrupted by wideband Gaussian noise.
(β_s and σ are the receiver input rms values of the analog Gaussian reflection and the wideband Gaussian noise, respectively).

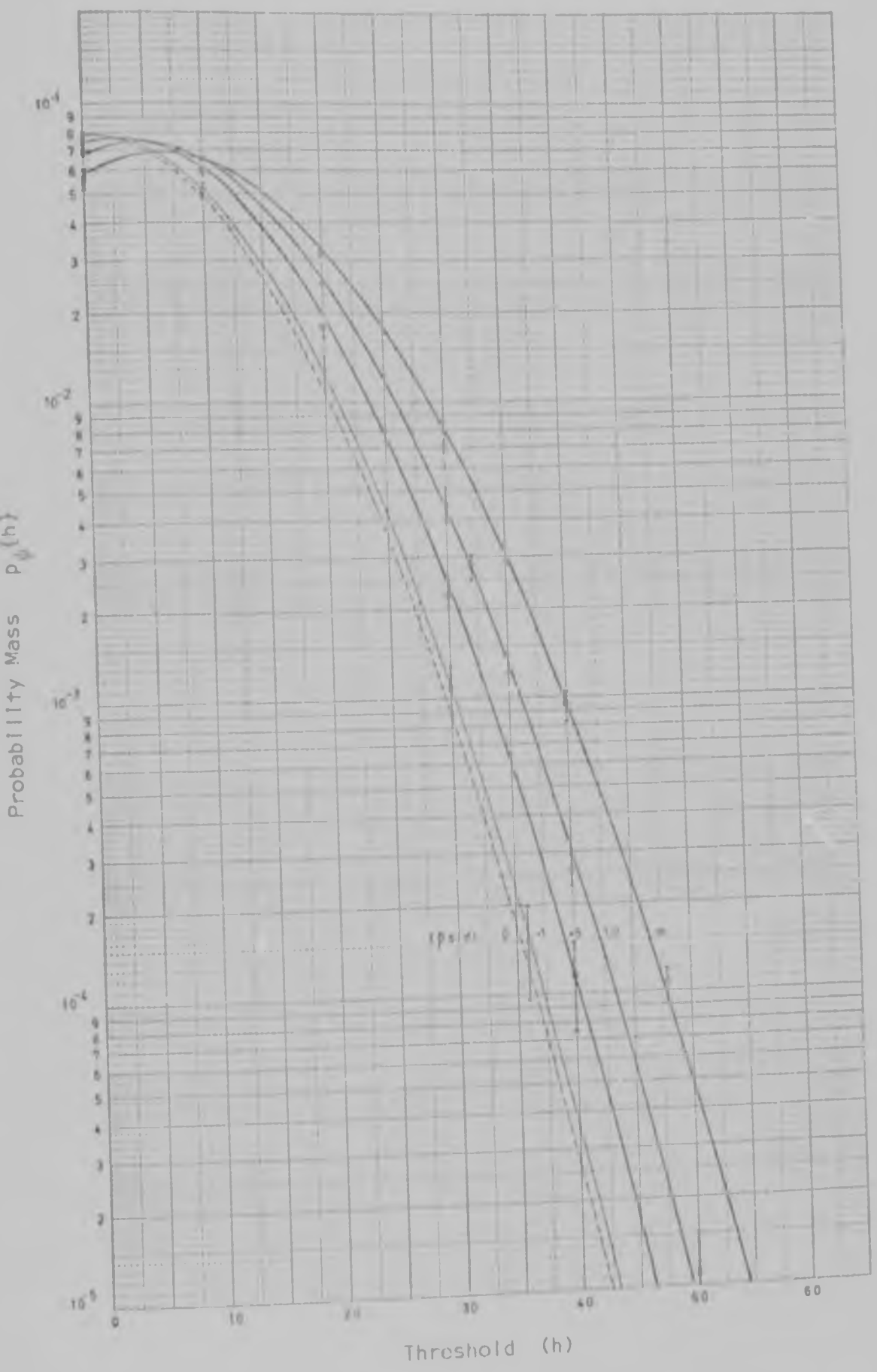

FIGURE 4-12 Probability mass functions of $\psi_0(\tau)$ for the 100 sample cross-correlation detection of an analog Gaussian reflection corrupted by wideband Gaussian noise. ($\tau = 5\pi/2\omega_b$).

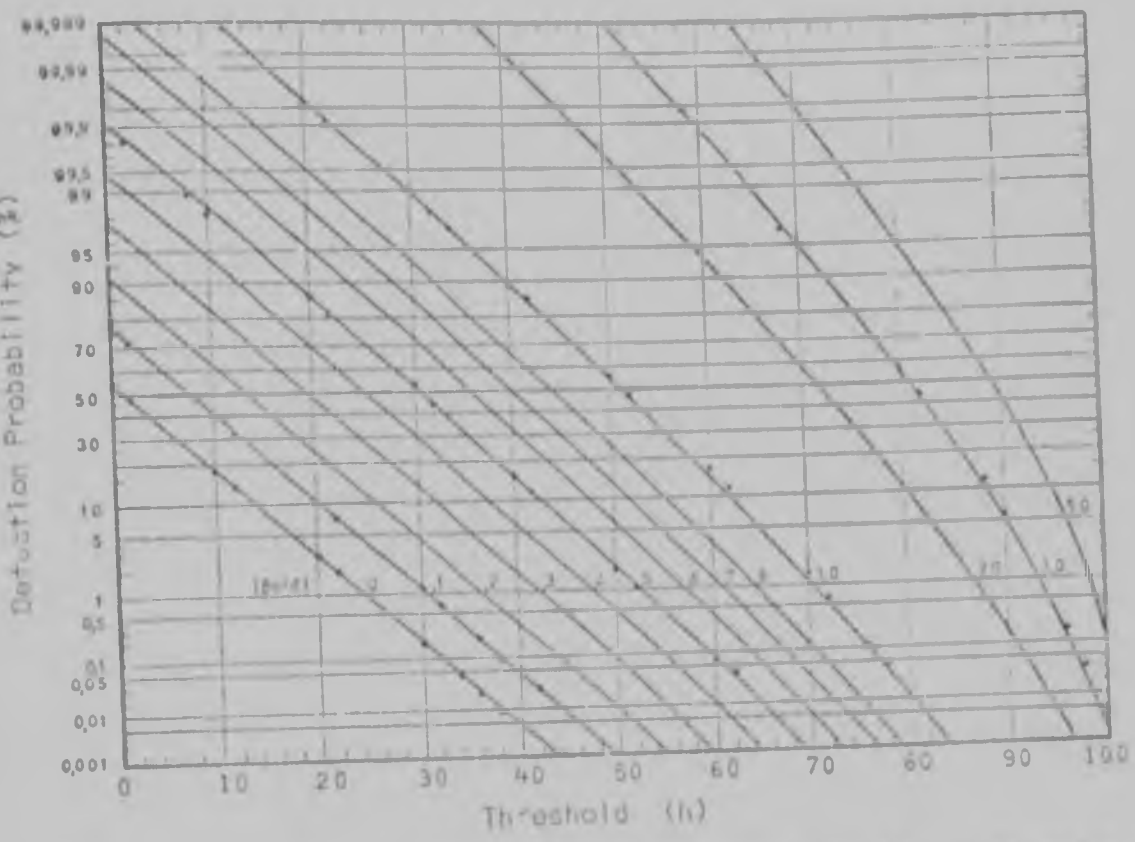

FIGURE 4-13 Detection probabilities of an analog Gaussian reflection corrupted by wideband Gaussian noise. (100 sample cross-correlation).

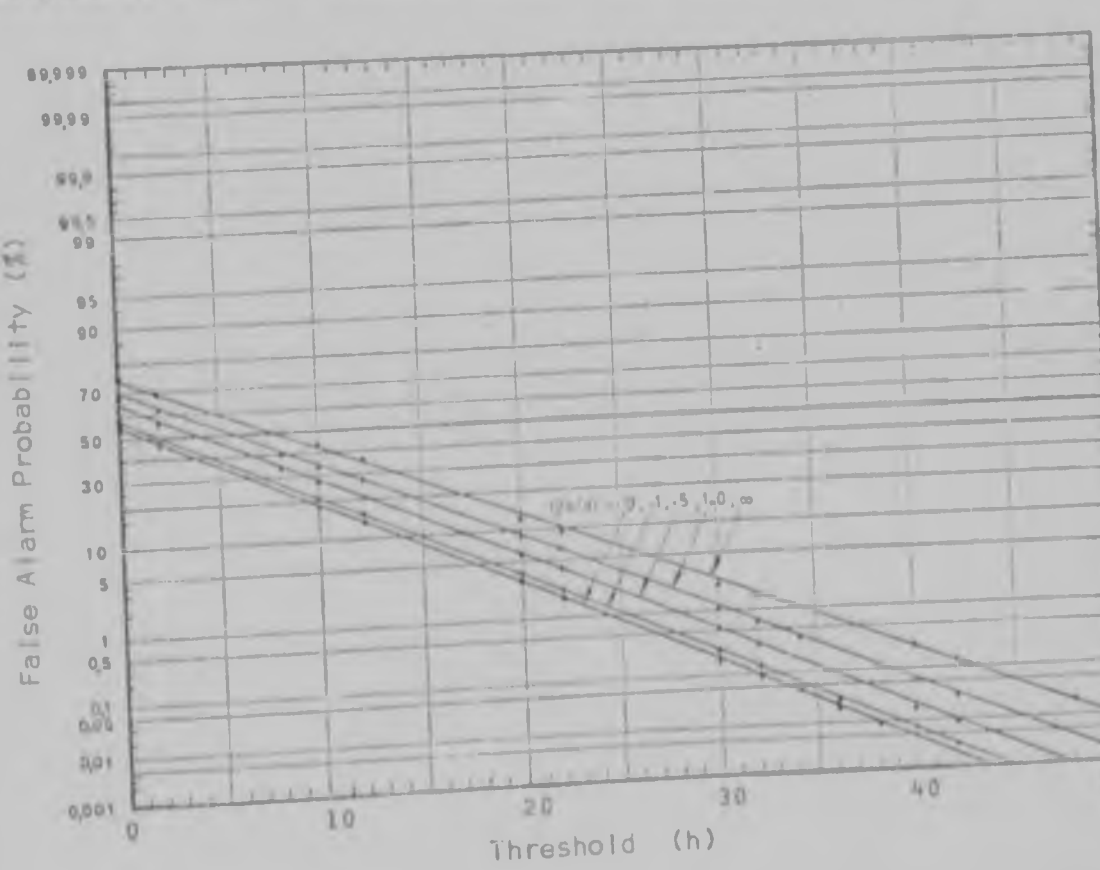

FIGURE 4-14 False alarm probabilities at delay $\tau = 5\pi/2\omega_b$ of an analog Gaussian reflection corrupted by wideband Gaussian noise. (100 sample cross-correlation).

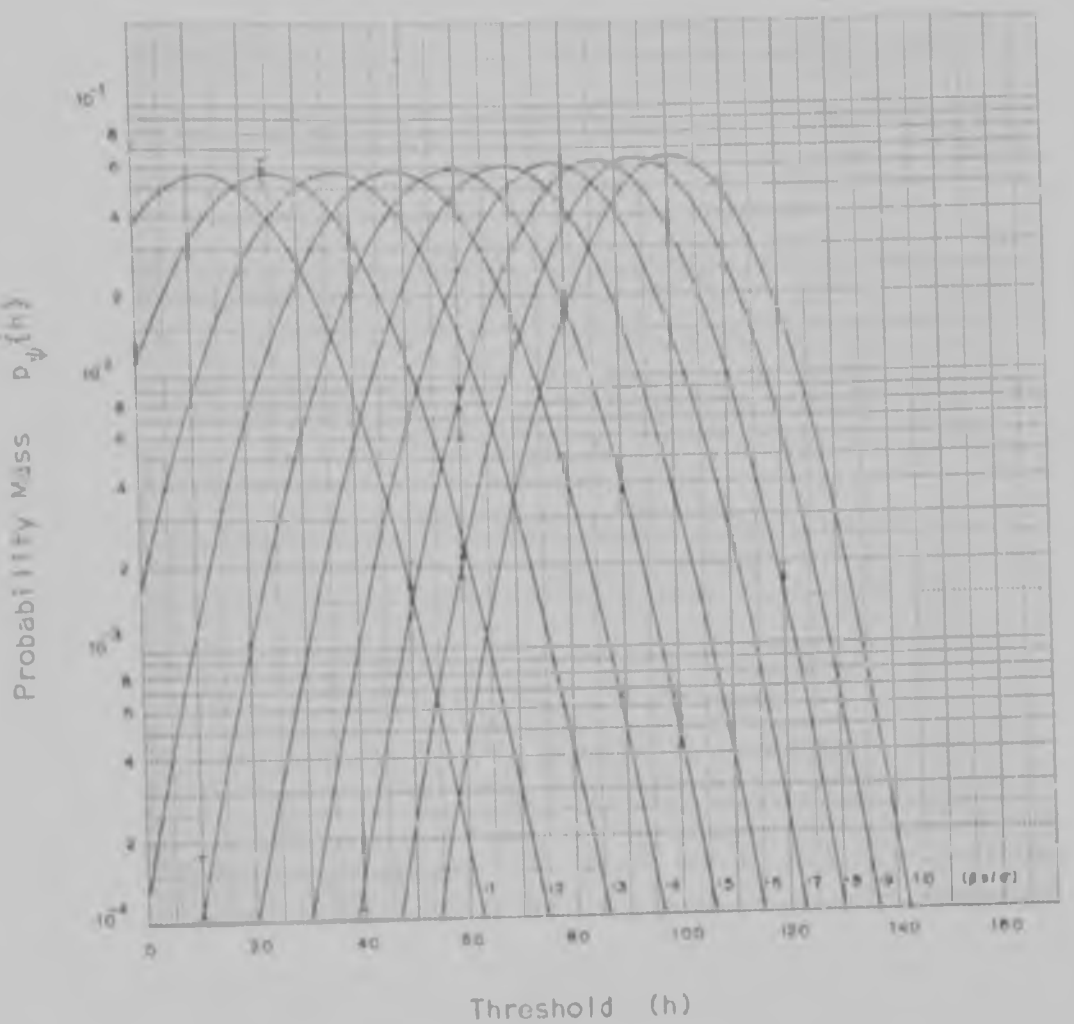

FIGURE 4-15 Probability mass functions of $\psi_n(0)$ for the 200 sample cross-correlation detection of an analog Gaussian reflection corrupted by wide-band Gaussian noise.

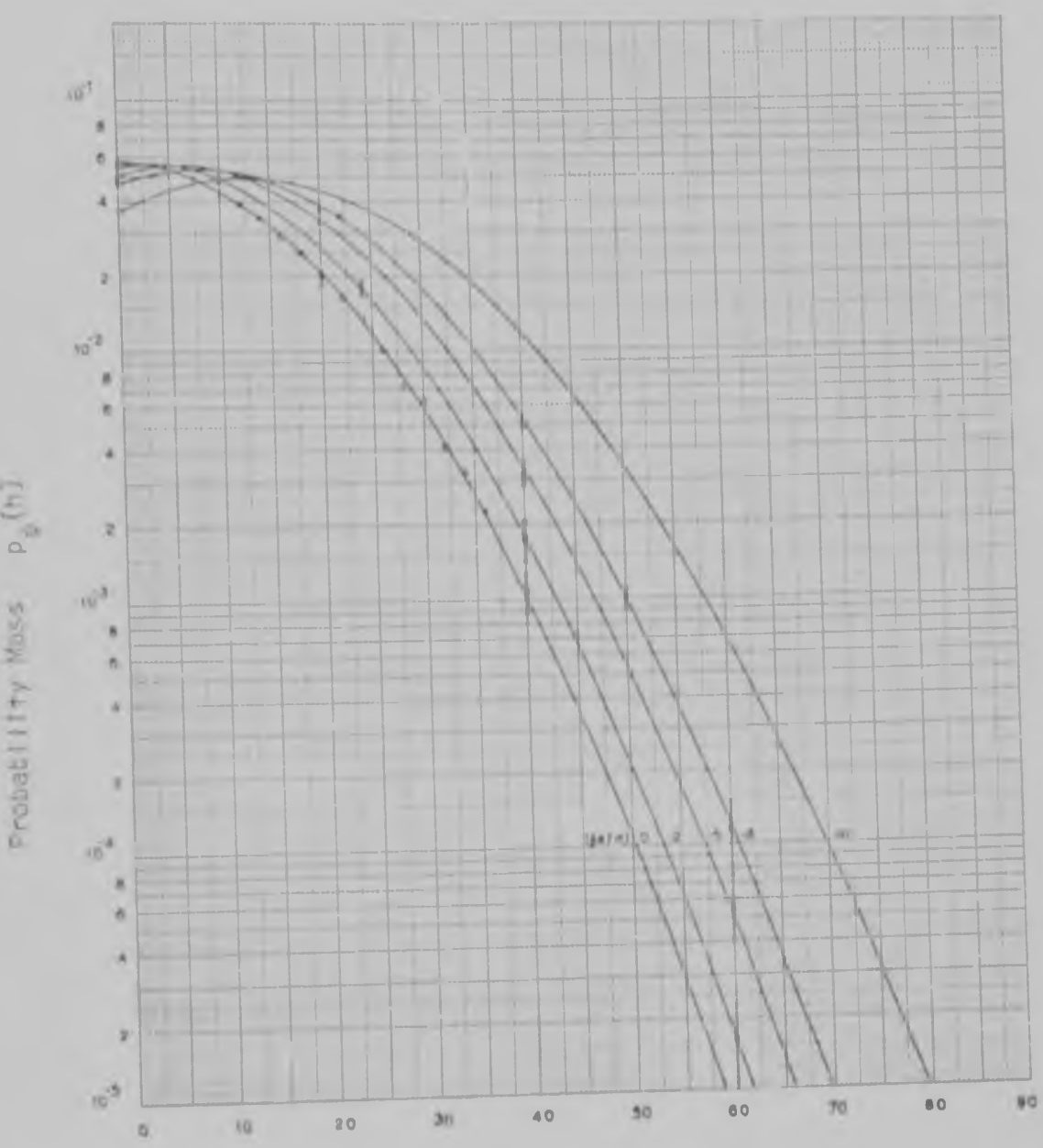

FIGURE 4-16 Probability mass functions of $\psi_0(\tau)$ for the 200 sample cross-correlation detection of an analog Gaussian reflection corrupted by wide-band Gaussian noise. ($\tau = 5\pi/2\omega_b$).

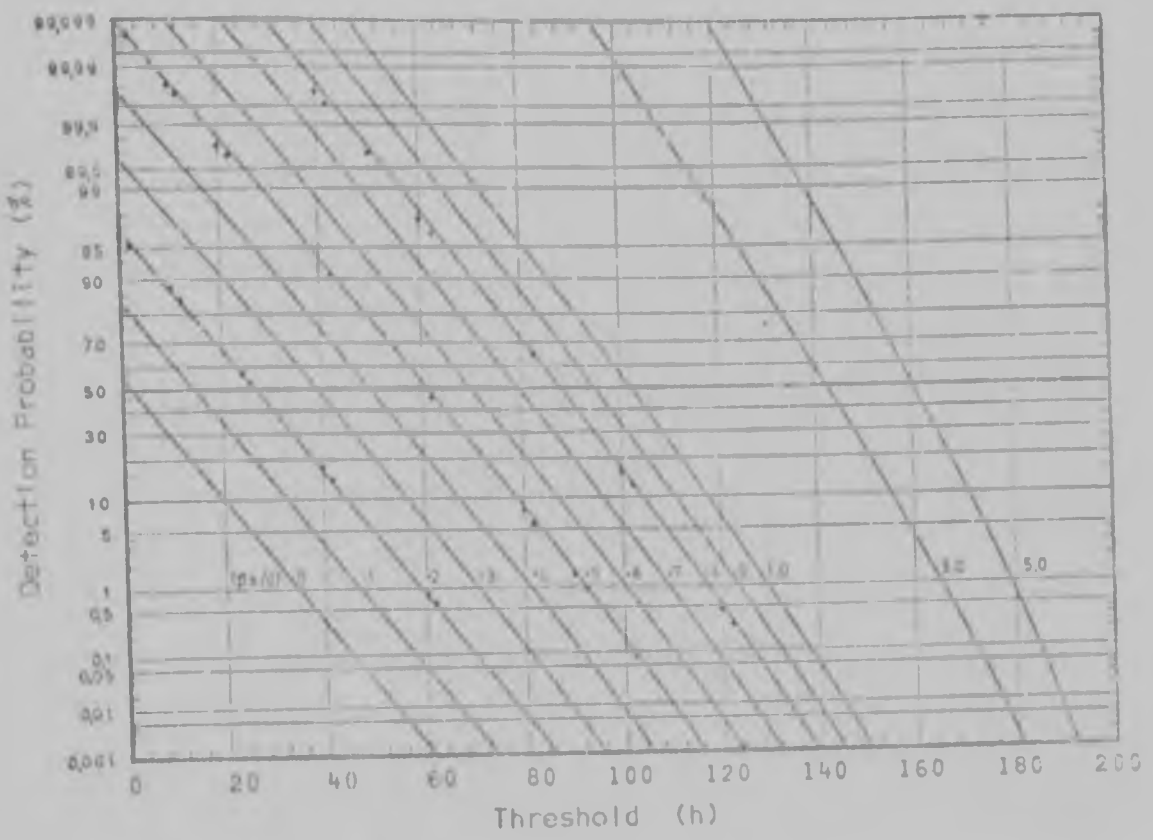

FIGURE 4-17 Detection probabilities of an analog Gaussian reflection corrupted by wideband Gaussian noise. (200 sample cross-correlation).

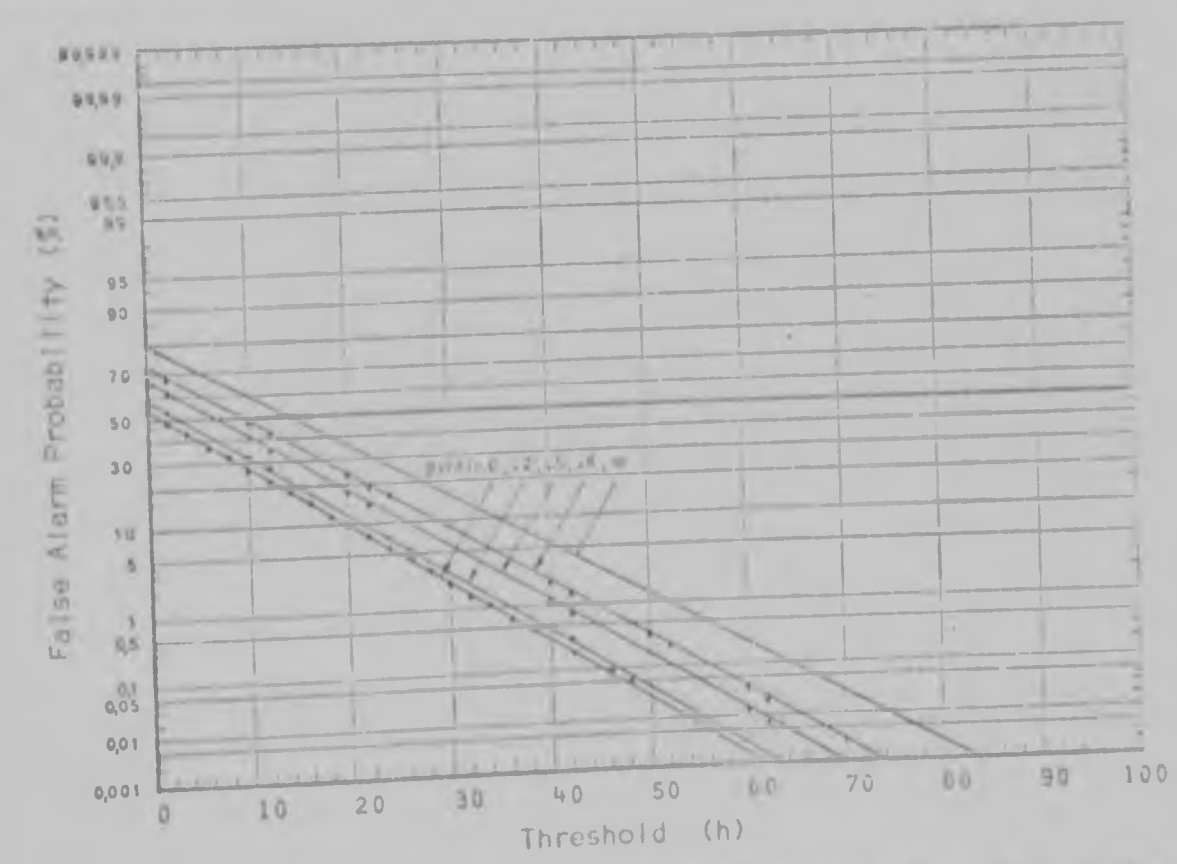

FIGURE 4-18 False alarm probabilities at delay $i = 5\pi/2\omega_b$ of an analog Gaussian reflection corrupted by wideband Gaussian noise. (200 sample cross-correlation).

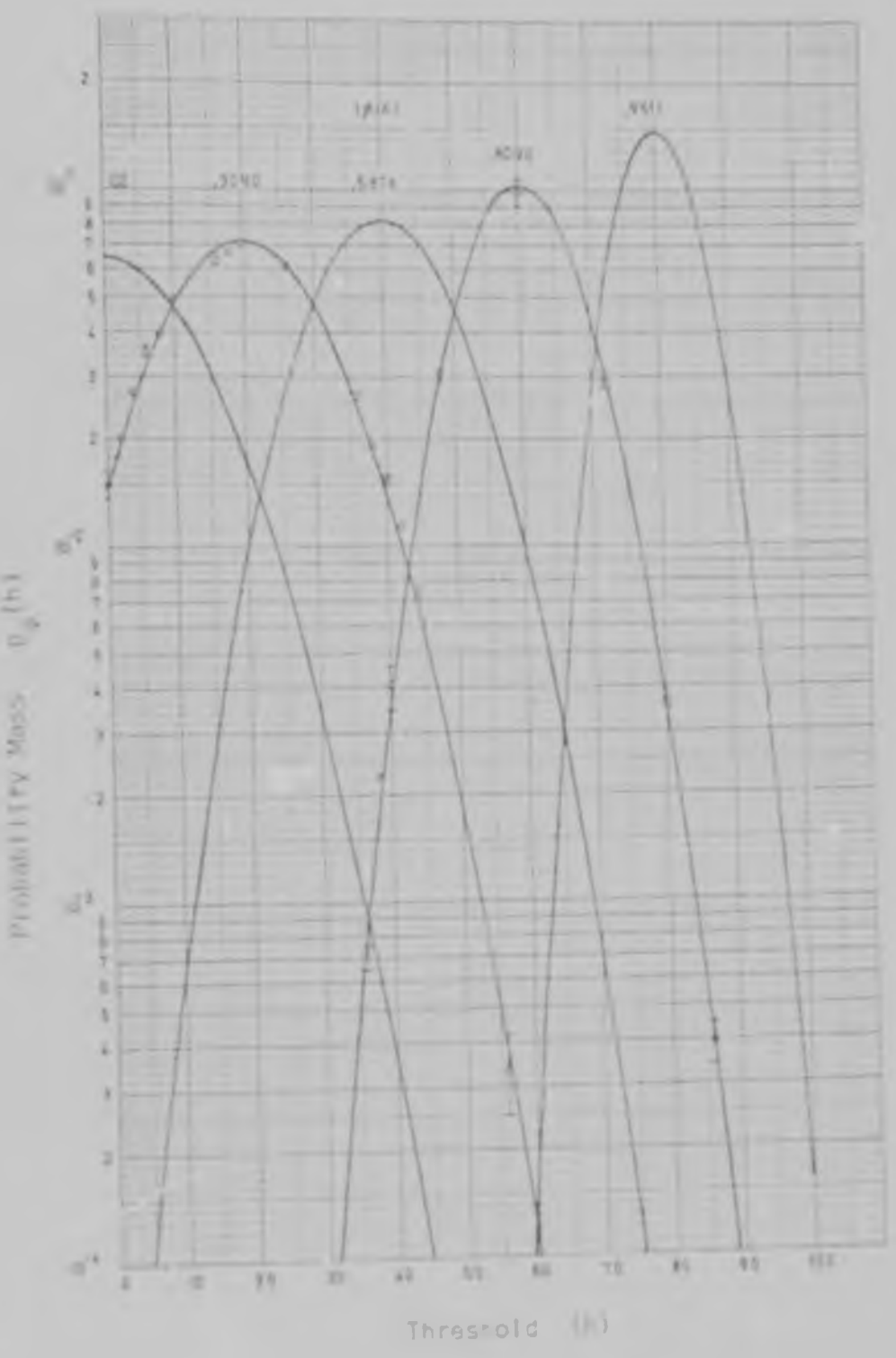

FIGURE 4-13 Probability mass functions of $P_0(h)$ for the 100 sample cross-correlation detection of a single-bit Gaussian reflection corrupted by a random phase sine wave. (Sine wave frequency = 3011 Hz).
(σ is the rms value of the single-bit Gaussian reflection at the receiver input, and A is the peak sine wave amplitude).

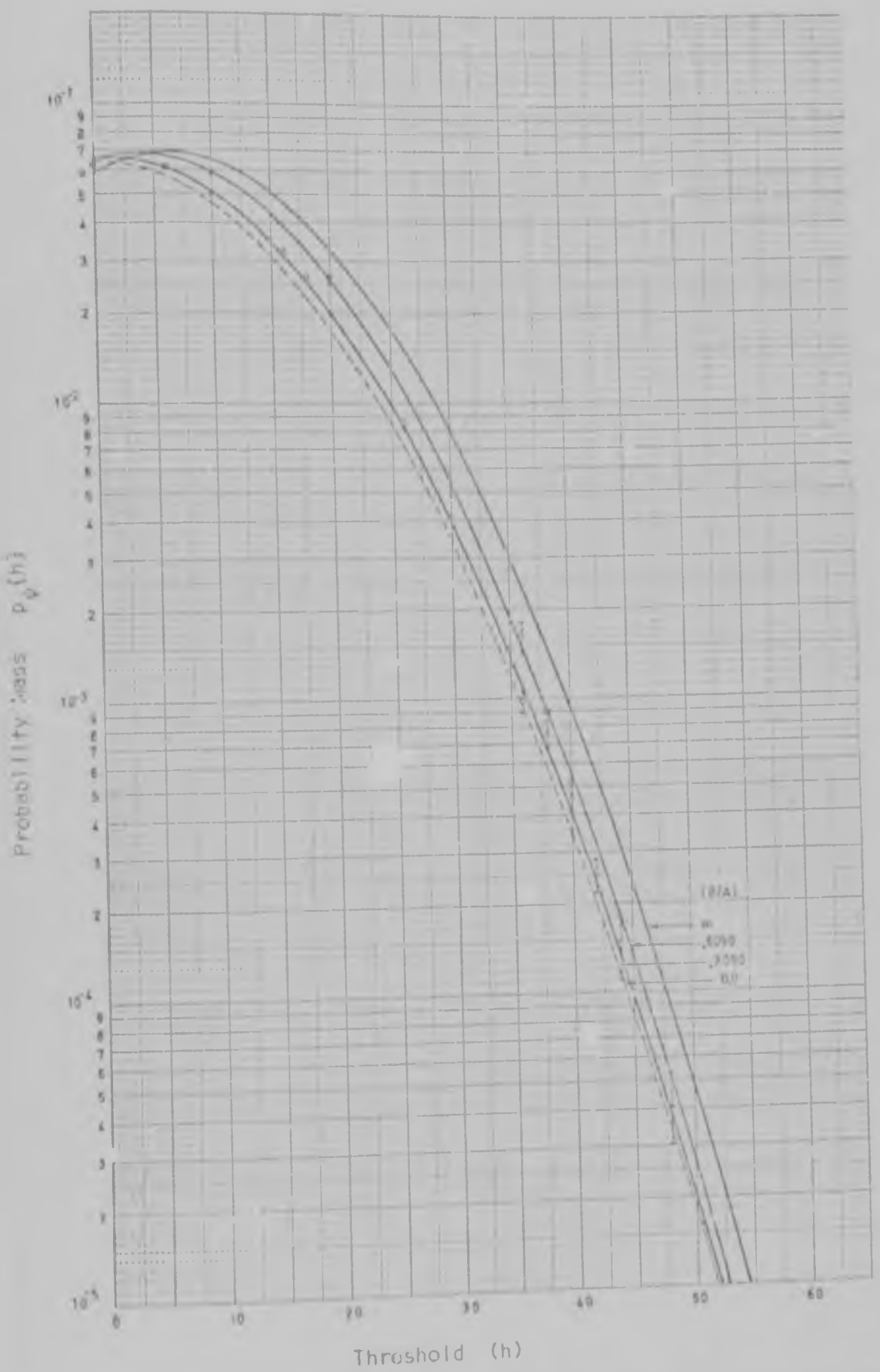

FIGURE 4-20 Probability mass functions of $\psi_0(\tau)$ for the 100 sample cross-correlation detection of a single-bit Gaussian reflection corrupted by a random phase sine wave. ($\tau = 5\pi/2\omega_b$). The curve for $(\beta/A)=\infty$ is identical to that for $(\beta s/\sigma)=\infty$ in Fig. 4-12.

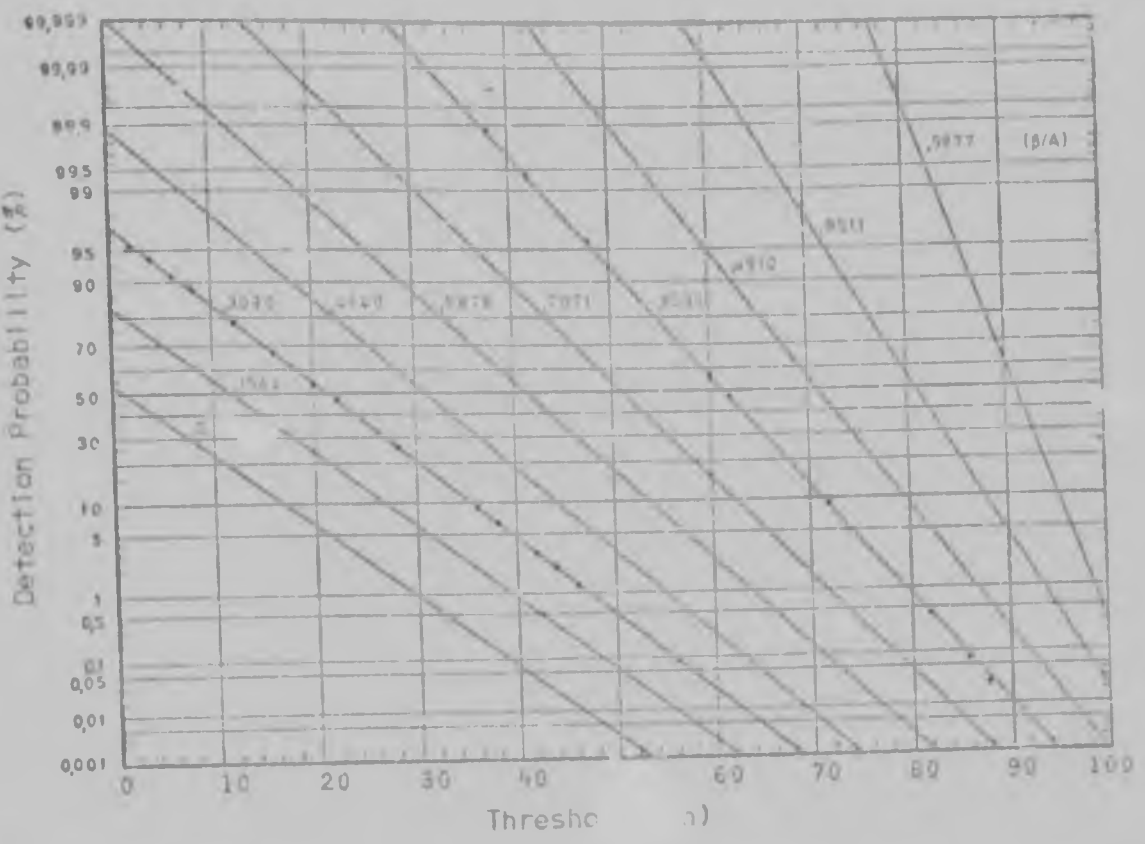

FIGURE 4-21 Detection probabilities of a single-bit Gaussian reflection corrupted by a random phase sine wave. (100 sample cross-correlation).

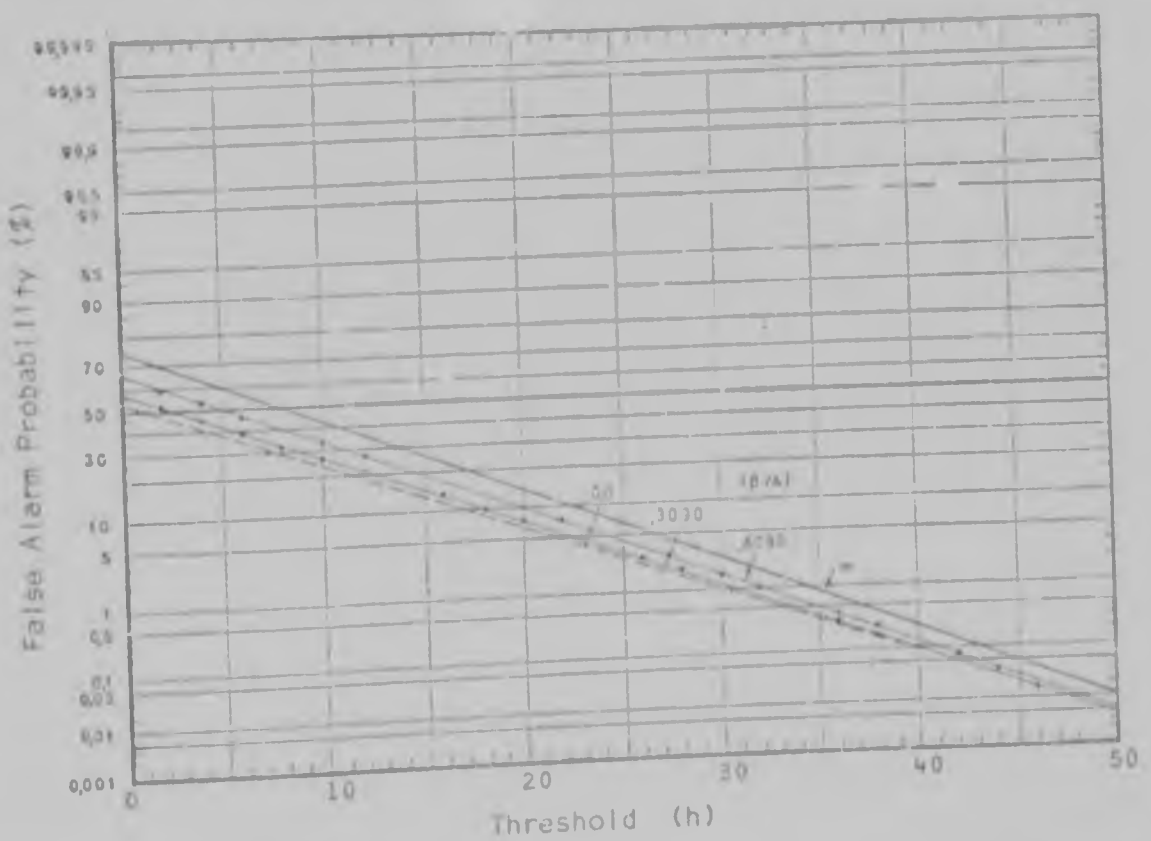

FIGURE 4-22 False alarm probabilities at delay $\tau = 5\pi/2 - b$ of a single-bit Gaussian reflection corrupted by a random phase sine wave. (100 sample cross-correlation).

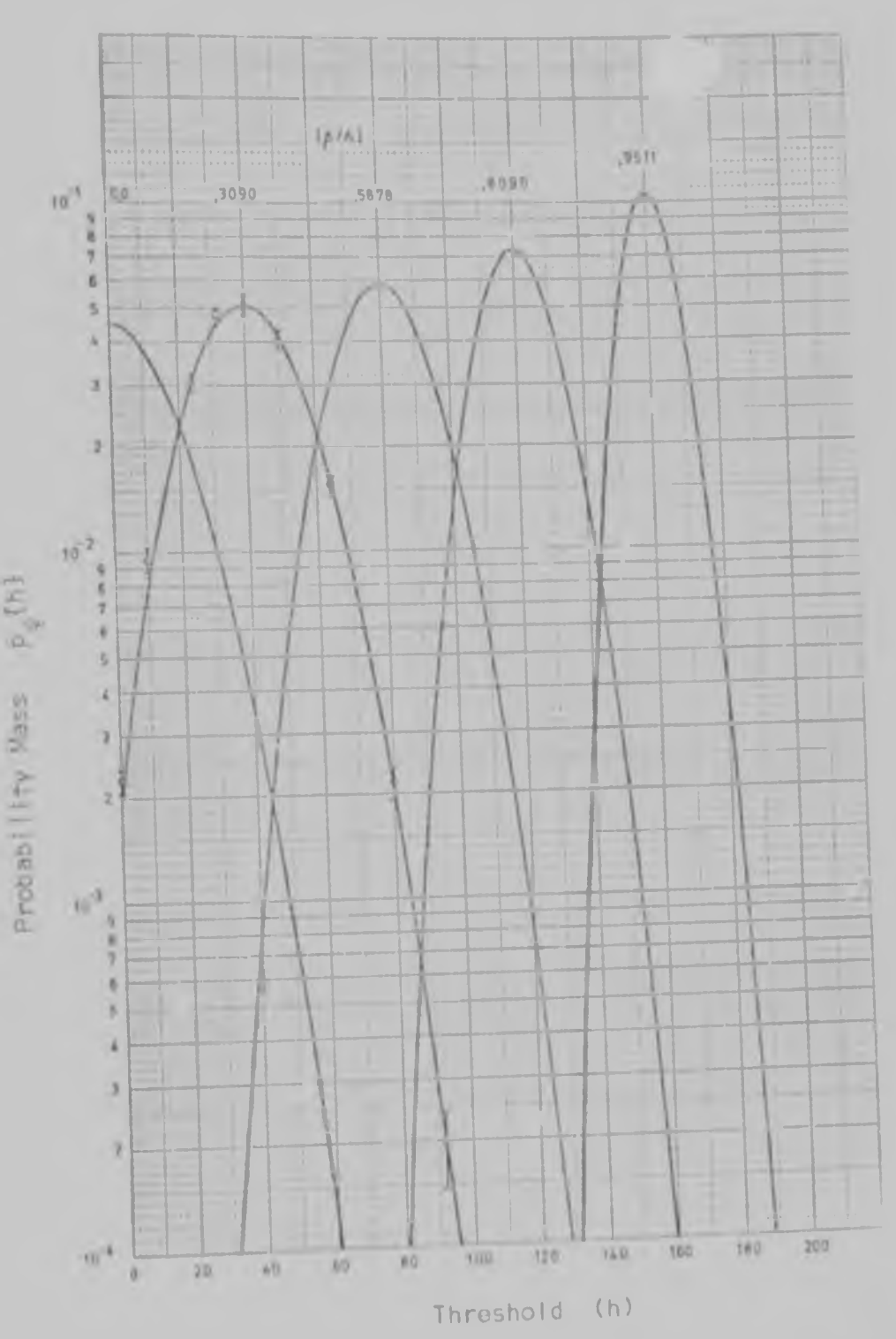

FIGURE 4-23 Probability mass functions of $\psi_D(0)$ for the 200 sample cross-correlation detection of a single-bit Gaussian reflection corrupted by a random phase sine wave. (Sine wave frequency = 3903 Hz).

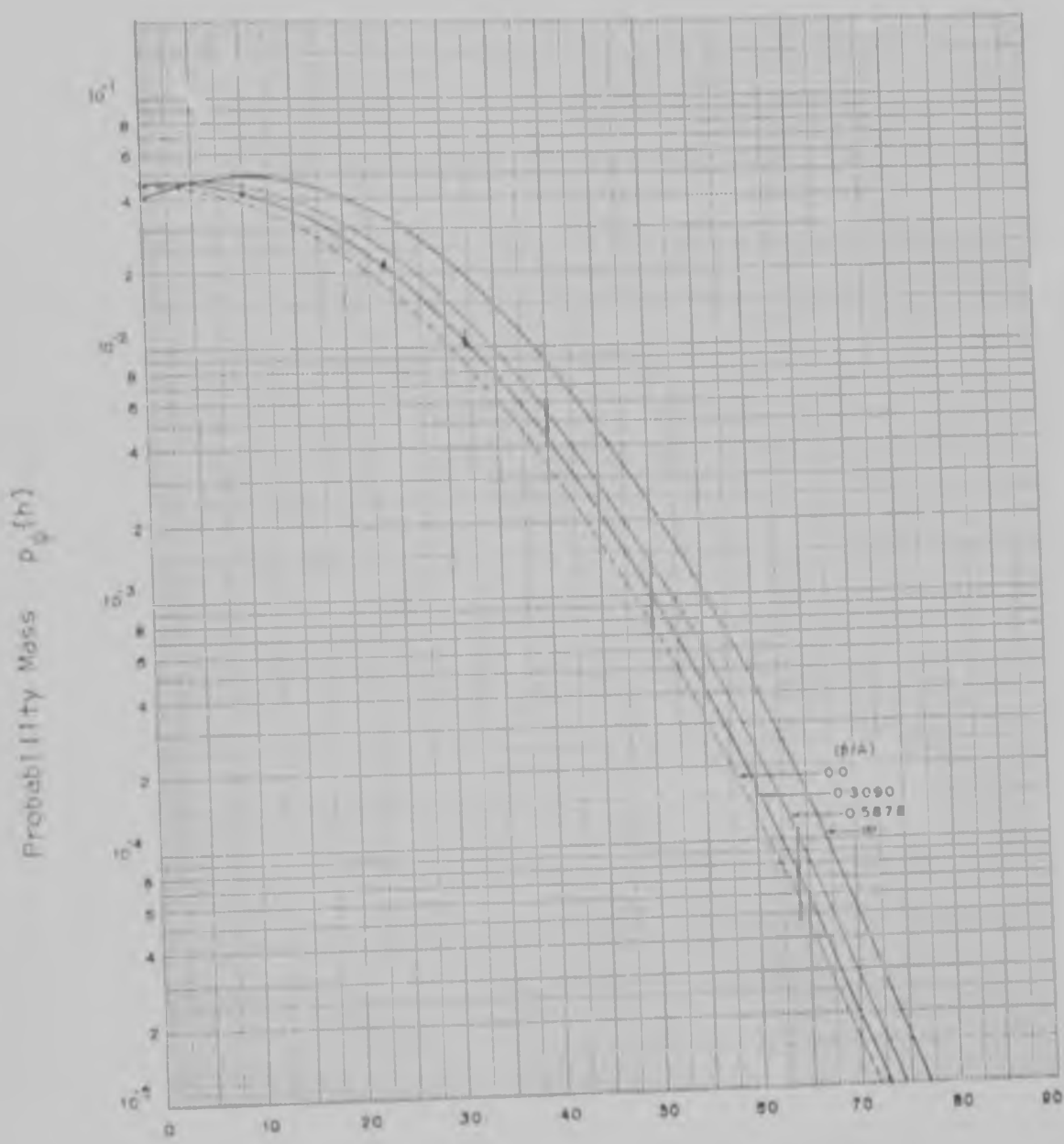

FIGURE 4-2: Probability mass functions of $p_0(\tau)$ for the 200 sample cross-correlation detection of a single-bit Gaussian reflection corrupted by a random phase sine wave. ($\tau = 5\pi/2\omega_b$).

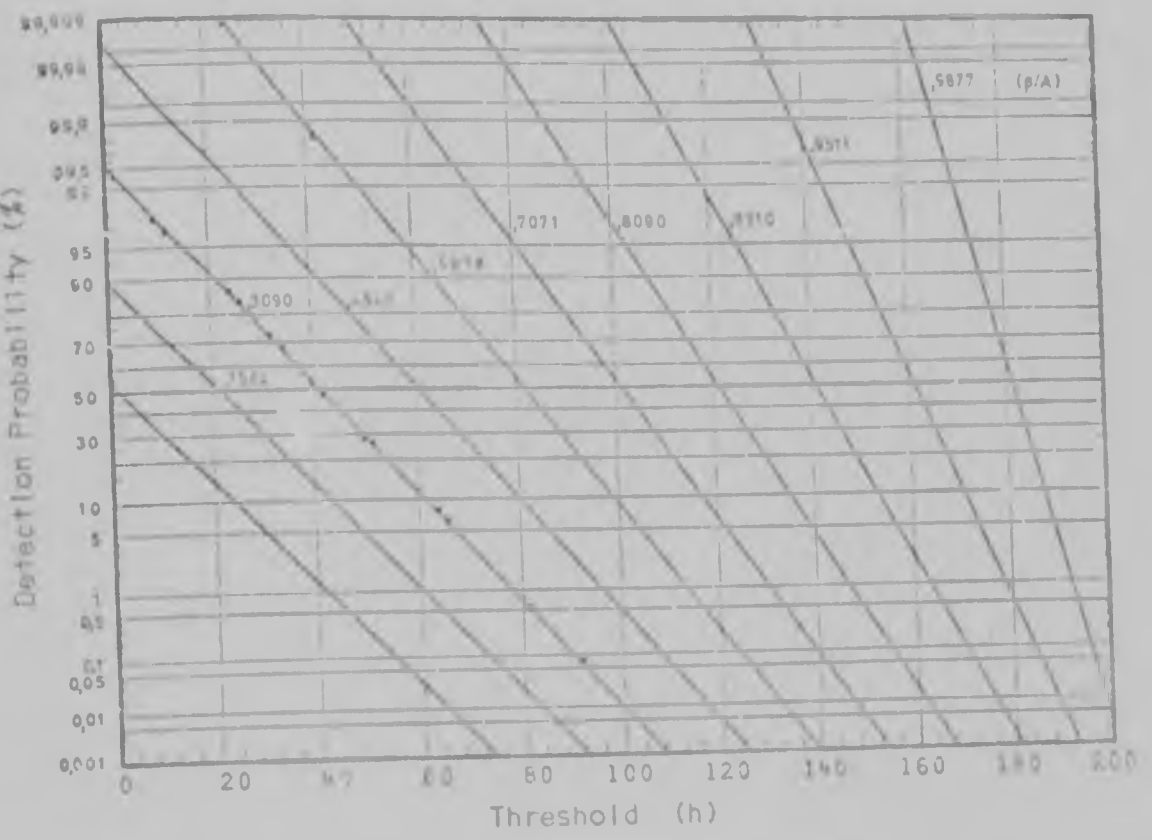

FIGURE 4-25 Detection probabilities of a single-bit Gaussian reflection corrupted by a random phase sine wave. (200 sample cross-correlation).

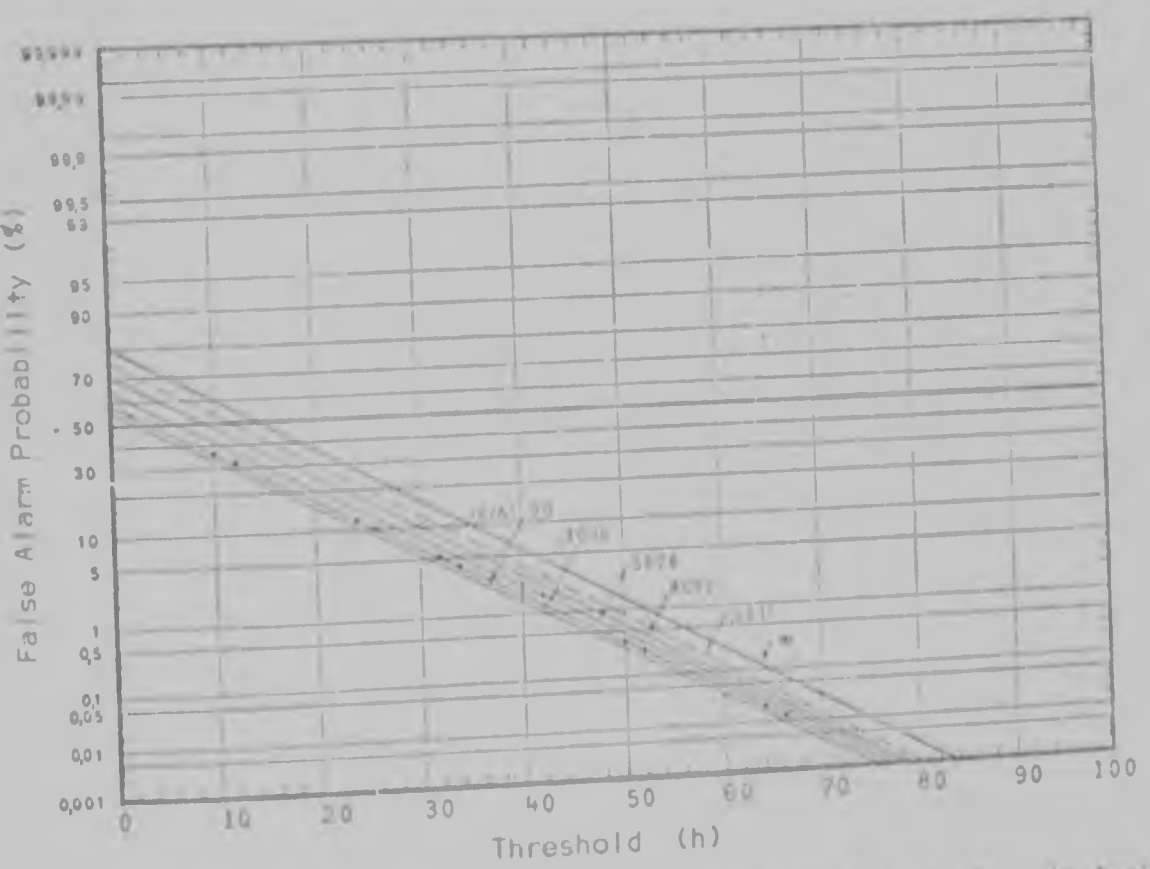

FIGURE 4-26 False alarm probabilities at delay $\tau = 5\tau/2 - b$ of a single-bit Gaussian reflection corrupted by a random phase sine wave. (200 sample cross-correlation).

CHAPTER V

PRACTICAL APPLICATION TO ACOUSTIC REFLECTION DETECTION

In this chapter one of the applications of the cross-correlator mentioned in Chapter one, that of acoustic reflection detection, is briefly investigated. The results are presented in the form of photographs of the monitoring oscilloscope trace. The apparatus used for the investigation is shown in Fig. 5-1.

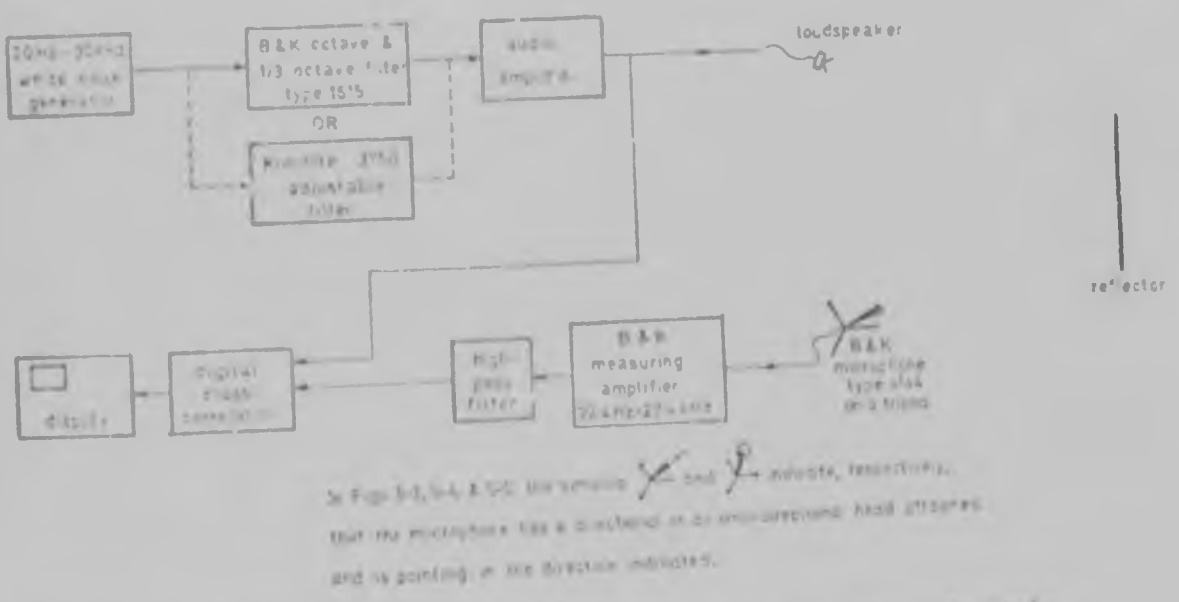

FIGURE 5-1 Apparatus for investigating the cross-correlator's performance in detecting acoustic reflections.

The first point that became apparent was that the noise signal centre frequency and the cross-correlator sampling frequency had to be matched. If the sampling frequency was too high, too few zero-crossings occurred within the 200 samples. This resulted in very large deviations

in the cross-correlation function, making the output unintelligible. Figure 5-2a shows the result of an 80 kHz sampling frequency on a noise signal having an octave bandwidth centred on 3.15 kHz. When the

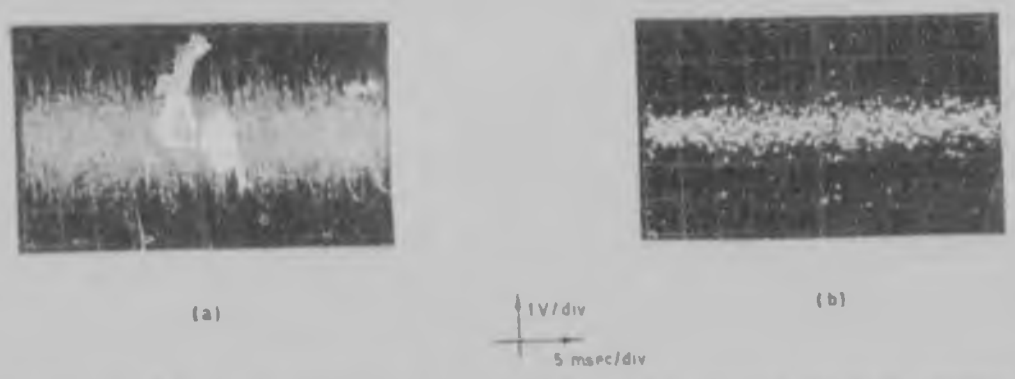

FIGURE 5-2[+] The effects of the sampling frequency on the cross-correlator output. (a) Frequency too high. (b) Frequency matched.

sampling frequency was reduced to 11 kHz, the cross-correlator output changed to that shown in Fig. 5-2b, revealing the presence of a reflection peak at 27.4 milliseconds delay. It was found that a sampling frequency of ten times the centre frequency of the noise signal, or less, yielded satisfactory results. This ensured that there were enough zero-crossings of the received and reference waveforms incorporated in the sets of samples being cross-correlated to avoid the excessive deviations illustrated in Fig. 5-2a. However, the lower the sampling frequency, the fewer the number of cross-correlations performed within the duration of the zero-delay peak. The increased possibility of missing the peak due to its lying in between two samples sets a lower limit on the sampling frequency. Generally speaking, the sampling frequency should be between one and five times the centre frequency of the noise signal spectrum, and not greater than ten times this frequency.

The bandwidth of the noise signal used was determined by (a) the transmitting loudspeaker's useful operating frequency bandwidth, (b)

[+]All the photographs were taken at $\frac{1}{4}$ second at f4 with ASA400 film.

the 'frequency selectivity' of the reflector, and (c) the receiving microphone's bandwidth. The latter constraint was in this case of no consequence as the microphone's bandwidth was much greater than that of the transmitting loudspeaker. The reasons for the other two constraints are fairly obvious:

(a) The loudspeaker distorted waveforms containing frequency components that were out of its operating frequency range. This caused the transmitted waveform to differ from the reference waveform, resulting in the cross-correlation peaks being attenuated. Thus, for example, it was difficult to detect cross-correlation peaks when using a single-cone, ten inch loudspeaker if the noise signal had a centre frequency above five kilohertz.

(b) The frequency selectivity of the reflector set both a lower and an upper limit on the signal bandwidth. If one used a very narrowband signal (less than a third octave) and its frequency spectrum lay in a poor reflection region for the reflector, it was difficult to detect the reflected signal cross-correlation peaks. Hence, although in most cases one-third octave bandwidth signals give perfectly satisfactory results (Fig. 5-3), when using them, several with different centre frequencies should be tried.

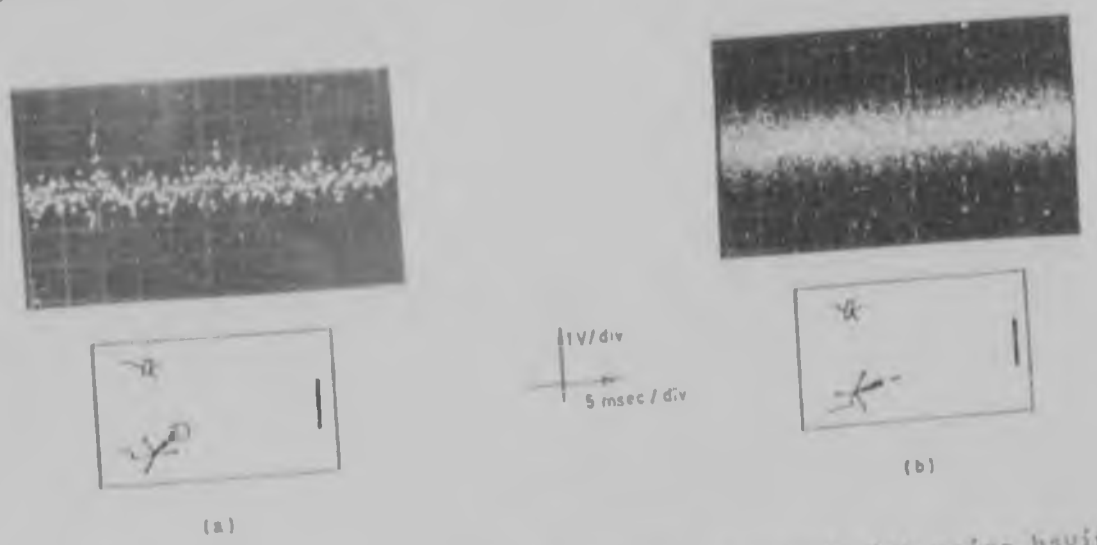

FIGURE 5-3 Cross-correlation functions obtained with noise having one-third octave bandwidths centred (a) on 3.15 kHz, (b) on 16 kHz.

If one used a very wideband signal and the reflector attenuated significant sections of the signal's spectrum, the reflected wave could become badly distorted and differ radically from the incident wave, once again resulting in diminished cross-correlation peaks. For instance, with the reflector used in this experiment, it was plainly audible that frequencies below about two kilohertz were hardly reflected at all. Figures 5-4a to 5-4g show the effect on the cross-correlator output of decreasing the signal bandwidth. Figure 5-4a illustrates the effect of too wide a bandwidth.

It is interesting to note the lack of variation in the spread or form (i.e. distribution) of the cross-correlation function values away from the central peaks as the signal bandwidth is varied. That the range or spread does not change ties in with the observations made in the theoretical analysis that the mean of $\Psi_p(\tau)$ varies over a very small range for $|\tau| > 0$, and that the variance of the distribution is determined primarily by the total number of samples, n, which is a constant. One would therefore expect the spread to remain virtually constant. That the form of the values of $\Psi_p(\tau)$ does not show any marked change (i.e. remains symmetrically distributed and does not develope any obvious 'high probability' or 'favoured' ranges) tends to suggest that the assumptions of convergence to normality are fairly robust, and may in fact hold even for bandwidths down to below an octave. This assumes, of course, that the signal centre frequency and the sampling frequency remain matched, as a very high sampling frequency in relation to the signal centre frequency would invalidate the assumption of independent numbers of zero crossings of the signal in non-overlapping intervals. This would then invalidate the evaluation of the cross-correlation function variance. Figure 5-2a is clear proof of this.

The directivity of the receiving microphone also has an effect on the cross-correlator output. This is illustrated in Fig. 5-5. It was shown in Chapter three that as the number of simultaneous reflections

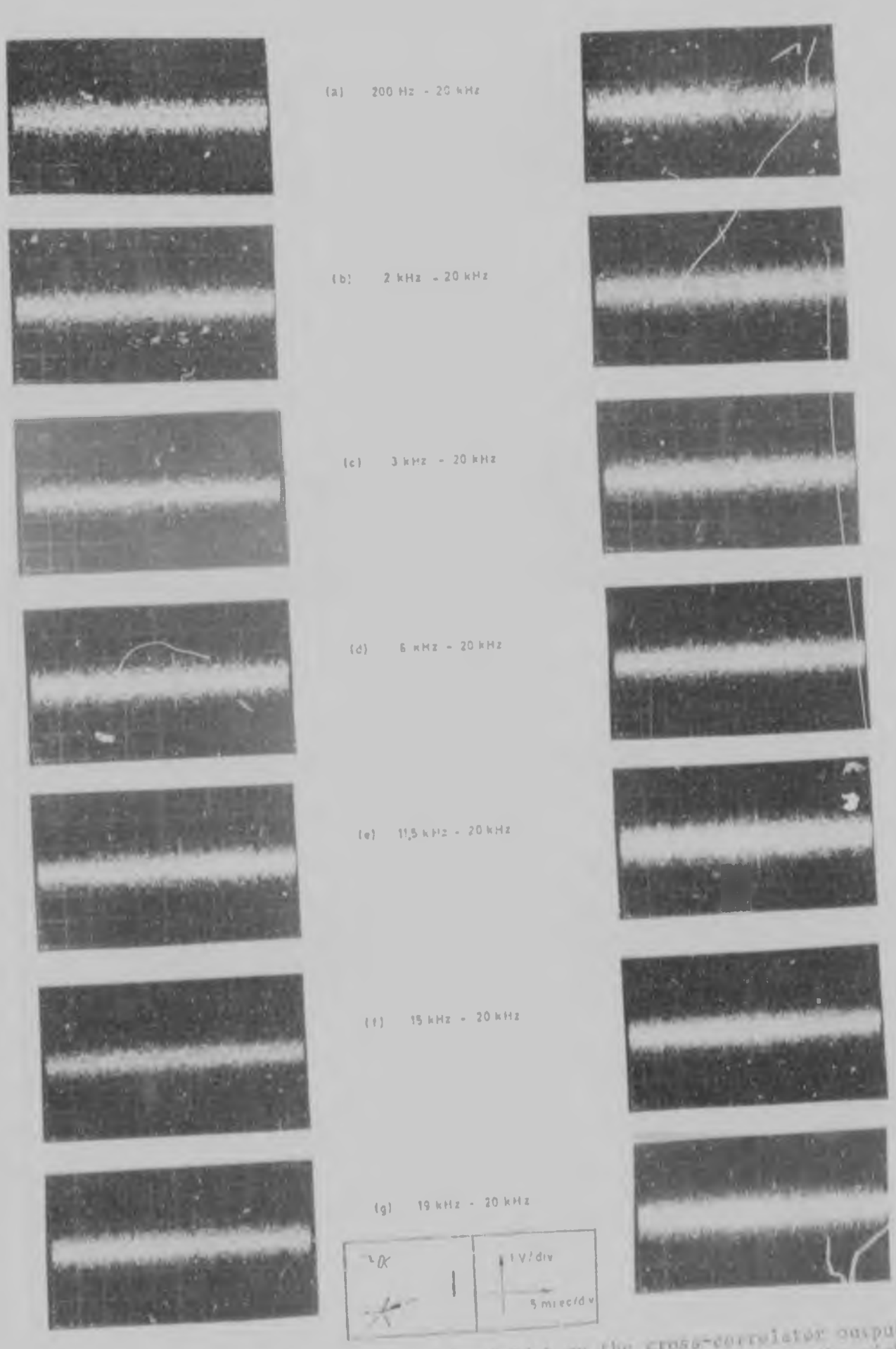

FIGURE 5-4 The effect of signal bandwidth on the cross-correlator output. The sampling frequency in the left hand column was 40 kHz and in the right hand column was 80 kHz.

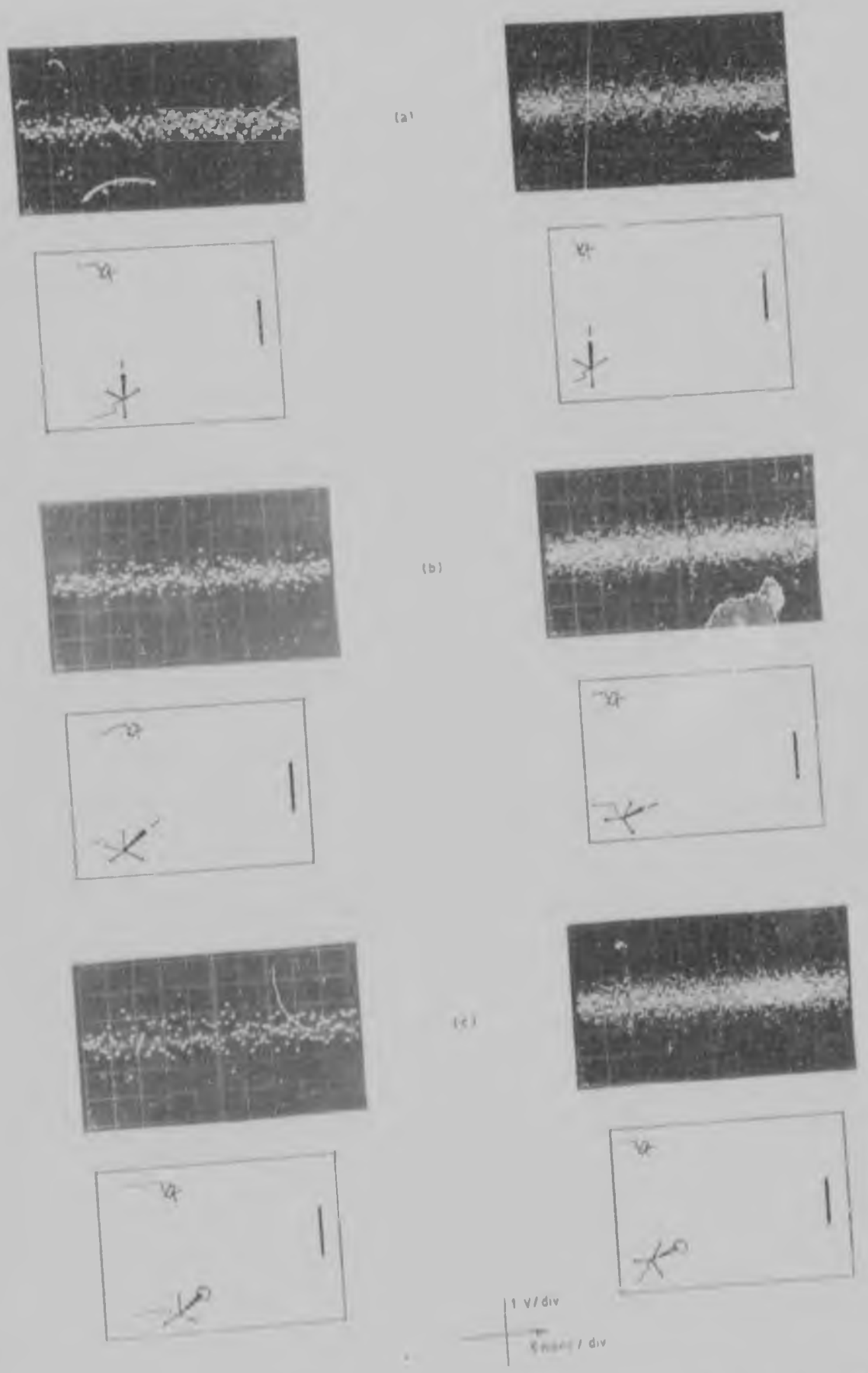

FIGURE 5-5 The effects of microphone directivity on the cross-correlator output. Both sets were taken using a Gaussian signal with an octave bandwidth centred on 3.15 kHz. The sampling frequencies of the left and right hand columns were 3.2 kHz and 40 kHz, respectively.

incident on the receiver increases, so the magnitudes of the individual peaks decrease. This was borne out by the experimental results, as can be seen in Fig. 5-5.

On other important observation was that it was advantageous to pass the received waveform through a high-pass filter having a low frequency cut-off at about 200 Hz. This cut out large, low frequency signals caused by draughts and air-conditioning etc., which distorted the zero crossing pattern of the received waveform causing large, low frequency deviations in the cross-correlator output which made the discerning of peaks more difficult.

To sum up, then:

(1) The noise signal centre frequency and the cross-correlator sampling frequency must be matched.

(2) The noise signal frequency spectrum should be well within the normal operating bandwidth of the transmitting loudspeaker.

(3) Octave bandwidth noise signals give consistently good results. If one-third octave or narrower bandwidth signals are used, several at different centre frequencies should be tried.

(4) Where possible use directional microphones, and

(5) high-pass filter the received waveform to cut out large, low frequency signals caused by draughts, air-conditioning etc..

CHAPTER VI

CONCLUSIONS

The purpose of this thesis has been to investigate the detection reliability of a single-bit digital cross-correlator for detecting either single-bit or analog Gaussian reflections. The output probability mass function has been derived for the cases of the reflected waveform being corrupted by either wideband Gaussian noise or a random phase sine wave, and theoretical predictions have been verified by close agreement with experimental results. Most of the conclusions to be drawn have appeared in the relevant places in the preceding chapters and so only the main ones are given here. The comparisons assume equal receiver input signal-to-noise ratios.

When the reflected waveform is corrupted by wideband Gaussian noise,

(a) the zero delay cross-correlation peaks and detection probabilities obtained using single-bit Gaussian signals are higher than those obtained with analog Gaussian signals, and

(b) the distributions of $\psi_0(\tau)$ for $|\tau|>0$, and hence the false alarm probabilities, are very similar for both single-bit and analog Gaussian signals.

When the reflected waveform is corrupted by a random phase sine wave,

(a) the zero delay cross-correlation peaks are again higher when single-bit as opposed to analog Gaussian signals are transmitted,

(b) the distributions of $\psi_0(\tau)$ for $|\tau|>0$, and thus the false alarm probabilities, obtained with either single-bit or analog Gaussian signals can

be expected to be similar; (they are identical for the two extremes of signal only or noise only at the receiver input).

(c) For single-bit Gaussian reflections and receiver input signal-to-noise ratios below 2.5 dB, the zero delay cross-correlation peaks are lower than those obtained when the corrupting waveform is wideband Gaussian noise, and, since the variances of the two sets of distributions are similar, the detection probabilities tend to be lower as well.

(d) For analog Gaussian reflections, the zero delay cross-correlation peaks are always lower than those obtained when the corrupting waveform is wideband Gaussian noise.

In general, therefore,

(a) although analog Gaussian signals require considerably reduced transmission bandwidths compared to single-bit Gaussian signals, their single reflection detection characteristics are not as good as those of the single-bit signals, and

(b) extraneous sinusoidal-type periodic waveforms are more detrimental to the cross-correlator's detection performance than wideband Gaussian noise is. (This result is of obvious importance to anyone wishing to jam the cross-correlation detector).

The performance of the cross-correlator under multiple reflection conditions was investigated in Chapter three and it was seen that if a single-bit Gaussian signal signal is transmitted, then for the special case of double reflections in a low extraneous noise level environment, only the larger of the two reflections will be detected. This effect was in fact shown to prevail regardless of the form of the single-bit waveform transmitted. However, when an analog Gaussian signal is transmitted, although the zero delay cross-correlation peaks are not as sharp and well-defined, this double reflection defect does not occur. This defect of single-bit waveforms is a serious disadvantage in multiple

reflection applications.

The false alarm probabilities of the cross-correlator depend upon the exact delay τ, and hence it is difficult to specify an 'average' false alarm rate for the detector. The only false alarm rate curve that is independent of τ is that for zero receiver input signal-to-noise ratio, and thus this curve could be used to give some measure of the average false alarm probabilities.

The detection probabilities evaluated here assume that the cross-correlation function will be calculated exactly at its peak value, i.e. at $\tau=0$. Since τ is continuous but the cross-correlation instants are discrete, this will probably rarely be the case. However, if the reflector is stationary, the correlator clock frequency can be adjusted until one of the sampling (and hence cross-correlation) instants does coincide with the cross-correlation peak. Alternatively, if the reflector is moving, it will pass through ranges corresponding to exact multiples of the sampling interval. In any event, in most practical applications the sampling frequency will be such that more than one cross-correlation is performed within the duration of the zero delay peak, so the probability of missing the peak altogether is remote. No trouble was experienced with this problem in the experiments described in Chapter five, even at very low sampling frequencies.

The results of Chapter five indicate that the performance of the cross-correlator in detecting acoustic reflections is adequate provided that the sampling rate and the signal centre frequency are matched. It appears that a sampling frequency of between one and ten times the signal centre frequency is suitable. Noise signals having one-third octave bandwidths give acceptable results in many cases; they must however, be used with care, especially if the reflector is frequency selective. When they or any other very narrowband Gaussian signals are used, it is advisable to try several having different centre frequencies. Wide

bandwidth Gaussian signals give good results when the transmitting loudspeaker can handle them without bad distortion, and the reflector does not attenuate large portions of the signal spectrum. Octave bandwidth Gaussian signals offered a good compromise between all the constraints and gave consistently satisfactory results. The experimental results bore out the theory of Chapter three by showing that the amplitudes of the individual cross-correlation peaks decrease as the number of simultaneous reflections received increases. This suggests the fairly obvious conclusion that directional microphones should be used where possible.

The theory developed here is applicable to Gaussian signals having frequency spectra other than the brick wall spectrum of the signal used in the theoretical analysis and experimental simulation. It must be remembered, though, that as the bandwidth of the signal is reduced, the assumption of independent numbers of zero crossings in non-overlapping intervals becomes less realistic. However, the results of Chapter five showed that as the signal bandwidth was reduced from 200 Hz-20 kHz to 19 kHz-20 kHz, there was no marked change in the form or spread of the cross-correlation function values away from the peaks (provided that the signal centre frequency and the sampling frequency were kept matched). As mentioned there, this is to be expected, and does suggest that the assumptions of independence between numbers of zero crossings in non-overlapping intervals etc. and the convergence theorems are fairly robust and may apply for narrow bandwidth signals, possibly down to below an octave. One may also surmise that if the reflected signal were to be bandpass filtered so as to exclude all frequency components outside the signal spectrum and hence improve the input signal-to-noise ratio, the resulting distributions would not differ greatly from those predicted using the assumptions and theory developed here. This surmise, however, is based only upon the above experimental observation, the robustness of the Central Limit theorems and the success of the theory in predicting

the infinite signal-to-noise ratio distributions, which indicated that the assumptions and convergence theorems certainly hold for the narrow-band signal used in the simulation. The mean values of the distributions will be as predicted since the expressions derived here for $\psi_{x_1x_1}(\tau)$ would be applicable in that case. Further, the variances have been seen to be dependent mainly upon the number of samples being cross-correlated. The topic has not been pursued further here and is a possible avenue for further research.

It is apparent from the theoretical and experimental results that the distributions of the cross-correlation function away from the central peaks are considerably less dependent upon or affected by the extraneous noise than the central peaks. As a result the correlator is susceptible to poor detection probabilities at high extraneous noise levels. Under these conditions some simple integration or averaging should be performed on the output.

As to future research, firstly there is the topic mentioned earlier of determining the effect on the cross-correlator output distributions of using very narrowband signals, and of bandpass filtering the received waveform. Another relevant topic is the determination of the output distributions when other types of random waveform, for example pseudo-random codes or Barker codes, are cross-correlated. The significance of these repeatable random waveforms is well known. Much of the theory developed for the derivation of the distribution of $\psi_{x_1}(\tau)$ for single-bit burst waveforms would be applicable in those cases, and the zero delay distributions of the two waveforms mentioned would be identical to those derived in Chapter two for single-bit Gaussian signals.

Very recently, high speed 'multiply and add' integrated circuits have made an appearance[38] and these will certainly help to remove one of the major obstacles to economical multiple-bit cross-correlators. Nevertheless, the simplicity of the single-bit cross-correlator will

still be an attraction in applications where it will suffice. Developments in surface acoustic wave devices promise to bring random waveform single-bit cross-correlation detection within the range of many everyday applications such as collision avoidance radars, and it is within the forseeable future that digital cross-correlators with two thousand bit capacities will become available in single LSI packages[39]. But regardless of how small the single-bit random waveform cross-correlator may become, its output will still have a probability distribution function that must be known if its detection performance is to be assessed.

APPENDIX A

AUTO-CORRELATION FUNCTIONS OF VARIOUS BANDLIMITED GAUSSIAN WAVEFORMS

$\rho_f(\tau)$ is the normalised auto-correlation function of $f_n(t)$ which is a bandlimited Gaussian waveform. The derivation of the expression for $\psi_x(\tau)$, the auto-correlation function of $\mathrm{sgn}[f_n(t)]$, i.e.

$$\psi_x(\tau) = \frac{2}{\pi} \cdot \mathrm{Arcsin}[\rho_f(\tau)] \qquad (2.1.7)$$

depends upon $f_n(t)$ and $f_n(t+\tau)$ being bivariate normally distributed, with zero mean and auto-covariance $\rho_f(\tau)$. Davenport and Root[40] show that if the input to a linear system is normally distributed, then the output will also be normally distributed; i.e. if $x(t)$ is Gaussian, then $\int_a^b x(t)h(t)dt$ is Gaussian also, as is $\int_{-\infty}^{\infty} x(\tau).b(t,\tau)d\tau$ for $h(t)$ and $b(t,\tau)$ linear systems. Hence, provided that the bandlimiting of $f_n(t)$ is linear and introduces no dc terms, eqn. (2.1.7) will hold for the single-bit version of $f_n(t)$, i.e. $x_1(t)$. Some examples of the auto-correlation function $\rho_f(\tau)$ of white noise passed through various bandlimiters are given below.

(1) Ideal bandpass filter of width $2\Delta\omega$, centred on ω_a.

$$\rho_f(\tau) = \left[\int_{-\omega_b}^{-\omega_a} + \int_{\omega_a}^{\omega_b}\right] \frac{1}{2(\omega_b-\omega_a)} \cos\omega\tau \, d\omega$$

$$= \frac{\sin\left[\frac{(\omega_b-\omega_a)}{2}\tau\right]}{\left[\frac{(\omega_b-\omega_a)}{2}\tau\right]} \cdot \cos\left[\frac{(\omega_b+\omega_a)}{2}\tau\right]$$

$$= \frac{\sin(\Delta\omega\tau)}{\Delta\omega\tau} \cdot \cos(\omega_a\tau) \quad \ldots\ldots\ldots\ldots\ldots\ldots\ldots\ldots \text{A1}$$

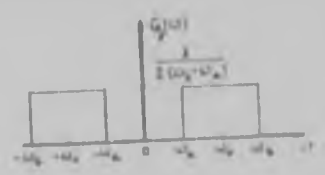

FIGURE A-1

for the special case of a low-pass filter (ω_a=0 in Fig. A-1),

$$\rho_f(\tau) = \frac{\sin(\omega_b\tau)}{\omega_b\tau} \quad \ldots\ldots\ldots\ldots\ldots\ldots\ldots\ldots\ldots\ldots \text{A2}$$

(2) Low-pass RC filter with cutoff frequency $\omega_c/2\pi$

$$\rho_x(\tau) = e^{-\omega_c|\tau|} \quad \text{. . . . . A3}$$

(3) Single-tuned filter[11]

$$G(\omega) = \frac{\Delta\omega}{\pi}\left[\frac{1}{\Delta\omega^2 + (\omega_0 - \omega)^2} + \frac{1}{\Delta\omega^2 + (\omega_0 + \omega)^2}\right]$$

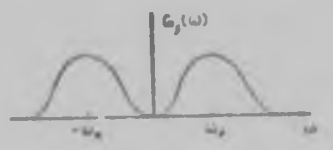

FIGURE A-2

where ω_0 is the centre frequency and $2\Delta\omega$ is the bandwidth

$$\rho_x(\tau) = e^{-\Delta\omega|\tau|}.\cos(\omega_0\tau) \quad \text{. . . . . A4}$$

APPENDIX B

EVALUATION OF THE AUTO-CORRELATION FUNCTI OF $X_2(t)$ [EQN. (2.1.10)]

$$x_2(t) = \mathrm{sgn}[\beta x_1(t) + n(t-\tau)] = \mathrm{sgn}[\beta a_1 + n_1]$$
$$x_2(t+\tau) = \mathrm{sgn}[\beta x_1(t+\tau) + n(t)] = \mathrm{sgn}[\beta a_2 + n_2]$$

so that

$$P_{++} = P\{\beta a_1 + n_1 \geq 0,\ \beta a_2 + n_2 \geq 0\}$$
$$= P\{\beta a_1 = \beta,\ n_1 \geq -\beta,\ \beta a_2 = \beta,\ n_2 \geq -\beta\} + P\{\beta a_1 = \beta,\ n_1 \geq -\beta,\ \beta a_2 = -\beta,\ n_2 \geq \beta\}$$
$$+ P\{\beta a_1 = -\beta,\ n_1 \geq \beta,\ \beta a_2 = \beta,\ n_2 \geq -\beta\} + P\{\beta a_1 = -\beta,\ n_1 \geq \beta,\ \beta a_2 = -\beta,\ n_2 \geq \beta\}$$

The probabilities involving n_1 and n_2 can be separated out as they are independent of a_1 and a_2 and of each other. Therefore

$$P_{++} = P\{n_1 \geq -\beta\}.P\{n_2 \geq -\beta\}.P\{a_1 = 1,\ a_2 = 1\} + P\{n_1 \geq -\beta\}.P\{n_2 \geq \beta\}.P\{a_1 = 1,\ a_2 = -1\}$$
$$+ P\{n_1 \geq \beta\}.P\{n_2 \geq -\beta\}.P\{a_1 = -1,\ a_2 = 1\} + P\{n_1 \geq \beta\}.P\{n_2 \geq \beta\}.P\{a_1 = -1,\ a_2 = -1\}$$

Substituting eqns. (2.1.3) (p. 15) and (3.1.9) (p. 47)

$$P_{++} = \tfrac{1}{4}\left[1+\mathrm{erf}(\beta/\sigma\sqrt{2})\right]^2 \tfrac{1}{4}\left[1+\psi_{x_1}(\tau)\right] + \tfrac{1}{4}\left[1+\mathrm{erf}(\beta/\sigma\sqrt{2})\right]\left[1-\mathrm{erf}(\beta/\sigma\sqrt{2})\right]\tfrac{1}{4}\left[1-\psi_{x_1}(\tau)\right]$$
$$+ \tfrac{1}{4}\left[1+\mathrm{erf}(\beta/\sigma\sqrt{2})\right]\left[1-\mathrm{erf}(\beta/\sigma\sqrt{2})\right]\tfrac{1}{4}\left[1-\psi_{x_1}(\tau)\right] + \tfrac{1}{4}\left[1-\mathrm{erf}(\beta/\sigma\sqrt{2})\right]^2 \tfrac{1}{4}\left[1+\psi_{x_1}(\tau)\right]$$
$$= \tfrac{1}{4} + \tfrac{1}{4}\left[\mathrm{erf}(\beta/\sigma\sqrt{2})\right]^2 \cdot \psi_{x_1}(\tau)$$

Equation (2.1.10) follows directly from $\psi_{x_1}(\tau) = 4P_{++} - 1$.

APPENDIX C

EVALUATION OF THE VARIANCE EXPRESSIONS [EQNS. (2.1.22) AND (2.1.24)]

AND METHOD OF COMBINING INDEPENDENT DISTRIBUTIONS

---

(1) From eqns. (2.1.20) and (2.1.21)

$$E\{x_1(t_i)x_2(t_i+\tau)x_1(t_j)x_2(t_j+\tau)\} = \begin{cases} \psi_{a_1}(t_j-t_i)\cdot\psi_{a_2}(t_j-t_i) & \text{for } t_j<t_i+\tau \\ [\psi_{a_1a_2}(\tau)]^2 & \text{for } t_j\geq t_i+\tau \end{cases}$$

Thus

$$\sum_{i=1}^{N_a}\sum_{j=i+1}^{N_a} E\{x_1(t_i)x_2(t_i+\tau)x_1(t_j)x_2(t_j+\tau)\}$$

$$= \psi_{a_1}(t_2-t_1)\psi_{a_2}(t_2-t_1)+\ldots+\psi_{a_1}(t_{N-N_a}-t_1)\psi_{a_2}(t_{N-N_a}-t_1)+[\psi_{a_1a_2}(\tau)]^2+[\psi_{a_1a_2}(\tau)]^2+\ldots$$

$$+\psi_{a_1}(t_3-t_2)\psi_{a_2}(t_3-t_2)+\ldots+\psi_{a_1}(t_{N-N_a+1}-t_2)\psi_{a_2}(t_{N-N_a+1}-t_2)+[\psi_{a_1a_2}(\tau)]^2+[\psi_{a_1a_2}(\tau)]^2+\ldots$$

etc.

Writing the terms $\psi_{a_1}(t_j-t_i)\psi_{a_2}(t_j-t_i)$ in the above expression as (j-i), for convenience, and remembering that $(t_j-t_i)=(j-i)\delta t$, the expansion becomes

terms= $\psi_{a_1}(t_j-t_i)\psi_{a_2}(t_j-t_i)$ — $(N-N_a-1)$ terms

$(2-1) + (3-1) + \ldots\ldots + (N-N_a-1)$

$+ (3-2) + (4-2) + \ldots + (N-N_a+1-2)$

$+ (N-N_a-1)$

$+ N_a-(N_a-1)$

all terms in first column $=\psi_{a_1}(\delta t)\psi_{a_2}(\delta t)$

Summing columns of like terms:-

$$\sum = \sum_{i=1}^{N-N_a-1}(N_a-i)\psi_{a_1}(i\delta t)\psi_{a_2}(i\delta t)$$

all terms= $[\psi_{a_1a_2}(\tau)]^2$ — $(2N_a-N)$ terms

$+ (N-N_a+1-1) + \ldots + (N_a-1-1) + (N_a-1)$

$+ (N-N_a+2-2) + \ldots + (N_a-2)$

$+ (N-N_a)$

Summing columns of like terms:-

$$\sum = [(2N_a-N)+\ldots+3+2+1][\psi_{a_1a_2}(\tau)]^2$$

$$= \tfrac{1}{2}(2N_a-N)(2N_a-N+1)[\psi_{a_1a_2}(\tau)]^2$$

Thus the double summation becomes

$$\sum_{i=1}^{N-N_a-1}(N_a-i)\,\psi_{x_1}(i\delta t)\,\psi_{x_2}(i\delta t)+\tfrac{1}{2}(2N_a-N)(2N_a-N+1)\left[\psi_{x_1x_2}(\tau)\right]^2 \quad \ldots\ldots\ldots \text{C1}$$

Substituting this into eqn. (2.1.16) yields eqn. (2.1.22).

(2) For the case where the double summation is over i=1 to (N-1) and j=(i+1) to N, the number of columns on the right hand side of the dividing line is N_a, and on the left hand side is $(N-N_a-1)$, as before. Therefore the terms on the right now add up to

$$\left[1+2+3+\ldots+N_a\right]\left[\psi_{x_1x_2}(\tau)\right]^2 = \tfrac{1}{2}.N_a(N_a+1)\left[\psi_{x_1x_2}(\tau)\right]^2 \quad \ldots\ldots\ldots\ldots \text{C2}$$

and those on the left (remembering that the 'triangle' of terms has (N-1) terms along the top and side instead of (N_a-1)) add up to

$$\sum_{i=1}^{N-N_a-1}(N-i)\,\psi_{x_1}(i\delta t)\,\psi_{x_2}(i\delta t) \quad \ldots\ldots\ldots\ldots\ldots\ldots \text{C3}$$

The total sum is then

$$\sum_{i=1}^{N-N_a-1}(N-i)\,\psi_{x_1}(i\delta t)\,\psi_{x_2}(i\delta t)+\tfrac{1}{2}.N_a(N_a+1)\left[\psi_{x_1x_2}(\tau)\right]^2 \quad \ldots\ldots\ldots\ldots \text{C4}$$

The N product terms in the case of continuous waveform cross-correlation are analogous to the N_a product terms in the case of burst waveform cross-correlation, and so the variance can he derived as in eqn. (2.1.16) to be

$$\mathrm{var}\left[\psi_x(\tau)\right] = N-\mu_x^2 + 2\sum_{i=1}^{N-1}\sum_{j=i+1}^{N}E\left\{x_1(t_i)x_2(t_i+\tau)x_1(t_j)x_2(t_j+\tau)\right\}$$

Substituting eqn. (C4) in this yields eqn. (2.1.24).

(3) Consider the two probability mass functions $p_a(n_1)$ and $p_b(n_2)$ of the sums of the N_a and N_b product terms (Fig. C-1a and b). Each term can have value +1 or -1 only, so the discrete mass function values occur at intervals of two. Whether they occur on even or odd numbers depends upon N_a and N_b. In this case (N_a+N_b) is even (100 or 200 samples), so either both are even

or both are odd.

As $p_a(n_1)$ and $p_b(n_2)$ can be assumed independent, $P[n_1=i, n_2=j]$ is equal to $p_a(i)p_b(j)$. Hence the probability of (n_1+n_2) being equal to k, say, is the sum of the products of all pairs of probabilities $p_a(n_1)p_b(n_2)$ for which $(n_1+n_2)=k$. For example, assuming that $N_a>N_b$,

$$p(-2)= p_a(N_b-2)p_b(-N_b)+ p_a(N_b-4)p_b(-N_b+2)+ \ldots + p_a(-1)p_b(-1)+ \ldots$$
$$\ldots + p_a(-N_b-2)p_b(N_b)$$

In general, for $[(n_1+n_2)=2j]\leq|N_a-N_b|$

$$p(2j)= \sum_{i=0}^{N_b} p_a(N_b+2j-2i)p_b(-N_b+2i) \qquad 2j\leq|N_a-N_b| \quad \ldots\ldots\ldots \text{C5}$$

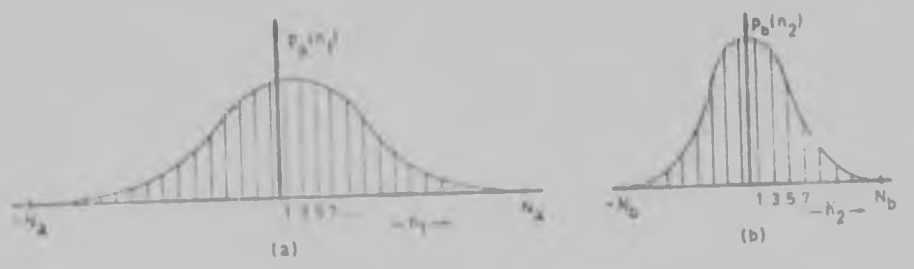

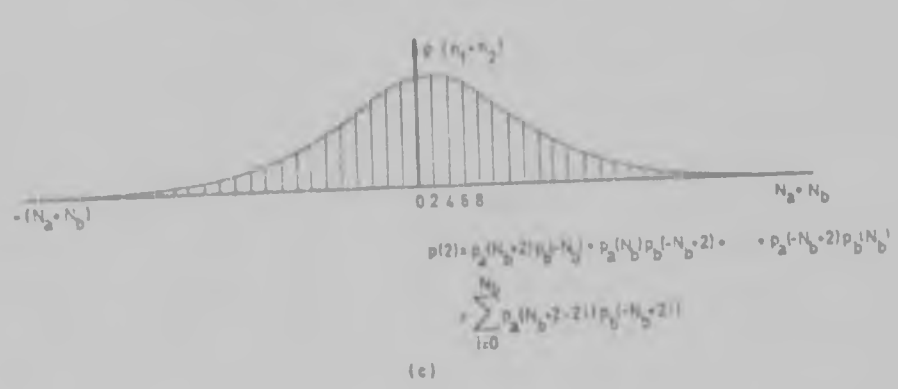

FIGURE C-1 Combination of independent probability mass functions.

For (n_1+n_2) outside this range, the summation does not involve all the $p_b(n_2)$ terms; for instance

$$p(N_a-1)= p_a(N_a)p_b(-1)+ p_a(N_a-2)p_b(1)+\ldots+ p_a(N_a-N_b-1)p_b(N_b)$$

A general expression for this situation would be

$$p(2j)= \sum_{i=\frac{N_b-N_a+2j}{2}}^{N_b} p_a(N_b+2j-2i)p_b(-N_b+2i) \qquad 2j\geq N_a-N_b \quad \ldots\ldots\ldots \text{C6}$$

and a similar expression holds for $2j\leq-(N_a-N_b)$, i.e.

$$p(2j) = \sum_{i=0}^{\left[\frac{N_b+N_a+2j}{2}\right]} p_a(N_b+2j-2i)\,p_b(-N_b+2i) \qquad 2j \leq -(N_a-N_b) \quad \ldots \text{C7}$$

These three general expressions for p(2j) are for N_a and N_b odd. If both are even, expressions similar to these can easily be derived. If $N_b > N_a$, their respective roles in the above analysis is simply reversed.

APPENDIX D

EVALUATION OF THE DOUBLE INTEGRAL IN EQN. (2.2.5)

(1) From eqn. (2.2.5)

$$P_{++}(\text{inst}) = \frac{1}{2\pi\beta s^2(1-\rho^2)^{1/2}} \int_0^\infty du \int_\eta^\infty \exp\left[\frac{-1}{2(1-\rho^2)}\left[\frac{u^2}{s^2} - \frac{2\rho u(v-\eta)}{\beta s^2} + \frac{(v-\eta)^2}{(\beta s)^2}\right]\right] dv$$

Letting $\alpha = u/s$ and $\lambda = (v-\eta)/\beta s$, this becomes

$$P_{++}(\text{inst}) = \frac{1}{2\pi(1-\rho^2)^{1/2}} \int_0^\infty d\alpha \int_{-\eta/\beta s}^\infty \exp\left[-\frac{\alpha^2 - 2\rho\alpha\lambda + \lambda^2}{2(1-\rho^2)}\right] d\lambda \quad \ldots\ldots\ldots \text{D1}$$

The related function $L(h,k,\rho)$ is defined in Ref. (41) as

$$L(h,k,\rho) = \frac{1}{2\pi(1-\rho^2)^{1/2}} \int_h^\infty d\alpha \int_k^\infty \exp\left[-\frac{\alpha^2 - 2\rho\alpha\lambda + \lambda^2}{2(1-\rho^2)}\right] d\lambda$$

and an expression for its Maclaurin series in terms of ρ is given

$$L(h,k,\rho) = Q(h)Q(k) + \sum_{m=0}^{\infty} \frac{Z^{(m)}(h)\, Z^{(m)}(k)}{(m+1)!} \rho^{m+1} \quad \ldots\ldots\ldots\ldots \text{D2}$$

where

$$Q(h) \triangleq \frac{1}{\sqrt{2\pi}} \int_{-h}^{\infty} e^{-x^2/2} dx \qquad \text{and} \qquad Z^{(i)}(h) \triangleq \frac{d^i}{dx^i}\left[\frac{1}{\sqrt{2\pi}} e^{-x^2/2}\right]_{x=h}$$

Now $Z^{(i)}(-h) = (-1)^i Z^{(i)}(h)$, and so eqn. (D1) can be written as

$$P_{++}(\text{inst}) = Q(0)Q(-\eta/\beta s) + \sum_{m=0}^{\infty} (-1)^m \frac{Z^{(m)}(0)\, Z^{(m)}(\eta/\beta s)}{(m+1)!} \rho^{m+1} \quad \ldots\ldots \text{D3}$$

(Consideration of the integral forms of the Maclaurin series terms yielding the factors $Z^{(m)}(h).Z^{(m)}(k)$ gives a rigorous justification for the simple modification of the expression for $L(h,k,\rho)$ to that for $L(h,-k,\rho)$). Also[41]

$$Z^{(m)}(0) = \begin{cases} 0 & m \text{ odd} \\ \dfrac{(-1)^{m/2}\, m!}{\sqrt{2\pi}\, 2^{m/2}\, (m/2)!} & m \text{ even} \end{cases}$$

so eqn. (D3) becomes

$$P_{++}(\text{inst}) = Q(0)Q(-\eta/\beta s) + \sum_{m=0}^{\infty}(-1)^m \frac{Z^{(2m)}(\eta/\beta}{(2m+1)\sqrt{2}\,{}^m m!}\,\rho^{2m+1} \quad \ldots\ldots\ldots \text{D4}$$

In general, from the definition of $Z^{(m)}(h)$, $Z^{(m)}(\eta/\beta s)$ consists of terms of the form $(\eta/\beta s)^{2j}\, Z^{(0)}(\eta/\beta s)$. Averaging over all η, these terms become

$$\overline{(\eta/\beta s)^{2j}\, Z^{(0)}(\eta/\beta s)} = \frac{1}{(\beta s)^{2j}}\left[\eta^{2j} \cdot \frac{e^{-\eta^2/2(\beta s)^2}}{\sqrt{2\pi}}\right]$$

$$= \frac{1}{2\pi\sigma(\beta s)^{2j}} \int_{-\infty}^{\infty} \eta^{2j}\, e^{-\eta^2/2(\beta s)^2}\, e^{-\eta^2/2\sigma^2}\, d\eta \quad \ldots \text{D5}$$

$$= \frac{1}{\pi\sigma(\beta s)^{2j}} \int_{0}^{\infty} \eta^{2j} e^{-a\eta^2}\, d\eta \qquad \left[a = \frac{1}{2(\beta s)^2} + \frac{1}{2\sigma^2}\right]$$

$$= \frac{1}{\pi\sigma(\beta s)^{2j}} \frac{1.3.5\ldots(2j-1)}{2^{j+1}\, a^{(2j+1)/2}} \quad \ldots\ldots\ldots\ldots \text{D6}$$

Substituting in the expression for $\overline{Z^{(2m)}(\eta/\beta s)}$, and rearranging,

$$\overline{Z^{(2m)}(\eta/\beta s)} = \frac{1.3\,5\ldots(2m-1)}{2\pi\sigma}\sqrt{\frac{\pi}{a}}\left[\frac{1}{2a(\beta s)^2} - 1\right]^m \quad \ldots\ldots\ldots\ldots \text{D7}$$

Substituting for a, and then substituting eqn. (D7) into eqn. (D4)

$$P_{++} = Q(0).\overline{Q(-\eta/\beta s)} + \frac{1}{2\pi}\sqrt{\frac{(\beta s/\sigma)^2}{1+(\beta s/\sigma)^2}} \sum_{m=0}^{\infty}(-1)^m \frac{(2m)!}{(2m+1)(2^m m!)^2}\left[\frac{(\beta s/\sigma)^2}{1+(\beta s/\sigma)^2}\right]^m (-1)^m.\rho^{2m+1}$$

$$= \tfrac{1}{2}.\tfrac{1}{2} + \frac{1}{2\pi}\sum_{m=0}^{\infty}\frac{(2m)!}{(2m+1)(2^m m!)^2}\left[\sqrt{\frac{(\beta s/\sigma)^2}{1+(\beta s/\sigma)^2}}\right]^{2m+1}\rho^{2m+1}$$

$$= \tfrac{1}{4} + \frac{1}{2\pi}.\text{Arcsin}\left[\sqrt{\frac{(\beta s/\sigma)^2}{1+(\beta s/\sigma)^2}}\cdot\rho\right]$$

Noting that $\rho = \rho_f(\tau)$, this is the same as eqn. (2.2.6)

(2) Similarly for the auto-correlation function of $x_2(t)$

$$P_{++}(\text{inst}) = \frac{1}{2\pi(1-\rho^2)^{1/2}} \int_{-\eta_1/\beta s}^{\infty} d\alpha \int_{-\eta_2/\beta s}^{\infty} \exp\left[-\frac{\alpha^2 - 2\rho\alpha\lambda + \lambda^2}{2(1-\rho^2)}\right] d\lambda$$

$$= Q(-\eta_1/\beta s)Q(-\eta_2/\beta s) + \sum_{m=0}^{\infty}\frac{Z^{(m)}(\eta_1/\beta s)\; Z^{(m)}(\eta_2/\beta s)}{(m+1)!}\,\rho^{m+1} \quad \ldots\ldots \text{D8}$$

by reasoning in the manner that led to eqn. (D3). For m odd, $Z^{(m)}(\eta/\beta s)$ is of the form $Z^{(0)}(\eta/\beta s)\left[a_1\eta + a_3\eta^2 + \ldots\ldots\right]$ and since

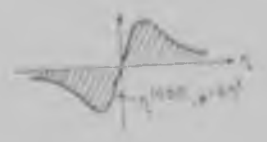

$$\int_{-\infty}^{\infty} \eta^{(\text{odd})}\, e^{-a\eta^2}\, d\eta = 0$$

eqn. (D8) consists of even order terms only; i.e.

$$P_{++}(\text{inst}) = Q(-\eta_1/\beta s)Q(-\eta_2/\beta s) + \sum_{m=0}^{\infty} \frac{Z^{(2m)}(\eta_1/\beta s)\, Z^{(2m)}(\eta_2/\beta s)}{(2m+1)!}\, \rho^{2m+1} \quad \ldots \text{D9}$$

and from eqn. (D7)

$$\overline{Z^{(2m)}(\eta_1/\beta s)} = \overline{Z^{(2m)}(\eta_2/\beta s)} = (-1)^m \frac{(2m)!}{2^m m!} \frac{1}{\sqrt{2\pi}} \left[\frac{(\beta s/\sigma)^2}{1+(\beta s/\sigma)^2}\right]^{m+\frac{1}{2}}$$

Substituting into eqn. (D9)

$$P_{++} = \tfrac{1}{2}\cdot\tfrac{1}{2} + \sum_{m=0}^{\infty} \left[\frac{(2m)!}{2^m m!}\right]^2 \frac{1}{(2m+1)!} \frac{1}{2\pi} \left[\frac{(\beta s/\sigma)^2}{1+(\beta s/\sigma)^2}\right]^{2m+1} \rho^{2m+1}$$

$$= \tfrac{1}{4} + \frac{1}{2\pi} \text{Arcsin}\left[\frac{(\beta s/\sigma)^2}{1+(\beta s/\sigma)^2}\cdot\rho\right] \quad \ldots \text{D10}$$

This last derivation could have been done less rigorously by assuming that since $n(t)$ and $\beta f_n(t)$ are Gaussian, their sum is Gaussian also. Thus $[\beta f_n(t) + n(t)]$ and $[\beta f_n(t+\tau) + n(t+\tau)]$ would be bivariate normally distributed with zero mean and normalised cross-covariance

$$\rho' = \frac{E\{[\beta f_n(t) + n(t)].[\beta f_n(t+\tau) + n(t+\tau)]\}}{\sqrt{E\{[\beta f_n(t) + n(t)]^2\}\; E\{[\beta f_n(t+\tau) + n(t+\tau)]^2\}}}$$

$$= \frac{(\beta s/\sigma)^2}{1+(\beta s/\sigma)^2} \cdot \rho_f(\tau)$$

For a zero mean bivariate normal distribution with cross-covariance ρ', the probability of both variates being greater than zero is $\frac{1}{4} + \frac{1}{2\pi}\text{Arcsin}[\rho']$, giving eqn. (D10). The rigorous proof assumes only that $\beta f_n(t)$ and $\beta f_n(t+\tau)$ are bivariate normally distributed (i.e. not with $n(t)$ added).

NOTE 1: The proof in this last paragraph indicates that one can assume $[\beta f_n(t) + n(t)]$ and $[\beta f_n(t+\tau) + n(t+\tau)]$ will follow a symmetrical bivariate normal distribution as well as $f_n(t)$ and $f_n(t+\tau)$, and this justifies the assumption on page 58.

APPENDIX E

EVALUATION OF ERROR PROBABILITY [EQN. (2.2.11)]

From eqn. (2.2.10)

$$p_e(\alpha) = \frac{1}{\sigma\sqrt{2\pi}}\left[\sigma\sqrt{\frac{\pi}{2}} - \alpha + \frac{\alpha^3}{3!\sigma^2} - \frac{3\alpha^5}{5!\sigma^4} + \frac{15\alpha^7}{7!\sigma^6} - \cdots\cdots\right]$$

In addition, if $\beta f_n(t_i) = \alpha$ at instant t_i, the probability of $n(t_i)$ changing the sign of $x_1(t_i)$ is

$$p_e(-\alpha) = \frac{1}{\sigma\sqrt{2\pi}}\int_{-\infty}^{-\alpha} e^{-y^2/2\sigma^2}\,dy = \frac{1}{\sigma\sqrt{2\pi}}\int_{\alpha}^{\infty} e^{-y^2/2\sigma^2}\,dy = p_e(\alpha)$$

Thus the total error probability, averaged over all α, is

$$p = 2\frac{1}{\beta s\sqrt{2\pi}}\int_0^{\infty} p_e(\alpha)\; e^{-\alpha^2/2(\beta s)^2}\,d\alpha$$

$$= \frac{2}{\beta s\sigma 2\pi}\left[\sigma\sqrt{\frac{\pi}{2}}\int_0^{\infty} e^{-\alpha^2/2(\beta s)^2}d\alpha - \int_0^{\infty}\alpha\, e^{-\alpha^2/2(\beta s)^2}d\alpha + \frac{1}{3!\sigma^2}\int_0^{\infty}\alpha^3 e^{-\alpha^2/2(\beta s)^2}d\alpha + \cdots\cdots\right]$$

$$= \frac{1}{\beta s\sigma\pi}\left[\sigma\sqrt{\frac{\pi}{2}}\cdot\tfrac{1}{2}\beta s\sqrt{2\pi} \qquad - (\beta s)^2 \qquad + \frac{1}{3!\sigma^2}2(\beta s)^4 - \cdots\cdots\right]$$

$$= \tfrac{1}{2} - \frac{1}{\pi}\left[(\beta s/\sigma) - \frac{1}{3}(\beta s/\sigma)^3 + \frac{1}{5}(\beta s/\sigma)^5 - \cdots\right]$$

$$= \tfrac{1}{2} - \tfrac{1}{\pi}\,\mathrm{Arctan}(\beta s/\sigma)$$

as in eqn. (2.2.11)

APPENDIX F

CALCULATION OF THE AVERAGE ERROR ZONE PERIOD

(1) T_b - the time spent by the sine wave in the error zone per exact number of half cycles:

For the waveform A.sin(ωt), the time spent above +β or below -β in one half cycle is $[\frac{\pi}{\omega} - \frac{2}{\omega}\,\mathrm{Arcsin}(\beta/A)]$. Letting $T' = \pi/\omega$,

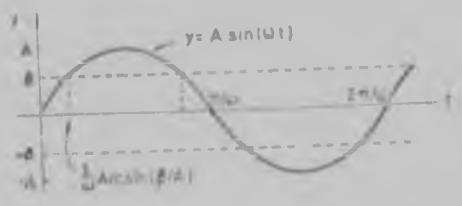

FIGURE F-1

$$T_b = T'[1 - \tfrac{2}{\pi}\mathrm{Arcsin}(\beta/A)]$$

If T' corresponded exactly to two half cycles of the sine wave, this would be equivalent to doubling ω; in this case there would be two error zone periods, each half as long, but adding up to the same total T_b. In fact, if T' corresponds to any exact number of half cycles of a sine wave, i.e. $T' = n\pi/\omega$ where n= 1,2,3...., the time spent by the sine wave above +β or below -β will be $T'[1 - \frac{2}{\pi}\mathrm{Arcsin}(\beta/A)]$, regardless of the actual number of half cycles in T'.

(2) $\overline{\Delta T_b}$ - the average time per fraction of a half cycle spent by the sine wave in the error zone:

The analysis assumes Φ to be evenly distributed between 0 and π radians, having probability density (1/π) within that region and zero elsewhere. The results would be identical if Φ were assumed to be evenly distributed between zero and 2π radians, and to have probability density (1/2π) within that region and zero outside it. The analysis will be split up into sections to account for all the various possibilities of T" (Fig. F-2).

FIGURE F-2

(a) $0 \leq T'' \leq (1/\omega)\text{Arcsin}(\beta/A)$. Consider the sinusoidal waveform in Fig. F-3 moving from right to left relative to the time axis as ϕ varies from 0 to π. The amount of time (ΔT_b) spent by the waveform above $+\beta$ within the vertical window 0 to T" will be considered in sections as follows:-

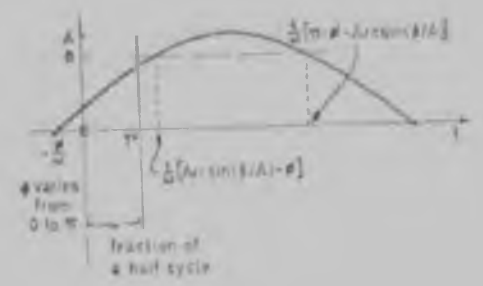

FIGURE F-3

For $0 \leq \phi \leq [\text{Arcsin}(\beta/A) - \omega T'']$,

$$\Delta T_b = 0$$

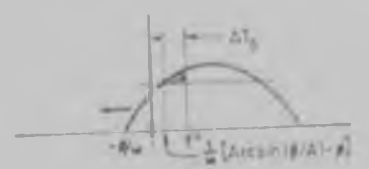

For $[\text{Arcsin}(\beta/A) - \omega T''] \leq \phi \leq \text{Arcsin}(\beta/A)$

$$\Delta T_b = T'' - \tfrac{1}{\omega}[\text{Arcsin}(\beta/A) - \phi]$$

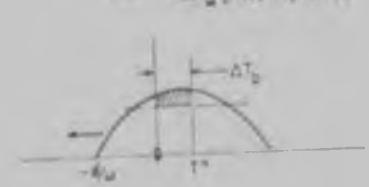

For $\text{Arcsin}(\beta/A) \leq \phi \leq (\pi - \text{Arcsin}(\beta/A) - \omega T'')$

$$\Delta T_b = T''$$

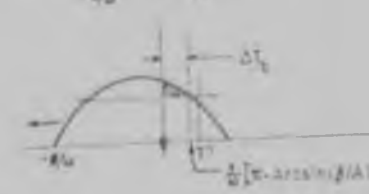

For $(\pi - \text{Arcsin}(\beta/A) - \omega T'') \leq \phi \leq [\pi - \text{Arcsin}(\beta/A)]$

$$\Delta T_b = T'' - \tfrac{1}{\omega}[\pi - \text{Arcsin}(\beta/A) - \phi]$$

And for $[\pi - \text{Arcsin}(\beta/A)] \leq \phi \leq \pi$

$$\Delta T_b = 0$$

Hence, averaging over all these intervals,

$$\overline{\Delta T_b} = \frac{1}{\pi}\left[\int_{\text{Arcsin}(\beta/A)-\omega T''}^{\text{Arcsin}(\beta/A)} \{T'' - \tfrac{1}{\omega}(\text{Arcsin}(\beta/A) - \phi)\}\, d\phi + \int_{\text{Arcsin}(\beta/A)}^{\pi-\text{Arcsin}(\beta/A)-\omega T''} T''\, d\phi + \int_{\pi-\text{Arcsin}(\beta/A)-\omega T''}^{\pi-\text{Arcsin}(\beta/A)} \{T'' - \tfrac{1}{\omega}[\pi - \text{Arcsin}(\beta/A) - \phi]\}\, d\phi\right]$$

$$= T''\left[1 - \tfrac{2}{\pi}\text{Arcsin}(\beta/A)\right] \quad \ldots\ldots\ldots\ldots\ldots\ldots\ldots\ldots\ldots \text{F1}$$

It is possible for T" to be greater than the error zone period per half cycle and still be less than $\frac{1}{\omega}\text{Arcsin}(\beta/A)$ (Fig. F-4)

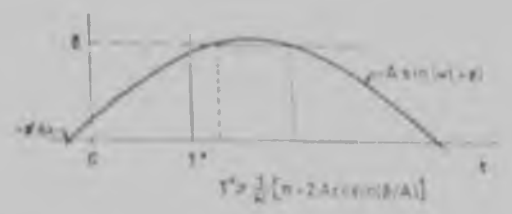

FIGURE F-4

An analysis similar to that above shows that in this case also

$$\overline{\Delta T_b} = T''\left[1 - \frac{2}{\pi}\text{Arcsin}(\beta/A)\right]$$

$\overline{\Delta T_b}$ can be evaluated in precisely the same way for all the other possibilities of T". The results are listed below. For convenience, let $S = \text{Arcsin}(\beta/A)$.

Range of T"	Relative size of T"	$\overline{\Delta T_b}$
$0 \leq T'' \leq \frac{1}{\omega} S$	$T'' \geq \frac{1}{\omega}[\pi - 2S]$	$T''\left[1 - \frac{2}{\pi} S\right]$
$\frac{1}{\omega}S \leq T'' \leq \frac{2}{\omega} S$	"	$T'' - \frac{ST''}{\pi} - \frac{S^2}{2\pi\omega} - \frac{\omega(T'')^2}{2\pi}$
$\frac{2}{\omega}S \leq T'' \leq \frac{1}{\omega}[\pi - S]$	"	$T''\left[1 - \frac{2}{\pi} S\right]$
$\frac{1}{\omega}[\pi - S] \leq T'' \leq \frac{\pi}{\omega}$	$T'' > \frac{1}{\omega}[\pi - 2S]$	$T''\left[1 - \frac{2}{\pi} S\right]$

APPENDIX G

EVALUATION OF THE VARIANCE OF $\Psi_s(0)$ FOR RANDOM SINE WAVE CORRUPTION

From the equation before eqn. (2.3.9)

$$\text{var}\,[\Psi_s(0)] = E\Big[\Big[\sum_{i=1}^{N} x_1(t_i)\,\xi(t_i)\Big]^2\Big] - \Big[E\Big[\sum_{i=1}^{N} x_1(t_i)\,\xi(t_i)\Big]\Big]^2 \quad \ldots\ldots \text{G1}$$

and since $x_1(t)$ and $\xi(t)$ are independent

$$E\Big[\sum_{i=1}^{N} x_1(t_i)\,\xi(t_i)\Big] = \sum_{i=1}^{N} E\{x_1(t_i)\}\,E\{\xi(t_i)\} = 0. \quad \ldots\ldots\ldots\ldots \text{G2}$$

and

$$E\Big[\Big[\sum_{i=1}^{N} x_1(t_i)\,\xi(t_i)\Big]^2\Big] = E\Big[\sum_{i=1}^{N} x_1^2(t_i)\,\xi^2(t_i)\Big] + 2\sum_{i=1}^{N-1}\sum_{j=i+1}^{N} E\{x_1(t_i)\,\xi(t_i)\,x_1(t_j)\,\xi(t_j)\}$$

$$= \sum_{i=1}^{N} E\{x_1^2(t_i)\}\,E\{\xi^2(t_i)\} + 2\sum_{i=1}^{N-1}\sum_{j=i+1}^{N} \Psi_{x_1}(t_j - t_i)\cdot\Psi_{\xi}(t_j - t_i) \quad \ldots\ldots \text{G3}$$

Now $E\{x_1^2(t_i)\} = 1$, and $\xi^2(t_i)$ is 1 in all the error zones and zero elsewhere. Hence, with the aid of Fig. 2-10 (p. 37),

$$E\{\xi^2(t_i)\} = \frac{\pi/\omega - t_{zzz}}{\pi/\omega} = 1 - \frac{2}{\pi}\,\text{Arcsin}(\beta/A)$$

Writing the double summation with just the (j-i) coefficients as in Appendix C, it becomes

All terms of form $\Psi_{x_1}(t_j - t_i)\,\Psi_{\xi}(t_j - t_i)$

(2-1) + (3-1) +.....+ (N-2) + (N-1)

+ (3-2) + (4-2) +.....+ (N-1-1)

all terms = $\Psi_{x_1}[(N-1)\delta t]\,\Psi_{\xi}[(N-1)\delta t]$

+[N-(N-1)]

all terms = $\Psi_{x_1}(\delta t)\,\Psi_{\xi}(\delta t)$

Summing columns of like terms:

$$\sum\sum = \sum_{i=1}^{N-1} (N-i)\,\Psi_{x_1}(i\delta t)\,\Psi_{\xi}(i\delta t) \quad \ldots\ldots \text{G5}$$

Substituting eqns. (G2) to (G5) into eqn. (G1) gives eqn. (2.3.9).

NOTE 1: (p. 37) The expression for the variance of the sum of the N_a product terms in the error zones is identical to eqn. (G1) with N replaced by N_a. Proceeding through the above analysis, and noting that the double summation matrix of terms has (N_a-1) terms along the top and side (instead of (N-1)) so that eqn. (G5) must have N replaced by N_a, the expression for the variance is the same as eqn. (2.3.9) but with N replaced by N_a.

APPENDIX H

AUTO-CORRELATION FUNCTION OF $\xi(t)$

The waveform $\xi(t)$ is illustrated below in Fig. H-1. Let $2\pi/\omega = T$ and $t_{nez} = 2\delta$.

FIGURE H-1

The auto-correlation function of $\xi(t)$ may be derived in sections, as follows:

$|\tau| < 2\delta$ (Fig. H-2)

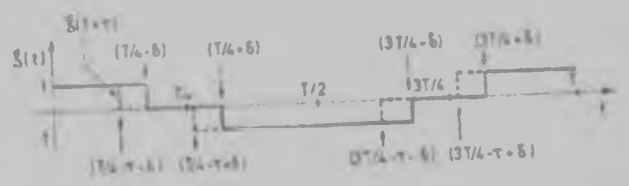

FIGURE H-2

$$\psi_\xi(\tau) = \frac{1}{T}\left[\int_0^{T/4-\delta-\tau} dt + \int_{T/4+\delta}^{3T/4-\delta-\tau} dt + \int_{3T/4-\delta}^{T} dt\right]$$

$$= 1 - (4\delta + 2\tau)/T$$

The remaining sub-ranges of τ may be treated likewise. The results are as follows: (remember that $T = 2\pi/\omega$ and $2\delta = t_{nez}$ here, by definition).

(1) $2\delta < T/4$	$\psi_\xi(\tau)$	(2) $2\delta \geq T/4$	$\psi_\xi(\tau)$
$0 \leq \tau \leq 2\delta$	$1-(4\delta+2\tau)/T$	$0 \leq \tau \leq (\frac{T}{2}-2\delta)$	$1-(4\delta+2\tau)/T$
$2\delta \leq \tau \leq (\frac{T}{2}-2\delta)$	$1-4\tau/T$	$(\frac{T}{2}-2\delta) \leq \tau \leq 2\delta$	0
$(\frac{T}{2}-2\delta) \leq \tau \leq \frac{T}{2}$	$-(2\tau-4\delta)/T$	$2\delta \leq \tau \leq \frac{T}{2}$	$-[(2\tau-4\delta)/T]$
$\frac{T}{2} \leq \tau \leq (\frac{T}{2}+2\delta)$	$-2[1-(\tau+2\delta)/T]$	$\frac{T}{2} \leq \tau \leq (T-2\delta)$	$-2[1-(\tau+2\delta)/T]$
$(\frac{T}{2}+2\delta) \leq \tau \leq (T-2\delta)$	$-[3-4\tau/T]$	$(T-2\delta) \leq \tau \leq (\frac{T}{2}+2\delta)$	0
$(T-2\delta) \leq \tau \leq T$	$(2\tau-4\delta)/T-1$	$(\frac{T}{2}+2\delta) \leq \tau \leq T$	$(2\tau-4\delta)/T-1$

In the limit as $2\delta \to 0$, $\xi(t)$ becomes a square wave with $\psi_\xi(\tau)$ given by

$0 \leq \tau \leq T/2$ $\quad \psi_\xi(\tau) = (1-4\tau/T)$

$T/2 \leq \tau \leq T$ $\quad \psi_\xi(\tau) = (4\tau/T-3)$

APPENDIX I

EVALUATION OF THE VARIANCE OF THE NON-ERROR ZONE PRODUCT TERMS SUM

As usual

$$var_{nez} = E\left\{\left[\sum_{i=1}^{N_a} x_1(t_i)y_2(t_i+\tau)\right]^2\right\} - E\left[\sum_{i=1}^{N_a} x_1(t_i)y_2(t_i+\tau)\right]$$

$$= E\left[\sum_{i=1}^{N_a} x_1^2(t_i)y_2^2(t_i+\tau)\right] - \mu_{nez}^2 + 2\sum_{i=1}^{N_a-1}\sum_{j=i+1}^{N_a} E[x_1(t_i)y_2(t_i+\tau)x_1(t_j)y_2(t_j+\tau)] \quad . \quad I1$$

where

$$\mu_{nez} = N_a \cdot \frac{\beta}{\pi} \text{Arcsin}(\beta/A) \cdot \psi_{x_1}(\tau) \qquad (2.3.14)$$

noting (a) that $y_2(t+\tau) = x_1(t+\tau).\gamma(t)$ and that $\gamma(t)$ and $x_1(t)$ are independent, and (b) that $E[x_1^2(t_i)x_1^2(t_i+\tau)] = 1$,

$$var_{nez} = \sum_{i=1}^{N_a} E[\gamma^2(t_i)] - \mu_{nez}^2 + 2\sum_{i=1}^{N_a-1}\sum_{j=i+1}^{N_a} \psi_{x_1}(t_j-t_i)E[x_1(t_i)x_1(t_i+\tau/x_1(t_j)x_1(t_j+\tau)] \quad . \quad . \quad . \quad . \quad . \quad I2$$

From Fig. I-1 it can be seen that $E[\gamma^2(t)] = E[\gamma(t)]$, and from eqn. (2.3.12)

$$E[\gamma(t)] = t_{nez}/(\pi/\omega) = \frac{2}{\pi}\text{Arcsin}(\beta/A)$$

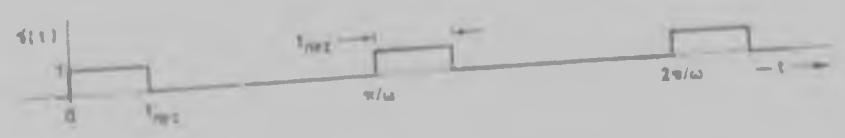

FIGURE I-1

Substituting this into eqn. (I2) yields eqn. (2.3.15)

$$var_{nez} = N_a \cdot \frac{2}{\pi}\text{Arcsin}(\beta/A) + 2\sum_{i=1}^{N_a-1}\sum_{j=i+1}^{N_a}\psi_{x_1}(t_j-t_i)E[x_1(t_i)x_1(t_i+\tau)x_1(t_j)x_1(t_j+\tau)] - \mu_{nez}^2 \quad . \quad . \quad . \quad . \quad . \quad . \quad . \quad . \quad . \quad I3$$

Now

$$E[x_1(t_i)x_1(t_i+\tau)x_1(t_j)x_1(t_j+\tau)] = \begin{cases} [\psi_{x_1}(t_j-t_i)]^2 & \text{for } t_j < (t_i+\tau) \\ [\psi_{x_1}(\tau)]^2 & \text{for } t_j \geq (t_i+\tau) \end{cases}$$

and the double summation may be simplified by expanding it in the way used in Appendix C:

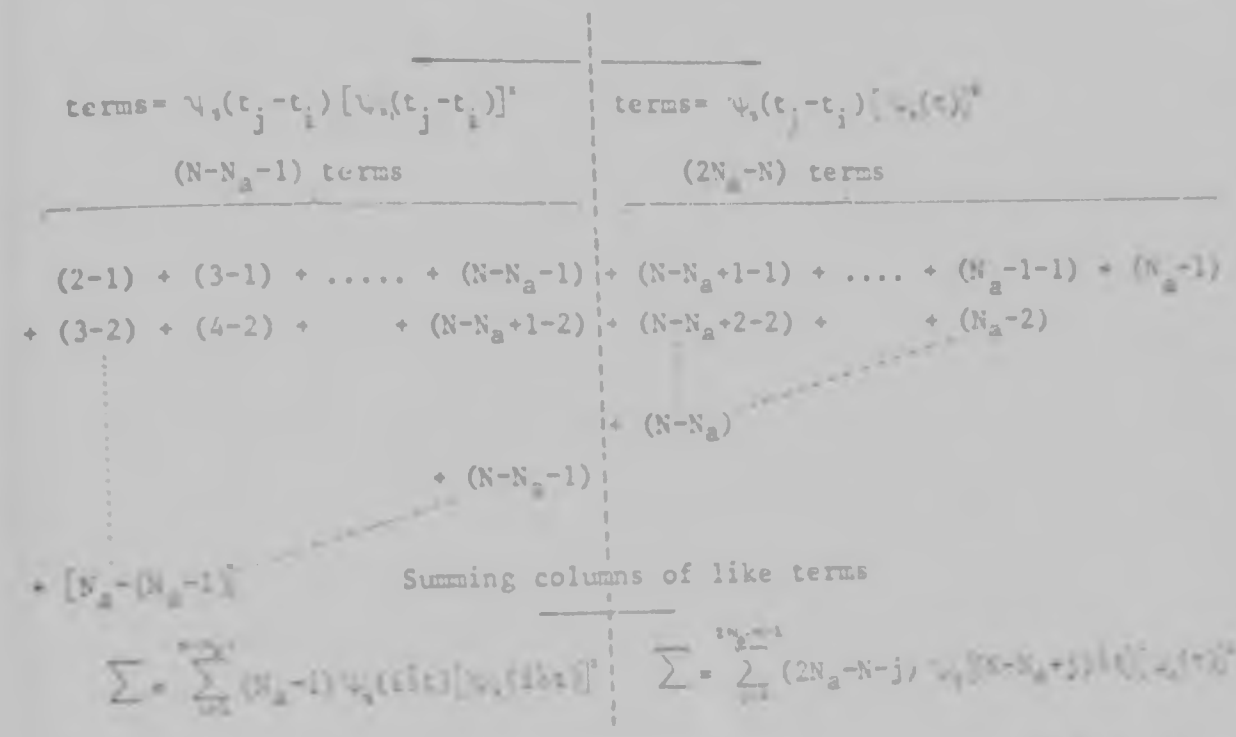

Substituting these two sums for the double summation in eqn. (13) leads to eqn. (2.3.16).

The variance of the non-error zone terms in the case of continuous waveform cross-correlation (p. 41) is the same as eqn. (11) except that the summations are all up to N instead of N_a, and μ_{nez} is replaced by μ_s from eqn. (2.3.18). Thus eqn. (13) becomes

$$\text{var}_{nez} = N\frac{2}{\pi}\text{Arcsin}(s/A) - \mu_s^2 + 2\sum_{i=1}^{N-1}\sum_{j=i+1}^{N}\psi_s(t_j-t_i)[x_1(t_i)x_1(t_{i+\tau})x_1(t_j)x_1(t_{j+\tau})]$$

The double summation matrix now has N_a terms to the right of the dotted line (from $(N-N_a)$ to $(N-1)$) and the first column goes from $(2-1)$ to $[N-(N-1)]$. Therefore the sums of the columns to the left and right of the dotted line become, respectively,

$$\sum_{i=1}^{N-N_a}(N-i)\psi_s(i\delta t)[\psi_s(i\delta t)]^2 \quad \text{and} \quad \sum_{j=1}^{N_a-1}(N_a-j)\psi_s[(N-N_a+j)\delta t][\psi_s(j\delta t)]^2.$$

Substituting the sum of these two for the double summation yields eqn. (2.3.19).

APPENDIX J

AUTO-CORRELATION FUNCTION OF $\gamma(t)$

For convenience, let $T = 2\pi/\omega$ and $2\delta = t_{nez}$ as in Appendix H. The auto-correlation function of $\gamma(t)$ will be derived for the two possible cases: (1) 2δ $(=t_{nez}) \leq T/4$ and (2) $2\delta \geq T/4$.

(1) $2\delta \leq T/4$

(a) $0 \leq \tau \leq 2\delta$ (Fig. J-1)

$$\psi_\gamma(\tau) = \frac{2}{T}\left[\int_0^{2\delta-\phi'-\tau} dt + \int_{\frac{T}{2}-\phi'}^{T/2} dt\right]$$
$$= \frac{2}{T}\left[2\delta-\tau\right]$$

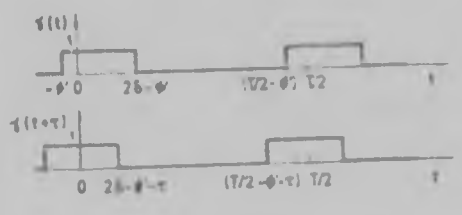

FIGURE J-1

The other sub-ranges of τ may be treated likewise. The results are tabulated below. (Note that $T = 2\pi/\omega$ and $2\delta = t_{nez}$)

(1) $2\delta \leq T/4$	$\psi_\gamma(\tau)$	(2) $2\delta \leq T/4$	$\psi_\gamma(\tau)$
$0 \leq \tau \leq 2\delta$	$2(2\delta-\tau)/T$	$0 \leq \tau \leq (\frac{T}{2}-2\delta)$	$2(2\delta-\tau)/T$
$2\delta \leq \tau \leq (\frac{T}{2}-2\delta)$	0	$(\frac{T}{2}-2\delta) \leq \tau \leq 2\delta$	$2(4\delta-\frac{T}{2})/T$
$(\frac{T}{2}-2\delta) \leq \tau \leq \frac{T}{2}$	$2(2\delta+\tau-\frac{T}{2})/T$	$2\delta \leq \tau \leq \frac{T}{2}$	$2(2\delta-\frac{T}{2}+\tau)/T$

APPENDIX K

DERIVATION OF VARIANCE EXPRESSION [EQN. (2.3.17)]

As before

$$\text{var}_{N_b} = \sum_{i=1}^{N_b} E\{x_1^2(t_i)\xi^2(t_i)\} + 2\sum_{i=1}^{N_b-1}\sum_{j=i+1}^{N_b} E\{x_1(t_i)\xi(t_i)x_1(t_j)\xi(t_j)\} - \left[\sum_{i=1}^{N_b} E\{x_1(t_i)\xi(t_i)\}\right]^2 \quad \ldots\ldots\ldots \text{K1}$$

In this case $\xi(t)$ is a square wave, so $E\{\xi(t_i)\} = 0 = E\{x_1(t_i)\}$ and $E\{\xi^2(t_i)\} = 1 = E\{x_1^2(t_i)\}$; substituting into eqn. (K1)

$$\text{var}_{N_b} = N_b + 2\sum_{i=1}^{N_b-1}\sum_{j=i+1}^{N_b} \psi_x(t_j-t_i)\,\psi_\xi(t_j-t_i). \quad \ldots\ldots\ldots\ldots\ldots\ldots \text{K2}$$

The double sum is analogous to that appearing in Appendix G except that the upper limit is N_b and not N. Hence its simplified expansion may be written down directly as in eqn. (G5), i.e.

$$\sum\sum = \sum_{i=1}^{N_b-1} (N_b-i)\,\psi_x(i\delta t)\,\psi_\xi(i\delta t)$$

Substituting this into eqn. (K2) gives eqn. (2.3.17)

$$\text{var}_{N_b} = N_b + 2\sum_{i=1}^{N_b-1} (N_b-i)\,\psi_{x_1}(i\delta t)\,\psi_\xi(i\delta t)$$

APPENDIX L

EVALUATION OF THE DOUBLE INTEGRAL IN EQN. (2.4.3)

Starting with eqn. (2.4.3) and letting $(\omega t+\phi)=\theta$,

$$P_{++}(\text{inst})=\frac{1}{2\pi\beta s^2(1-\rho_\epsilon^2)^{1/2}}\int_0^\infty d\alpha\int_0^\infty \exp\left[\frac{-1}{2(1-\rho_\epsilon^2)}\left[\frac{\alpha^2}{s^2}-\frac{2\rho_\epsilon\alpha(\epsilon-A\sin\theta)}{\beta s^2}+\frac{(\epsilon-A\sin\theta)^2}{(\beta s)^2}\right]\right]d\epsilon$$

Letting $(\epsilon-A\sin\theta)/\beta=\lambda$ and $1/(2\pi s^2\sqrt{1-\rho_\epsilon^2})=k$, this becomes

$$P_{++}(\text{inst})=k\int_0^\infty d\alpha\int_{-(A\sin\theta)/\beta}^\infty \exp\left[-\frac{\alpha^2-2\rho_\epsilon\alpha\lambda+\lambda^2}{2(1-\rho_\epsilon^2)s^2}\right]d\lambda \quad \ldots\ldots\ldots\ldots \text{L1}$$

which is of the general form

$$k\int_{-u_1}^\infty d\alpha\int_{-u_2}^\infty \exp\left[-\frac{\alpha^2-2\rho_\epsilon\alpha\lambda+\lambda^2}{2(1-\rho_\epsilon^2)s^2}\right]d\lambda=F(u_1,u_2). \quad \ldots\ldots \text{L2}$$

Using the method of McFadden[36] this can be expanded in a two dimensional Maclaurin series in terms of u_1 and u_2. Substituting zero for u_1 and $(A\sin\theta/\beta)$ for u_2 would give $P_{++}(\text{inst})$. This can then be averaged (term by term) by integrating with respect to θ over the range zero to 2π and multiplying by $p(\theta)=1/2\pi$.

$$F(u_1,u_2)=F(0,0)+\left.\frac{\partial F}{\partial u_1}\right|_0 u_1+\left.\frac{\partial F}{\partial u_2}\right|_0 u_2+\frac{1}{2!}\left[\left.\frac{\partial^2 F}{\partial u_1^2}\right|_0 u_1^2+\left.\frac{\partial^2 F}{\partial u_1\partial u_2}\right|_0 u_1u_2+\left.\frac{\partial^2 F}{\partial u_2^2}\right|_0 u_2^2\right]+\ldots \quad \text{L3}$$

Also needed is the expression for differentiating an integral; i.e. if

$$I[a(t),b(t)]=\int_{a(t)}^{b(t)} R(\alpha,\beta)\,d\alpha$$

then

$$\frac{dI}{dt}=R[b(t),\beta]\cdot\frac{db(t)}{dt}-R[a(t),\beta]\cdot\frac{da(t)}{dt}+\int_{a(t)}^{b(t)}\frac{\partial R(\alpha,\beta)}{\partial t}\,d\alpha \quad \ldots\ldots \text{L4}$$

It can be seen from eqn. (L1) that the first and last terms are zero, and by inspection, all terms in eqn. (L3) containing factor u_1 will be zero and all terms with $u_2(=A\sin\theta/\beta)$ raised to an odd power will average to

zero over one cycle of θ. Therefore

$$F(u_1,u_2) = F(0,0) + \frac{1}{2!}\frac{\partial^2 F}{\partial u_1^2}\Big|_0 u_2^2 + \frac{1}{4!}\frac{\partial^4 F}{\partial u_1^4}\Big|_0 u_2^4 + \frac{1}{6!}\frac{\partial^6 F}{\partial u_1^6}\Big|_0 u_2^6 + \cdots \quad \text{L5}$$

Applying eqn. (L4) to eqn. (L2)

$$F(u_1,u_2) = \left[\tfrac{1}{4} + \tfrac{1}{2\pi}\mathrm{Arcsin}(\rho_s)\right] - \left[\frac{\rho_s}{2!\,2\pi s^2(1-\rho_s^2)^{1/2}}\right]u_2^2 + \left[\frac{\rho_s(3-2\rho_s^2)}{4!\,2\pi s^4(1-\rho_s^2)^{3/2}}\right]u_2^4 -$$

$$-\left[\frac{\rho_s(15-20\rho_s^2+8\rho_s^4)}{6!\,2\pi s^6(1-\rho_s^2)^{5/2}}\right]u_2^6 + \left[\frac{\rho_s(105-210\rho_s^2+168\rho_s^4-48\rho_s^6)}{8!\,2\pi s^8(1-\rho_s^2)^{7/2}}\right]u_2^8 + \cdots \quad \text{L6}$$

Integrating term by term over $0 \le \theta \le 2\pi$ and multiplying by $1/2\pi$,

$$P_{++} = \tfrac{1}{4} + \frac{1}{2\pi}\mathrm{Arcsin}(\rho_s) - \frac{1}{2\pi}\left\{\frac{\rho_s(A/\theta s)^2}{2!\,(1-\rho_s^2)^{1/2}}\cdot\tfrac{1}{2} - \frac{\rho_s(3-2\rho_s^2)(A/\theta s)^4}{4!\,(1-\rho_s^2)^{3/2}}\cdot\tfrac{1}{2}\cdot\tfrac{3}{4} + \right.$$

$$\left. \frac{\rho_s(15-20\rho_s^2+8\rho_s^4)(A/\theta s)^6}{6!\,(1-\rho_s^2)^{5/2}}\cdot\tfrac{1}{2}\cdot\tfrac{3}{4}\cdot\tfrac{5}{6} + \cdots\cdots\right\} \quad \text{L7}$$

Remembering that $\Psi_{++}(\tau) = 4P_{++} - 1$ and substituting eqn. (L7) yields eqn. (2.4.4) directly.

APPENDIX M

AUTO-CORRELATION FUNCTION OF $X_2(t)$ [EQN. (3.2.7)]

$$x_2(t) = \mathrm{sgn}[\beta f_n(t) + \gamma f_n(t+\Delta) + n(t)] = \mathrm{sgn}[w(t) + n_1(t)] \quad \text{M1}$$

$$x_2(t+\tau) = \mathrm{sgn}[\beta f_n(t+\tau) + \gamma f_n(t+\tau+\Delta) + n(t+\tau)] = \mathrm{sgn}[w(t+\tau) + n_2(t)] \quad \text{M2}$$

$w(t)$ and $w(t+\tau)$ are linear functions of $f_n(t)$, $f_n(t+\Delta)$, $f_n(t+\tau)$ and $f_n(t+\tau+\Delta)$ and hence will have a bivariate normal distribution function. Comparing eqn. (M1) to eqn. (2.2.2) on page 25, it is clear that the analysis of the auto-correlation function of $x_2(t)$ in the present case is exactly analogous to that of the auto-correlation function of $x_2(t)$ in Section 2.2.1 with $\beta f_n(t)$ replaced by $w(t)$. Therefore the auto-correlation function of $x_2(t)$ in eqn. (M1) can be written down as in eqn. (2.2.8) (p. 26)

$$\psi_{x_2}(\tau) = \frac{2}{\pi} \mathrm{Arcsin}\left[\frac{(\lambda s/\sigma)^2}{1+(\lambda s/\sigma)^2} \cdot \rho_w(\tau)\right] \quad \text{M3}$$

where λs is the standard deviation of $w(t)$, i.e.

$$\lambda s = \sqrt{E[w(t)]^2} = s\sqrt{\beta^2 + 2\rho_f(\Delta)\beta\gamma + \gamma^2} \quad \text{M4}$$

and $\rho_w(\tau)$ is the normalised auto-covariance of $w(t)$ which is

$$\rho_w(\tau) = \frac{E[w(t)w(t+\tau)]}{E[w(t)]^2}$$

$$= \frac{(\gamma^2+\beta^2)\rho_f(\tau) + \gamma\beta[\rho_f(\tau+\Delta) + \rho_f(\tau-\Delta)]}{(\beta^2 + 2\beta\gamma\rho_f(\Delta) + \gamma^2)} \quad \text{M5}$$

APPENDIX N

SPECIMEN SET OF EXPERIMENTAL READINGS

The readings given below are the complete set taken for the experimental points plotted on the 0.309 signal-to-noise ratio curves in Figs. 4-19 to 4-22, (100 sample cross-correlation of a single-bit Gaussian signal with a reflection corrupted by a 3903 Hz random phase sine wave). The left hand sets of readings are the zero-delay counts (the number of times that $\psi_s(0) \geq h$), and the right hand sets are the false alarm counts (the number of times that $\psi_s(\tau) \geq h$).

h	0		2		2 contd.		4		6	
N_h	96878	57042	95311	50837	95411	50977	93235	44169	90548	38175
	96643	57062	95187	50938	95454	50713	93314	44029	90607	38284
	96809	57072	95172	50786	95061	50720	93194	44484	90488	38203
	96711	56967	95133	50638	95202	50688	93203	44316	90581	37857
	96826	57254	95427	50824			93333	44309	90464	37957
	96669	57133	95318	50969			93211	44249		

h	8		10		12		16		18	
N_h	86935	31860	82912	26640	78061	21628	66643	13192	60457	10010
	87012	32200	83201	26564	77957	21302	66649	13278	60305	10179
	87085	31977	83141	26378	78203	21451	66862	13249	60407	10052
	87047	32273	82997	26455	77974	21626	66675	13414	60446	9958
	86921	32064	[illegible]	[illegible]	78247	21321	66718	13253	60305	10056
			83021	26274			66923	13318		
			82853	26416						
			83179	26492						

h	20		22		26		28		36	
N_h	53883	7428	46575	5399	32606	2646	26696	1746	9308	296
	53713	7392	46858	5338	32575	2713	26715	1799	9395	283
	53633	7407	46739	5362	32519	2613	26770	1798	9373	279
	53638	7419	46636	5439	32651	2608	26808	1801	[illegible]	[illegible]
	53794	7434	46744	5479	32483	2766	26614	1783	9378	273
			46737	5436	32833	2639	26456	1815	9380	261
					32821	2597	26819	1725	9299	279
					32751	2673	26703	1817	9354	252
					33100	2613	26632	1819		
					32968	2669	[illegible]	[illegible]		

▨ reading rejected for one of the reasons discussed in Chapter four.

h	38		40		42		44		46	
N_h	6805	172	4782	113	3220	53	2161	50	1378	18
	6548	129	4799	109	3276	59	2194	31	1389	17
	6608	173	4754	112	3289	60	2116	30	1323	16
	6805	188	4767	100	3203	57	2018	24	1337	14
	6647	180	4619	106	3267	59	2089	32	1358	20
	6743	182	4776	82	3271	53	2102	38	1425	12
	6674	169	4784	106	3239	56	2090	37	1291	21
	6770	180	4800	95	3162	56	2084	32	1330	17
							2081	27	1347	25
									1355	11
									1330	15

h	56	58
N_h	95	49
	83	65
	80	51
	105	60
	83	54
	85	48

——— zero delay counts only.

▨ reading rejected for one of the reasons discussed in Chapter four.

APPENDIX O

CALCULATION OF CONFIDENCE INTERVALS

Most of the methods for estimating confidence intervals for the difference between the means of two groups of readings assume that the readings are normally distributed, or are most efficient when they are. As discussed in Section 4.5, the Central Limit Theorem suggests that the N_h readings will approach normality for large N_R.

The standard deviations s.d.1 and s.d.2 of the sets of the N_h and N_{h+2} readings may be tested for equality using the ratio test[42]. (This test also assumes the sets of readings to be normally distributed). The ratio $\{(s.d.1)^2/(\text{true s.d.1})^2\}/\{(s.d.2)^2/(\text{true s.d.2})^2\}$ follows the F distribution. To test if the standard deviations are equal, the true standard deviations are assumed equal and the ratio $\{(s.d.1)^2\}/\{(s.d.2)^2\}$ is compared to unity. If it lies within the range $F_{n_1-1,n_2-1;\alpha/2}$ to $1/F_{n_2-1,n_1-1;\alpha/2}$, there is no significant difference between the standard deviations at the $(1-\alpha)$ confidence level. n_1 and n_2 are the number of samples used for the s.d.1 and s.d.2 estimates, respectively.

Consider the readings of N_{40} and N_{42} from the 100 sample cross-correlation of an analog Gaussian signal with a reflection corrupted by wideband Gaussian noise, $(\beta s/\sigma) = 0.1$:

N_{40}: 50, 42, 51, 54, 54, 49, 51, 55, 52, 50

N_{42}: 22, 26, 14, 20, 22, 24, 23, 20, 26, 20

$\overline{N_{40}} = 50.8$ s.d.1 = 4.44 where $s.d. = \sqrt{\frac{1}{(N-1)}\left\{\Sigma x_i^2 - \frac{[\Sigma x_i]^2}{N}\right\}}$

$\overline{N_{42}} = 21.7$ s.d.2 = 3.53

In this case the 95 per cent limits, $F_{9,9;.025}$ and $1/F_{9,9;.025}$, are 4.03 and 0.248. $[(s.d.1)^2]/[(s.d.2)^2]$ is equal to 1.58, indicating no significant

difference at the 95 per cent confidence level.

Where sets of readings are normally distributed and have equal variances, the t-test may be applied to finding the confidence interval of the difference between their means.[37][43] This test is sensitive to skewness in small numbers of samples, but this sensitivity is of less consequence when the sets of samples are equal sized and similarly distributed. Applying it to the two sets of readings above gives

Mean difference = 29.1

90 per cent confidence limits = 26.3 to 31.9

The second method of determining the confidence limits of the mean difference $(m_1 - m_2)$, applicable only to equal sized groups of readings, is to calculate the ranges r_1 and r_2 of the two groups and set limits on $(m_1 - m_2)$ using[44]

$$(\mu_1 - \mu_2) = (m_1 - m_2) \pm \alpha(r_1 + r_2)$$

α being tabulated in Reference (44) and more fully in Reference (45). This method is liable to be sensitive to large departures of the readings from normality. Applying it to the example above,

$r_1 = (55-42) = 13$

$r_2 = 12$

$\alpha = 0.125$ for 90 per cent confidence limits.

Thus

$$(\mu_1 - \mu_2) = 29.1 \pm 0.125 \times 25$$

$$= 26.0 \text{ to } 32.2 \qquad \text{(c.f. 26.3 to 31.9)}$$

Both the above methods yield compatible answers. The second method is computationally the easiest, but is only applicable to equal sized groups of readings. The t-test was used in this thesis.

Certain sets of readings caused trouble in that their standard

deviations were obviously not equal. Those on page 67 are an example:

N_{60}: 97284, 97248, 97258

N_{62}: 96211, 96433, 96665, 96420, 96444, 96703, 96583, 96612, 96425

The standard deviation of N_{60} is 18.57 and that of N_{62} is 154.54; regarding the N_{60} readings as virtually constant (compared to those of N_{62}), the 90 per cent limits on the mean of N_{62} can be estimated from the t distribution to be 96499.5 ±119.1. Therefore the limits on the mean difference are approximately 763.8 ±119.1, or 644.7 to 882.9. Applying the t-test directly to the estimation of the 90 per cent limits on the difference between their means gives the limits as 594.7 to 933. Thus, even though the test is not strictly applicable due to the differing variances, it still gives one a fair idea of the confidence limits. Fortunately, there were only three instances in the entire set of experimental readings where the above situation arose.

APPENDIX P

TABLES OF EXPERIMENTAL RESULTS PLOTTED IN FIGURES 4-3 TO 4-26

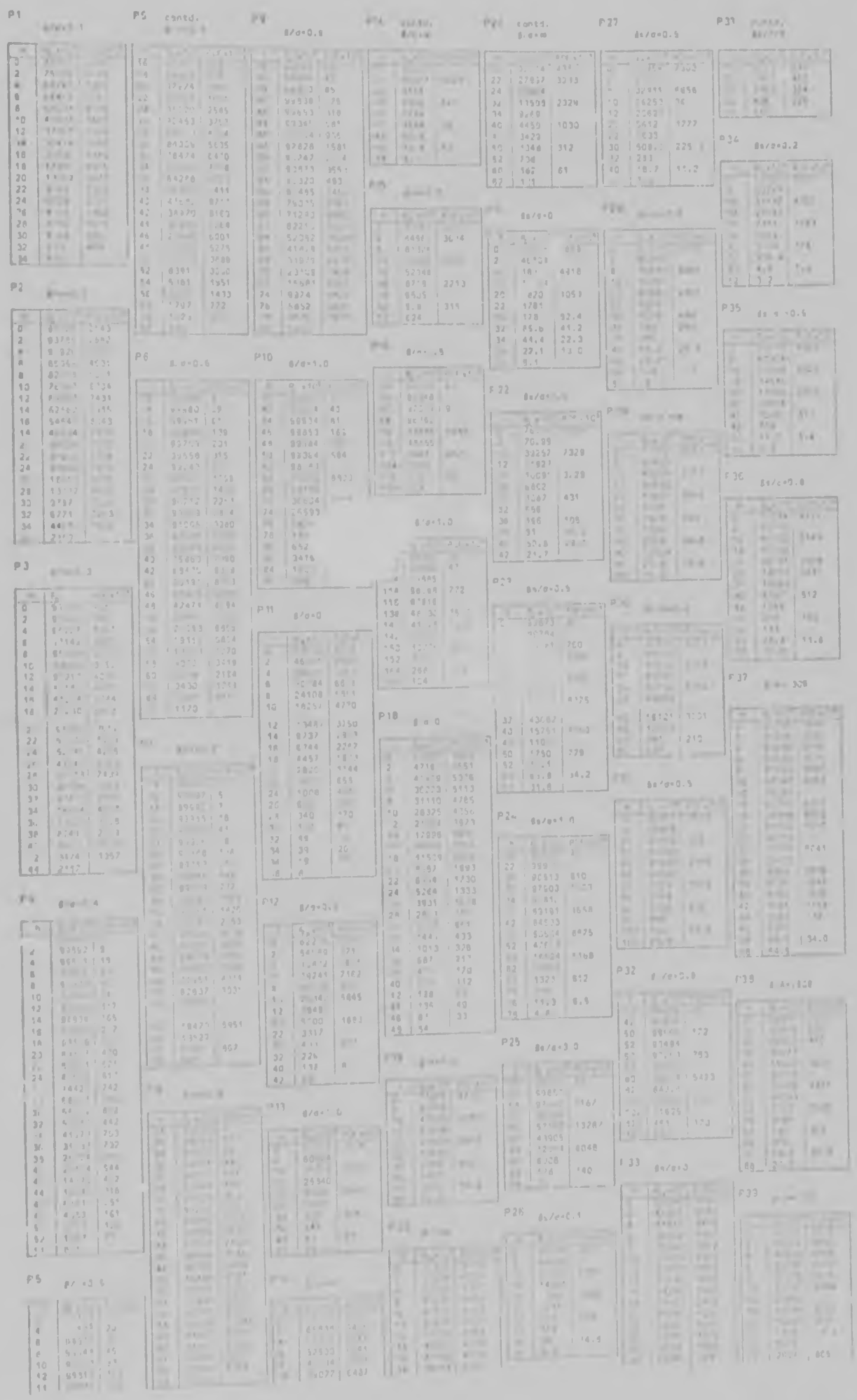

P39 contd.
β/A=.309

h	P_{FA} x10^5	PDF x10^5
28	1789	
36	274.7	96.3
38	178.4	75.4
40	103	46.4
42	56.6	25.2
44	31.4	14.5
46	16.9	

P40
β/A=.809

h	P_{FA} x10^5	PDF x10^5
0	64891	6161
2	58730	6599
4	52131	6669
6	45462	
10	32615	5893
12	26722	
20	9690	2615
22	7075	
30	1481	504
32	977	
36	365	162
38	203	
40	114.6	50.3
42	63.7	
48	8.0	4.1
50	3.9	

P41
β/A=.309

h	P_0 x10^5	PDF x10^5
0	99494	223
2	99271	
10	97350	952
12	96398	
24	85820	3070
26	82750	
32	71511	4849
34	66662	
40	51874	5079
42	46795	
50	29022	4127
52	24895	
64	7617	1554
66	6063	
80	764.2	215.5
82	548.7	
92	71.4	19.2
94	52.2	

P42
β/A=.5878

h	P_0 x10^5	PDF x10^5
40	99884	37
42	99786	

P43
β/A=.309

h	P_{FA} x10^5	PDF x10^5
0	57920	4664
2	53256	
10	35426	4217
12	31209	
24	12079	2153
26	9926	
32	5006	1078
34	4008	
40	1829	471
42	1358	
50	350	98
52	252	
64	21.8	7.8
66	14.0	

P44
β/A=.5875

h	P_{FA} x10^5	PDF x10^5
40	2285	590
42	1696	

APPENDIX Q

VOLTMETER READING INTERPRETATION

The two types of voltmeter used for measuring the noise signal and the sine wave levels were a Hewlett Packard True rms voltmeter and a Hewlett Packard average responding vacuum tube voltmeter (VTVM).

(a) True rms voltmeter

No conversion factors were required with this meter.

(b) Average responding VTVM

In this meter the input is rectified and applied to a moving coil meter calibrated to read the rms value of a sine wave. When the input is zero mean Gaussian noise with variance σ^2, the average deviation from zero of the rectified input is

$$2\int_0^\infty x\,\frac{1}{\sigma\sqrt{2\pi}}\exp\left[-x^2/2\sigma^2\right]dx = \sigma\sqrt{\frac{2}{\pi}}$$

For a sine wave,

$$V_{rms'\ av} = \pi/2\sqrt{2}$$

thus

$$\sigma\sqrt{\frac{2}{\pi}} = \text{meter reading} \times 2\sqrt{2}/\pi$$

and therefore

$$\sigma = \text{meter reading} \times 1.129$$

For zero mean Gaussian noise, σ is the same as the rms value.

When the input is a switching waveform that swings symmetrically about zero between +V and -V, say, the average and rms value of the rectified input is V. The meter reading must therefore be multiplied by $\pi/2\sqrt{2}$, i.e. 1.11. For example, for an rms value of 0.25 volts, the meter must read 0.278 volts.

APPENDIX R

VOLTAGES USED FOR THE EXPERIMENTAL READINGS

(a) Single-bit Gaussian reflection corrupted by wideband Gaussian noise

Signal-to-noise ratio (β/σ)	β (volts)	Ave. resp. VTVM reading (volts)	σ (volts)	Ave. resp. VTVM reading (volts)
0	0	0	0.25	0.222
0.1	0.05	0.056	0.50	0.443
0.2	0.10	0.111	0.50	0.443
0.3	0.20	0.222	0.667	0.591
0.4	0.15	0.166	0.375	0.332
0.5	0.20	0.222	0.40	0.356
0.6	0.25	0.278	0.416	0.368
0.7	0.25	0.278	0.358	0.317
0.8	0.25	0.278	0.313	0.277
0.9	0.25	0.278	0.278	0.246
1.0	0.25	0.278	0.25	0.222
∞	0.25	0.278	0	0

(b) Analog Gaussian reflection corrupted by wideband Gaussian noise

	100 samples		200 samples	
Signal-to-noise ratio ($\beta s/\sigma$)	βs (volts)	σ (volts)	βs (volts)	σ (volts)
0	0	0.25	0	0.25
0.1	0.25	2.50		
0.2			0.15	0.75
0.5	0.30	0.60	0.25	0.50
0.8			0.25	0.313
1.0	0.30	0.30		
∞	0.25	0	0.25	0

(c) Single-bit Gaussian reflection corrupted by a random phase sine wave

		100 samples		200 samples	
β/A	Signal-to-noise ratio ($\beta\sqrt{2}/A$)	β (volts)	$A/\sqrt{2}$ (volts)	β (volts)	$A/\sqrt{2}$ (volts)
0.309	0.436	0.20	0.458	0.20	0.458
0.588	0.831			0.20	0.240
0.809	1.143	0.343	0.30		

APPENDIX S

COMPUTER PROGRAMS FOR THE THEORETICAL DISTRIBUTIONS

PROGRAM 1: Probability mass function of $\Psi_b(0)$ for the cross-correlation of a single-bit Gaussian signal and a reflection corrupted by wideband Gaussian noise. The program has been used for up to 500 samples and signal-to-noise ratios of zero to five.

```
      DO 11 II=1,5
      N=100*II                          N is the number of samples cross-correlated
      DO 10 JK=1,9
      B=.1*JK
      SIG=1.                                        B/SIG corresponds to (β/σ)
      WRITE(6,1) N,B,SIG
    1 FORMAT(1X,'T/DT=',I8,3X,'BETA=',F5.2,3X,'SIGMA=',F5.2)
      P=.5*(1-ERF(B/(SIG*1.41422)))
      SUM=0.
      WRITE(6,2)
    2 FORMAT(//3X,'BINOMIAL DISTRIB OF ERRORS FOR TAU=0')
      WRITE(6,3)
    3 FORMAT(//3X,'PSI(0)',10X,'PROB',17X,'SUM')
      N1=.1*N-10*B
      DO 8 J=N1,N
      M=N
      FACT=1.
      IF(J.LT.(N-J)) GO TO 4
      NL=N-J
      Z=1-P
      JJ=NL
      GO TO 5
    4 NL=J
      JJ=NL
      Z=P
    5 DO 6 I=1,NL
      FACT=(FACT*M*Z*(1-Z))/JJ
      M=M-1
    6 JJ=JJ-1
      FACT=FACT*((1-Z)**(N-Z*NL))
      C=N-2*J
      SUM=SUM+FACT
    7 PROB=FACT
      IF(PROB.LT.(.1E-10).AND.J.GT.(N/2)) GO TO 10
    8 WRITE(6,9) C,PROB,SUM
    9 FORMAT(2X,F7.2,5X,E14.6,8X,E14.6)
   10 CONTINUE
   11 CONTINUE
      END
```

Evaluation of the binomial distribution ${}_NC_r\ p^r(1-p)^{N-r}$ (=PROB)

C corresponds to the threshold h

SUM is the Detection probability

PROGRAM 2: Probability mass function of $\Psi_b(\tau)$ for the cross-correlation of a burst-type single-bit Gaussian signal and a reflection corrupted by wideband Gaussian noise. The program has been used for up to 1000 samples for all signal-to-noise ratios.

```
      DIMENSION P(1001),P(1001)
      TAU=21.*3.E6
C     WHERE 21.*3 IS THE OUTPUT N OF THE SIGNAL
C     AND 3.E6 IS THE CORRELATION INSTANT
      DT=.01*.01*21.
C     WHERE .01*21 IS THE INTERVAL BETWEEN CORRELATIONS
      PI=3.1415927
      DO 260 I2=1,10
      NT=100*I2
```

NT is the total number of samples

COMPUTER PROGRAMS FOR THE THEORETICAL DISTRIBUTIONS

PROGRAM 1: Probability mass function of $\Psi_s(0)$ for the cross-correlation of a single-bit Gaussian signal and a reflection corrupted by wideband Gaussian noise. The program has been used for up to 500 samples and signal-to-noise ratios of zero to five.

```
      DO 11 II=1,5
      N=100*II                    N is the number of samples cross-correlated
      DO 10 JK=1,9
      B=.1*JK
                                  B/SIG corresponds to (β/σ)
      SIG=1.
      WRITE(6,1) N,B,SIG
    1 FORMAT(1X,'T/DT=',I8,3X,'BETA=',F5.2,3X,'SIGMA=',F5.2)
      P=.5*(1-ERF(B/(SIG*1.41422)))
      SUM=0.
      WRITE(6,2)
    2 FORMAT(//3X,'BINOMIAL DISTRIB OF ERRORS FOR TAU=0')
      WRITE(6,3)
    3 FORMAT(//3X,'PSI(0)',10X,'PROB',17X,'SUM')
      M1=.1*N-10*B
      DO 8 J=M1,N
      M=N
      FACT=1.
      IF(J.LT.(N-J)) GO TO 4
      NL=N-J
      Z=1-P
      JJ=NL
      GO TO 5
    4 NL=J
      JJ=NL
      Z=P
    5 DO 6 I=1,NL
      FACT=(FACT*M*Z*(1-Z))/JJ
      M=M-1
    6 JJ=JJ-1
      FACT=FACT*((1-Z)**(N-2*NL))
      C=N-2*J                     Evaluation of the binomial
      SUM=SUM+FACT                distribution  ${}_NC_r\ p^r(1-p)^{N-r}$
    7 PROB=FACT                   (=PROB)
      IF(PROB.LT.(.1E-10).AND.J.GT.(N/2)) GO TO 10
    8 WRITE(6,9) C,PROB,SUM       C corresponds to the threshold h
    9 FORMAT(2X,F7.2,5X,E14.6,8X,E14.6)   SUM is the Detection probability
   10 CONTINUE
   11 CONTINUE
      END
```

PROGRAM 2: Probability mass function of $\Psi_s(\tau)$ for the cross-correlation of a burst-type single-bit Gaussian signal and a reflection corrupted by wideband Gaussian noise. The program has been used for up to 1000 samples for all signal-to-noise ratios.

```
      DIMENSION P(1001),PR(1001)
      T40=21.*0.064
C     WHERE 21=M2 IS THE CUTOFF # OF THE SIGNAL
C     AND .064=S IS THE CORRELATION INSTANT
      DT=.01281*21.
C     WHERE .01281 IS THE INTERVAL BETWEEN CORRELATIONS
      PI=3.1415927
      DO 260 I2=1,10              NT is the total number of samples
      NT=100*I2
```

```
008           N=NT-5
009           N1=N
010           SIG=1.
011           DO 250 I3=1,10
012           B=I3*.1
013           XX=EPF(B/(SIG*1.4142))
014           X=2.*PI*TAU
015           ROE=XX*(2./PI)*ARSIN(SIN(X)/X)
016           EAN=N*ROE
      C       WHERE EAN IS THE MEAN OF THE SUM OF N PRODUCTS
017           VAR=0.
018           DO 10 I=1,4
019           XXX=2.*PI*I*21.*.01281
020           VAR=VAR+2.*(N-I)*((XX*(2./PI)*ARSIN(SIN(XXX)/XXX))**2)
021     10    CONTINUE
022           VAR=VAR+2.*(N-4.)*(N-5.)*.5*((ROE)**2)
023           VAR=VAR+N-(EAN)**2
024           STD=SQRT(VAR)
025           SD=2.*SQRT(N*.5*(1.+ROE)*.5*(1.-ROE))
      C       SD IS THE STAN.DEV. RESULTING FROM CENTRAL LIMIT THM
026           WRITE(6,20) NT,B,SIG
027     20    FORMAT('1',3X,'SAMPLE NO=',F7.1,3X,'B=',F5.2,3X,'SIG=',F6.3)
028           WRITE(6,30) ROE,EAN,STD,SD
029     30    FORMAT(/3X,'ROE=',E14.6,3X,'MEAN=',F6.2,3X,'S.D.=',F7.2,3X,'CF. RO
              2DT(NPQ)=',F7.2)
030           SUM=0.
031           N9=N-1
032           DO 70 J=1,N9
033           A=2.*J-N
      C       WHERE A IS THE VALUE OF THE PRODUCT SUM
034           B=(A+1.-EAN)/(STD*1.4142)
035           C=(A-1.-EAN)/(STD*1.4142)
036           PR(J+1)=.5*(ERF(B)-ERF(C))
037           SUM=SUM+PR(J+1)
038     70    CONTINUE
      C       WHERE PR(J+1) CORRESPONDS TO VALUE OF PSI 2J-N
039           PR(N+1)=0.
040           PR(1)=0.
041           WRITE(6,75) SUM
042     75    FORMAT(/1X,'SUM OF PROBS FOR CORR OVER(T-TAU)=',E14.6)
      C       WORKING OUT THE BINOMIAL DISTRIBUTION DUE TO CORR OVER TAU
043           SUM1=0.
044           N2=N1-1
045           DO 120 J1=1,N2
046           M1=N1
047           F=1.
048           IF(J1.LT.(N1-J1)) GO TO 90
050           N4=N1-J1
051           Z1=1.-.5
      C       Z1 IS THE PROB THAT ANY ONE PROD TERM IS +1
052           JJJ=N4
053           GO TO 100
054     90    N4=J1
055           Z1=.5
056           JJJ=N4
057     100   DO 110 I1=1,N4
058           F=(F*M1*Z1*(1.-Z1))/JJJ
059           M1=M1-1
060     110   JJJ=JJJ-1
061           F=F*((1.-Z1)**(N1-2.*N4))
062           J2=J1+1
063           P(J2)=F
064     120   CONTINUE
065           P(N1+1)=.5**N1
      C       WHERE P(J+1) IS THE PROB OF J SUCCESSES (PROD=1)
      C       SO CORR. SUM=2.*J-N1-P(1) CORRESPONDS TO SUM=-N1
066           P(1)=.5**N1
067           WRITE(6,140)
068     140   FORMAT(///2X,'FINAL DISTRIBUTION OF PSI(TAU)')
069           WRITE(6,150)
070     150   FORMAT(///2X,'VAL OF PSI(TAU)',4X,'PROB(PSI(TAU))',5X,'SUM OF PROBS
              3')
      C       THE FOLLOWING ASSUMES TAU/DT<(T-TAU)/DT. IF NOT REVERSE THEIR ROLES
071           SUMB=0.
072           N6=1+NT/2
073           DO 200 J=1,N6
074           PRO=0.
075           IF(J.LT.(N1+1)) GO TO 160
077           N5=N1+1
078           GO TO 170
079     160   N5=J
080     170   DO 180 I=1,N5
081     180   PRO=PRO+P(I)*PR(J+1-I)
082           SUMB=SUMB+PRO
083           C2=-NT+2.*J-2.
```

N is the number of samples in $T-\tau$
N1 is the number of samples in τ

B/SIG corresponds to (β/σ)

ROE equals $\psi_{xx}(\tau)$

VAR is the variance of the distribution over $(T-\tau)$

PR(I) are the Normal density function values for the sum of the N product terms in $(T-\tau)$

Similar to PROGRAM 1
N1 corresponds to N,
M1 to M, F to FACT
and P to PROB.
P=(1-P)=0.5 here.

Combining the two distributions as in Appendix C(3)

C2 corresponds to the threshold h (for h negative)

```
084             M4=20*(1+12)
085             IF(C2.LT.(-M4)) GO TO 200
087             WRITE(6,190) C2,PRO,SUMB
088       190   FORMAT(5X,F7.1,2(8,E14.6,5X,E14.6))
089       200   CONTINUE
          C     THIS GIVES PRODUCTS FOR PSI NEGATIVE
090             N7=(M4+EAN)/2.+1
091             DO 240 J=1,N7
092             PRO=0.
093             IF((2.*J).GT.(N-N1)) GO TO 210
095             N8=N1+1
096             GO TO 220
097       210   N8=(NT+2-2*J)/2
098       220   DO 230 I=1,N8
099       230   PRO=PRO+P(N1+2.-I)*PR(N-(NT/2.)+J+I)
100             SUMB=SUMB+PRO
101             C3=2.*J                          C3 corresponds to the threshold h
102             WRITE(6,190) C3,PRO,SUMB                 (for h positive)
103       240   CONTINUE
104       250   CONTINUE
105       260   CONTINUE
106             STOP
107             END
```

PROGRAM 3: Probability mass function of $\psi_s(0)$ for the cross-correlation of an analog Gaussian signal and a reflection corrupted by wideband Gaussian noise. The program has been used for up to 500 samples and signal-to-noise ratios of zero to five.

```
002             DO 110 II=1,10
003             N=100*II                 N is the number of samples cross-correlated
004             DO 100 JK=1,8
005             B=.1*JK                                  B/SIG corresponds to (Bs/σ)
006             SIG=1.
007             WRITE(6,10)
008       10    FORMAT('1'1X,'DISTRIB OF PSI(0),UNCLIPPED NOISE+ NOISE')
009             WRITE(6,20) N,B,SIG
010       20    FORMAT(1X,'SAMPLE NO=',I5,3X,'BETA=',F5.2,3X,'SIGMA=',F5.2)
011             P=.5*(1-(2/3.14159)*ATAN(B/SIG))
012             SUM=0.
013             WRITE(6,30)
014       30    FORMAT(//3X,'PSI(0)',10X,'PROB',17X,'SUM')
015             N1=.1*N-10*B
016             DO 80 J=N1,N
017             M=N
018             FACT=1.
019             IF(J.LT.(N-J)) GO TO 40
021             NL=N-J
022             Z=1-P
023             JJ=NL
024             GO TO 50
025       40    NL=J                                     see PROGRAM 1 for comments
026             JJ=NL
027             Z=P
028       50    DO 60 I=1,NL
029             FACT=(FACT*M*Z*(1-Z))/JJ
030             M=M-1
031       60    JJ=JJ-1
032             FACT=FACT*((1-Z)**(N-2*NL))
033             C=N-2*J
034             SUM=SUM+FACT
035       70    PROB=FACT
036             IF(PROB.LT.1.E-25.AND.J.GE.(N/2)) GO TO 100
038       80    WRITE(6,90) C,PROB,SUM
039       90    FORMAT(1X,F7.2,5X,E14.6,8X,E14.6)
040       100   CONTINUE
041       110   CONTINUE
042             STOP
043             END
```

PROGRAM 4: Probability mass function of $\psi_s(t)$ for the cross-correlation of a continuous analog Gaussian signal and a reflection corrupted by wideband Gaussian noise. The program has been used for 100 and 200 samples for all signal-to-noise ratios.

```
002           REAL*8 PRO,XX,PI,X,EAN,VAR,XXX,STD,B1,C1,B,SIG,RCE1,RCE12,ROE2
003           REAL*8 ROE
              C
              C     THIS PROGRAM ASSUMES THAT OVER THE WHOLE CORRELATION PERIOD C TO T
              C     THE RECEIVED WAVEFORM IS SGN(B*F(T)+N(T)) I.E. ONLY ONE DISTRIBUTION
              C     HAS TO BE DERIVED
              C
004           PI=4.*DATAN(1.D0)
005           SIG=1.D0
006           DO 110 I2=1,2
007           W=20.**.5*I2
              C     W IS THE BANDWIDTH OF THE SIGNAL
008           DT=W/79.249
              C     WHERE 79.25 KHZ IS THE CORRELATION FREQUENCY
009           TAU=5.*DT
010           X=2.*PI*TAU
011           ROE=DSIN(X)/X
012           DO 100 III=1,2
013           N=100*III
014           DO 90 I3=1,10
015           B=.1*I3
016           WRITE(6,5) W
017     5     FORMAT('1',1X,'DISTRIBUTION FOR UNCLIPPED NOISE+NOISE, W(KHZ)=',F6
              3.1)
018           XX=B**2/(1.D0+B**2)
019           ROE12=DARSIN(DSQRT(XX)*ROE)*2.D0/PI
020           EAN=W=ROE12
              C     WHERE EAN IS THE MEAN OF THE SUM OF N PRODUCTS
021           VAR=0.
022           DO 10 I=1,4
023           XXX=2.*PI*I*DT
024           ROE1=DARSIN(DSIN(XXX)/XXX)*2.D0/PI
025           ROE2=DARSIN(XX*DSIN(XXX)/XXX)*2.D0/PI
026           VAR=VAR+2.D0*(N-I)*ROE1*ROE2
027     10    CONTINUE
028           VAR=VAR+2.*(N-4.)*(N-5.)*.5*(ROE12)**2)
029           VAR=VAR+N-(EAN)**2
030           STD=DSQRT(VAR)
031           SD=2.*SQRT(N*.5*(1.+ROE12)*.5*(1.-ROE12))
              C     SD IS THE STAN.DEV. RESULTING FROM CENTRAL LIMIT THM
032           WRITE(6,20) N,B,SIG
033     20    FORMAT(/3X,'SAMPLE NO=',I4,3X,'B=',F7.2,3X,'SIG=',F6.3)
034           WRITE(6,30) ROE12,EAN
035     30    FORMAT(/3X,'ROE12=',E14.6,3X,'MEAN=',F6.2)
036           WRITE(6,31) STD,SD
037     31    FORMAT(/3X,'S.D.=',F8.4,3X,'CF. S.D. FOR INDEPENDENT TERMS=',F7.2)
038           WRITE(6,35)
039     35    FORMAT(//5X,'FINAL DISTRIBUTION OF PSI(TAU)')
040           WRITE(6,40)
041     40    FORMAT(//2X,'VAL OF PSI(TAU)',4X,'PROB(PSI(TAU))',6X,'SUM OF PROBS
              3')
042           SUM=0.
043           IF(III.EQ.2) GO TO 45
045           N3=10
046           N4=80
047           GO TO 50
048     45    N3=45
049           N4=155
050     50    DO 70 J=N3,N4
051           NA=N-2*J
052           B1=(NA*1.-EAN)/(STD*DSQRT(2.D0))
053           C1=(NA-1.-EAN)/(STD*DSQRT(2.D0))
054           PRO=.5*(DERF(B1)-DERF(C1))
055           SUM=SUM+PRO
              C     PRO IS THE PROBABILITY THAT THE PRODUCT SUM EQUALS NA
056     70    WRITE(6,72) NA,PRO,SUM
057     72    FORMAT(6X,I4,10X,E14.6,5X,E14.6)
058     80    CONTINUE
059     90    CONTINUE
060     100   CONTINUE
061     110   CONTINUE
062           STOP
063           END
```

DT is the sampling interval in milliseconds. $X = \omega_b T$

N is the total number of samples

B is the signal-to-noise ratio ($\beta s/\sigma$)

Evaluating the distribution variance from eqn. (2.2.16)

NA is the threshold level h

SUM is the False Alarm probability

PROGRAM 5: Probability mass function of $\psi_n(0)$ for the cross-correlation of a single-bit Gaussian signal and a reflection corrupted by a random phase 3903 Hz sine wave. The program has been used for up to 500 samples and signal-to-noise ratios between zero and unity.

```
002           PI=3.14159227
003           A=1.
004           DO 400 II=1,2
005           NTN=100*II
006           DO 360 I1=1,10                          NTN is the total number of samples
007           K=I1
008           B=A*SIN((PI/2.)*(1.-.1*K))
      C       A=SINE AMPLITUDE,B=SIGNAL AMPLITUDE FOR EXACTLY
      C       K SAMPLES/ERROR ZONE,NTN=TOTAL NO OF SAMPLES
009           DT=.012811E-03
010           F=1./(20.*DT)
      C       DT IS THE SAMPLING INTERVAL,F=SINE FREQUENCY
011           T=1./F
012           WT=NTN*DT
013           MM=2*F*WT
014           ST=MM/(2.*F)
015           S=ARSIN(B/A)
016           DST=WT-ST
      C       WT=WAVEFORM DURATION,MM=LARGEST NO OF EXACT HALFWAVES
      C       IN WT, ST=DURATION OF MM-HALFWAVES,DST=REMAINDER
017           X1=S/(2.*PI*F)
018           X2=2.*X1
019           IF(DST.GT.X1.AND.DST.LT.X2) GO TO 20
021           DET=DST*(1.-2.*S/PI)
022           GO TO 30
023     20    DET=DST*(1.-S/PI)-(S**2)/(4.*(PI**2)*F)-F*(DST**2)
024     30    ET=ST*(1.-2.*S/PI)+DET
      C       ET IS THE TOTAL PART OF ST SPENT IN ERROR ZONE.DET IS
      C       THE PART OF DST
025           EN=ET/DT
026           EAN=NTN-EN
      C       EN=NO OF SAMPLES IN ERROR ZONE.EAN=MEAN OF SUM OF NTN SAMPLES
027           VAR=0.
028           MT=NTN-1
029           DO 300 I=1,MT
030           TAU=DT*(NTN-I)
031           X=2.*PI*TAU*21.E03                                  ROE= Ψ1((N-i)δt)
032           ROE=(2./PI)*ARSIN(SIN(X)/X)
033           NN=TAU/T
034           EXT=TAU-NN*T
      C       AS SINE IS PERIODIC,CURR FUNC IS ALSO.EXT IS THE
      C       DIFF BETWEEN TAU & NO OF WHOLE CYCLES I.E TAU
035           DEL=X2
036           T1=-DEL*T/2.
037           T2=DEL*T/2.
038           T3=T-DEL
039           IF(DEL.GE.(T/4.)) GO TO 200
041           IF(EXT.GE.(0.0).AND.EXT.LT.DEL) GO TO 40
043           IF(EXT.GE.DEL.AND.EXT.LT.T1) GO TO 50
045           IF(EXT.GE.T1.AND.EXT.LT.(T/2.)) GO TO 60
047           IF(EXT.GE.(T/2.).AND.EXT.LT.T2) GO TO 70
049           IF(EXT.GE.T2.AND.EXT.LT.T3) GO TO 80
051           IF(EXT.GE.T3.AND.EXT.LE.T) GO TO 90
053     200   IF(EXT.GE.(0.0).AND.EXT.LT.T1) GO TO 40
055           IF(EXT.GE.T1.AND.EXT.LT.DEL) GO TO 100
057           IF(EXT.GE.DEL.AND.EXT.LT.(T/2.)) GO TO 30
059           IF(EXT.GE.(T/2.).AND.EXT.LT.T3) GO TO 70
061           IF(EXT.GE.T3.AND.EXT.LT.T2) GO TO 100
063           IF(EXT.GE.T2.AND.EXT.LE.T) GO TO 90
065     40    R=1.-2.*(DEL+EXT)/T                                 Defining the
066           GO TO 300                                           auto-correlation
067     50    R=1.-4.*EXT/T                                       function Ψ1(TAU)
068           GO TO 300                                           of ξ(t)
069     60    R=-2.*(EXT-DEL)/T
070           GO TO 300
071     70    R=-2.*(1.-(EXT+DEL)/T)
072           GO TO 300
073     80    R=-(3.-4.*EXT/T)
074           GO TO 300
075     90    R=(2.*(EXT-DEL)/T)-1.
076           GO TO 300
077     100   R=0.0
078     300   VAR=VAR+I*R*ROE                                     VAR is the variance of
079           VAR=VAR+2.*B**                                      Ψs(0) from eqn. (2.3.9)
080           STD=SQRT(VAR)
081           WRITE(6,310)
082     310   FORMAT('1',/1X,'DISTRIB OF PSI(0) FOR SIGNAL=SINEWAVE')
083           WRITE(6,320) NTN,A
084     320   FORMAT(/1X,'SAMPLE SIZE=',I2,3X,'STD=',F4.2,3X,'A=',F6.4)
085           WRITE(6,330) B,ST,DST
086     330   FORMAT(1X,'SIGNAL AMPLITUDE=',F7.4,3X,'WAVEFORM DURATION=',F7.4,3X,'S.D.=',F6.3)
087           WRITE(6,340)
088     340   FORMAT(/2X,'PSI(0)',8X,'FREQ',8X,'SUM')
089           SUM=0.0
090           NINI=NTN+1
```

```
091             DO 360 J=1,NTN1
092             M=2*(J-1)-NTN
093             X=(M+1.-EAN)/(STD*1.4142)
094             Y=(M-1.-EAN)/(STD*1.4142)
095             P=.5*(ERF(X)-ERF(Y))
096             SUM=SUM+P
097             M1=EAN-60*II
098             M2=EAN+60*II
099             IF(M.LT.M1.OR.M.GT.M2) GO TO 360
101             WRITE(6,350) M,P,SUM
102     350     FORMAT(2X,I5,4X,E14.5,2X,E14.6,)
103     360     CONTINUE
104     400     CONTINUE
105             STOP
106             END
```

M is the threshold h, P is the probability mass function value at h, and SUM is the Detection probability

PROGRAM 6: Probability mass function of $\psi_s(\tau)$ for the cross-correlation of a continuous single-bit Gaussian signal and a reflection corrupted by a random phase 3903 Hz sine wave. The program has been used for up to 500 samples and signal-to-noise ratios between zero and unity.

```
002             PI=4.*ATAN(1.)
003             A=1.
004             DO 370 II=1,2
005             NTN=100*II
006             DO 360 II=1,10
007             B=SIN(PI/2.*(1.-.1*(II)))
008             S=ARSIN(B/A)
        C       A=PEAK SINE AMPLITUDE,B=SIGNAL AMPLITUDE
        C       FOR EXACTLY II SAMPLES /ERROR ZONE. NTN=TOTAL SAMPLE NO.
009             DT=.01281E-03
010             TAU=5.*DT
011             X=2.*PI*21.E03*TAU
012             ROE=2.*ARSIN(SIN(X)/X)/PI
013             F=1./(20.*DT)
014             T=1./F
        C       DT=SAMPLING INTERVAL,F=SINE FREQUENCY
015             TT=T/2.
016             X1=5/12.*PI*F)
017             X2=2.*X1
018             VAR1=0.
019             NA=NTN-5
020             EAN=NTN*2.*S*ROE/PI
021             T2=TT-X2
022             DO 150 L=1,NA
023             TTL=(NTN-NA+L-1)*DT
024             T1=AMOD(TTL,TT)
        C       AS GAMMA FUNC IS PERIODIC; SO IS ITS CORR FUNC.
        C       T1 IS THE DELAY REDUCED TO LESS THAN ONE CYCLE.
025             IF(X2.LT.(T/4.)) GO TO 100
027             IF(T1.GE.(0.).AND.T1.LE.T2) GO TO 110
029             IF(T1.GE.T2.AND.T1.LE.X2) GO TO 120
031             IF(T1.GE.X2.AND.T1.LE.TT) GO TO 130
033     100     IF(T1.GE.(0.).AND.T1.LE.X2) GO TO 110
035             IF(T1.GE.X2.AND.T1.LE.T2) GO TO 140
037             IF(T1.GE.T2.AND.T1.LE.TT) GO TO 130
039     110     ROE2=(X2-T1)/TT
040             GO TO 150
041     120     ROE2=(2.*X2-TT)/TT
042             GO TO 150
043     130     ROE2=(X2-TT+T1)/TT
044             GO TO 150
045     140     ROE2=0.
046     150     VAR1=VAR1+(NA-L+1)*ROE2
047             VAR1=VAR1*2.*(ROE**2)
048             ND=NTN-NA-1
049             DO 90 K=1,ND
050             TL=K*DT
051             A1=2.*PI*21.E03*TL
052             ROE1=2.*ARSIN(SIN(A1)/A1)/PI
053             T1=AMOD(TTL,TT)
054             IF(X2.LT.(T/4.)) GO TO 40
056             IF(T1.GE.(0.).AND.T1.LE.T2) GO TO 50
058             IF(T1.GE.T2.AND.T1.LE.X2) GO TO 60
060             IF(T1.GE.X2.AND.T1.LE.TT) GO TO 70
062     40      IF(T1.GE.(0.).AND.T1.LE.X2) GO TO 80
064             IF(T1.GE.X2.AND.T1.LE.T2) GO TO 90
```

X2 corresponds to t_{nez} (=2δ)

Defining ROE2 as $\psi_s[(N-N_a+i)\delta t]$ in eqn. (2.3.19)

ROE1= $\psi_s(i\delta t)$ in eqn. (2.3.19)

```
066             IF(T1.GE.T2.AND.T1.LE.TT) GO TO 70
068     50      ROE2=(X2-T1)/TT
069             GO TO 90
070     60      ROE2=(2.*X2-TT)/TT
071             GO TO 90
072     70      ROE2=(X2-TT+T1)/TT
073             GO TO 90
074     80      ROE2=0.
075     90      VAR1=VAR1+(NTN-K)*ROE2*(ROE1**2)*2.
076             VAR1=VAR1+NTN*S**2./PI-(EAN**2)
077             T4=TT+X2
078             T5=T-X2
079             VAR2=0.
080             MM=NTN-1
081             DO 290 LL=1,MM
082             TTT=LL*DT
083             T3=AMOD(TTT,T)
084             IF(X2.GE.(T/4.)) GO TO 200
086             IF(T3.GE.(0.).AND.T3.LT.X2) GO TO 210
098             IF(T3.GE.X2.AND.T3.LT.T2) GO TO 220
090             IF(T3.GE.T2.AND.T3.LT.TT) GO TO 230
092             IF(T3.GE.TT.AND.T3.LT.T4) GO TO 240
094             IF(T3.GE.T4.AND.T3.LT.T5) GO TO 250
096             IF(T3.GE.T5.AND.T3.LE.T) GO TO 260
098     200     IF(T3.GE.(0.).AND.T3.LT.T2) GO TO 210
100             IF(T3.GE.T2.AND.T3.LT.X2) GO TO 270
102             IF(T3.GE.X2.AND.T3.LT.TT) GO TO 230
104             IF(T3.GE.TT.AND.T3.LT.T5) GO TO 240
106             IF(T3.GE.T5.AND.T3.LT.T4) GO TO 270
108             IF(T3.GE.T4.AND.T3.LE.T) GO TO 260
110     210     R=1.-(X2+T3)/TT
111             GO TO 280
112     220     R=1.-2.*T3/TT
113             GO TO 280
114     230     R=-(T3-X2)/TT
115             GO TO 280
116     240     R=-2.*(1.-(T3+X2)/T)
117             GO TO
118     250     R=-(3. 4.*T3/T)
119             GO TO 280
120     260     R=(T3-X2)/TT-1.
121             GO TO 290
122     270     R=0.0
123     280     A2=2.*PI*21.E03*TTT
124             R1=2.*ARSIN(SIN(A2)/A2)/PI
125     290     VAR2=VAR2+(NTN-LL)*R*R1
126             VAR2=VAR2*2.+NTN*(1.-2.*S/PI)
127             VAR=VAR1+VAR2
128             STD=SQRT(VAR)
129             SV=STD*SQRT(2.)
130             WRITE(6,300)
131     300     FORMAT('1',/1X,'DISTRIB OF PSI(T) FOR SIGNAL+SINEWAVE')
132             WRITE(6,310) NTN,S,A
133     310     FORMAT(/1X,'SAMPLE NO=',I4,3X,'BETA=',F6.4,3X,'A=',F6.4)
134             WRITE(6,320) F,EAN,STD
135     320     FORMAT(1X,'SINE FREQ=',F9.0,2X,'MEAN=',F8.2,2X,'S.D=',F7.3)
136             WRITE(6,330)
137     330     FORMAT(/3X,'PSI(T)',8X,'PROB',11X,'SUM')
138             SUM=0.0
139             DO 340 J=1,80
140             M=82-2*J
141             X=(M+1.-EAN)/SV
142             Y=(M-1.-EAN)/SV
143             P=.5*(ERF(X)-ERF(Y))
144             SUM=SUM+P
145     340     WRITE(6,350) M,P,SUM
146     350     FORMAT(2X,I5,5X,E14.6,2X,E14.6)
147     360     CONTINUE
148     370     CONTINUE
149             STOP
150             END
```

Defining ROE2 as $\psi_1(i\delta t)$ in eqn. (2.3.19)

VAR1 corresponds to var_{nez} in eqn. (2.3.19)

Defining R as $\psi_3(i\delta t)$ in eqn. (2.3.20)

R1= $\psi_2(i\delta t)$ in eqn. (2.3.20)

VAR2 corresponds to var_{ez} in eqn. (2.3.20)

M is the threshold h, P is the probability mass function value at h, and SUM is the False Alarm probability

APPENDIX T

THE DESIGN OF THE CROSS-CORRELATOR

In this appendix some of the general points in the design of the single-bit digital cross-correlator are discussed. The detailed drawings of the circuitry, printed circuit board layouts, etc., have not been included as they are of no vital importance to this thesis. They are, however, to be found in the separate manual that is kept with the instrument.

From consideration of the correlation function of the narrowband Gaussian signal (Fig. T-1) it was decided that the correlation function

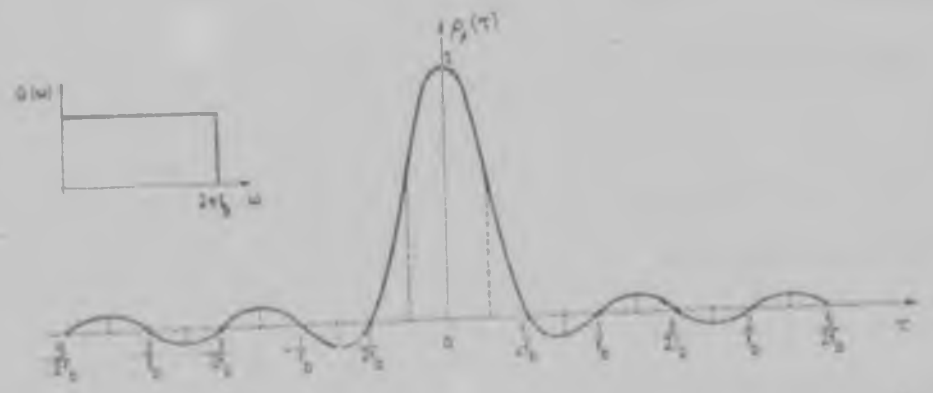

FIGURE T-1 Normalised auto-correlation function of bandlimited Gaussian noise.

should be evaluated at least every $(1/4f_b)$ seconds. For real time operation, this set the sampling rate at $4f_b$ samples/second, i.e. 8×10^4 samples/second for a Gaussian signal with a 20 kHz cut-off frequency.

For economy of circuitry serial processing was chosen. Thus between each sampling instant the two sets of samples have to be circulated around shift registers to perform the cross-correlation, and the result has to be processed and displayed. The computation is performed by an up/down

counter with the mode controlled by an Exclusive-Or gate having $x_1(t_i)$ and $x_2(t_i+\tau)$ as inputs. With a sampling rate of 80 kHz, the time between samples is 12.5 μs, and of this it was decided that 10 μs would be used for circulating the two waveforms, and 2.5 μs for processing, displaying and resetting the counters, etc.. For 200 sample cross-correlation this set the necessary shift register and up/down counter clocking rates at 20 MHz.

The narrowband Gaussian noise source chosen was a Sescosem 4.3 volt zener diode operating in the knee region. This was found to give a very large noise output extending up to well over 1 MHz. This was amplified and passed through a fifth order elliptic filter having less than 1 dB ripple in the pass band, cut-off frequency around 20 kHz, and having a response more than 40 dB down at 25 kHz, and more than 35 dB down above that frequency. The output of the filter was re-amplified and fed to the comparator feeding the reference signal register. The frequency spectrum of this comparator input (i.e. of $x_n(t)$) is shown in Fig. 4-2 on page 70.

Figure T-2 shows the instrument in its present form as a general purpose single-bit digital cross-correlator. It has three operating modes:

(a) AUTOMATIC - Automatically feeds in 100 or 200 reference and received waveform samples (single-bit) and cross-correlates the received waveform with the reference waveform up to the delay set on the selecting potentiometer (up to five seconds); it then feeds in two new sets of samples and repeats the process, etc..

(b) THEORETICAL - For verifying the mathematical predictions; i.e. it feeds in 100 or 200 reference and received waveform samples, and then cross-correlates the received waveform with the reference waveform six times, for $\tau = 0$ up to $\tau = 5/4f_b$. If $\psi_b(\tau)$ is greater than or equal to the set threshold h for $\tau = 0$, it pulses the Detection counter, and if $\psi_b(\tau)$

is greater than or equal to h for $\tau = 5/4f_b$, it pulses the False Alarm counter. It performs this set of ations N_R times. where N_R can be set to 10^2, 10^3,.... 10^7, and then stops automatical.y.

(c) MANUAL - On pressing the START button, it feeds in the reference and received waveform samples and then cross-correlates the received waveform with the reference waveform until stopped manually.

There is a SYNC output for triggering the oscilloscope used for the visual display, and the cross-correlator can be externally clocked.

A block diagram of the general operation of the instrument is given in Fig. T-3, and a simplified schematic is given in Fig. T-4.

FIGURE T-2 The single-bit digital cross-correlator in its present form.

AUTO- Start cross-correlating and continue for time t, as set. Then take new set of samples and repeat automa lcally, etc..

THEOR-Start cross-correlating and continue for 5 shifts of the received waveform. Then feed in new set of samples and repeat. Stop after 10^5, 10^6 etc. ,repetitions, as set.

MAN- Start cross-correlating and continue (with same set of samples) until stopped.

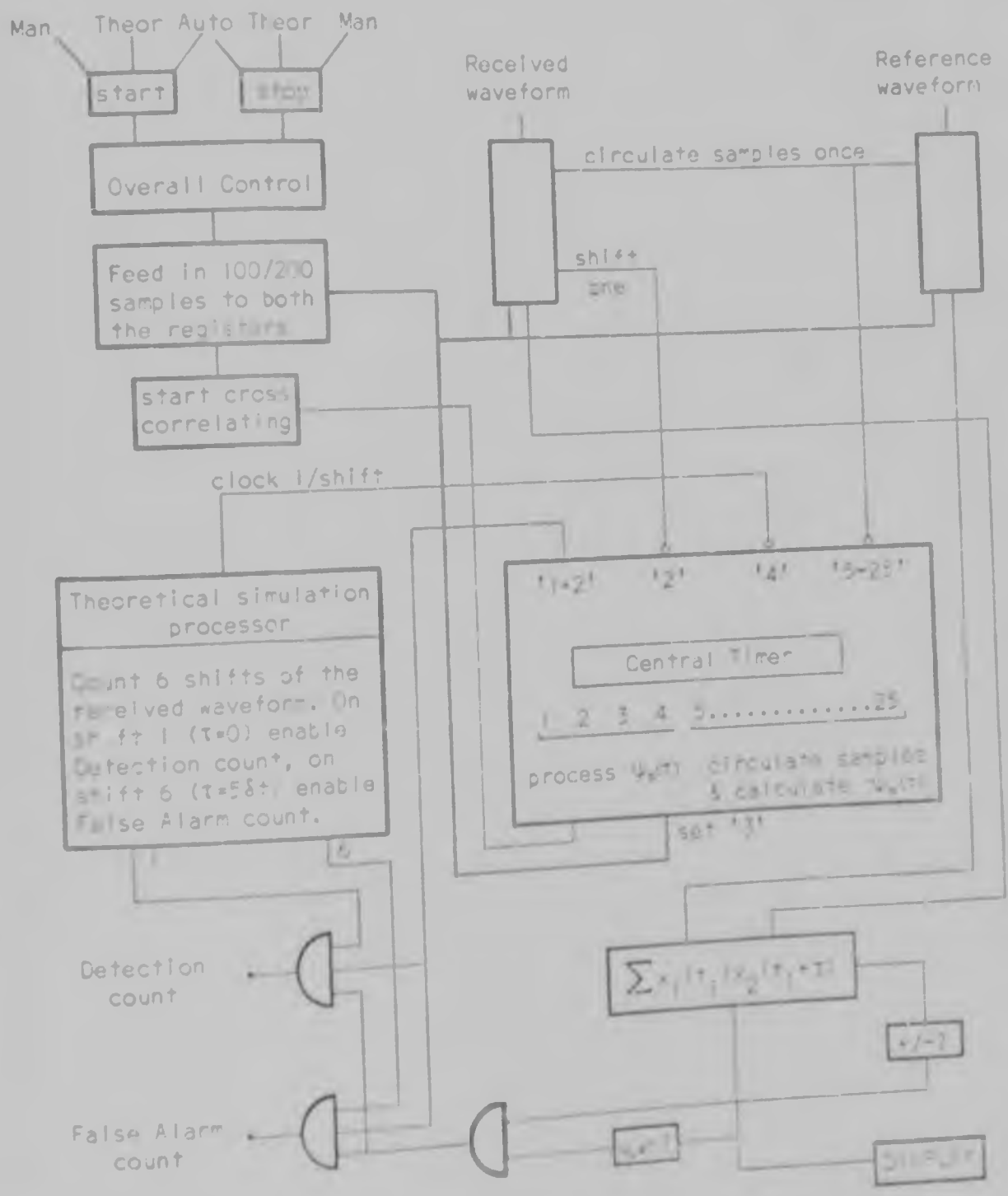

FIGURE T-3 Block diagram of cross-correlator operation.

REFERENCES

1. Van Vleck, J. H.:'The Spectrum of Clipped Noise', R. R. L. Report 51, July 21, 1943.

2. Lampar , D. G.:'The Probability Distribution for the Filtered Output of a Multiplier whose Inputs are Correlated, Stationary Time Series', IRE Trans., IT-2(2), March 1956, pp. 4-11.

3. Roe, G. M., and White, G. M.:'Probability Density Functions for Correlators with Noisy Reference Signals', IRE Trans., IT-7(1), January 1961, pp. 13-18.

4. Jacobson, M. J.:'Output Probability Distribution of a Correlator Detector with Signal Plus Noise Inputs', Jour. Acoust. Soc. Amer., 35(7), July 1963, pp. 1041-1048.

5. Cooper, D. C.:'The probability Density Function for the Output of a Correlator with Bandpass Input Waveforms', IEEE Trans., IT-11(2), April 1965, pp. 190-195.

6. Stremmler, F., and Jensen, T.:'The Probability Density Function for the Output of an Analog Crosscorrelator with Bandpass Inputs', IEEE Trans., IT-16(5), September 1970, pp. 627-629.

7. Murarka, N. P.:'The Probability Density Function for Correlators with Noisy Reference Inputs', IEEE Trans., COM-19(5), October 1971, pp. 711-714.

8. Andrews, L. C.:'The Probability Density Function for the Output of a Cross-correlator with Bandpass Inputs', IEEE Trans., IT-19(1), January 1973, pp. 13-19.

9. Andrews, L. C.:'Output Probability Density Functions for Cross-correlators Using Sampling Techniques', IEEE Trans., AES-10(1), January 1974, pp. 78-81.

10. Thomas, J. B., and Williams, T. R.:'On the Detection of Signals in Non Stationary Noise by Product Arrays', Jour. Acoust. Soc. Amer., 31(4), April 1959, pp. 453-462.

11. Ekre, H.:'Polarity Coincidence Correlation Detection of a Weak Noise Source', IEEE Trans., IT-9(1), January 1963, pp. 18-23.

12. Cheng, M. C.:'The Clipping Loss in Correlation Detectors for Arbitrary Signal-to-Noise Ratios', IEEE Trans., IT-14(3), May 1968, pp. 332-339.

13. Gassner, R. L., McGillem, C. D., and Cooper, G. R.:'A Wideband Digital Correlator', Proc. Nat. Electron. Conf., 1965, pp. 656-661.

14. McGillem, C. D., Cooper, G. R., and Waltman, W. B.:'An Experimental Random Signal Radar', Proc. Nat. Electron. Conf., 1967, pp. 409-412.

15. Aein, J. M.:'Normal Approximations to the Error Rate for Hard-limiting Correlators', IEEE Trans., COM-15(1), February 1967, pp. 44-51.

16. Collins, J. H., and Hagon, P. J.:'Surface Wave Delay Lines Promise Filters for Radar, Flat Tubes for Television, and Faster Computers', Electronics, 43(2), January 19, 1970, pp. 110-120.

17. Kino, G. S., and Shaw, J.:'Acoustic Surface Waves', Sci. Amer., 227, 1972, pp. 51-68.

18. Maines, J. D., and Paige, E. G. S.:'Surface-acoustic-wave Components, Devices and Applications', IEE Review, 120(10R), October 1973, pp. 1078-1110.

19. Morgan, D. P.:'Surface Acoustic Wave Devices and Applications - 5 - Signal Processing Using Programmable Non-Linear Convolvers', Ultrasonics, 12(2), March 1974, pp. 74-83.

20. Grant, P. M., Collins, J. H., Darby, B. J., and Morgan, D. P.:'Potential Applications of Acoustic Matched Filters to Air Traffic Control Systems', IEEE Trans., MTT-21(4), April 1973, pp. 288-300.

21. Broch, J. T.:'On the Applicability and Limitations of the Cross-correlation and Cross-spectral Density Techniques', Bruel & Kjaer Tech. Review, 4, 1970, pp. 3-27.

22. Lange, F. H.:'Correlation Techniques', London, ILIFFE, 1967.

23. Drake, A. W.:'Fundamentals of Applied Probability Theory', New York, McGraw Hill, 1967, p. 129.

24. Speigel, M. R.:'Theory and Problems of Statistics', New York, McGraw Hill (Schaum's Outline Series), 1961, p. 122.

25. Wozencraft, J. M., and Jacobs, I. M.:'Principles of Communication Engineering', 2nd. Ed., New York, John Wiley & Sons, 1967, pp. 106-108.

26. Kendall, M. G., and Stuart, A.:'The Advanced Theory of Statistics - Volume 1 - Distribution Theory', 2nd Ed., London, Charles Griffin, 1963, p. 193.

27. Feller, W.:'An Introduction to Probability Theory and its Applications Volume 2', New York, John Wiley & Sons, 1966, p. 258.

28. Kendall, M. G., and Stuart, A., op.cit., p. 224 and p. 234.

29. McFadden, J. A.:'The axis Crossing Intervals of Random Functions-II', IRE Trans., IT-4(1), March 1958, pp. 14-24.

30. Rice, S. O.:'Mathematical Analysis of Random Noise', in 'Selected Papers on Noise and Stochastic Processes', (N. Wax, Ed.), New York, Dover, 1954, p. 187.

31. Davenport, W. B., and Root, W. L.:'An Introduction to the Theory of Random Signals and Noise', New York, McGraw Hill, 1958, pp. 147-148.

32. Kendall, M. G., and Stuart, A., see Ref. 26, p. 350.

33. Gupta, S. S.:'Probability Integrals of Multivariate Normal and Multivariate t', Annals of Maths. Stats., 34, 1963, pp. 792-839.

34. Kendall, M. G., and Stuart, A., see Ref. 26, p. 352.

35. Lee, Y. W.:'Statistical Theory of Communication', New York, John Wiley & Sons, 1960, pp. 195-198.

36 McFadden, J. A.:'The Correlation Function of a Sine Wave Plus Noise After Extreme Clipping', IRE Trans., IT-2(2), June 1956, pp. 82-83.

37. ..od, A. M.:'Introduction to the Theory of Statistics', New York, McGraw Hill, 1950, pp. 264-267.

38.'Research and Development', Electronics and Power, 21 March 1974, p. 225.

39. Altman, L.:'Bipolar Logic Steps up to LSI, with the Smart Money on I^2L', Electronics, 47, 21 February 1974, pp. 91-96.

40. Davenport, W. B., and Root, W. L., see Ref. 31, p. 155.

41. Abramowitz, M., and Stegun, I. A.(Eds.):'Handbook of Mathematical Functions', Washington D.C., NBS, Applied Maths Series 55, 1964, pp. 931-940.

42. Bowker, A. H., and Lieberman, G. J.:'Engineering Statistics', New Jersey, Prentice Hall, 1959, pp. 187-188.

43. Ouencuille, M. H.:'Rapid Statistical Calculations', London, Charles Griffin, 1959, p. 8.

44. Ibid., p. 12.

45. Lord, E.:'The Use of Range in Place of Standard Deviation in the t-test', Biometrika, 34, 1947, pp. 41-67.

(e) The normal case, having the matrix of the linear block Hurwitzian, but $\mathrm{Re}\,[B(s)] \neq 0$, $\mathrm{Re}\,[s] \neq 0$. We introduce the function $B'(s) = B(s)$, where $B'(s)$ satisfies the condition of eqn. 7, and, from expr. 8, for $B'(s)$, we have

$$\mathrm{Re}\,[(1+jcq)\,B'(j\omega)] + \frac{1}{k_0} \geq 0 \quad . \quad . \quad . \quad . \quad . \quad (19)$$

Using the same notation as in the previous cases, we have the condition of stability (i.p.s.):

$$X - qY - \frac{1}{k_0} \geq 0 \quad . \quad . \quad . \quad . \quad . \quad . \quad . \quad . \quad . \quad (20)$$

Expr. 20 shows that, in this case, the condition of stability is the same as in case (*b*). Thus the frequency absolute-stability criterion, may be applied to a large class of systems with a modified formulation, where the m.t.l. may be to the right or to the left of the p.l.

GH. CARTIANU

Radiocommunication Department of the Polytechnic Institute of Bucharest
Bucharest, Romania

IL. PILAT

Economic Cybernetic Department
Academy of Economic Sciences
Bucharest, Romania

3rd February 1975

References

1 POPOV, V. M.: 'L'hyperstabilite des systemes automatiques' (Dunod, Paris, 1973)
2 POPOV, V. M.: 'Ob absolutiutnoi ustoicivoisti nelineinih sistem avtomaticekovo regulirovania', *Avtom. & Telemekh.*, 1961, 22, (8)
3 LEFSCHETZ, S.: 'Stability of nonlinear control systems' (Academic Press, 1965)
4 MINORSKY, N.: 'Theory of nonlinear control systems' (McGraw-Hill, 1969), p. 91
5 AIZERMAN, M. A., and GANTMAHER, F. R.: 'Absolutnaia ustoicivosti regulruemih sistem', *Izd. Akad. Nauk SSSR*, 1963

SINGLE-BIT CROSSCORRELATION FUNCTION OF SINGLE-BIT BANDLIMITED GAUSSIAN WAVEFORM AND TWO SIMULTANEOUS REFLECTIONS CORRUPTED BY NOISE

Indexing terms: Correlation methods, Signal detection

The derivation of the single-bit crosscorrelation function of a single-bit bandlimited Gaussian waveform and two reflections corrupted by wideband Gaussian noise is given. It is seen that single-bit waveforms should not be used in single-bit crosscorrelation detectors when low extraneous noise levels and double simultaneous reflections can be expected.

In a previous letter,[1] the single-bit crosscorrelation function of a single-bit bandlimited Gaussian waveform and one reflection corrupted by wideband noise was derived. In many practical crosscorrelation detection systems, however, situations arise where two or more reflections are incident on the receiver simultaneously. Therefore, in this letter, the single-bit crosscorrelation function of a single-bit bandlimited Gaussian waveform and two attenuated, delayed reflections corrupted by wideband Gaussian noise is derived.

The two waveforms being crosscorrelated are

$$x_1(t) = \mathrm{sgn}\,[f_n(t)] \quad . \quad . \quad . \quad . \quad . \quad . \quad . \quad . \quad . \quad (1)$$

and

$$x_2(t+\tau) = \mathrm{sgn}\,[\beta x_1(t+\tau) + \gamma x_1(t+\tau+\Delta) + n(t+\tau)] \quad (2)$$

where $f_n(t)$ is zero-mean Gaussian noise, bandlimited to $\omega_b/2\pi$ hertz and having variance σ^2; $n(t)$ is wideband Gaussian noise with zero mean and variance σ'^2, and β and γ are attenuation factors. The crosscorrelation function of $x_1(t)$ and $x_2(t+\tau)$ can be written as[1]

$$R_{x_1x_2}(\tau) = 4P_{++} - 1 \quad . \quad . \quad . \quad . \quad . \quad . \quad . \quad . \quad . \quad (3)$$

where P_{++} is the joint probability of $x_1(t)$ and $x_2(t+\tau)$ both being equal to $+1$. For $x_2(t+\tau)$ to be equal to $+1$, either

(*a*) $\beta x_1(t+\tau) = \beta$, $\gamma x_1(t+\tau+\Delta) = \gamma$ and $n(t+\tau) \geq -(\beta+\gamma)$

(*b*) $\beta x_1(t+\tau) = \beta$, $\gamma x_1(t+\tau+\Delta) = -\gamma$ and $n(t+\tau) \geq (\gamma-\beta)$

(*c*) $\beta x_1(t+\tau) = -\beta$, $\gamma x_1(t+\tau+\Delta) = \gamma$ and $n(t+\tau) \geq (\beta-\gamma)$

(*d*) $\beta x_1(t+\tau) = -\beta$, $\gamma x_1(t+\tau+\Delta) = -\gamma$ and $n(t+\tau) \geq -(\beta+\gamma)$.

Letting $y_1 = f_n(t)/s$, $y_2 = f_n(t+\tau)/s$ and $y_3 = f_n(t+\tau+\Delta)/s$, P_{++} is therefore

$$\begin{aligned} P_{++} = {} & P\{y_1 \geq 0, y_2 \geq 0, y_3 \geq 0\}\, P\{n(t+\tau) \geq -(\beta+\gamma)\} \\ & + P\{y_1 \geq 0, y_2 \geq 0, y_3 < 0\}\, P\{n(t+\tau) \geq (\gamma-\beta)\} \\ & + P\{y_1 \geq 0, y_2 < 0, y_3 \geq 0\}\, P\{n(t+\tau) \geq (\beta-\gamma)\} \\ & + P\{y_1 \geq 0, y_2 < 0, y_3 < 0\}\, P\{n(t+\tau) \geq (\beta+\gamma)\} \end{aligned}$$
$$. \quad . \quad . \quad . \quad (4)$$

Now[2]

$$P\{y_1 \geq 0, y_2 \geq 0, y_3 \geq 0\} = \frac{1}{8} + \frac{1}{4\pi}(\mathrm{Sin}^{-1}\rho_{12} + \mathrm{Sin}^{-1}\rho_{13} + \mathrm{Sin}^{-1}\rho_{23}) \quad (5)$$

where ρ_{12} is the covariance of y_1 and y_2, and ρ_{13} and ρ_{23} are similarly defined. The other joint probabilities in eqn. 4 may be derived by noting that

$$P\{y_1 \geq 0, y_2 \geq 0, y_3 < 0\} = P\{y_1 \geq 0, y_2 \geq 0, -y_3 \geq 0\}$$

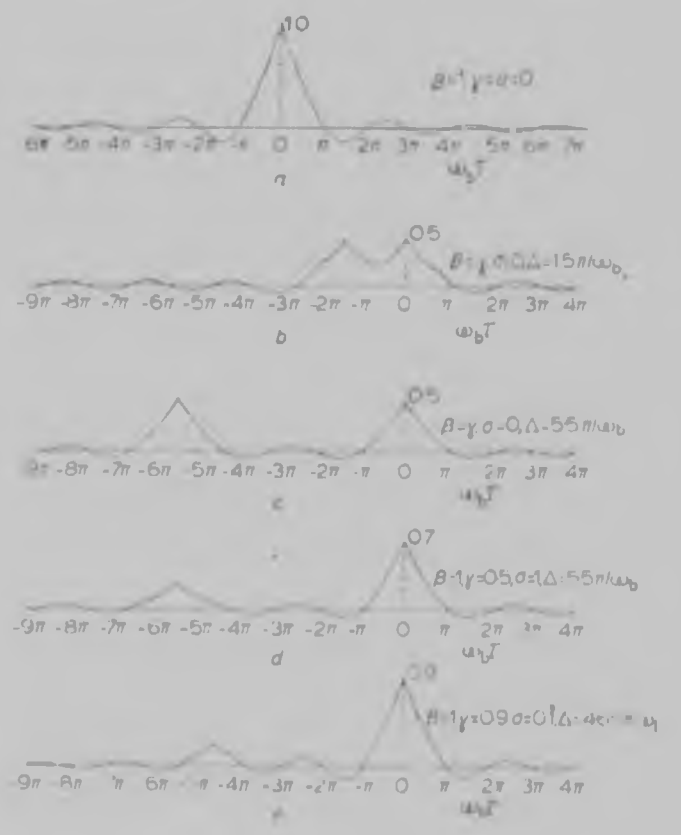

Fig. 1 *Single-bit crosscorrelation functions of single-bit Gaussian waveform and two reflections*

Noting also that the covariance matrix of y_1, y_2 and $-y_3$ is

$$\begin{bmatrix} 1 & \rho_{12} & -\rho_{13} \\ & 1 & -\rho_{23} \\ & & 1 \end{bmatrix}$$

it follows that

$$P\{y_1 \geqslant 0,\ y_2 \geqslant 0,\ -y_3 \geqslant 0\} = \frac{1}{8} + \frac{1}{4\pi}\{\mathrm{Sin}^{-1}\rho_{12} - \mathrm{Sin}^{-1}\rho_{13} - \mathrm{Sin}^{-1}\rho_{23}\} \quad (6)$$

The other joint probabilities in eqn. 4 can be derived similarly. Also,

$$P\{n(t+\tau) \geqslant -(\beta+\gamma)\} = \frac{1}{2}\left\{1 + \mathrm{erf}\left(\frac{\beta+\gamma}{\sigma\sqrt{2}}\right)\right\} \quad (7)$$

where

$$\mathrm{erf}(U) \triangleq \frac{2}{\sqrt{\pi}}\int_0^U e^{-u^2}\,du$$

Deriving similar expressions for the other probabilities in eqn. 4 involving $n(t+\tau)$ and substituting into eqn. 4,

$$P_{++} = \frac{1}{4} + \frac{1}{4\pi}\left[\mathrm{erf}\left(\frac{\beta-\gamma}{\sigma\sqrt{2}}\right)\{\mathrm{Sin}^{-1}\rho_{12} - \mathrm{Sin}^{-1}\rho_{13}\} + \mathrm{erf}\left(\frac{\beta+\gamma}{\sigma\sqrt{2}}\right)\{\mathrm{Sin}^{-1}\rho_{12} + \mathrm{Sin}^{-1}\rho_{13}\}\right] \quad (8)$$

ρ_{12} is the same as the normalised autocorrelation function of $f_n(t)$, i.e. $\rho(\tau)$. Similarly, ρ_{13} is the same as $\rho(\tau+\Delta)$. Thus, from eqns. 3 and 8,

$$\psi_{x_1x_2}(\tau) = \frac{1}{\pi}\left[\mathrm{erf}\left(\frac{\beta-\gamma}{\sigma\sqrt{2}}\right)\mathrm{Sin}^{-1}\rho(\tau) - \mathrm{Sin}^{-1}\rho(\tau+\Delta),\right.$$

$$\left. + \mathrm{erf}\left(\frac{\beta+\gamma}{\sigma\sqrt{2}}\right)\{\mathrm{Sin}^{-1}\rho(\tau) + \mathrm{Sin}^{-1}\rho(\tau+\Delta)\}\right] \quad (9)$$

As the extraneous noise $n(t)$ tends to zero, $\psi_{x_1x_2}(\tau)$ becomes critically dependent on the greater of β and γ. For $\sigma = 0$, if $\beta > \gamma$, eqn. 9 becomes

$$\psi_{x_1x_2}(\tau) = \frac{2}{\pi}\mathrm{Sin}^{-1}\rho(\tau)$$

and, if $\gamma > \beta$,

$$\psi_{x_1x_2}(\tau) = \frac{2}{\pi}\mathrm{Sin}^{-1}\rho(\tau+\Delta)$$

In other words, only the larger of the two reflections will be detected. The conclusion to be drawn is that single-bit waveforms should not be used for single-bit crosscorrelation reflection detection in applications where low extraneous noise levels and double simultaneous reflections can be expected, as there is a definite chance that the smaller of the two reflections will be missed, even though it may only be slightly smaller. This, incidentally, applies to the single-bit crosscorrelation detection of any single-bit waveform, pseudorandom, square, or whatever.

Eqn. 9 is plotted in Fig. 1 for some representative values of β, γ, σ and Δ. $f_n(t)$ is assumed to have a 'brick-wall' frequency spectrum from zero to $\omega_0/2\pi$ hertz.

An extension of this type of analysis to more than two simultaneous reflections will not, in general, be possible. The reason is that multivariate normal distributions of order higher than three would be involved, and it is only in exceptional circumstances[3, 4] that joint probabilities of the form of eqn. 5 can be evaluated exactly in this case.

T. E. HOWARD

31st January 1975

Department of Electrical Engineering
University of the Witwatersrand
Jan Smuts Avenue, Johannesburg, S. Africa

References

1 HOWARD, T. E.: 'Probability distribution of the crosscorrelation function of finite-duration single-bit random waveforms', *Electron. Lett.*, 1972, 8, pp. 560–562 and Errata, *ibid.*, 1973, 9, p. 72
2 KENDALL, M. G., and STUART, A.: 'The advanced theory of statistics Vol. 1 Distribution theory' (Charles Griffin, London, 1963, 2nd edn.), p. 352
3 GUPTA, S. S.: 'Probability integrals of multivariate normal and multivariate *t*', *Ann. Math. Stat.*, 1963, 34, pp. 792–839
4 CHENG, M. C.: 'The clipping loss in correlation detectors for arbitrary signal-to-noise ratios', *IEEE Trans.*, 1968, IT-14, pp. 382–389

TRACKING SENSITIVITY: AN ALTERNATIVE ALGORITHM FOR LINEAR NONRECIPROCAL CIRCUITS

Indexing terms: Computer-aided circuit analysis, Linear network analysis, Sensitivity analysis

A previous algorithm by Leung and Spence for computing component tracking sensitivity is occasionally incapable of application. An alternative algorithm is presented that is always applicable and which is believed to be computationally more attractive than Leung and Spence's for circuits containing of the order of 20 or fewer nodes. The similarity between these techniques and some earlier work by Branin for computing the steady-state a.c. analysis of a circuit is also pointed out.

Introduction: In a recent letter,[1] Leung and Spence develop an algorithm for obtaining the 'tracking sensitivity' of a transfer impedance with respect to large changes in some global parameter K, e.g. temperature. Their technique involves reducing a particular matrix to diagonal form by means of a similarity transformation; a process that is occasionally not possible. For example, if we try to apply Leung and Spence's algorithm to the circuit shown in Fig. 1, with the component values g_i and sensitivities s_i shown, we find ourselves trying to diagonalise the matrix

$$Y_t\,Y_n^{-1} = \begin{bmatrix} 1 & -1 \\ 0 & 1 \end{bmatrix}\begin{bmatrix} 1 & -1 \\ -2 & 3 \end{bmatrix} = \begin{bmatrix} 1 & -1 \\ 0 & 1 \end{bmatrix}\begin{bmatrix} 3 & 1 \\ 2 & 1 \end{bmatrix} = \begin{bmatrix} 1 & 0 \\ 2 & 1 \end{bmatrix}$$

which is impossible. In this letter, we point out how this shortcoming may be easily rectified, as well as providing a technique that is believed to be computationally more attractive than Leung and Spence's for circuits having of the order of 20 or fewer nodes. We also point out the connection between

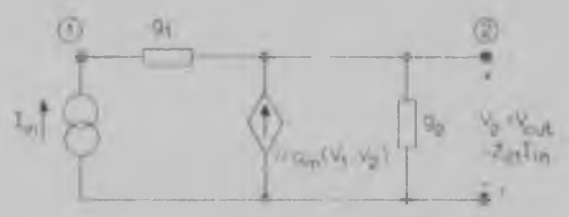

Fig. 1 *Circuit example for which diagonalisation fails*

Table 1

Component g_i $g_i = g_{is}(1 + s_i K)$	Nominal value g_{is}	Sensitivity coefficient s_i
	S	
g_1	1	1
g_2	1	1
g_m	1	α 1

For any specified set of coefficients p_i giving a nonzero right-hand side in eqn. 16, a necessary and sufficient condition for eqn. 16 to be uniquely solvable for the $(n+1)\times 1$ matrix $M-I$ (and thus the matrix M which completes the observer design) is that the matrix J should be nonsingular. The condition for this to be so may be expressed in familiar control-engineering terms by noting that a sequence of nonsingular elementary row operations converts J to the form

$$b_0\theta = b_0\begin{bmatrix} f_2^{\mathrm{T}} \\ f_2^{\mathrm{T}}Q \\ \vdots \\ f_2^{\mathrm{T}}Q^{n-1} \end{bmatrix} \qquad (18)$$

θ is the observability matrix formed from f_2^{T} and Q. Thus, given $b_0 \neq 0$, a necessary and sufficient condition for arbitrary assignment of the coefficients $p_0, p_1, \ldots p_{n-1}$ to be possible is that (f_2^{T}, Q) should be an observable pair. A computer program has been devised by T. Y. Yip to implement the above scheme, to display the dynamic performances of the systems so designed and to evaluate performance indices. The results of many design studies have been very encouraging and the observability test has invariably been satisfied. The possibility of extending the idea to multi-input multi-output systems is being explored.

H. M. POWER
T. Y. YIP

23rd October 1972

Department of Electrical Engineering
University of Salford
Salford M5 4WT, England

References

1 WOLFE, H. M.: 'Effect of zero-crossable feedback on numerators of transfer functions', *Electron. Lett.*, 1970, **6**, pp. 470–471
2 KAILATH, T., and PAYNE, H. J.: 'Pole and zero assignment for linear multivariable systems using output feedback', *Stanford Univ. Rep.*, 1972, **8**, pp. 518–523
3 LUENBERGER, D. G.: 'Observing the state of a linear system', *IEEE Trans.*, 1964, **MIL-8**, pp. 74–80
4 LUENBERGER, D. G.: 'Observers for multivariable systems', *ibid.*, 1966, **AC-11**, pp. 190–197
5 NAGUMO, M., and YASUTOMI, S. C.: 'The synthesis of optimum transient response systems and zero-lock forms', *Trans. Am. Inst. Elec. Engrs.*, 1953, **72**, Pt. 2, pp. 279–288
6 POWER, H. M.: 'On the solution of a matrix equation in the theory of Luenberger observers', *IEEE Trans.*, 1971, **AC-16** (to be published)
7 WOLOVICH, W. A.: 'Linear multivariable systems' (McGraw-Hill, 1971), p. 182

PROBABILITY DISTRIBUTION OF THE CROSSCORRELATION FUNCTION OF FINITE-DURATION SINGLE-BIT RANDOM WAVEFORMS

Indexing terms: Correlation theory, Error statistics

The duration errors of a digital crosscorrelator, arising from the clipped, bandlimited Gaussian waveforms are investigated, and the probability distribution of the crosscorrelator due to finite-duration sequences and distortion by additional Gaussian noise is derived and compared with experimental results.

Much work has been done on deriving the autocorrelation functions of Gaussian noise,[1] sine waves plus noise[2] etc. and the effects of amplitude limiting on these functions.[3, 4] However, in all practical correlators, waveforms of noninfinite duration are correlated, resulting in a distribution of the correlation function about the 'infinite-duration' value. Knowledge of this distribution is essential in determining the detection reliability of the correlator. In this letter, the probability distribution of the crosscorrelation function of severely clipped, bandlimited Gaussian noise, and an attenuated, delayed replica, distorted by wideband Gaussian noise, is derived and compared with the actual distribution measured on a digital crosscorrelator.

Consider the two waveforms

$$x_1(t) = \mathrm{sgn}\,\{f_n(t)\}$$

$$x_2(t+\tau) = \mathrm{sgn}\,\{\beta x_1(t+\tau) + n(t+\tau)\}$$

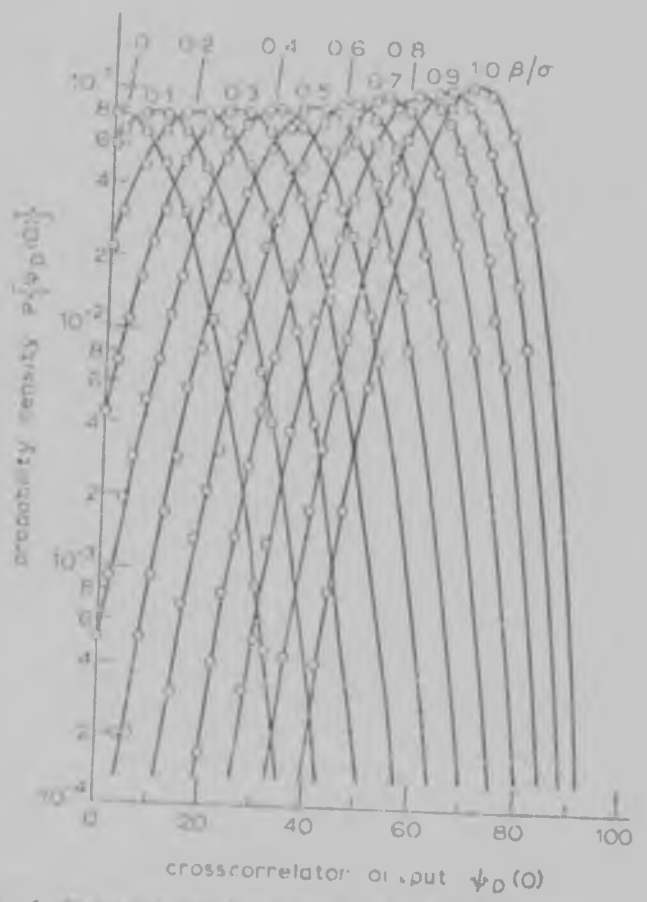

Fig. 1 *Probability-density functions of $\psi_{xx}(0)$ for 760 samples*
Theoretical points joined with smooth curves
——— theoretical
○○○ experimental

where $f_n(t)$ is a random Gaussian waveform of zero mean, bandlimited to $f_0/2\pi$ hertz, and $n(t)$ is wideband Gaussian noise of zero mean and variance σ^2. β is an attenuation factor. It has been shown[5, 6] that the crosscorrelation function of $x_1(t)$ and $x_2(t+\tau)$ can be written as

$$\psi_{x_1x_2}(\tau) = 4P_{++} - 1 \qquad (1)$$

where P_{++} is the probability that $x_1(t) = +1$ and also that $x_2(t+\tau) = +1$. For $x_2(t+\tau)$ to be $+1$, either $\beta x_1(t+\tau) > n$ and $n(t+\tau) > -\beta$, or $\beta x_1(t+\tau) < -\beta$ and $n(t+\tau) < +\beta$. Therefore

$$P_{++} = P\{x_1(t) = 1\}[P\{x_1(t+\tau) = 1 \mid x_1(t) = 1\} \times \{\tfrac{1}{2} + \tfrac{1}{2}\,\mathrm{erf}\,(\beta/\sigma\sqrt{2})\} + P\{x_1(t+\tau) = 1 \mid x_1(t) = 1\}\{1 - \tfrac{1}{2}\,\mathrm{erf}\,(\beta/\sigma\sqrt{2})\}] \qquad (2)$$

where

$$\mathrm{erf}\,(\theta) = \frac{2}{\sqrt{\pi}}\int_0^{\theta} e^{-u^2}\,du$$

$P\{x_1(t+\tau) = 1 \mid x_1(t) = 1\}$ is the probability of an even number of zero crossings in time τ and is[4] $\frac{1}{2}\{1 + \rho(\tau)\}$, where $\rho(\tau)$ is the autocorrelation function of $x_1(t)$. Similarly, $P\{x_1(t+\tau) = -1 \mid x_1(t) = 1\}$ is $\frac{1}{2}\{1 - \rho(\tau)\}$. On substituting

in eqn. 2, and substituting eqn. 2 into eqn. 1,

$$\psi_{x_1 x_2}(\tau) = \operatorname{erf}(\beta/\sigma_N\sqrt{2})\,\rho(\tau) \quad . \quad . \quad . \quad . \quad . \quad . \quad . \quad (3)$$

The autocorrelation function of $x_2(t)$ is derived similarly as

$$\psi_{x_2}(\tau) = \{\operatorname{erf}(\beta/\sigma_N\sqrt{2})\}^2\,\rho(\tau) \quad . \quad . \quad . \quad . \quad . \quad . \quad . \quad (4)$$

Consider a digital correlator. N samples, δt apart, of $x_1(t)$ and $x_2(t+\tau)$ are stored, and the products of corresponding sample pairs are added to form the crosscorrelation operation, i.e.

$$\psi_D(\tau) = \sum_{i=1}^{N} x_1(t_i)\,x_2(t_i+\tau) \quad . \quad . \quad . \quad . \quad . \quad . \quad . \quad (5)$$

The distribution of $\psi_D(\tau)$ will be considered for $\tau = 0$ and $|\tau| > 0$.

For $\tau = 0$ and no extraneous noise in $x_2(t)$, $\psi_D(0) = N$, since all the product terms are $+1$. With noise present, $\psi_D(0)$ will be reduced by 2 for every instant t_i at which either (*a*) $n(t_i) > +\beta$ when $\beta x_1(t_i) = -\beta$ or (*b*) $n(t_i) < -\beta$ when $x_1(t_i) = +\beta$. The probability of *a* or *b* occurring is $p = \frac{1}{2}\operatorname{erfc}(\beta/\sigma_N\sqrt{2})$, which, as $n(t)$ is the wideband Gaussian noise, is independent of t_i. Hence the number of times *a* or *b* occurs in N instants follows a binomial distribution[5] with mean Np. Hence $\psi_D(0)$ will also follow a binomial distribution with mean

$$\begin{aligned}\psi_D(0) &= N - 2Np \\ &= N\operatorname{erf}(\beta/\sigma_N\sqrt{2}) \quad . \quad . \quad . \quad . \quad . \quad . \quad . \quad . \quad (6)\end{aligned}$$

This agrees with eqn. 3. Fig. 1 compares theoretical and experimental distributions of $\psi_D(0)$.

For $|\tau| > 0$ over the period t_1 to $(t_N - \tau)$, $x_1(t_i)$ is being crosscorrelated with sgn $\{\beta x_1(t_i+\tau) + n(t_i+\tau)\}$, and over the period $(t_N - \tau)$ to t_N with sgn $\{n(t_i+\tau)\}$. Hence two distributions must be derived, and their combination yields the distribution of $\psi_D(\tau)$. (*a*) For the period t_1 to $(t_N - \tau)$, as a large number N' of similarly distributed product terms are being summed, the central limit theorem suggests the distribution will approach normality for $N' > 30$. The mean of this sum will be

$$\mu = N'\operatorname{erf}(\beta/\sigma_N\sqrt{2})\,\rho(\tau) \quad . \quad . \quad . \quad . \quad . \quad . \quad . \quad (7)$$

where[1, 3]

$$\rho(\tau) = \frac{2}{\pi}\sin^{-1}\{\sin(\omega_b\tau)/(\omega_b\tau)\}$$

The variance of the sum can be calculated from

$$\begin{aligned}&\operatorname{var}\left\{\sum_{i=1}^{N'} x_1(t_i)\,x_2(t_i+\tau)\right\} \\ &= E\left\{\left[\sum_{i=1}^{N'} x_1(t_i)\,x_2(t_i+\tau)\right]^2\right\} - \left[E\left\{\sum_{i=1}^{N'} x_1(t_i)\,x_2(t_i+\tau)\right\}\right]^2 \\ &= E\left\{\sum_{i=1}^{N'} x_1^2(t_i)\,x_2^2(t_i+\tau)\right\} \\ &\quad + 2E\left\{\sum_{j>i}^{N'}\sum^{N'} x_1(t_i)\,x_2(t_i+\tau)\,x_1(t_j)\,x_2(t_j+\tau)\right\} - \mu^2 \\ &= N' - \mu^2 + 2\sum_{j>i}^{N'}\sum^{N'} E\{x_1(t_i)\,x_2(t_i+\tau)\,x_1(t_j)\,x_2(t_j+\tau)\} \quad (8)\end{aligned}$$

$$\begin{aligned}&E\{x_1(t_i)\,x_2(t_i+\tau)\,x_1(t_j)\,x_2(t_j+\tau)\} \\ &= P_{++++} - P_{+++-} - P_{++-+} \\ &\quad - P_{+-++} - P_{-+++} + P_{++--} + P_{+--+} + P_{-++-} + P_{--++} - P_{+---} - P_{-+--} - P_{--+-} + P_{----} \quad (9)\end{aligned}$$

where $P_{++-+} = P\{x_1(t_i) = 1,\ x_2(t_i+\tau) = 1,\ x_1(t_j) = 1,\ x_2(t_j+\tau) = -1\}$ and P_{-+++} etc. are similarly defined.

Assuming that the number of zero crossings of $x_1(t)$ or $x_2(t)$ in any τ interval is independent of the number in any other τ overlapping interval, these joint probabilities may be calculated as follows:

(*a*) $t_j > (t_i + \tau)$, so that the nonoverlapping intervals are t_i to τ, t_j to $(t_i+\tau)$ and $(t_i+\tau)$ to $(t_j+\tau)$.

$$\begin{aligned}P_{++++} &= P\{x_1(t_i) = 1\}\,P\{x_1(t_j) = 1 \mid x_1(t_i) = 1\} \\ &\quad \times P\{x_2(t_i+\tau) = 1 \mid x_1(t_j) = 1\} \\ &\quad \times P\{x_2(t_j+\tau) = 1 \mid x_2(t_i+\tau) = 1\} \\ &= \tfrac{1}{2}\{1 + \rho(t_j - t_i)\}\,\tfrac{1}{2}\{1 + \psi_{x_1x_2}(t_i+\tau-t_j)\} \\ &\quad \times \tfrac{1}{2}\{1 + \psi_{x_1}(t_j - t_i)\} \quad . \quad . \quad . \quad . \quad . \quad . \quad . \quad (10)\end{aligned}$$

Similarly,

$$\begin{aligned}P_{+++-} &= \tfrac{1}{8}\{1 + \rho(t_j - t_i)\}\{1 + \psi_{x_1x_2}(t_i+\tau-t_j)\} \\ &\quad - \rho(t_j - t_i)\,\psi_{x_1}(t_j - t_i) = \psi^2_{x_1x_2}(t_i+\tau-t_j) \\ &\quad \times \{1 - \psi_{x_2}(t_j+t_i)\}\end{aligned}$$

Hence, from eqn. 9,

$$E\{x_1(t_i)\,x_2(t_i+\tau)\,x_1(t_j)\,x_2(t_j+\tau)\} = 0$$

(*b*) $t_j < (t_i + \tau)$, so that the nonoverlapping intervals are t_i to $(t_i+\tau)$, $(t_i+\tau)$ to t_j and t_j to $(t_j+\tau)$. As before,

$$E\{x_1(t_i)\,x_2(t_i+\tau)\,x_1(t_j)\,x_2(t_j+\tau)\} = \psi^2_{x_1x_2}(\tau)$$

All the values of $\psi_{x_1x_2}(t_j - t_i)$ are known from eqn. 3, and hence the variance of the sum of N' products can be found.

Over the period $(t_N - \tau)$ to t_N, a signal $x_1(t)$ is being crosscorrelated with $x_2(t+\tau) = \operatorname{sgn}\{n(t+\tau)\}$, and thus the mean of the sum of these $(N - N')$ products is zero, and, since each product term is independent, the sum is binomially distributed, tending to normal as $(N - N')$ increases, and with variance $(N - N')$.

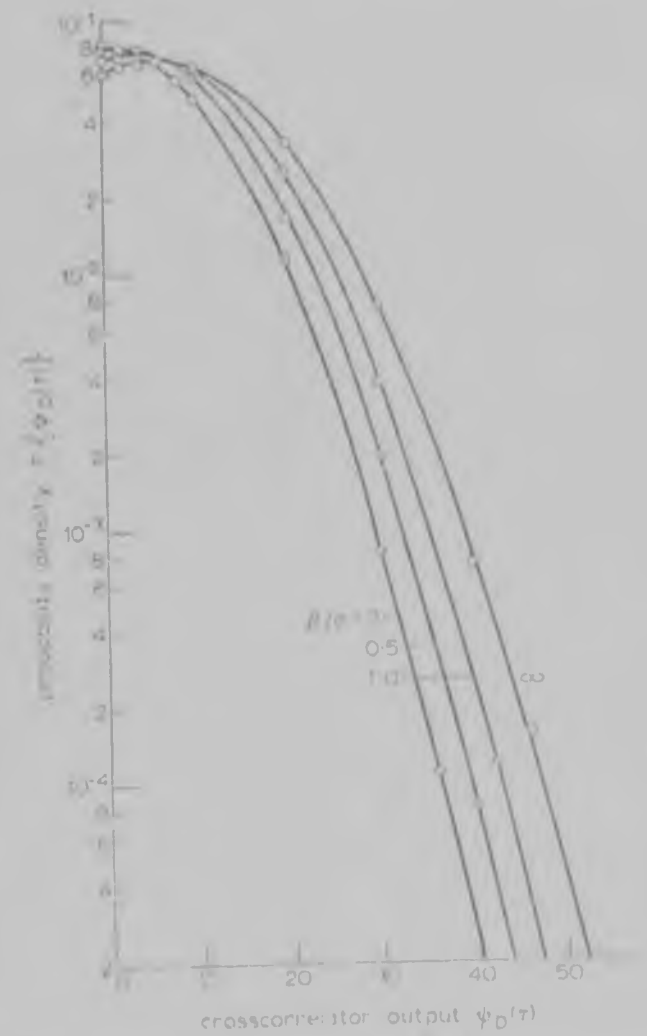

Fig. 2 *Probability density functions of $\{n(t)\}$ for 100 samples*
Theoretical points joined with a smooth curve
theoretical
experimental

The output of the correlator is the sum of the N' and the $(N-N')$ products, so that the distribution of $\psi_t(\tau)$ can be obtained by combining the two distributions derived above. If, over t_1 to t_N, $x_2(t+\tau) = \text{sgn}\{n(t+\tau)\}$, $\psi_n(\tau)$ would be binomially distributed about zero, tending to normal for large N, and with variance N.

For verification of the theory, a crosscorrelator with $N = 100$ or 200 was built. The cutoff frequency of $f_n(t)$ was 21 kHz, sample spacing $\delta t = 12.81\ \mu$s and $\tau = s \times 12.81\ \mu$s, giving $N' = 95$ or 195 and a variance, from eqn. 8, of

$$\text{var} = N' - \mu^2 + 2\{(N'-1)\psi_{x_1x_2}(\delta t) + (N'-2)\psi_{x_1x_2}(2\delta t) + (N'-3)\psi^2_{x_1x_2}(3\delta t) + (N'-4)\psi^2_{x_1x_2}(4\delta t) + \tfrac{1}{2}(N'-4)(N'-5)\psi_{x_1x_2}(\tau)\} \quad \ldots\ldots\ldots \quad (11)$$

The theoretical and experimental results are shown in Fig. 2. For clarity, only those for $N = 100$ are shown. Similar agreement between theory and experiment was obtained with 200 samples.

These probability distributions for $\mu = 0$ make it possible to predict the detection and false-alarm probability of the correlator operating in a noisy environment, and hence to have a measure of its reliability and to compare it with other systems.

Work is at present proceeding on the analysis of the cross-correlation of 1-bit random waveforms, and its application to the measurement of multipath reflections and similar problems in the field of acoustics.

The author gratefully acknowledges the financial support, in the form of a scholarship given by S. J. Fuchs Ltd., and the assistance given by the members of the Fuchs Electronics Laboratory, in particular Martyn Schrire, in building up the correlator. He also acknowledges the help and guidance given by his supervisor, Prof. H. E. Hanrahan.

J. E. HOWARD

Department of Electrical Engineering
University of the Witwatersrand
Jan Smuts Avenue, Johannesburg, South Africa

16th October 1972

References

1 [illegible] S. [illegible]: 'Mathematical analysis of random noise' *in* 'Selected papers on noise and stochastic processes' (Dover, 1954), p. 188
2 [illegible] MIDDLETON, J. [illegible]: 'The correlation function of a sine wave plus Gaussian noise after extreme clipping', *IRE Trans.*, 1956, IT-2, pp. 82–83
3 DAWSON, J. L., and UHLENBECK, G. E.: 'Threshold signals' (McGraw-Hill, 1950), p. 353
4 MIDDLETON, J. A.: 'The axis-crossing intervals of random functions', *IRE Trans.*, 1956, IT-4, pp. 146–150
5 DRAKE, A. W.: 'Fundamentals of applied probability theory' (McGraw-Hill, 1967), p. 121
6 BRUEL, J. J.: 'On the applicability and limitations of the cross-correlation and cross-spectral density techniques', *Bruel & Kjaer Tech. Rev.*, 1970, 4, pp. 3–27

HIGH-POWER AVALANCHE IMPATT REFLECTION AMPLIFIER USING THE RUCKER COMBINING CIRCUIT

Indexing terms: IMPATT devices, Microwave amplifiers, Stability

The analysis by Kurokowa of the Rucker multidevice symmetrical oscillator circuit has been applied to the design of a single-tuned high-power IMPATT amplifier. It is shown that the stability of the amplifier régime can be predicted from a simple circuit model. An experimental circuit has successfully demonstrated the different circuit regimes when operating in a single coherent mode.

The oscillator circuit proposed by Rucker[1] to combine the output powers from several active devices which share a common load was analysed by Kurokowa[2] using an eigenvector approach. It was shown that the Rucker circuit could be operated in a single mode with the appropriate circuit-loading conditions. In this letter, the analysis has been successfully applied to the design of a single-tuned high-power reflection IMPATT amplifier and locked oscillator.

There are several approaches which can be used to coherently combine solid-state devices. The hybrid ring[3] and 3 dB coupler[4] offer a relatively simple method of combining two separate amplifier modules when the amplitudes and phases of the signal are carefully matched. For several modules, this circuit technique can become physically unwieldy. The fabrication of parallel arrays of diodes[5] in which the arrays are formed in a single diode chip and mounted in a package has also been successfully applied for high-power operation. This approach, however, eventually suffers from its limited capability in heat dissipation. Paralleling individually encapsulated devices closely together has been shown to work,[6] although, in the experience of the authors, when more than two devices are used, the circuit becomes very difficult to stabilise in a single mode owing to the interactive coupling between each device. In Rucker's circuit, the power-combining properties form an integral part of the circuit itself. The active devices are physically located half a wavelength apart in a coaxial-line configuration and separated by a stabilising resistor. The circuit behaves in a coherent way, as though the devices were connected in parallel. For those high-power applications requiring a low external Q factor, such as an amplifier or locked oscillator, Rucker's circuit has the necessary attributes.

Kurokowa analysed the n port ($n = 5$) symmetrical Rucker oscillator circuit, and determined the eigenvectors and corre-

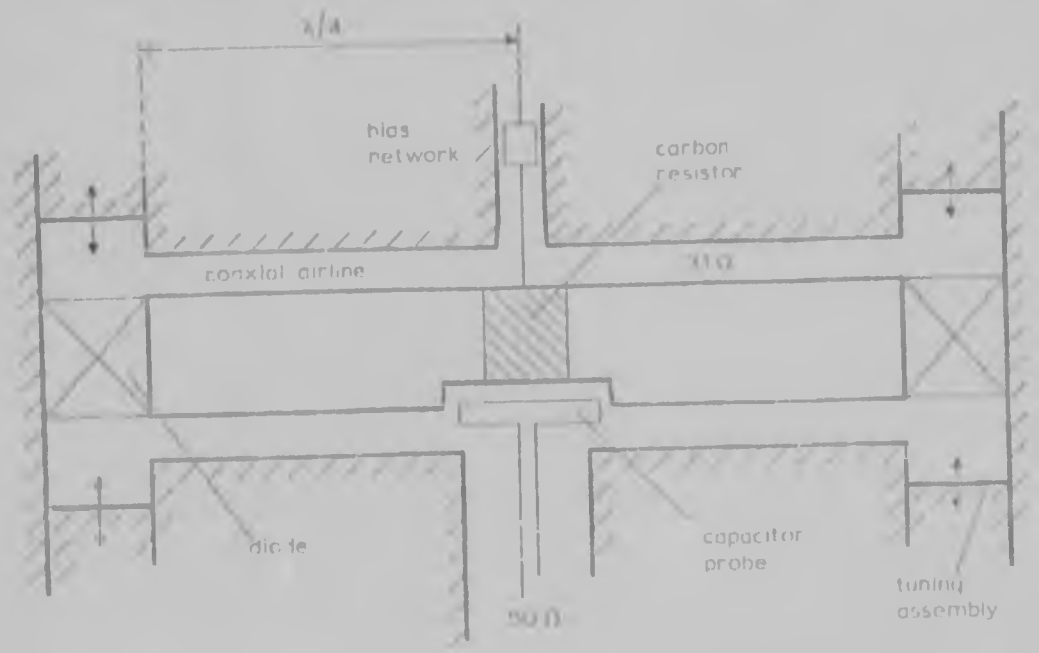

Fig. 1 *Schematic of the amplifier-combining circuit*

conclude anything about the far sidelobes. It might therefore be better not to make the approximation that the L pattern is circularly symmetrical, but also to consider the effect of the crosspolarisation field components.

H. A. J. M. VAN HOOF

23rd January 1974

Laboratory for Electronic Developments of the Armed Forces, Oegstgeest, Netherlands

References

A DIJK, J., and MAANDERS, E. J.: 'Some errors in the calculation of the radiation patterns of reflector antennas using Kirchhoff integration', *Electron. Lett.*, 1973, 9, pp. 512–513

B KINBER, B. E.: 'The condition of shadowing and diffraction correction to current distribution', *Radiotekh. & Elektron.*, 1960, 5, pp. 1407–1416

C KINBER, B. E.: 'Side lobe radiation of reflector antennas', *ibid.*, 1961, 6, pp. 545–558

D TARTAKOVSKII, E. B., and TANDIT, V. E.: 'Current distribution on the reflector of a reflector antenna', *ibid.*, 1960, 5, pp. 918–925

E TANDIT, V. E., and TARTAKOVSKII, E. B.: 'The radiation of a reflector antenna in the shadow region', *ibid.*, 1960, 5, pp. 1398–1406

PROBABILITY-DENSITY FUNCTION OF OUTPUT OF SINGLE-BIT CROSS-CORRELATOR FOR DETECTING GAUSSIAN REFLECTIONS IN NOISE

Indexing terms: Correlators, Digital systems, Signal detection

The detection errors of a single-bit digital crosscorrelator for detecting bandlimited Gaussian reflections in noise are investigated, and the probability density function of the correlator output due to finite-interval crosscorrelation and corruption of the received waveform by wideband Gaussian noise is derived and compared with experimental results.

The use of crosscorrelators for detecting random waveform reflections is well established.[1] Although sophisticated crosscorrelators are available, the single-bit digital serial crosscorrelator is of great interest, owing to its simplicity and inexpensiveness. The detection reliability of such an instrument is most readily assessed by an examination of the distribution of its output that results from the finite correlation interval and the corruption of the received waveform by noise. In a previous letter,[2] this distribution was derived for the single-bit crosscorrelation of a severely clipped bandlimited Gaussian signal and an attenuated reflection corrupted by wideband noise. Although severely clipped waveforms have the advantage that their peak and average powers are the same, the original analogue waveforms offer the great advantage that their transmission-bandwidth requirements are considerably less than those of the severely clipped versions. In this letter, therefore, the probability density function of the single-bit crosscorrelation function of full analogue bandlimited Gaussian noise, and an attenuated reflection, corrupted by wideband Gaussian noise, are derived. This is compared with experimental results, and the detection reliability is shown to be worse than if the clipped waveform is transmitted.

Consider the two waveforms

$$\left.\begin{aligned} z_1(t) &= \operatorname{sgn}\{f_n(t)\} = \operatorname{sgn}\{v_1(t)\} \\ \text{and} \\ z_2(t+\tau) &= \operatorname{sgn}\{\beta f_n(t+\tau) + n(t+\tau)\} = \operatorname{sgn}\{v_2(t+\tau)\} \end{aligned}\right\} \quad (1)$$

where $f_n(t)$ is a random Gaussian waveform of zero mean and variance s^2, bandlimited to $\omega_b/2\pi$ hertz, and $n(t)$ is wideband Gaussian noise of zero mean and variance σ^2. β is an attenuation factor and $f_n(t)$ and $f_n(t+\tau)$ follow a bivariate normal distribution, and, for the purposes of computation, $v_2(t+\tau)$ may be regarded as a Gaussian waveform having the same amplitude distribution as $\beta f_n(t+\tau)$, but with its mean value shifted to $n(t+\tau)$. Hence[3] $v_1(t)$ and $v_2(t+\tau)$ will also follow a bivariate normal distribution with mean $\{0, n(t+\tau)\}$ and variances $\{s^2, (\beta s)^2 + \sigma^2\}$. It has been shown[3] that the crosscorrelation function of $z_1(t)$ and $z_2(t+\tau)$ can be written as

$$\psi_{z_1 z_2}(\tau) = 4P_{++} - 1 \quad \ldots \quad (2)$$

where P_{++} is the probability that $x_1(t) > 0$ and $x_2(t+\tau) > 0$, averaged over all $n(t+\tau)$. Letting $n(t+\tau) = \eta$,

$$P_{++} = \frac{1}{2\pi\beta s^2(1-\rho^2)^{\frac{1}{2}}} \int_{-\infty}^{\infty} d\eta \int_{0}^{\infty} \exp\left[\frac{-1}{2(1-\rho^2)}\left\{\frac{x^2}{s^2} - \frac{2\rho x(x-\eta)}{\beta s^2} + \frac{(x-\eta)^2}{(\beta s)^2}\right\}\right] dx \quad (3)$$

Evaluating as in Reference 5,

$$P_{++} = Q(0)\,Q(-\eta/\beta s) + \sum_{m=0}^{\infty} (-1)^m \frac{Z^{(m)}(0)\,Z^{(m)}(\eta/\beta s)}{(m+1)!}\,\rho^{m+1} \quad \ldots \quad (4)$$

where

$$Q(x) \Delta \frac{1}{\sqrt{(2\pi)}} \int_{x}^{\infty} \exp(-u^2/2)\,du$$

$$Z^{(\lambda)}(x) \Delta \frac{d^\lambda}{dx^\lambda}\left\{\frac{1}{\sqrt{(2\pi)}} \exp(-x^2/2)\right\}$$

Averaging P_{++} over all η gives $\overline{P_{++}}$:

$$\overline{P_{++}} = \tfrac{1}{4} + \frac{1}{2\pi} \sum_{m=0}^{\infty} \frac{(2m)!}{(2m+1)\{2^m m!\}^2} \left[\sqrt{\left\{\frac{(\beta s/\sigma)^2}{1+(\beta s/\sigma)^2}\right\}}\right]^{2m+1} \times \rho^{2m+1}$$

$$= \tfrac{1}{4} + \frac{1}{2\pi} \sin^{-1}\left[\sqrt{\left\{\frac{(\beta s/\sigma)^2}{1+(\beta s/\sigma)^2}\right\}}\,\rho(\tau)\right] \quad \ldots \quad (5)$$

where[4, 6] $\rho(\tau) = \rho = \sin(\omega_b\tau)/\omega_b\tau$. Substituting in eqn. 2,

$$\psi_{z_1 z_2}(\tau) = \frac{2}{\pi} \sin^{-1}\left[\sqrt{\left\{\frac{(\beta s/\sigma)^2}{1+(\beta s/\sigma)^2}\right\}}\,\rho(\tau)\right] \quad (6)$$

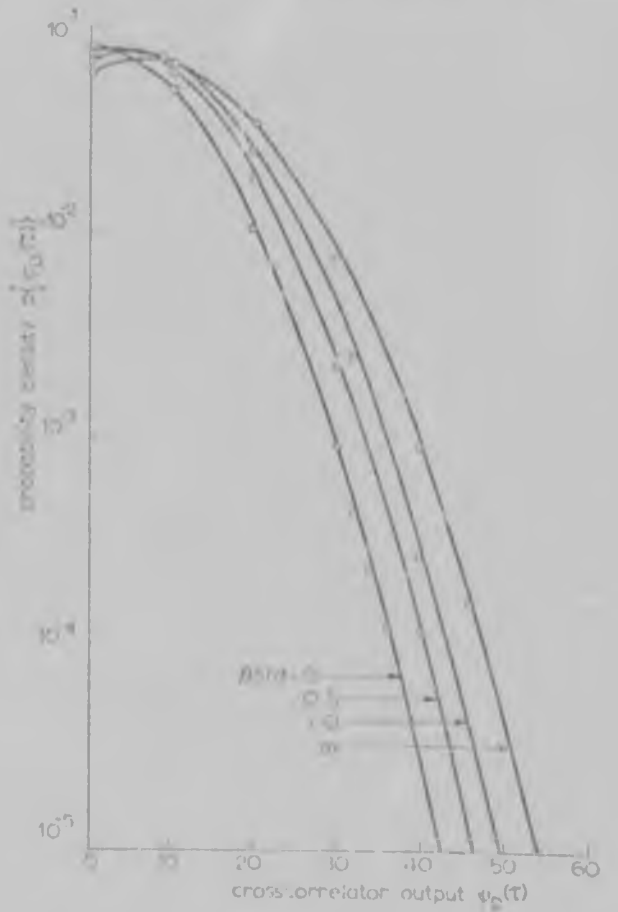

Fig. 1. *Probability density functions of $\Psi_D(0)$ for 100 samples*
Experimental points joined by a smooth curve

Considering the autocorrelation function of $z_2(t)$ yields

$$\psi_{z_1z_2}(\tau) = \frac{2}{\pi}\sin^{-1}\left\{\frac{(\beta s/\sigma)^2}{1+(\beta s/\sigma)^2}\cdot\rho(\tau)\right\}$$

which agrees with the result of Ekre.[7]

Consider a digital crosscorrelator. N samples, δt apart, of $z_1(t)$ and $z_2(t+\tau)$ are stored, and the products of corresponding sample pairs added to form the crosscorrelation; i.e.

$$\psi_D(\tau) = \sum_{i=1}^{N} z_1(t_i)z_2(t_i+\tau) \quad . \quad . \quad . \quad . \quad . \quad . \quad . \quad . \quad (7)$$

For $\tau = 0$, it was shown in the previous letter[1] that the number of instants N_t at which $n(t)$ causes the sign of $\beta f_n(t) + n(t)$ to differ from that of $f_n(t)$ follows a binomial distribution with mean Np and variance $Np(1-p)$, where

$$p = \overline{\text{prob}\{n(t_i) > -\beta f_n(t_i), f_n(t_i) < 0\}} + \overline{\text{prob}\{n(t_i) < -\beta f_n(t_i), f_n(t_i) > 0\}}$$

$$= \frac{2}{\beta s\sqrt{(2\pi)}}\int_0^\infty\left\{\frac{1}{\sigma\sqrt{(2\pi)}}\int_y^\infty \exp(-t^2/2\sigma^2)\,dt\right\}\exp\{-y^2/2(\beta s)^2\}\,dy \quad (8)$$

Expanding the inner integral in a Maclaurin series,

$$p = \tfrac{1}{2} - \frac{1}{\pi}\tan^{-1}(\beta s/\sigma)$$

and therefore

$$\psi_D(0) = (N-2Np) = N\frac{2}{\pi}\tan^{-1}(\beta s/\sigma) \quad . \quad (9)$$

which agrees with eqn. 6. Since $P\{\psi_D(0) = N-2N_t\}$ is equivalent to $P\{N_t$ error instants$\}$, the distribution of $\psi_D(0)$ can be derived directly from that of N_t. Fig. 1 compares the theoretical and experimental distributions of $\psi_D(0)$.

Unlike the previous case,[2] where burst waveforms of duration T were transmitted, $f_n(t)$ was transmitted continuously, and hence $z_2(t+\tau) = \text{sgn}\{\beta f_n(t+\tau)+n(t+\tau)\}$ over the whole crosscorrelation interval T. Thus only one distribution has to be derived for $|\tau| > 0$. The sum of the N products will behave like that of the N products in Reference 2, tending to normal for large N, with mean and variance given by

$$\mu = \psi_D(\tau) = N\psi_{z_1z_2}(\tau) \quad . \quad . \quad . \quad . \quad . \quad . \quad . \quad . \quad (10)$$

and

$$\text{var}\{\psi_D(\tau)\} = N - \mu^2 + 2\sum_{i=1}^{N-1}\sum_{j=i+1}^{N} E\{z_1(t_i)\,z_2(t_i+\tau)\,z_1(t_j)\,z_2(t_j+\tau)\} \quad (11)$$

It was shown in Reference 2 that

$$E\{z_1(t_i)\,z_2(t_i+\tau)\,z_1(t_j)\,z_2(t_j+\tau)\} = \begin{cases}\psi_{z_1}(t_j-t_i)\,\psi_{z_2}(t_j-t_i) & t_j < t_i+\tau \\ \{\psi_{z_1z_2}(\tau)\}^2 & t_j \geqslant t_i+\tau\end{cases}$$

Expanding the double summation and collecting like terms,

$$\text{var}\{\psi_D(\tau)\} = N-\mu^2+N_a(N_a+1)\{\psi_{z_1z_2}(\tau)\}^2+2\sum_{i=1}^{N-N_a-1}(N-i)\,\psi_{z_1}(i\delta t)\,\psi_{z_2}(i\delta t) \quad (12)$$

where $\psi_{z_1}(\tau) = (2/\pi)\sin^{-1}\{\rho(\tau)\}$ and N_a is the number of samples in the period $T-\tau$. Theoretical and experimental distributions of $\psi_D(\tau)$ are shown in Fig. 2.

To verify the theory, a digital crosscorrelator having $N = 100$ or 200 was used. The cutoff frequency of $f_n(t)$ was 21 kHz, the sample spacing $\delta t = 12{\cdot}81\ \mu$s and $\tau = 5\delta t$, giving $N_a = 95$ or 195. Similar agreement was obtained between theory and experiment with 200 samples. Comparison of Fig. 1 with the first Figure in Reference 2 shows that the detection reliability is greater when clipped noise, as opposed to analogue noise, is transmitted. For instance, taking β/σ in Reference 2 and $\beta s/\sigma$ as equivalent, the mean value of $\psi_D(0)$ for $\beta/\sigma = \beta s/\sigma = 1$ occurs at a level of 69 for clipped noise and at a level of only 50 for analogue noise. However, comparison of the respective Figs. 2 shows that the false-alarm performances of the two detection schemes are very similar. Therefore a lower central crosscorrelation peak is the price to be paid for the decreased transmission bandwidth.

Acknowledgments: The author gratefully acknowledges the financial support in the form of a scholarship given by C. I. Fuchs Ltd., and the guidance of his supervisor, Prof. H. E. Hanrahan.

J. E. HOWARD

Department of Electrical Engineering
University of the Witwatersrand
Jan Smuts Avenue, Johannesburg, South Africa

24th January 1974

References

1 BROCH, J. T.: 'On the applicability and limitations of the cross-correlation and cross-spectral density techniques', *Bruel & Kjaer Tech. Rev.*, 1970, 4, pp. 3–27
2 HOWARD, J. E.: 'Probability distribution of the crosscorrelation function of finite-duration single-bit random waveforms', *Electron. Lett.*, 1972, 8, pp. 560–562 and Errata, *ibid.*, 1973, 9, p. 72
3 MCFADDEN, J. A.: 'The correlation function of a sine wave plus Gaussian noise after extreme clipping', *IRE Trans.*, 1956, IT-2, pp. 82–83
4 WOZENCRAFT, J. M., and JACOBS, M. J.: 'Principles of communication engineering' (Wiley, 1967), chap. 3
5 ABRAMOWITZ, M. and STEGUN, I. A.: 'Handbook of mathematical functions' (NBS, Washington DC, 1964)
6 RICE, S. O.: 'Mathematical analysis of random noise' *in* 'Selected papers on noise and stochastic processes' (Dover, 1954), p. 188
7 EKRE, H.: 'Polarity coincidence correlation detection of a weak noise source', *IEEE Trans.*, 1963, IT-9, pp. 18–23

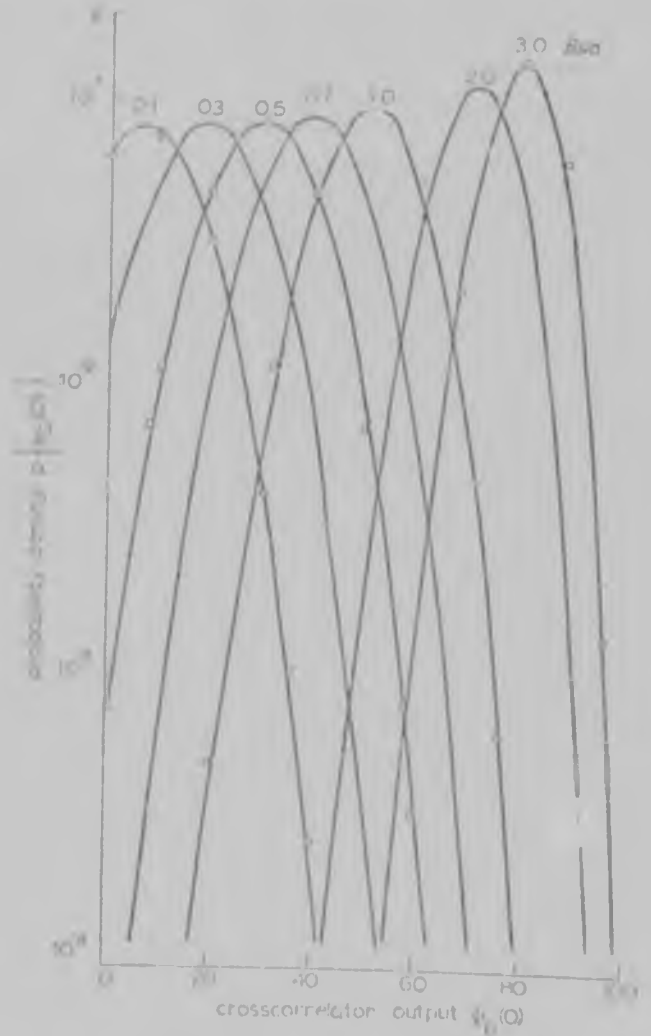

Fig. 2. *Probability density functions of $\Psi_D(0)$ for 100 samples*
Experimental points joined by a smooth curve

These equations might then be implemented by [illegible] submachines interconnected in a nonhierarchical manner, as shown in Fig. 2b. The required storage is then only [illegible] bits, representing a [illegible]% reduction on the requirement for the original machine.

To summarise, the technique offers the following advantages:

(*a*) The most economical use of storage is obtained, since no redundant variables are required in the submachines.

(*b*) The submachines have only one output, and can be realised from commercially available memory units, involving little or no redundancy.

(*c*) Apart from those with redundant inputs, the submachines are of uniform structure.

(*d*) The use of smaller storage units leads to a reduced access time for the system.

A. M. A. HUSSAIN
M. E. WOODWARD

Department of Electronic & Electrical Engineering
University of Technology
Loughborough, Leics. LE11 3TU, England

20th May 1974

References

1 HOWARD, R. V.: 'Partition methods for read-only memory sequential machines', *IEEE Trans.*, 1970, C-19, pp. [illegible]
2 HUSSAIN, A.: 'Decomposition structure of sequential machines', *Int. & Control*, 1962, 5, pp. [illegible]

ERRATA

WAIT, J. R., and SPIES, K. P.: 'Low-frequency impedance of a circular loop over a conducting ground', *Electron. Lett.*, 1973, 9, pp. 346–348

We regret that the following errors have occurred in the above letter:

In eqn. 7, A_2 should be I^2

In eqn. 13, the lower limit of integration should be 0

In the unnumbered equation following eqn. 13, the factor $(2/i)$ should be $(2/i)^4$

STREET, M. A., and SHINN, D. H.: 'Site shielding for Earth-station antennas', *Electron. Lett.*, 1974, 10, pp. 120–121

The authors would like to make the following correction to their letter:

Reference 4 is to CCIR Report 391, 1970

HOWARD, J. E.: 'Probability-density function of single-bit crosscorrelator for detecting Gaussian reflections in noise', *Electron. Lett.*, 1974, 10, pp. 71–72

We regret that the following errors have occurred in the above letter:

In eqn. 9, $\psi_D(0)$ should be $\overline{\psi_D(0)}$

Figs 1 and 2 should be interchanged, and the subcaptions should read 'Theoretical points joined by a smooth curve'

HOLMES, J. N.: 'Variable-frame-rate coding scheme for speech-analysis/synthesis systems', *Electron. Lett.*, 1974, 10, pp. 101–102

We regret that the following error has occurred in the above letter:

Reference 3 is to Vol. AE-21

THAJCHAYAPONG, P., and RAYNER, P. J. W.: 'Design of recursive digital filters approximating to arbitrary prescribed magnitude responses', *Electron. Lett.*, 1974, 10, p.p. 159–161:

We regret that the following error has occurred in the above letter:

In eqn. 3*c*, the symbol $\leqslant$ should be $\geqslant$